CHEMICAL REVIEWS

REVIEW

pubs.acs.org/CR

Relativistic Pseudopotentials: Their Development and Scope of Applications

Michael Dolg* and Xiaoyan Cao

Theoretical Chemistry, University of Cologne, Greinstrasse 4, 50939 Cologne, Germany

CONTENTS

Special Issue: 2012 Quantum Chemistry

Received: April 25, 2011
Published: September 13, 2011

dx.doi.org/10.1021/cr2001383 | *Chem. Rev.* 2012, 112, 403–480

1. INTRODUCTION

The concept of valence and core electrons is familiar to every chemist and underlying, for example, the ordering of the elements in the periodic table. For many qualitative considerations the chemistry of an element is only determined by its valence electrons, which actively participate in chemical bonding. In this picture the core electrons remain essentially inert and at most play an indirect role, for example, by providing together with the nucleus somewhat modified effective potentials for the valence electrons of the elements within a group of the periodic table. These do not only lead to quantitative differences for atoms, for example, in ionization potentials, electron affinities and excitation energies, but also for molecules, for example, the strengths of the chemical bonds formed by these atoms, and thus affect their chemical behavior.

The method of effective core potentials (ECPs) makes use of these ideas in first-principles electronic structure theory calculations. The main goals are a considerable reduction of the computational effort by avoiding the costly explicit treatment of the atomic cores in the calculations and at the same time an implicit treatment of the major relativistic effects for the valence electron system. The elimination of the atomic cores from the calculations allows to treat all elements of a group of the periodic table on equal footing. Since the same number of valence electrons has to be dealt with, one can expect that the same computational effort is required for all elements of a column of the periodic table and one may also hope that a similar accuracy is achieved, that is, a bias in the quality of the results caused by largely different system sizes is avoided. Clearly, such an expectation rests on the discussible assumption that the ECP formalism works equally well for all elements of a group of the periodic table.

Relativistic contributions, which become non-negligible quantitatively and sometimes even qualitatively for heavy elements and thus cannot be neglected for accurate investigations, require an additional computational effort at the all-electron (AE) level. Within ECP approaches they are included usually by means of a simple parametrization of a suitably chosen valence-only (VO) model Hamiltonian with respect to relativistic AE reference data. If spin−orbit (SO) effects can be neglected the scalar-relativistic ECP approaches can make use of the whole unchanged machinery of nonrelativistic quantum chemistry, nevertheless leading to results comparable to those of more costly scalar-relativistic AE calculations. SO effects can be accounted for in ECP approaches using various strategies, which range from a simple perturbative treatment subsequent to scalar-relativistic calculations, that is, as the last step of the calculation, to their rigorous variational inclusion already from the beginning of the calculation. Since for most investigations targeting chemical problems the results obtained with modern ECP schemes are usually not less accurate than those derived from more costly, but also approximate relativistic AE calculations, it is not too surprising that ECPs became a workhorse of relativistic quantum chemistry and produced more results than any other relativistic method.[1,2]

The present article intends to describe the most important aspects of the theoretical background of ECPs. The two main branches of the method will be discussed, that is, the pseudopotential (PP) and the model potential (MP) approach. During the long history of ECPs many schemes were proposed and developed, which cannot all be discussed in detail here. Thus, we emphasize only those modern variants of the PP and MP approaches, which experience a widespread use today. When doing this we mainly focus on schemes applied to chemical problems, that is, molecules, using Gaussian basis sets and only very briefly touch those constructed for the treatment of solids with plane-wave basis sets. At the same time we restrict the discussion to static calculations and exclude applications in, for example, Car−Parrinello molecular dynamics.

Besides presenting the formalisms we also summarize some selected calibration studies and a few characteristic applications. It is quite obvious that due to the by now huge number of applications of ECPs this selection has to be quite subjective and necessarily also incomplete. Fortunately a relatively large number of review articles focusing on various aspects of ECPs has appeared,[3−31] where the reader can find further information. Some more general information about relativistic quantum chemistry can be found in condensed form in reviews by Pyykkö[1,2] and Schwarz,[32] as well as in more detail in books edited during the past decade by Hess,[33] Schwerdtfeger,[34,35] Hirao and Ishikawa,[36] and Barysz and Ishikawa.[37] The basics of relativistic electronic structure methods were recently summarized in monographs by Dyall and Faegri[38] and by Grant.[39] Additional information is available from the www-database for

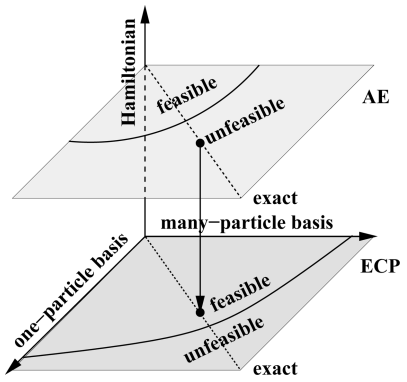

Figure 1. Coordinate system of quantum chemical ab initio methods. The basic goal of ECP approaches is illustrated by the arrow: by reducing somewhat the accuracy of the Hamiltonian, larger one- and many-body basis sets can be applied, that is, for a given system the wave function description becomes more accurate. Alternatively the computational effort is reduced or the size of accessible systems is increased.

relativistic theory of atoms and molecules (RTAM) provided by Pyykkö,[40] as well as the printed collections summarizing work from 1916 to 1999.[41−43]

Throughout this review, we use atomic units in the equations, that is, the rest mass of the electron $m_{0,e}$, the elementary charge e, the reduced Planck's constant $\hbar = h/(2\pi)$, and the Coulomb constant $1/(4\pi\varepsilon_0)$ are used as units for mass, charge, action/angular momentum, and Coulomb force. In this system of units, the velocity of light has a value of $c \approx 137.0359895$. $\alpha = 1/c$ denotes the fine structure constant. We also make use of the Dirac bracket notation as described, for example, in the book of Szabo and Ostlund.[44]

2. QUANTUM CHEMICAL PREREQUISITES

This initial section aims at readers not too familiar with quantum chemical approaches and can be skipped by those who are specialists. A more detailed description is available, for example, from the book of Szabo and Ostlund.[44] The methods and approximations discussed in this article can be located in a three-dimensional coordinate system of quantum chemical ab initio methods, see Figure 1, which can be viewed as a modification of the two-dimensional chart of quantum chemistry proposed by Pople in 1965.[45]

It is commonly accepted that quantum mechanics needs to be applied to chemistry to obtain an accurate nonempirical theoretical description of atoms, molecules, and solids. The central equation to solve is the time-dependent Schrödinger equation[46]

$$\hat{H}|\Psi\rangle = i\frac{\partial}{\partial t}|\Psi\rangle \tag{1}$$

with $\hat{H}$ being the Hamiltonian defining the system and $|\Psi\rangle$ the wave function describing its state. In this review, we will only consider cases where the Hamiltonian $\hat{H}$ does not explicitly depend on time. Thus the separation ansatz

$$|\Psi\rangle = |\psi\rangle \cdot e^{-iEt} \tag{2}$$

applies and leads to the time-independent Schrödinger equation for stationary states with total energy E and described by the wave function $|\psi\rangle$

$$\hat{H}|\psi\rangle = E|\psi\rangle \tag{3}$$

We will further assume that the so-called Born−Oppenheimer (BO) approximation[47] holds. It allows an approximate separation of the Schrödinger eq 3 in a nuclear part and an electronic part, which treats the electrons in the field of the nuclei at fixed positions and corresponds to the basic equation for most quantum chemistry electronic structure methods. Note that only the BO approximation allows the chemist, for example, to draw the well-known structural formulas with chemical symbols of the atoms denoting the positions of the atomic nuclei/cores in space as well as dashes and dots representing valence electron pairs and unpaired valence electrons, respectively. However, further approximations are needed to arrive at such a simple schematic representation of atoms, molecules and solids on the basis of quantum chemical considerations.

We consider a general configuration space Hamiltonian for n electrons and N nuclei, in the absence of external fields, that is

$$\hat{H} = \sum_{i}^{n} \hat{h}(i) + \sum_{i<j}^{n} \hat{g}(i,j) + \sum_{\lambda<\mu}^{N} \frac{Z_\lambda Z_\mu}{r_{\lambda\mu}} \tag{4}$$

The indices i and j denote electrons, whereas λ and μ stand for nuclei. Z_λ is the charge of the nucleus λ. The one- and two-particle operators $\hat{h}$ and $\hat{g}$ may be of relativistic, quasirelativistic or nonrelativistic form, each choice defining a plane in the coordinate system of ab initio methods perpendicular to the Hamiltonian axis, see Figure 1.

The exact solution of the time-independent Schrödinger eq 3, even under the assumption of the Born−Oppenheimer approximation, is infeasible except for a few one-electron systems. A large part of quantum chemistry therefore deals with the development of methods for the approximate, albeit sufficiently accurate solution of eq 3. Two main strategies evolved during the last almost nine decades, i.e., wave function-based theory (WFT)[46,48] and density functional theory (DFT).[49,50] We will mainly make use of WFT in the following, since it allows to develop an ab initio formalism and yields better insight in the underlying approximations of the methods discussed in this article. Note, however, that this choice does not imply that the ECP schemes cannot be derived for or applied in the framework of DFT.

A central method of ab initio WFT is the Hartree−Fock (HF) approach.[51−55] Here the most simple ansatz for a many-electron wave function, which obeys the Pauli antisymmetry principle[56] and the indistinguishability of the electrons as elementary particles, is used. The so-called Slater determinant[57] for a (closed-shell) n electron system is an antisymmetrized linear combination of products of n one-electron wave functions, that is, orthonormal spin−orbitals $|\varphi\rangle$

$$|\Phi_{\mathrm{HF}}\rangle = \frac{1}{\sqrt{n!}} \det||\varphi_1(1)\rangle|\varphi_2(2)\rangle...|\varphi_n(n)\rangle| \tag{5}$$

The HF wave function does not solve the Schrödinger eq 3; however, it maps approximately the unsolvable many-electron problem to effective one-electron problems, that is, the (canonical) Fock equation for the spin−orbitals $|\varphi\rangle$ and their orbital energies ε

$$\hat{F}|\varphi_i\rangle = \varepsilon_i|\varphi_i\rangle \tag{6}$$

Here $\hat{F}$ denotes the Fock-operator, an effective one-electron Hamiltonian, taking into account the (average) interactions of an electron in the spin−orbital $|\varphi\rangle$ with the nuclei and all other

dx.doi.org/10.1021/cr2001383 |Chem. Rev. 2012, 112, 403–480

electrons in the system. Since the Fock-operator $\hat{F}$ actually depends on its own occupied eigenfunctions $|\varphi\rangle$, the Fock eq 6 has to be solved iteratively by means of the self-consistent field (SCF) procedure.[51,52] The Fock equation is obtained for the exact Hamiltonian in eq 3 and the approximate (normalized) wave function in eq 5 by applying the Ritz−Rayleigh variational principle

$$E_{\mathrm{HF}} = \langle \Phi_{\mathrm{HF}} | \hat{H} | \Phi_{\mathrm{HF}} \rangle \geq E_0 \tag{7}$$

with E_0 being the exact ground state energy. We note here in passing that because of the unboundedness from below of the Dirac Hamiltonian only the stationarity of the energy expression can be required in the fully relativistic Dirac−Hartree−Fock (DHF) case, $\delta E_{\mathrm{DHF}} = \delta \langle \Phi_{\mathrm{DHF}} | \hat{H} | \Phi_{\mathrm{DHF}} \rangle = 0$. The energy variation is performed with respect to changes of the orbitals $|\varphi\rangle$, under the constraint that they form an orthonormal set, that is, $\langle \varphi_i | \varphi_j \rangle = \delta_{ij}$. Most calculations apply the formalism of Roothaan[58] and Hall,[59] where the orbitals $|\varphi\rangle$ are expanded as linear combinations of one-particle basis functions $|\chi\rangle$

$$|\varphi_i\rangle = \sum_j c_{ij} |\chi_j\rangle \tag{8}$$

for example, Gaussian[60,61] or more rarely Slater[62] functions. The quality of this one-particle basis set decides how close one may approach the best possible HF solution, that is, the HF limit to be reached when using a complete one-particle basis set. Thus, the one-particle basis set axis is one of two axes spanning the plane defined by a given Hamiltonian in Figure 1.

The difference between the HF limit energy E_{HF} and the exact energy E in eq 3 is called correlation energy[63] and results from the momentary response of the electrons to their mutual interactions, which are only treated on average in the HF formalism. Several strategies were developed to systematically approach the exact energy E and exact wave function $|\psi\rangle$ in ab initio quantum chemistry. These mostly use expansions of the wave function in a basis of Slater determinants $|\Phi\rangle$

$$|\psi_I\rangle = \sum_J C_{IJ} |\Phi_J\rangle \tag{9}$$

for example, the multiconfiguration Hartree−Fock SCF (MCHF, MCSCF) approach,[64] the configuration interaction (CI) approach,[57,65] many-body perturbation theory (MBPT),[66,67] or the coupled-cluster (CC) ansatz.[68] For a given one-particle basis set $\{|\chi_i\rangle\}$ one may in these schemes systematically construct larger/better many-electron basis sets $\{|\Phi_I\rangle\}$ thus approaching the corresponding Hamiltonian limit, which corresponds to a full configuration interaction (FCI). The many-particle basis set axis is another axis spanning the plane defined by a given Hamiltonian in Figure 1. Usually it is impracticable to use complete one- or many-particle basis sets and thus a major task of a computational quantum chemist is to select besides a suitable Hamiltonian also the optimum combination of one- and many-particle basis sets. Hereby the chosen Hamiltonian already sets some practical limitations due to the related required computational effort. Not always the theoretically best founded Hamiltonian will allow in practical calculations to approach the experimental result closest. Typically a suitable compromise with a less rigorous Hamiltonian and the possibility to use more extended one- and many-electron basis sets performs best.

The partitioning of a many-electron system into subsystems, which may be treated at different levels of theory, has been investigated by several scientists, see, for example, the review given by Huzinaga and references cited therein.[16] Staying at the effective independent-particle picture of the HF method one may exploit that the determinantal wave function eq 5 and the total energy eq 7 are invariant with respect to unitary transformations of the spin−orbitals $|\varphi\rangle$. Using one of several well-established orbital localization methods,[69−71] one can arrive at orbitals centered at or in close vicinity to the nuclei, which may be classified either as energetically low-lying core orbitals, or energetically high-lying valence orbitals representing lone pairs, and at usually energetically high-lying valence orbitals centered between two (or more) nuclei representing covalent chemical bonds. Taking only the lone pairs and bonding orbitals into account and representing the core orbitals together with the nucleus by the symbol of the element, such a localized orbital HF solution provides a similar picture of the electron distribution in a molecule as the structural formulas frequently used by chemists.

Since the computational effort to obtain approximate solutions of the Schrödinger eq 3 with standard approaches formally scales with the fourth (HF) or higher powers (CI, CC, MBPT) of the number of orbitals, a large amount of effort goes into the development of computational WFT methods which, by exploiting, e.g., the locality of electron correlation, seek to reduce the steep scaling of the computing time with system size and at best reach a linear dependence for extended systems. However, when increasing the system size by going from light to heavy atoms these techniques do not lead to reductions of the computational effort, and despite their chemical similarity, the elements of one column of the periodic table often cannot be treated on equal footing, for example, with a comparable accuracy. It was therefore tempting from the beginning of the development of quantum chemistry to remove the atomic cores, as long as they remain sufficiently inert and transferable between various situations, from the explicit treatment of the remaining valence electrons. A relief from the *nightmare of inner shells* discussed by van Vleck and Sherman[72] was provided already very early in the history of quantum chemistry by introducing pseudopotentials (PPs), for example, by Hellmann for molecules[73] and by Gombas in the theory of metals.[74,75] As a variant of effective core potentials (ECPs) the PPs, as well as the more rigorous model potentials (MPs), aim to model as accurately as possible the interaction of a valence electron with the core of an atom, that is, the nucleus and the core electrons/orbitals removed from the explicit quantum chemical treatment. We note that also essentially all semiempirical schemes restrict their explicit calculations to the valence electron system in the field of the atomic cores.

3. RELATIVISTIC ALL-ELECTRON REFERENCE SCHEMES

The commonly used ECP method does not only have the advantage to reduce the computational effort compared to an AE calculation by limiting the number of electrons treated explicitly but also allows an implicit incorporation of the most important relativistic effects[1,2,76,77] merely by parametrization with respect to suitable relativistic AE reference data. Many technical problems connected to relativistic AE Hamiltonians are circumvented by ECP approaches, which makes them attractive tools for heavy-element quantum chemical studies. Questions to be answered are, for example, to which extent relativistic operators

acting mainly in the vicinity of the nucleus can be modeled in PP methods by operators acting mainly in the spatial valence region, or how accurately a relativistic two-electron operator such as the Breit term can be modeled by effective one-electron operators at the ECP level.

Relativistic AE approaches are discussed here only very briefly for the following two reasons: First, relativistic ECPs are usually derived from (atomic) relativistic AE reference calculations, e.g., (multiconfiguration (MC)) Dirac−Hartree−Fock (DHF) calculations[78−83] or approximate two- and/or one-component (scalar-relativistic) calculations using, e.g., the Wood−Boring (WB)[84] or Cowan−Griffin (CG)[85] Hamiltonian, the approximate second-order Dirac equation derived by Barthelat, Pelissier and Durand,[86] the Douglas−Kroll−Hess (DKH)[87−91] Hamiltonian, or the relativistic scheme of Nakajima and Hirao obtained by elimination of the small components (RESC).[92] In view of the limits of accuracy of ECP parametrizations it is interesting to see which relativistic contributions are so pronounced, that they still can be realistically taken into account in an ECP adjustment of a given accuracy, and which can safely be omitted.

Second, at least for small systems, relativistic AE methods can be used to calibrate ECP methods, e.g., to check the ECP transferability from the atom to molecules (or solids), or from uncorrelated to correlated calculations. A number of molecular electronic structures codes based on DHF solutions are available for this purpose, for example, MOLFDIR,[93] DIRAC,[94] BERTHA,[95,96] and others.[97−101] In this context, it should be noted that modern ECPs can reach a fairly high accuracy, for example, not only the incorporation of the dominant Dirac one-electron relativistic effects is achieved, but also smaller contributions because of the Breit interaction between two electrons, the finite nucleus or even quantum electrodynamic corrections can be accounted for. Since these contributions are often neglected in quantum chemical AE calculations for all but the smallest systems, ECP schemes can sometimes even reach a better overall accuracy than approximate relativistic AE methods.[102] For calibration studies it is important to remember that every ECP can model only the AE method it was adjusted to, that is, one should distinguish between the accuracy of the used reference data and the accuracy of the ECP approach itself. This point is sometimes overlooked in calibration studies.[103] Thus, the Hamiltonian coordinate of an ECP plane in Figure 1 is certainly smaller than the one of the AE approach underlying the specific ECP model, but it may actually be larger than the ones of other AE schemes omitting some relativistic contributions which are implicitly included in the ECP under consideration.

3.1. Dirac−Coulomb−Breit Hamiltonian

In the most accurate electronic structure calculations for atoms, molecules and also solids the Dirac (D) one-particle Hamiltonian is applied in eq 4

$$\hat{h}_{\mathrm{D}}(i) = c\hat{\vec{\alpha}}_i \cdot \hat{\vec{p}}_i + (\hat{\beta}_i - \mathbf{I}_4)c^2 + \sum_{\lambda} \hat{V}_\lambda(r_{i\lambda}) \tag{10}$$

Here c denotes the velocity of light ($c \approx 137.0359895$ au). Equation 10 is correct to all orders of the fine-structure constant $\alpha = 1/c$. To have the same zero of energy as in the nonrelativistic case the rest energy c^2 of the electron was subtracted. Further $\mathbf{I}_4$ denotes the 4×4 unit matrix, and $\hat{\vec{p}}_i = -i\hat{\vec{\nabla}}_i$ is the momentum operator acting on the i-th electron, with the vector differential (del or nabla) operator $\hat{\vec{\nabla}}_i = (\partial/\partial x_i, \partial/\partial y_i, \partial/\partial z_i)$. $\hat{\vec{\alpha}}_i$ is a three-component vector whose elements together with $\hat{\beta}_i$ are the 4×4 Dirac matrices

$$\hat{\vec{\alpha}} = \begin{pmatrix} \vec{0} & \hat{\vec{\sigma}} \\ \hat{\vec{\sigma}} & \vec{0} \end{pmatrix} \text{ and } \hat{\beta} = \begin{pmatrix} \mathbf{I}_2 & \mathbf{0}_2 \\ \mathbf{0}_2 & -\mathbf{I}_2 \end{pmatrix} \tag{11}$$

These can be expressed in terms of the three-component vector of the 2×2 Pauli matrices $\hat{\vec{\sigma}}$

$$\hat{\sigma}_x = \begin{pmatrix} 0 & 1 \\ 1 & 0 \end{pmatrix}, \ \hat{\sigma}_y = \begin{pmatrix} 0 & -i \\ i & 0 \end{pmatrix}, \ \hat{\sigma}_z = \begin{pmatrix} 1 & 0 \\ 0 & -1 \end{pmatrix} \tag{12}$$

the 2×2 unit matrix $\mathbf{I}_2$ and the 2×2 zero matrix $\mathbf{0}_2$. $\hat{V}_\lambda(r_{i\lambda})$ denotes the electrostatic potential generated by the λ-th nucleus at the position of the i-th electron

$$\hat{V}_\lambda(r_{i\lambda}) = -\frac{Z_\lambda}{r_{i\lambda}} \tag{13}$$

Frequently a finite nucleus is used,[104] for example, a Gaussian-type charge distribution

$$\rho_\lambda(r) = \rho_{0,\lambda} \exp(-\eta_\lambda r^2) \text{ with } 4\pi \int_0^\infty \mathrm{d}r r^2 \rho_\lambda(r) = Z_\lambda \tag{14}$$

The parameter η_λ can be determined from the nuclear radius R_λ, which is related to the nuclear mass according to

$$\eta_\lambda = 3/(2R_\lambda^2) \text{ with } R_\lambda = 2.2677 \times 10^{-5} M_\lambda^{1/3} \tag{15}$$

Other variants of charge distributions are also in use, for example, a finite hard sphere

$$\rho_\lambda(r) = \begin{cases} \rho_{0,\lambda} & \text{if} \quad r \le R_\lambda \\ 0 & \text{otherwise} \end{cases} \tag{16}$$

or a Fermi-type nuclear model

$$\rho_\lambda(r) = \frac{\rho_{0,\lambda}}{1 + e^{(r - c_\lambda)/a_\lambda}} \tag{17}$$

Here the parameter c_λ (half-charge radius) is the radius at which $\rho_\lambda(r) = 0.5\rho_{0,\lambda}$. The parameter a_λ is related to the skin thickness t_λ ($t_\lambda/a_\lambda = 4\ln 3$), which is the interval across which $\rho_\lambda(r)$ falls from $0.9\rho_{0,\lambda}$ to $0.1\rho_{0,\lambda}$.[83] Besides providing a more realistic model than the point charge nucleus, the finite nuclear models have the practical advantage that the wave function at the nucleus is more well-behaved and the size of the highest exponents in basis set expansions can be somewhat reduced. The Gaussian charge distribution eq 14 is easy to implement and a natural choice for Gaussian basis sets.

The Dirac Hamiltonian eq 10 does not only describe an electron, but also its antiparticle, the positron. Because of the structure of the Dirac Hamiltonian the corresponding relativistic wave function for a one-particle system turns out to be a four-component vector (four-spinor), the two upper components (upper bispinor) being large for the electronic states, the two lower ones (lower bispinor) being large for the positronic states (charge degrees of freedom in the wave function). The general properties of the solutions of the one-particle Dirac equation also

dx.doi.org/10.1021/cr2001383 |Chem. Rev. 2012, 112, 403–480

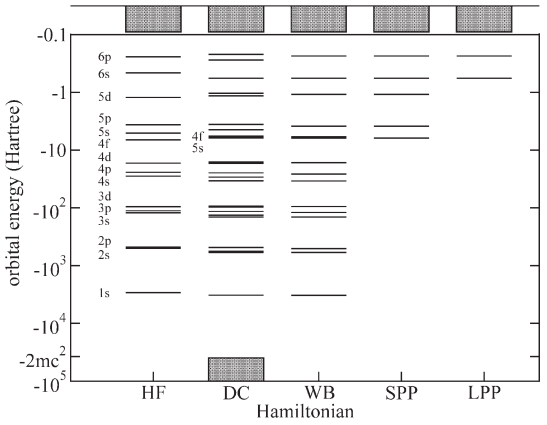

Figure 2. Schematic spectrum of occupied one-particle levels of the Pb atom in its $6s^26p^2$ ground state configuration from nonrelativistic HF, relativistic DHF/DC and scalar-relativistic WB calculations as well as for a scalar-relativistic small-core (22 valence electrons in 5s, 5p, 5d, 6s, 6p) and a corresponding large-core (4 valence electrons in 6s, 6p) PP. Note the logarithmic scale for the one-particle energies. The continua were added schematically, and bound unoccupied levels between 6p and the upper continuum are not displayed. Thick lines indicate a (near-) degeneracy of levels.

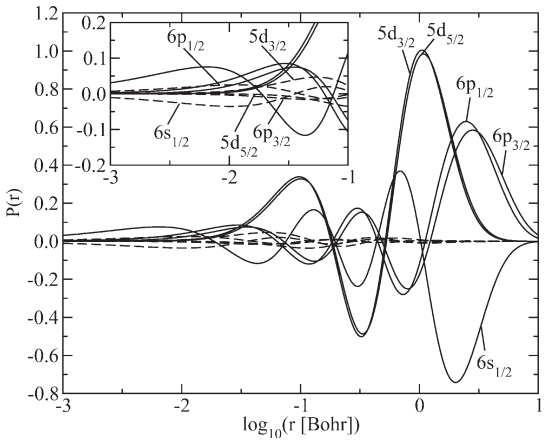

Figure 3. Large (upper; solid lines) and small (lower; dashed lines) components of the valence spinors of Pb in the $6s^2$ $6p^2$ ground state configuration from MCDHF calculations using the program GRASP.[83] The small components have a noticeable contribution only in the core region and are shown in the inset.

hold true for the orbitals used in an independent-particle description of a many-electron system, e.g., in the (MC)DHF approach. Figure 2 displays the occupied one-particle levels from AE HF and DHF calculations performed with the GRASP code[83] for the Pb ($Z = 82$) atom in its $6s^26p^2$ ground state configuration. The continua for $\varepsilon \geq 0$ and $\varepsilon \leq -2c^2$ were schematically added, and possible unoccupied bound levels between 6p and the upper continuum are not displayed. In relativistic quantum chemistry, where one is interested in the electronic states, it is common to use the terms large components and small components for the upper and lower components, respectively. Figure 3 shows for the Pb atom in its ground state configuration that the small components are nonnegligible only in the core region, that is, the chemical behavior of an element is determined by the large components. Saue showed, for example, that for Rn ($Z = 86$) the small component density only contributes with 0.7% (0.6281 electrons) to the total density, is essentially localized within a radius of 0.15 Å and arises to 65% (99.9%) from the shells 1s−2p (1s−5d).[105] This is a motivation to eliminate the small components, that is, the charge degrees of freedom from the Dirac Hamiltonian, and to construct transformed AE Hamiltonians which lead to two-component spinors. The odd and even components of the four-spinor, as well as of two-spinors approximating it, may be related to spin up and down, respectively, of the particle (spin degrees of freedom).

In the simplest and most commonly encountered case of relativistic AE calculations the two-particle terms in eq 4 are just the nonrelativistic electrostatic Coulomb (C) interaction (yielding the Dirac−Coulomb (DC) Hamiltonian correct to $O(\alpha^0)$)

$$\hat{g}_C(i,j) = \frac{1}{r_{ij}} \tag{18}$$

This choice is motivated by the fact that for the relativistic effects in chemistry, for example, on bond distances and binding energies, the one-particle Dirac relativistic contributions are by far larger than contributions arising from relativistic corrections to the Coulomb electron−electron repulsion.[106] The most rigorous two-electron interaction which can be derived from quantum electrodynamics (QED) is the frequency-dependent Breit interaction, given here in Coulomb gauge[107]

$$\hat{g}_{\omega,\mathrm{CB}}(i,j) = \frac{1}{r_{ij}} - \frac{\hat{\vec{\alpha}}_i \cdot \hat{\vec{\alpha}}_j}{r_{ij}} e^{ir_{ij}\omega_{ij}/c} + \frac{(\hat{\vec{\alpha}}_i \cdot \hat{\vec{\nabla}}_i)(\hat{\vec{\alpha}}_j \cdot \hat{\vec{\nabla}}_j)}{\omega_{ij}^2 r_{ij} c^2} (e^{ir_{ij}\omega_{ij}/c} - 1) \tag{19}$$

where the frequency of the exchanged photon is taken from the orbital energy difference, that is, $\omega_{ij} = |\varepsilon_i - \varepsilon_j|$. In the limit $c \rightarrow \infty$ the Gaunt (G) term

$$\hat{g}_{\mathrm{CG}}(i,j) = \frac{1}{r_{ij}} - \frac{\hat{\vec{\alpha}}_i \cdot \hat{\vec{\alpha}}_j}{r_{ij}} \tag{20}$$

is obtained, which can be interpreted to contain besides the Coulomb interaction also the magnetic interaction between two electrons. The Gaunt term is quite frequently added to the Dirac one-particle Hamiltonian (yielding the Dirac−Coulomb−Gaunt (DCG) Hamiltonian correct to $O(\alpha^0)$), since it does not require the evaluation of additional two-electron integrals. The retardation of the interaction due to the finite velocity of light is accounted for in addition to the magnetic interaction by the frequency-independent Breit (B) interaction (yielding the Dirac−Coulomb−Breit (DCB) Hamiltonian correct to $O(\alpha^2)$)

$$\hat{g}_{\mathrm{CB}}(i,j) = \frac{1}{r_{ij}} - \frac{1}{2r_{ij}}\left[\hat{\vec{\alpha}}_i \cdot \hat{\vec{\alpha}}_j + \frac{(\hat{\vec{\alpha}}_i \cdot \hat{\vec{r}}_{ij})(\hat{\vec{\alpha}}_j \cdot \hat{\vec{r}}_{ij})}{r_{ij}^2}\right] \tag{21}$$

It is often sufficient to treat the Gaunt- and Breit-interaction not variationally, but merely by first-order perturbation theory after the approximate solution of the Dirac−Coulomb−Hamiltonian problem.[83] The contribution of higher-order relativistic corrections such as the vacuum polarization or the self-energy of the electron can be derived from quantum electrodynamics (QED). These are usually neglected due to their expected negligible impact on chemical properties. It is noteworthy, however, that for

dx.doi.org/10.1021/cr2001383 |Chem. Rev. 2012, 112, 403–480

the first ionization potential of the gold atom the contributions of vacuum polarization and self-energy of the electron are estimated to contribute with −0.021 eV.[108] Modern ECPs can indeed be adjusted with roughly this accuracy and the implicit inclusion of such significant QED effects in valence-only calculations therefore should be possible.

Technical problems of relativistic electronic structure calculations based on the above-described Hamiltonians arise mainly from the fact that the Dirac−Hamiltonian is not bounded from below and thus an energy-minimization without additional precautions may lead to a variational collapse. In addition, at the many-electron level an infinite number of unbound states with one electron in the positive and one in the negative continuum are degenerate with the desired bound solution. A mixing-in of these unphysical states is possible without changing the energy and might lead to the so-called Brown−Ravenhall continuum dissolution,[109] which is sometimes also called Brown−Ravenhall disease.[110−112] A variational collapse at the one- or many-electron level can be avoided if a no-pair Hamiltonian is constructed, that is, the Hamiltonian is projected onto the desired electronic states by means of suitable operators $\hat{P}_+$ as suggested by Sucher[110,113]

$$\hat{H}_{\mathrm{np}} = \hat{P}_+ \hat{H} \hat{P}_+ \tag{22}$$

In practice the projection is achieved if the Hamiltonian is formulated in Fock space and the occupation of negative energy states is forbidden. Thus Dirac−Hartree−Fock (DHF) calculations, as well as subsequent wave function-based correlated calculations, are not plagued by continuum dissolution. In (atomic) finite difference calculations the undesired solutions are avoided by imposing suitable boundary conditions.[81,83]

For practical calculations using finite basis sets a more important aspect is the coupling of the upper and lower components of the wave function via $\hat{\vec{\alpha}}_i \cdot \hat{\vec{p}}_i$, which may lead to a variational collapse because of the so-called finite basis set disease.[111,112,114] If the basis set used to describe the lower components does not span the function space corresponding to first derivatives of basis functions expanding the upper components, zero or near-zero kinetic energy matrix elements may result. The kinetic energy may thus not be able to balance the potential energy, resulting in too low total energies. Consequently a routinely used remedy are so-called kinetically balanced basis sets. A comparison of the various prescriptions to construct kinetically balanced basis sets was given recently by Kutzelnigg and co-workers.[115] A different approach to avoid the problems resulting from the unboundedness of the Dirac operator and to arrive at accurate solutions is the relativistic free complement method of Nakashima and Nakatsuji.[116]

The problems related to the unboundedness of the Dirac Hamiltonian from below have been successfully solved for practical calculations, especially for atomic finite difference DHF calculations, which are used to generate AE reference data for the ECP adjustment. For further details concerning difficulties (and practical solutions) associated with relativistic AE Hamiltonians the reader is referred to, for example, a review article by Kutzelnigg,[117] and the books of Dyall and Faegri[38] and Grant.[39]

Since the ECP approach is an approximate method, the adjustment of highly accurate ECPs was for many decades not considered to be feasible. It is thus understandable that various still very popular, and for most chemical problems sufficiently accurate, sets of ECPs are based on AE reference data, which is not obtained with the DCB Hamiltonian, but rather with the simpler DC Hamiltonian, some two- or one-component approximations of it such as the Douglas−Kroll−Hess (DKH),[87−91] Cowan−Griffin (CG),[85] or Wood−Boring (WB)[84] Hamiltonians, or even at the nonrelativistic level. A number of other approximate relativistic AE schemes exist,[86,92,118−127] some of which also have been used occasionally to obtain reference data for the ECP adjustment.[86,92] An overview of some of the methods is given by Karwowski and Kobus[128] and Barysz.[129] In the sections 3.2 and 3.3, we only concentrate on the DKH, CG and WB approaches, which are used in some currently popular ECP schemes. Some motivation to rely on the corresponding approximate reference data is given in the discussion of relativistic effects in section 4.

3.2. Douglas−Kroll−Hess Hamiltonian

The elimination of the small components from the Dirac equation to order α^2, for example, by using the classical Foldy−Wouthuysen (FW) transformation,[130,131] leads to the Pauli Hamiltonian,[38,39] which because of the occurrence of unbound operators such as the $-(1/8)\alpha^2\hat{\vec{p}}^4$ mass-velocity term can lead to a collapse in variational calculations. The same is true for the Breit−Pauli Hamiltonian, which can be derived from quantum electrodynamics (QED).[132] Although a perturbative treatment of relativistic contributions based on the Pauli Hamiltonian is valid for light elements, it can fail for heavier ones. A more suitable transformation leading to a variationally stable Hamiltonian was devised by Douglas and Kroll[133] and later further developed and put to work by Hess and co-workers in the context of quantum chemical calculations.[87−90] A review was published recently by Nakajima and Hirao.[91] The coupling of the upper and lower bispinor of an electronic solution of the Dirac equation is due to the odd terms in $\hat{h}_{\mathrm{D}}$ in eq 10, that is, terms anticommuting with $\hat{\beta}$. Using an unitary transformation expanding the Hamiltonian in powers of the external potential $\hat{V}$ the effect of the odd terms can be reduced and an approximate two-component Hamiltonian can be extracted by eliminating them from the result. The Douglas−Kroll−Hess (DKH) approach starts with a free-particle FW transformation $\hat{U}_0$ of $\hat{h}_{\mathrm{D}}$

$$\hat{h}_1(i) = \hat{U}_0(i)\hat{h}_{\mathrm{D}}(i)\hat{U}_0^{-1}(i) = \hat{\beta}\hat{E}_i + \hat{\varepsilon}_1(i) + \hat{\mathcal{O}}_1(i) \tag{23}$$

where $\hat{\varepsilon}_1$ and $\hat{\mathcal{O}}_1$ are even and odd operators of order $\hat{V}$, respectively.

$$\begin{aligned} \hat{\varepsilon}_1(i) &= \hat{A}_i(\hat{V}(i) + \hat{R}_i\hat{V}(i)\hat{R}_i)\hat{A}_i, \\ \hat{\mathcal{O}}_1(i) &= -\hat{\beta}\hat{A}_i(\hat{V}(i)\hat{R}_i - \hat{R}_i\hat{V}(i))\hat{A}_i \end{aligned} \tag{24}$$

with

$$\hat{U}_0(i) = \hat{A}_i(I + \hat{\beta}\hat{R}_i),\ \hat{A}_i = \sqrt{\frac{\hat{E}_i + c^2}{2\hat{E}_i}} \tag{25}$$

$$\hat{R}_i = \frac{c\hat{\vec{\sigma}}_i \cdot \hat{\vec{p}}_i}{\hat{E}_i + c^2}, \qquad \hat{E}_i = \sqrt{c^4 + c^2 p_i^2} \tag{26}$$

If $\hat{V}$ is the hydrogen potential at the Bohr radius, then $\hat{A}$, $\hat{R}$, $\hat{V}$, and $\hat{E}_p$ can be estimated to be of order α^0, α^1, α^0, and α^{-2}, respectively. Therefore $\hat{\varepsilon}_1$ and $\hat{\mathcal{O}}_1$ are of order α^2 and α^1, respectively.

dx.doi.org/10.1021/cr2001383 |Chem. Rev. 2012, 112, 403–480

The nth order DKH transformation of the Dirac Hamiltonian is given by

$$\hat{h}_{\mathrm{DKH}n}(i) = \hat{U}_n(i)\hat{U}_{n-1}(i)\ldots\hat{U}_1(i)\hat{U}_0(i)\hat{h}_{\mathrm{D}}(i)\hat{U}_0^{-1}(i)\hat{U}_1^{-1}(i)\ldots\hat{U}_{n-1}^{-1}(i)\hat{U}_n^{-1}(i) \quad (27)$$

with

$$\hat{U}_n(i) = (1 + \hat{W}_n^2(i))^{1/2} + \hat{W}_n(i) \quad (28)$$

Here $\hat{W}_n$ is an integral operator with the kernel

$$\hat{W}_n(\vec{p}_i, \vec{p}_i') = \frac{\beta}{\hat{E}_i + \hat{E}_{i'}}\hat{O}_n(\vec{p}_i, \vec{p}_i') \quad (29)$$

The odd operator $\hat{O}_n$ is of order n in the external potential $\hat{V}$ and is generated by the previous n transformations. The application of $\hat{U}_1$ to $\hat{h}_1$ yields

$$\hat{h}_{\mathrm{DKH2}}(i) = \hat{\beta}\hat{E}_i + \hat{\varepsilon}_1(i) + \hat{\mathcal{O}}_2(i) + \hat{\varepsilon}_2(i) + \ldots \quad (30)$$

with

$$\hat{\mathcal{O}}_2(i) = [\hat{W}_1(i), \hat{\varepsilon}_1(i)], \quad \hat{\varepsilon}_2(i) = -\frac{1}{2}[\hat{W}_1(i), \hat{\mathcal{O}}_1(i)] \quad (31)$$

In comparison to $\hat{\mathcal{O}}_1$ the amplitude of the odd term in $\hat{\mathcal{O}}_2$ is reduced from order α to order α^5, whereas compared to $\hat{\varepsilon}_1$ the even term $\hat{\varepsilon}_2$ is of order α^4 instead of order α^2. Thus, after two DKH transformations the resulting second-order DKH2 Hamiltonian, which is bounded from below and thus variationally stable, has even terms correct to order α^6, and the lowest-order odd terms are of order α^4. For the one-electron case the odd terms may be systematically removed in this way order by order.

For many-electron systems the DKH transformation may be applied to the two-electron interaction $\hat{g}(i,j)$. In scalar-relativistic calculations, the first transformation of the two-electron operators was found to be about as important as the fifth-order transformation of the one-electron operators[90]

$$\hat{U}_0(i)\hat{U}_0(j)\hat{g}(i,j)\hat{U}_0^{-1}(j)\hat{U}_0^{-1}(i) = \hat{g}(i,j) + [\hat{U}_0(i), \hat{g}(i,j)]\hat{U}_0^{-1}(i) + [\hat{U}_0(j), \hat{g}(i,j)]\hat{U}_0^{-1}(j) + [\hat{U}_0(i), [\hat{U}_0(j), \hat{g}(i,j)]]\hat{U}_0^{-1}(j)\hat{U}_0^{-1}(i) \quad (32)$$

In standard applications, one can neglect the commutators and use the untransformed Coulomb operator for the electron−electron interaction without significant loss of accuracy.

Samzow and Hess applied the DK transformation to the DCB Hamiltonian[134] and arrived, after separating spin by use of the Dirac relation

$$(\hat{\vec{\sigma}}_j\cdot\hat{\vec{p}}_j f(r_j))(\hat{\vec{\sigma}}_j\cdot\hat{\vec{p}}_j) = (\hat{\vec{p}}_j f(r_j))\cdot\hat{\vec{p}}_j + i\hat{\vec{\sigma}}_j\cdot[(\hat{\vec{p}}_j f(r_j)) \times \hat{\vec{p}}_j] \quad (33)$$

at the DKH SO term. Keeping only the lowest order α^2 contributions, the Breit−Pauli (BP) SO operator can be derived. Both Hamiltonians are closely related and can be written as sums over one- and two-electron terms, that is

$$\hat{H}^{\mathrm{SO}} = \sum_i \hat{h}_1^{\mathrm{SO}}(i) + \sum_{i\neq j}\hat{h}_2^{\mathrm{SO}}(i,j) \quad (34)$$

The DKH one-particle SO term

$$\hat{h}_{1,\mathrm{DKH}}^{\mathrm{SO}}(i) = \hat{B}_i\hat{h}_{1,\mathrm{BP}}^{\mathrm{SO}}(i)\hat{B}_i \quad (35)$$

is related to the Pauli one-particle SO term

$$\hat{h}_{1,\mathrm{BP}}^{\mathrm{SO}}(i) = \sum_\lambda \frac{Z_\lambda}{2c^2}\hat{\vec{s}}\cdot\left(\frac{\vec{r}_{i\lambda}}{r_{i\lambda}^3}\times\hat{\vec{p}}_i\right) \quad (36)$$

by the kinematic factor

$$\hat{B}_i = \frac{2c^2\hat{A}_i}{\hat{E}_i + c^2} \quad (37)$$

where $\hat{A}$ and $\hat{E}$ are defined in eqs 25 and 26, respectively. The DKH two-electron SO term

$$\hat{h}_{2,\mathrm{DKH}}^{\mathrm{SO}}(i,j) = -\frac{1}{2c^2}\left[\hat{B}_i\hat{A}_j\hat{\vec{s}}\cdot\left(\frac{\vec{r}_{ij}}{r_{ij}^3}\times\hat{\vec{p}}_i\right)\hat{B}_i\hat{A}_j + \hat{B}_j\hat{A}_i 2\hat{\vec{s}}\cdot\left(\frac{\vec{r}_{ij}}{r_{ij}^3}\times\hat{\vec{p}}_i\right)\hat{B}_i\hat{A}_j\right] \quad (38)$$

exhibits a similar relation to the BP two-electron SO term

$$\hat{h}_{2,\mathrm{BP}}^{\mathrm{SO}}(i,j) = -\frac{1}{2c^2}(\hat{\vec{s}} + 2\hat{\vec{s}})\cdot\left(\frac{\vec{r}_{ij}}{r_{ij}^3}\times\hat{\vec{p}}_i\right) \quad (39)$$

both accounting for the spin-same-orbit and spin-other-orbit interactions. Note that for low momenta $\hat{E}\rightarrow c^2$ and thus $\hat{A}\rightarrow 1$ and $\hat{B}\rightarrow 1$, that is, the DKH SO Hamiltonian reduces to the BP SO Hamiltonian. Because of the $1/r^3$ singularity the BP SO operator can only be used in low-order perturbation theory after a scalar-relativistic DKH AE calculation, whereas the DKH SO operator is also suitable for variational calculations.[134]

Calculations using the above SO Hamiltonians require relatively expensive evaluations of one- and especially two-electron integrals. Therefore Blume and Watson investigated to which extent the BP two-electron SO terms eq 39 can be folded into an effective one-electron SO operator analogous to eq 36 when using an effective nuclear charge Z_λ^{eff}.[135,136] Using Z_λ^{eff} as an adjustable parameter SO operators of this type were also used in PP calculations.[137−140] Hess and co-workers proposed a mean field SO method for both the structurally related DKH and BP SO Hamiltonians leading to an effective atomic one-electron SO Hamiltonian which is applicable in correlated calculations.[141] The atomic mean field (AMFI) SO method[141] was also used in MP and PP calculations.[142,143]

The DKH2 and DKH3 formalism was mainly used in the development of MPs, both for an implicit and an explicit inclusion of relativistic contributions, see sections 7.2 and 7.4, as well as to generate reference data for calibration of both PPs and MPs. The approach is in the meantime available in a large number of quantum chemistry codes using finite basis sets, whereas a finite difference implementation has not been reported to the best of our knowledge.

3.3. Cowan−Griffin and Wood−Boring Hamiltonian

The elimination of the lower bispinor from the Dirac equation leads to the two-component Wood−Boring (WB) equation.[84]

The (electronic) eigenvalues of the Dirac Hamiltonian are obtained exactly if during the solution of the WB equation the energy-dependent Hamiltonian

$$\hat{h}_{\mathrm{WB}}(i) = \frac{1}{2}(\hat{\vec{\sigma}}_i \cdot \hat{\vec{p}}_i)\left(1 + \frac{E_i - \hat{V}(i)}{2c^2}\right)^{-1}(\hat{\vec{\sigma}}_i \cdot \hat{\vec{p}}_i) + \sum_{\lambda} V_{\lambda}(r_{i\lambda}) \quad (40)$$

is iterated. The energy-dependence of the WB Hamiltonian leads to (slightly) nonorthogonal orbitals, e.g., for the Pb ground state the maximum nonorthogonality is observed for the 1s and 2s core orbitals, that is, $\langle 1s|2s\rangle = 0.0405$, and significantly smaller values for the 6s and 6p valence orbitals, that is, $\langle ns|6s\rangle \leq 0.0013$ and $\langle np|6p\rangle \leq 0.0009$ for $n = 1-5$, respectively.[144] Wood and Boring used this Hamiltonian in molecular DFT/X_α AE calculations. The application of the Dirac relation eq 33 allows the partitioning of spin-independent and spin-dependent parts, and therefore the derivation of a scalar-relativistic WB Hamiltonian, which is formally obtained by replacing $\hat{\vec{\sigma}}_i \cdot \hat{\vec{p}}_i$ by $\hat{\vec{p}}_i$ in eq 40.

In the development of ECPs the WB Hamiltonian is mainly used in atomic finite difference calculations as an alternative to the more involved DHF/DC approach, which was in early implementations often plagued by convergence problems, to generate reference data for energy-consistent PPs,[145−155] see section 6.1. In its spectral representation it is used as SO operator within the MP approach,[156,157] see section 7.1.

Applying the central field approximation one obtains from eq 40 for an one-electron atom the following equation for the radial function $P_{n\kappa}(r)$, corresponding to the upper component of the solution of the Dirac equation:

$$(\hat{h}_{\mathrm{S}} + \hat{h}_{\mathrm{MV}} + \hat{h}_{\mathrm{D}} + \hat{h}_{\mathrm{SO}})P_{n\kappa}(r) = \varepsilon_{n\kappa}P_{n\kappa}(r) \quad (41)$$

The relativistic quantum number κ in eq 41 is defined in terms of the quantum numbers of orbital and total angular momentum, l and j, as

$$\kappa = \mp (j + 1/2) \text{ for } j = l \pm 1/2 \quad (42)$$

The radial function $P_{n\kappa}(r)$ is related to the orbital $|\varphi_{n\kappa m}\rangle$ by

$$\langle \vec{r}\,|\varphi_{n\kappa m}\rangle = \frac{1}{r}P_{n\kappa}(r)\chi_{\kappa m}(\vec{r}/r) \quad (43)$$

with $\chi_{\kappa m}$ denoting the spinor spherical harmonics. In the WB AE approach the nonrelativistic Schrödinger Hamiltonian

$$h_{\mathrm{S}}(i) = -\frac{1}{2}\frac{d^2}{dr^2} + \frac{l(l+1)}{2r^2} + \hat{V} \quad (44)$$

is supplemented by three energy-dependent relativistic terms, that is, a mass-velocity (MV), a Darwin (D), and a spin−orbit (SO) term

$$\hat{h}_{\mathrm{MV}} = -\frac{\alpha^2}{2}[\varepsilon_{n\kappa} - \hat{V}]^2, \quad \hat{h}_{\mathrm{D}} = -\frac{\alpha^2}{4}\frac{d\hat{V}}{dr}B_{n\kappa}\left(\frac{d}{dr} - \frac{1}{r}\right)$$
$$\hat{h}_{\mathrm{SO}} = -\frac{\alpha^2}{4}\frac{d\hat{V}}{dr}B_{n\kappa}\frac{\kappa+1}{r}, \quad B_{n\kappa} = \left(1 + \frac{\alpha^2}{2}[\varepsilon_{n\kappa} - \hat{V}(r)]\right)^{-1} \quad (45)$$

For one-electron systems one has $\hat{V} = -Z/r$ in eqs 41, 44, and 45, which can be solved iteratively and yield the same one-particle energies as the corresponding Dirac-equation. In the many-electron case the correct nonlocal Hartree−Fock potential $\hat{V}$ is used in eq 44, however a local approximation $\hat{V} \approx \hat{V}(r)$ to it is inserted in eq 45.[85,144] Similar to the energy $\varepsilon_{n\kappa}$ also the local potential approximation $\hat{V}$ has to be iterated, as it is the case for $\hat{V}$.

Averaging over spin yields $\kappa = -1$, that is, the SO term $\hat{h}_{\mathrm{SO}}$ vanishes for the scalar-relativistic WB approach. The CG approach in addition neglects the Darwin term $\hat{h}_{\mathrm{D}}$ for angular quantum numbers $l > 0$, and the corresponding one-electron energies become identical with eigenvalues of the Klein−Gordon equation for spin-0 particles. The numerical results for energy differences, i.e., excitation energies, ionization potentials and electron affinities, of the scalar-relativistic WB and CG approaches seem to agree for not too highly charged ions typically within 0.01− 0.05 eV, for example, for the d transition elements the largest difference of 0.05 eV occurs for the ionization from the 5d shell of Hg.[158,147] A comparative study of several quasirelativistic methods used in atomic structure calculations was given by Karwowski and Kobus.[128]

4. RELATIVISTIC AND ELECTRON CORRELATION EFFECTS

In the ECP approach all relativistic contributions originating from the atomic cores are usually folded into the parameter set and the valence electrons are treated formally nonrelativistically, see section 5. Correlation effects are usually treated explicitly in the valence shell, whereas core−valence contributions may be modeled by a CPP, see section 5.5. In the following both relativistic and electron correlation effects will be briefly discussed. There is a number of excellent review articles focusing on relativistic effects, which the reader is referred to for further details.[1,2,32,76,77,159]

4.1. Definition and Evaluation

Relativistic effects/contributions may be defined as the difference of the results of a relativistic and a nonrelativistic calculation, that is, calculations with the speed of light in atomic units $c \approx 137.0359895$ and $c \rightarrow \infty$, respectively. Ideally for both the relativistic (r) and the nonrelativistic (nr) case the exact form of the operators $\hat{X}_{\mathrm{r}}$ and $\hat{X}_{\mathrm{nr}}$, as well as the exact wave functions $|\Psi_{\mathrm{r}}\rangle$ and $|\Psi_{\mathrm{nr}}\rangle$ are available for the evaluation of the relativistic contribution ΔX_{r}

$$\Delta X_{\mathrm{rel}} = \langle\Psi_{\mathrm{r}}|\hat{X}_{\mathrm{r}}|\Psi_{\mathrm{r}}\rangle - \langle\Psi_{\mathrm{nr}}|\hat{X}_{\mathrm{nr}}|\Psi_{\mathrm{nr}}\rangle \quad (46)$$

However, such a pleasant situation is very rare. For chemistry the hydrogen atom and hydrogen-like ions with nuclear charge Z are probably the most important cases where eq 46 can be rigorously used. Both the Dirac and the Schrödinger equation can be solved analytically, that is, the energy expectation values/eigenvalues after subtracting the rest energy c^2 of the electron are

$$E_{n\kappa} = \pm c^2\left[1 + \left(\frac{Z/c}{n - |\kappa| + \sqrt{\kappa^2 - (Z/c)^2}}\right)^2\right]^{-1/2} - c^2 \quad (47)$$

and

$$E_n = -\frac{Z^2}{2n^2} \quad (48)$$

dx.doi.org/10.1021/cr2001383 |Chem. Rev. 2012, 112, 403–480

The relativistic quantum number κ is defined in eq 42. In contrast to the nonrelativistic result eq 48 two sets of solutions exist in the relativistic case eq 47. These are separated by $\sim 2c^2$, that is, the rest energy of an electron-positron pair. The Dirac equation is not merely a wave equation valid for an electron, but rather for spin $-1/2$ particles as both electrons and positrons. The solutions in eq 47 near the zero of energy are called electronic states and have to be compared to the nonrelativistic solutions in eq 48 to evaluate the relativistic contribution to the total energy of a one-electron system. The negative energy solutions near $-2c^2$ do not correspond to electronic states and are sometimes called positronic states. A Taylor expansion of eq 47 yields (after neglecting (Z/c) under the square root) as the leading term the nonrelativistic energy increasing as Z^2, and a first correction term increasing as Z^4. Since the prefactor of this lowest-order relativistic energy contribution is $1/c^2$, one may expect that the correction becomes chemically relevant only for heavy nuclei.

For a many-electron system the exact relativistic Hamiltonian is not known (see section 3) and neither the nonrelativistic nor the relativistic Schrödinger equation is analytically solvable. Thus, the relativistic contribution depends on the approximate relativistic many-electron Hamiltonian $\tilde{\hat{H}}_r$ as well as on the approximate nonrelativistic and relativistic many-electron wave functions $|\tilde{\Psi}_{nr}\rangle$ and $|\tilde{\Psi}_r\rangle$, that is, the one- and many-electron basis sets (bs) and the computational method (cm) applied to determine the expansion coefficients. In case one is interested in a quantity other than the energy, the operator $\hat{X}_r$ might also be available only in some approximate form $\tilde{\hat{X}}_r$. Thus, in practice one can only evaluate an approximate relativistic contribution $\Delta\tilde{X}_r$

$$\Delta\tilde{X}_r = \langle\tilde{\Psi}_r^{cm,bs}|\tilde{\hat{X}}_r|\tilde{\Psi}_r^{cm,bs}\rangle - \langle\tilde{\Psi}_{nr}^{cm,bs}|\hat{X}_{nr}|\tilde{\Psi}_{nr}^{cm,bs}\rangle \quad (49)$$

Typical examples are the various relativistic bond length contractions obtained for AgH, see Figure 6 in the the review article of Pyykkö,[2] and for AuH, see Figure 1 in a publication of Schwerdtfeger et al.[160]

Correlation effects/contributions can be defined as the difference between the result for the exact correlated (c) solution $|\Psi_c\rangle$ of the many-electron problem and the best possible uncorrelated (uc) one $|\Psi_{uc}\rangle$, which is obtained at the independent-particle level at the basis set limit (∞). Denoting the exact HF limit solution by $|\Psi_{uc}^{HF,\infty}\rangle$, one can write

$$\Delta X_c = \langle\Psi_c|\hat{X}|\Psi_c\rangle - \langle\Psi_{uc}^{HF,\infty}|\hat{X}|\Psi_{uc}^{HF,\infty}\rangle \quad (50)$$

For $\Delta X_c = \Delta E_c$ and $\hat{X} = \hat{H}$ this corresponds in the nonrelativistic case to the definition of the correlation energy given by Löwdin.[63] Again, since an exact wave function $|\Psi_c\rangle$ is usually not available, an approximate correlated solution $|\tilde{\Psi}_c\rangle$ has to be used. Although a FCI is sometimes said to provide an 'exact' solution, it is only feasible in a finite one-particle basis set. Moreover, although the exact HF limit solution $|\Psi_{uc}^{HF,\infty}\rangle$ can be achieved for atoms and possibly for linear molecules by finite difference methods, one has to settle down, at least in the general polyatomic case, with an approximate HF solution $|\tilde{\Psi}_{uc}^{HF,bs}\rangle$ obtained for a finite one-particle basis set. Finally, the evaluation depends on the way relativistic contributions are included in the calculation, for example, correlation contributions evaluated at the nonrelativistic and at an approximate relativistic level are of similar magnitude, but usually do not agree. Whereas one can assume that in the nonrelativistic case the exact form of the operator $\hat{X}_{nr}$ is known, one might have to use an approximate form $\tilde{\hat{X}}_r$ in the relativistic case. Therefore only an approximate correlation contribution is accessible, that is,

$$\Delta\tilde{X}_c = \langle\tilde{\Psi}_c^{cm,bs}|\hat{X}|\tilde{\Psi}_c^{cm,bs}\rangle - \langle\tilde{\Psi}_{uc}^{HF,bs}|\hat{X}|\tilde{\Psi}_{uc}^{HF,bs}\rangle \quad (51)$$

In summary, both relativistic and correlation contributions depend on the way they are calculated and they are coupled. One may hope that at least for light elements, where relativistic contributions are weak, the coupling is also weak, whereas for heavier ones the relativistic changes of the wave function and the electron density will certainly lead to changed correlation contributions. Instead of an exact expression

$$\langle\Psi_{r,c}|\hat{X}_r|\Psi_{r,c}\rangle = \langle\Psi^{HF,\infty}|\hat{X}_{nr}|\Psi^{HF,\infty}\rangle + \Delta X_r + \Delta X_c + \Delta\Delta X_{r,c} \quad (52)$$

one has to rely on a corresponding approximate one

$$\left\langle\tilde{\Psi}_{c,r}^{cm,bs}|\tilde{\hat{X}}_r|\tilde{\Psi}_{c,r}^{cm,bs}\right\rangle = \left\langle\tilde{\Psi}_{nr,uc}^{HF,bs}|\hat{X}_{nr}|\tilde{\Psi}_{nr,uc}^{HF,bs}\right\rangle + \Delta\tilde{X}_r + \Delta\tilde{X}_c + \Delta\Delta\tilde{X}_{r,c} \quad (53)$$

Therefore, it is always necessary to state exactly the level of theory at which relativistic effects were evaluated. It has been pointed out by Schwarz that, e.g., for different approaches the evaluation of the first expectation value in eq 53 may still lead to similar numerical results, which however due to the different relativistic methods applied may lead to differing interpretations.[159,161] Thus, besides many wrong interpretations there may exist more than one which is correct.

Often it is convenient to discuss relativistic effects at the independent-particle level, for example, by comparing DHF/DC or DHF/DCB results to nonrelativistic HF results. This allows to break down the whole effect into contributions of individual orbitals or shells, which is handy for the interpretation as well as often for a qualitative prediction of relativistic effects. In the following we will only consider a few aspects, which are relevant to motivate the inclusion of relativistic contributions in the ECP parametrization. We try to single out which relativistic contributions need to be taken into account in order to be able to achieve a certain accuracy, e.g., an accuracy of at least 0.1 eV in energy differences such as excitation energies, ionization potentials, electron affinities and binding energies and 0.01 Å in bond distances.

4.2. Examples for Atoms

One distinguishes direct and indirect relativistic effects. The direct effects arise from substituting the nonrelativistic Hamiltonian by a relativistic one and have been shown to originate mainly in the spatial core region,[159,162] that is, close to the nucleus. Direct scalar-relativistic effects act on all orbitals, especially those which have a significant amplitude in the core region, and always lead to a contraction and stabilization. Moreover, direct spin−orbit (SO) effects lead for shells with angular momentum symmetry $l > 0$ to a SO splitting yielding two subshells with total angular momentum quantum numbers $j = l - 1/2$ and $j = l + 1/2$, see, for example, the orbital plots for Hg^{79+} published by Burke and Grant.[2,163] Compared to the scalar-relativistic solutions with angular momentum symmetry l the spinors with $j = l - 1/2$ experience a stabilization and contraction, whereas those with $j = l + 1/2$ undergo a destabilization and expansion.

dx.doi.org/10.1021/cr2001383 |Chem. Rev. 2012, 112, 403–480

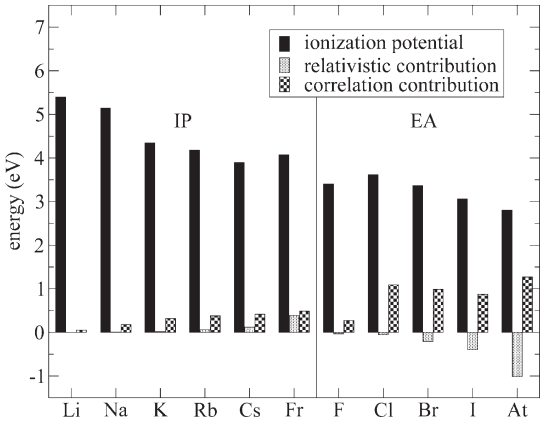

Figure 4. Experimental ionization potentials of the alkaline atoms and experimental electron affinities of the halogen atoms in comparison to the corresponding differential relativistic and electron correlation effects. Nonrelativistic HF and relativistic DHF results were evaluated with GRASP.[83]

Indirect relativistic effects occur only in many-electron atoms and are a consequence of the direct effects. They are caused by relativistic changes of the inner compact orbitals, which lead to modified effective potentials for the outer more diffuse ones. Again, in a many-electron atom all orbitals experience indirect effects, however their magnitude and sign depends strongly on their spatial extension compared to the other occupied shells.

As a rule one usually finds for the valence orbitals of a many-electron atom that the s and p shells are stabilized and contracted, mainly by dominating direct relativistic effects, whereas the d and f shells are destabilized and expanded, mainly by dominating indirect relativistic effects. The expansion and destabilization can be explained by the reduced effective nuclear charge acting on the outer orbitals, which results from the strong contraction of the inner shells and the more efficient shielding of the nuclear charge related to it. However, indirect relativistic stabilization also is observed, for example, for heavy post-d elements such as Au or Hg. The outermost d shell is strongly destabilized and somewhat expanded by dominating indirect relativistic effects. Therefore the valence s shell experiences an increased effective nuclear charge and thus an additional stabilization and contraction. A detailed analysis of relativistic effects in the neutral atoms of d- and f-block elements was provided by Autschbach et al.[164]

Desclaux published in 1973 results of nonrelativistic HF and relativistic DHF/DC calculations for the atoms with nuclear charges from 1 to 120.[165] From the ratios of relativistic and nonrelativistic orbital energies and $\langle r \rangle$ expectation values one can get a quick overview over the importance of relativistic effects for all elements of the periodic table. An illustrative use of the data tabulated by Desclaux is the graphical localization of the well-known *gold maximum* of relativistic effects by plotting the ratio of relativistic and nonrelativistic $\langle r \rangle$ expectation values for the 6s orbitals of Cs (Z = 55) to Fm (Z = 100).[2,77] An overview over atomic relativistic calculations for larger series of elements has been given by Pyykkö.[1] Nowadays tabulations of atomic results somewhat lost their importance, since the corresponding atomic structure codes are readily available[80,81,83,166] and one can quickly obtain the data for essentially any configuration/state of the atom/ion one is interested in. This is not the case for correlated calculations, which require a significantly higher computational effort than the HF/DHF studies. Often relativistic effects are counteracted by correlation effects, which usually favor a higher number of paired electrons and also a higher occupation of f and d shells.

The discussion of relativistic atomic orbital contractions and expansions is actually more involved than a comparison of $\langle r \rangle$ expectation values obtained with a nonrelativistic and a relativistic wave function may imply. The nonrelativistic Schrödinger one-electron Hamiltonian cannot be obtained from the relativistic Dirac Hamiltonian directly by merely applying the limit $c \rightarrow \infty$, but rather a transformation from the Dirac picture to the Schrödinger picture has to precede, for example, the Foldy–Wouthuysen transformation.[130,131] This is connected to the finding that the operator $\hat{\vec{r}}$ represents a physical quantity $\hat{\vec{r}}_{\mathrm{charge}}$ and $\hat{\vec{r}}_{\mathrm{mass}}$ in the Dirac and Schrödinger picture, respectively.[167] The comparison of $\langle r \rangle$ expectation values from DHF and HF calculations thus not only reveals relativistic changes of the wave functions but also so-called picture change effects. The picture change contributions can become very large for the innermost shells (up to 50% for 1s) and become insignificant for valence shells (e.g., < 0.1% for 6s).[167] Since the discussion of ECPs one mainly deals with valence shells, the picture change contributions will not be explicitly considered in this article.

A simple example for the importance of relativistic and correlation contributions are the ionization potentials of the alkaline ions plotted in Figure 4. The nonrelativistic HF values are clearly dominating. The differential relativistic and correlation contributions were evaluated as differences between AE DHF and HF results and experimental data and AE DHF results, respectively. The relativistic and correlation contributions increase slowly with nuclear charge, both leading to higher ionization potentials. The relativistic contributions to the total energy increase as $\sim Z^{4.34}$, the one to the ionization potentials of Na to Fr with $\sim Z^{2.00}$ (the value for Li is below 0.001 eV and was excluded). The correlation contributions to the alkaline atom ionization potentials are somewhat larger than the relativistic contributions and arise mainly from core–valence correlation. For the electron affinities of the halogen atoms also displayed in Figure 4 the correlation contributions increase the electron affinity and are above 1 eV, except for F. The relativistic contributions decrease the electron affinity, mainly due to the large contributions of the SO interaction, which lowers the energy of the neutral atom. If an accuracy of ~0.1 eV is desired for main group elements, relativistic contributions have to be included already for the post-3d main group elements.

The simple rules concerning dominating direct and indirect relativistic effects acting on different orbitals are very well illustrated by the work of Martin and Hay, who evaluated differential relativistic and correlation effects, that is, contributions to energy differences, in excitation and ionization energies of the third- to fifth-row transition metals.[158] Differential relativistic effects were evaluated as differences between scalar-relativistic CG and nonrelativistic HF results, whereas differential correlation effects were obtained as differences between experimental data and scalar-relativistic CG HF results. The lowest LS states of s^2d^n, s^1d^{n+1}, d^{n+2}, s^1d^n, and d^{n+1} were considered. Results for $s^2d^n - s^1d^{n+1}$ energy differences in atoms at the beginning and end of each row are displayed in Figure 5. In accordance with their increase with Z the largest contributions for each row are always found at the end of the row, with the *gold maximum* at the end of the 5d series.[2,77] For example, the Cu, Ag and Au $s^2d^9 \rightarrow s^1d^{10}$ excitation energies are relativistically increased by 0.43, 1.05, and 3.27 eV, respectively. For Ni, Pd and Pt $s^2d^n \rightarrow d^{n+2}$ the

dx.doi.org/10.1021/cr2001383 |*Chem. Rev.* 2012, 112, 403–480

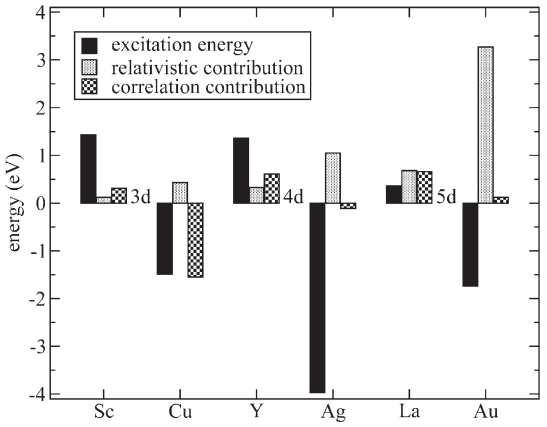

Figure 5. Experimental $s^2d^n \rightarrow s^1d^{n+1}$ excitation/deexcitation energies for the lowest LS states of selected 3d (Sc, Cu), 4d (Y, Ag), and 5d (La, Au) transition metals in comparison to the corresponding differential relativistic and electron correlation effects. Data taken from Martin and Hay.[158]

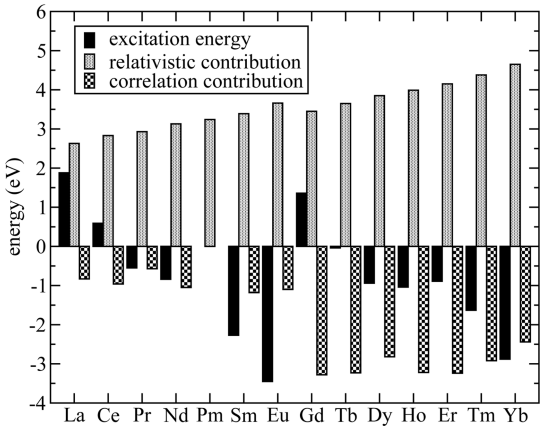

Figure 6. Experimental $f^nd^1s^2 \rightarrow f^{n+1}s^2$ excitation/deexcitation energies for the lowest LSJ states of selected the lanthanide atoms in comparison to the corresponding differential relativistic and electron correlation effects. Data taken from Dolg and Stoll.[20]

relativistic contributions are even larger, e.g., 0.57, 1.57, and 5.15 eV, respectively. The correlation contributions are often of opposite sign, that is, −1.55, −0.10, and 0.12 eV for Cu, Ag and Au $s^2d^9 \rightarrow s^1d^{10}$ and −4.33, −1.19, and −0.66 eV for Ni, Pd and Pt $s^2d^n \rightarrow d^{n+2}$. Since for the lightest transition element Sc the differential relativistic contribution is already 0.12 eV, one has to include relativistic effects for all transition metals, if an accuracy of ∼0.1 eV is desired.

Similar differential relativistic contributions are available for the lanthanides[20,145] and actinides[149] by the comparison of scalar-relativistic WB and nonrelativistic HF results. In case of the lanthanides also correlation contributions were estimated. The results for $f^nd^1s^2 - f^{n+1}s^2$ energy differences are displayed in Figure 6. It is noteworthy that at a nonrelativistic level both lanthanides and actinides might preferably be divalent. This can be seen from Figure 6 by subtracting from the experimental excitation energy the relativistic contribution, which leads to strongly negative results, that is, a favored $f^{n+1}s^2$ configuration. Thus only the very strong indirect relativistic destabilization of the f shell favors higher valencies. In case of Ce and Th the

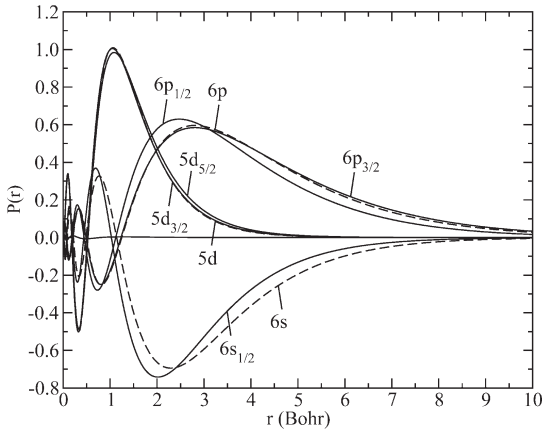

Figure 7. Relativistic valence spinors (solid lines) and nonrelativistic valence orbitals (dashed lines) of Pb in the $6s^2\ 6p^2$ ground state configuration from state averaged MCDHF and MCHF calculations using the program GRASP.[83] Note that $5d_{3/2}$ and 5d, as well as $6p_{3/2}$ and 6p nearly coincide.

experimentally observed ground state configurations $4f^15d^16s^2$ and $6d^27s^2$ are relativistically stabilized against the nonrelativistic ground state configurations $4f^26s^2$ and $5f^27s^2$ by about 2.73 and 9.47 eV, respectively.[168] (Note that in Figure 4 of the original publication the Ce configurations $4f^26s^2$ and $5d^26s^2$ were erroneously interchanged for the relativistic case and thus the relativistic contribution of 4.13 eV mentioned in the text is wrong.) It is obvious that for lanthanides, as well as for the heavier actinides, relativistic contributions have to be included, often even for qualitative considerations.

To investigate which relativistic contributions for heavy main group atoms should be included in the adjustment of ab initio ECPs we consider some examples of atomic and molecular DHF calculations for the group 14 elements. Figure 7 shows the relativistic and nonrelativistic valence orbitals of Pb in its ground state configuration. The relativistic contraction of the 6s shell as well as the SO splitting of the 6p shell are clearly visible. The nonrelativistic 6p orbital has a similar radial shape as the relativistic $6p_{3/2}$ spinor. Since the $6p_{1/2}$ spinor is more compact in the valence region, an overall relativistic contraction of the 6p shell results. It also has to be noted that the relativistic $^3P_0$ ground state has a contribution of over 90% from $6p^2_{1/2}$ for Pb, whereas it is only 67% for C, where LS coupling is a good description, cf. Figure 8. When neglecting the remaining very small fine structure splitting in C, the situation encountered there essentially corresponds to the nonrelativistic limit for all heavier homologues. Figure 8 also reveals that for group 14 elements heavier than Si LS coupling begins to break down and an intermediate coupling scheme has to be applied. The pure jj coupling is approximately reached at Pb and provides an excellent description for Eka-Pb.

Table 1 lists atomic $s^2p^2\ J = 0+ \rightarrow s^1\ p^3\ J = 2-$ excitation energies of the group 14 elements.[83] It can be seen that the one-particle relativistic effects are substantially larger than the two-particle ones. If one assumes a target accuracy of 0.1 eV, one-particle relativistic contributions need only to be accounted for Ge and the heavier homologues, whereas for an refined accuracy of about 0.01 eV all group 14 elements need to be treated including one-particle (Dirac) relativistic contributions, whereas for Sn, Pb, and Eka-Pb two-particle (Breit) relativistic contributions and even contributions of quantum electrodynamics

dx.doi.org/10.1021/cr2001383 |Chem. Rev. 2012, 112, 403–480

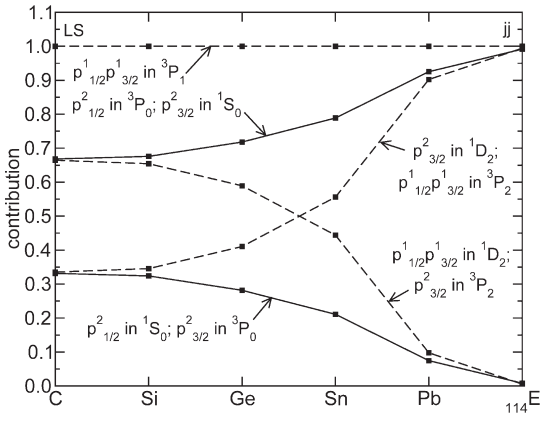

Figure 8. Contributions of relativistic *jj*-coupled configurations to the $s^2 p^2$ LSJ states $^3P_{0,1,2}$, $^1D_2$, and $^1S_0$ of the group 14 elements C to Eka-Pb. The ground state is a $^3P_0$ state and has contributions from $p^2_{1/2}$ and $p^2_{3/2}$ (solid lines). Calculated using the program GRASP.[83]

Table 1. Finite Nucleus Contributions $\Delta\Delta E_{fn}$, Contributions of the Dirac (One-Particle) Relativity $\Delta\Delta E_D$ and the Breit (Two-Particle) Relativity in the Low-Frequency Limit for the Exchanged Photon $\Delta\Delta E_{B,lfl}$ and the Corresponding Frequency-Dependent Interaction $\Delta\Delta E_B$, as well as Quantum Electrodynamical Contributions $\Delta\Delta E_{QED}$ (Vacuum Polarization, Self-Energy) for the s^2p^2 $J = 0+ \rightarrow s^1 p^3$ $J = 2-$ Excitation Energies ΔE (all in eV) of Group 14 Elements (Nuclear Charge Z, Nuclear Mass M) from Average-Level Multi-Configuration Dirac−Hartree−Fock Calculations Using the Code GRASP[83] with Extensions for QED Corrections by Thierfelder and Schwerdtfeger[108]

X	Z	M	ΔE	ΔΔE$_{fn}$	ΔΔE$_D$	ΔΔE$_{B,lfl}$	ΔΔE$_B$	ΔΔE$_{QED}$
C	6	12.01	2.625	0.000	0.019	−0.002	−0.002	−0.001
Si	14	28.09	2.706	0.000	0.073	−0.002	−0.002	−0.002
Ge	32	72.64	3.727	0.000	0.457	−0.004	−0.004	−0.008
Sn	50	118.71	3.407	−0.001	1.077	−0.008	−0.008	−0.013
Pb	82	207.2	5.958	−0.016	3.780	−0.023	−0.027	−0.034
Eka-Pb	114	289	11.651	−0.417	10.481	−0.060	−0.070	−0.070

(QED) such as vacuum polarization and self-energy need to be considered. It was pointed out by Thierfelder and Schwerdtfeger that for ionization potentials from the valence s shell of heavy elements the QED contributions become as important as those of the Breit interaction.[108] The results of Table 1 indicate that this somewhat surprising finding also holds for the lowest excitations out of the valence s shell. It is also interesting to see that for heavy elements such as Pb contributions due to the finite nucleus become non-negligible and yield very large corrections for superheavy elements such as Eka-Pb.

4.3. Examples for Molecules

In molecules, relativistic bond length contractions and, somewhat more rarely, expansion are observed, as well as bond stabilizations and destabilizations. The bond contractions and expansions may occur parallel to orbital contractions and expansions but cannot necessarily be explained to be caused by them. For an extensive list of examples and references we refer to the review by Pyykkö,[2] and for a detailed analysis of possible interpretations to articles by Schwarz.[32,159,161] If a heavy (relativistic) atom A and a more electronegative light (nonrelativistic) atom B form a polar molecule $A^{\delta+}B^{\delta-}$ and the highest valence orbital of A is relativistically stabilized, the electron transfer from A to B requires more energy and thus the binding energy decreases. An example is AuF, where a 25% destabilization of the bond was calculated.[169] If on the other hand B is less electronegative, a polar molecule $A^{\delta-}B^{\delta+}$ is formed, the electron transfer from B to A yields more energy and the binding energy increases. An example is AuLi, where a 30% stabilization of the binding energy is observed.[169] If SO effects in the orbitals involved in covalent bonding are relevant, things get somewhat more involved. In a diatomic molecule the $p_{1/2,1/2}$ spinor forms 1/3 pσ and 2/3 pπ components, whereas the $p_{3/2,1/2}$ spinor forms 2/3 pσ and 1/3 pπ components.[76,170,171] Bonds as, e.g., in TlH or Tl_2 are therefore destabilized by SO effects. The $p_{3/2,3/2}$ spinor forms only a π component and thus the bonds of BiH and Bi_2 are not destabilized by SO effects.

Table 2. X−H Bond Distances R_e (Å) and Binding Energies E_b (eV) from Molecular Dirac−Hartree−Fock Calculations Using the Dirac−Coulomb−Gaunt Hamiltonian[a]

XH$_4$	R$_e$	ΔR$_D$	ΔR$_G$	E$_b$	ΔE$_D$	ΔE$_G$
CH$_4$	1.08323	−0.00013	0.00009	13.7068	−0.0142	−0.0027
SiH$_4$	1.48677	−0.00089	0.00017	9.6455	−0.0542	−0.0027
GeH$_4$	1.55793	−0.00637	0.00051	8.3850	−0.3709	−0.0024
SnH$_4$	1.73369	−0.02143	0.00089	6.8421	−0.8066	−0.0035
PbH$_4$	1.73703	−0.07236	0.00167	5.1561	−2.3661	−0.0220

[a] ΔR_D, ΔE_D and ΔR_G, ΔE_G denote the relativistic Dirac (one-particle) and Gaunt (two-particle) contributions. Data taken from Visser et al.[106]

Further support for the modeling of only the DC Hamiltonian can be obtained from, for example, molecular DHF/DC(+G) calculations for the group 14 tetrahydrides by Visser et al.[106] The results for bond lengths and binding energies are listed in Table 2. Here it is essentially only the one-particle (Dirac) relativity which significantly influences the results. It was pointed out by Dyall in a related study of the group 14 di- and tetrahydrides, that first-order perturbation theory including only mass-velocity and Darwin terms is sufficiently accurate only up to Ge ($Z = 32$).[100,172] In case of the tetrahydrides the relativistic bond length contractions obtained in first-order perturbation theory based on a nonrelativistic HF solution and by using the Dirac−Coulomb Hamiltonian at the DHF level agreed within 0.002 Å, whereas the relativistic corrections to the harmonic (a_1 breathing) frequencies evaluated by first-order perturbation theory are overestimated by about 2, 4, and 22 cm^{-1} for GeH_4, SnH_4, and PbH_4, respectively, corresponding to relative errors of up to 80% for PbH_4. The $XH_4 \rightarrow XH_2 + X_2$ HF reaction energies derived from first-order perturbation theory are too large by 0.2, 3.4, and 13.3 kcal/mol for X = Ge, Sn, and Pb, respectively. In view of errors due to finite basis sets or incomplete correlation treatments it appears to be safe to neglect the two-particle (Breit, modeled here by Gaunt) contributions. However, since the inclusion of terms beyond the DC relativity today is straightforward and routine in atomic finite difference calculations needed to generate AE reference data for ECP adjustments,[83] these terms are included in modern ECPs and even may become important for accurate calculations of atomic and molecular excitation energies.[102,173−175]

As it is the case for all first-principles calculations electron correlation effects are important in ECP calculations when

dx.doi.org/10.1021/cr2001383 |Chem. Rev. 2012, 112, 403–480

electron pairs are formed, for example, when bonds are formed or broken. If accurate valence correlation energies can be obtained with PPs and MPs is discussed in section 9.3. Of special interest in ECP schemes using large cores are static and dynamic core-polarization effects, that is, polarization of the spherical core occurring at the HF level, as well as by core−valence correlation effects. Meyer and Rosmus demonstrated in ab initio pair-natural orbital coupled electron-pair (PNO-CEPA) AE calculations on the hydrides LiH−BH and NaH−AlH that core−valence correlation may affect bond lengths, vibrational frequencies, dipole moments, etc., as strongly as valence correlation.[176,177] The computational effort to account for these effects explicitly however was found to be high, so that it was proposed to include them only implicitly by means of an effective core polarization potential (CPP).[178,179] At the two-valence-electron correlated AE level it was found that, for example, core−valence correlation shortens the bond distance of K_2 by 5.1%, and increases the binding energy, vibrational frequency and ionization potential by 2.1, 9.5, and 8.8%, respectively.[179] The CPP approach can be adapted to ECP schemes,[180] which will be further discussed in section 5.5.

5. VALENCE-ONLY MODEL HAMILTONIAN FOR ATOMS AND MOLECULES

In ECP methods, we seek an effective valence-only (VO) Hamiltonian for n_v valence electrons treated explicitly in the calculations and N cores, that is,

$$\hat{H}_v = \sum_i^{n_v} \hat{h}_v(i) + \sum_{i<j}^{n_v} \hat{g}_v(i,j) + \hat{V}_{cpp} + V_{cc} \tag{54}$$

The subscripts c and v refer to core and valence, respectively. $\hat{h}_v$ and $\hat{g}_v$ denote effective one- and two-electron operators. $\hat{V}_{cpp}$ is a core-polarization potential (CPP), further described in section 5.5, and V_{cc} represents the repulsion between all cores and nuclei of the system. For a neutral system, n_v is obtained from the total number of electrons n by subtracting the number of core electrons n_c, that is, the difference between the nuclear charge Z_λ and the core charge Q_λ for every core λ

$$n_v = n - n_c = n - \sum_\lambda^N (Z_\lambda - Q_\lambda) \tag{55}$$

Nonrelativistic, scalar-relativistic as well as quasi-relativistic ECPs use a valence-only model Hamiltonian which is formally of nonrelativistic form, that is,

$$\hat{h}_v(i) = -\frac{1}{2}\hat{\nabla}_i^2 + \hat{V}_{cv}(i) \quad \text{and} \quad \hat{g}_v(i,j) = \frac{1}{r_{ij}} \tag{56}$$

If we neglect $\hat{V}_{cpp}$ and V_{cc} in eq 54 for a moment, it is usually assumed that all relativistic contributions can be folded into the Hamiltonian by means of parametrization of the ECP $\hat{V}_{cv}$ and that the nonrelativistic kinetic energy operator as well as the nonrelativistic Coulomb interaction between the electrons suffices.

Two main branches of ECPs may be distinguished, that is, model potentials (MPs), which try to model as accurately as possible the AE (HF) potential for the valence electrons and thus produce valence orbitals with a correct nodal structure, and pseudopotentials (PPs), which after a formal transformation from the valence orbitals to pseudovalence orbitals with a simplified radial nodal structure lead to further savings in the one-electron basis sets. Since nowadays PPs are more popular than MPs we will focus in the current review somewhat more on the former type of ECPs. In both PP and MP approaches it has also been attempted to include relativistic terms explicitly, that is, the Dirac one-particle Hamiltonian eq 10 in the context of PPs[181,182] (section 6.6) or the DKH Hamiltonian eq 27 in the context of MPs[183−187] (section 7.4).

Besides relativistic contributions the ECP $\hat{V}_{cv}$ has to account for all interactions of the valence electron with the nucleus and the (removed) core electron system, as well as for (the absence of explicit) core−valence orthogonality constraints. The leading term for an atom is the Coulomb electron−core attraction, that is,

$$\hat{V}_{cv}(i) = -\frac{Q}{r_i} + \Delta\hat{V}_{cv}(i) \tag{57}$$

In case of a molecule it is usually assumed that the ECP $\hat{V}_{cv}$ simply is a superposition of N atomic contributions

$$\hat{V}_{cv}(i) = \sum_\lambda^N \left[-\frac{Q_\lambda}{r_{\lambda i}} + \Delta\hat{V}_{cv}^\lambda(i) \right] \tag{58}$$

This assumption is the basis for the atomic adjustment of the valence-only model Hamiltonian parameters, which is essential for the efficiency of the approach. Considering various core definitions for each element, various AE approaches to generate the reference data and also various methods to adjust the ECPs there are already a significant number of possible parametrizations for each of the ∼120 chemical elements. A molecular adjustment would require parametrizations for (at least) the much larger number of pairs of elements. In addition, in the atomic adjustment finite difference methods, or at least very large one-particle basis sets, can be applied and guarantee a basis set independence of the derived parameter sets, which would be less straightforward to achieve in a molecular adjustment.

V_{cc} may be written as the leading point charge Coulomb repulsion between cores/nuclei and, if required, pairwise additive corrections accounting for deviations from the point charge approximation (section 5.6:

$$V_{cc} = \sum_{\lambda<\mu}^N \left[\frac{Q_\lambda Q_\mu}{r_{\lambda\mu}} + \Delta V_{cc}^{\lambda\mu}(r_{\lambda\mu}) \right] \tag{59}$$

The corrections $\Delta V_{cc}^{\lambda\mu}$ account, for example, for mutually penetrating cores, where besides modified electrostatic contributions also orthogonality constraints and the Pauli-repulsion between the electron shells localized on different cores has to be taken into account. These corrections are usually only required for those special cases where large ECP cores are used. Since large-core ECPs are often not too well transferable between different systems and thus have only a limited range of usage, the corrections have to be derived only for the few cases under consideration. We note that $\hat{V}_{cpp}$ has both atomic as well as molecular contributions, however, the latter evolve automatically as products of atomic terms and thus do not need to be adjusted separately for the molecular case (section 5.5).

Unless otherwise noted we will consider in the remainder of this article a VO model Hamiltonian of the following form:

$$\hat{H}_v = -\frac{1}{2}\sum_i^{n_v}\hat{\nabla}_i^2 + \sum_{i<j}^{n_v}\frac{1}{r_{ij}} + \sum_i^{n_v}\sum_\lambda^N \left[-\frac{Q_\lambda}{r_{\lambda i}} + \Delta\hat{V}_{cv}^\lambda(i) \right] + \hat{V}_{cpp} + V_{cc} \tag{60}$$

dx.doi.org/10.1021/cr2001383 |Chem. Rev. 2012, 112, 403–480

The main task for the ECP development is to find an analytical form for $\Delta\hat{V}_{cv}$, as well as for $\hat{V}_{cpp}$ and V_{cc}, which is sufficiently accurate and at the same time easily applicable in practical calculations.

5.1. Underlying Approximations

A number of severe approximations has to be made in order to arrive at a computationally practical VO scheme using the Hamiltonian eq 60. These are related to the choice of the operators $\hat{h}_v$ and $\hat{g}_v$, as well as the one of $\hat{V}_{cpp}$ and V_{cc}. To compensate for the errors resulting from the underlying approximations the effective VO Hamiltonian usually contains free parameters in $\Delta\hat{V}_{cv}$, $\hat{V}_{cpp}$, and $\hat{V}_{cc}$, which can be adjusted to reproduce as accurately as possible AE or experimental reference data. In a series of papers, Schwarz analyzed carefully the various approximations and consequences underlying the PP approach.[188−192]

First of all one has to separate the core and valence electron systems. The exact quantum mechanical partitioning of many-electron system into independent subsystems is not feasible, but it can be achieved approximately within an independent-particle picture, for example, at the HF level,[16,193,194] where groups of (localized) orbitals can be used to define, for example, the core and valence electron subsystems. Whereas the core−valence separation is exact at the independent-particle level, it is not for the exact wave function. Although the core systems as well as the valence system can still be described separately at a correlated level, core−valence correlation effects have been neglected. Clearly, the assumption of valence-only methods is usually that core correlation effects can safely be omitted for the problems of interest. In case of core−valence correlation either the same assumption is made or it is attempted to describe the effect by constructing suitable effective operators, which may be added to the valence-only Hamiltonian. CPPs (section 5.5), which were initially used in AE calculations to take dynamic core−valence polarization, that is, core−valence correlation, into account[178,179] are now quite popular especially in large-core PP methods.[180,195−197]

Second, one has to assume that the atomic cores are inert and remain unchanged when they are transferred from one system to another. When describing the core electron systems within the independent-particle approximation this corresponds to a freezing of the core orbitals for a special state, for example, in their atomic ground state situation, and using them unchanged for all others, for example, also for molecules. The underlying frozen-core (FC) approximation[193] is an assumption made in all VO schemes. Clearly, the size of the core is an important factor for both the accuracy (small cores preferable) as well as the efficiency (large cores preferable) of the VO approach. Here chemical intuition is usually not sufficient to find the best compromise, and rather results of AE FC calculations provide useful hints as outlined in section 5.2. In addition to dynamic core-polarization, that is, core−valence correlation, CPPs (section 5.5) can also be used to account to a certain extent for static core-polarization, for example, correct for the FC errors in VO schemes.

Third, to really eliminate the core electrons and possibly also core orbitals from the calculation one has to replace their contributions in an AE FC Hamiltonian for the valence electrons by an ECP modeling the real nonlocal HF potential. Often it is assumed that the ECPs are just atomic effective one-electron Hamiltonians entering $\hat{h}_v$, which may be cast into a computationally convenient analytical form with adjustable parameters, also allowing for an implicit treatment of relativistic contributions. Molecular ECPs are usually constructed as a superposition of the atomic ECPs. At the stage of the construction of the atomic ECPs most of the differences in the various ECP (MP and PP) schemes arise. Details will be discussed for PPs in section 5.3 and for MPs in section 5.4.

A brief explanation of the nomenclature used here and in previous reviews[25,27,29,31,198] is in order, since during the almost eight decades since the work of Hellmann[73] various authors used different names for their approaches. We hereby assume that one wants to model HF AE results for the valence electron system, which is the main topic of this review. The MP approach attempts to construct analytical effective potentials modeling directly the original nonlocal HF potential for the valence electrons in orbitals which have the full nodal structure of the AE valence orbitals. It originates from the Huzinaga−Cantu equation[199] and could be referred to as a "model HF potential approach". The PP approach in practice tries to construct analytical effective potentials modeling the nonlocal HF potential for (nodeless) pseudo-valence orbitals, that is, orbitals which after a formal transformation still yield the correct orbital energies, but have a simplified radial nodal structure. The method is (formally) based on the Phillips−Kleinman equation[200] and could be referred to as a "model HF pseudopotential approach". Thus, both approaches belong to effective core potential (ECP) methods. In order to keep the nomenclature simple, we use the terms model potential (MP) and pseudopotential (PP) in context with ECP approaches using valence orbitals with the correct and with a simplified nodal structure, respectively. The nomenclature used here is consistent, for example, with the one used by Seijo and Barandiáran.[24] We note here in passing that the MP approach is more general than just being a variant of the ECP method, since it can also be used to model environments of a group of atoms of interest, for example, the environment of embedded clusters in solid state physics.[16,24,201]

Fourth, ECP methods often assume that the atomic cores of a system do not interact with each other except for their mutual Coulomb repulsion, however, for very large cores this assumption of a simple pairwise Coulomb repulsion might be too crude. Mutually "penetrating" or "overlapping" cores need to be accounted for by additional pairwise additive corrections modeling, for example, the exponentially decaying Pauli repulsion between closed shell cores (section 5.6).

5.2. Size of the Core

One of the most important decisions to be made when constructing an ECP besides the choice of the reference data is the choice of the size of the core. Large cores are attractive since they lead to large computational savings, whereas small cores allow a higher accuracy to be reached. Of course, when relativistic contributions are implicitly taken into account as it is the case for most ECP approaches, too small cores may also lead to errors since the nonrelativistic kinetic energy together with a relativistically parametrized ECP might not correctly describe the relativistic kinematics. Thus a compromise is needed. Hereby one has to have in mind which system should be modeled and what method should be applied to it. For example, whereas for the treatment of middle-sized Hg_n ($n \leq 55$) clusters, the Hg atom may be modeled as a two-electron system,[202] one would rather use a more reliable 20-electron Hg ECP in order to obtain an accurate potential curve for Hg_2 at the CCSD(T) level.[203−205] However, if instead of CCSD(T) one uses the QMC approach,

dx.doi.org/10.1021/cr2001383 |Chem. Rev. 2012, 112, 403–480

Table 3. Relative Dirac−Hartree−Fock (DHF) Energies (eV), Obtained with the Dirac−Coulomb (DC) Hamiltonian, of the 2*J* + 1-Weighted Average of All *J* Levels Belonging to a Nonrelativistic Configuration[83] with Respect to the Value for the C $2s^2$ $2p^2$ and Pb $6s^2$ $6p^2$ Ground State Configurations[a]

		C		Pb			
					FCE		
		DHF/DC	FCE 4 ve	DHF/DC	4 ve	14 ve	22 ve
M^{4+}		144.224	0.027	89.837	1.586	0.070	0.002
s^1		79.841	0.007	49.239	0.580	0.018	0.000
	p^1	87.924	0.002	60.021	0.882	0.042	0.001
s^2		34.039	0.003	19.387	0.110	0.002	0.000
s^1	p^1	40.339	0.000	28.017	0.247	0.009	0.000
	p^2	50.521	0.001	38.674	0.467	0.027	0.000
s^2	p^1	9.995	0.000	6.159	0.017	0.000	0.000
s^1	p^2	18.035	0.001	14.640	0.092	0.006	0.000
	p^3	28.994	0.005	25.116	0.249	0.020	0.000
s^2	p^2	0.000	0.000	0.000	0.000	0.000	0.000
s^1	p^3	8.786	0.002	8.271	0.038	0.005	0.000
	p^4	20.253	0.006	18.516	0.156	0.018	0.000
m.a.e.			0.004		0.369	0.018	0.000

[a] The frozen-core errors (FCE; eV) in the relative energies are given for 4, 14, and 22 valence electron (ve) systems. The frozen core was taken from the neutral atom in the ground state configuration. The mean absolute errors (m.a.e.) are listed in the last line.

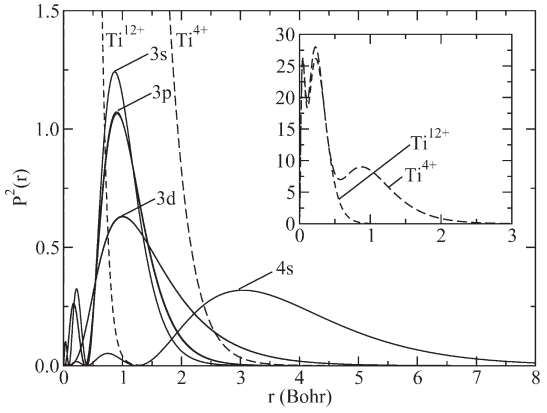

Figure 9. Orbital densities for Ti ([Ar] $3d^2$ $4s^2$) from multiconfiguration Dirac−Hartree−Fock calculations with the Dirac−Coulomb Hamiltonian using the program GRASP.[83] The Ti^{12+} (Ne-core; small-core ECPs) and Ti^{4+} (Ar core; large-core ECPs) densities are also plotted.

the treatment of Hg as a two-electron system using a PP becomes attractive again.[206] Also, when using plane-wave basis sets a large core is computationally desirable, whereas Gaussian basis sets in principle also treat small cores very well.

Results of AE FC HF or DHF calculations provide a good impression of the errors which result for a specific size of the core. Using standard atomic codes[80,81,83,166] these can be routinely carried out at the finite difference level. It has to be noted, however, that additional FC errors arise at the correlated level. Table 3 lists the frozen core errors for C ([He] core) as well as Pb ([Xe] $4f^{14}$ $5d^{10}$, [Xe] $4f^{14}$, and [Kr] $4d^{10}$ $4f^{14}$ cores; see also Figure 2). When treating C and Pb according to the chemical

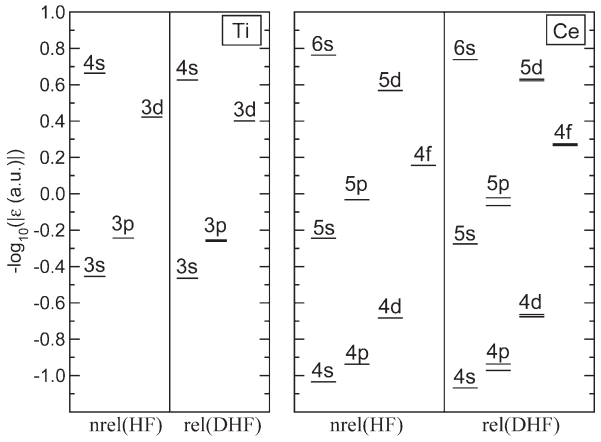

Figure 10. Orbital energies for Ti ([Ar] $3d^2$ $4s^2$) and Ce ([Xe] $4f^1$ $5d^1$ $6s^2$) from multiconfiguration Dirac−Hartree−Fock calculations with the Dirac−Coulomb Hamiltonian using the program GRASP.[83] In some cases the SO splitting is too weak to be resolved. Note the logarithmic *y*-axis.

intuition as four-valence-electron systems the FC errors are below 0.03 eV for C, but may amount to more than 1 eV for Pb. The reason is the larger radial overlap of the Pb 6s and 6p valence orbitals with the Pb^{78+} core shells, especially the diffuse 5d shell. Including 5d to the valence space, that is, treating Pb as a 14-valence-electron system, reduces the FC errors to 0.07 eV or less. Negligible FC errors far below 0.01 eV are found when the 5s and 5p shells are also included in the valence space and Pb is treated as a 22-valence-electron system. Thus, the treatment of all elements of a column of the periodic table on equal footing by ECP methods will not always lead to the same accuracy. More than one choice of the core is possible for heavy elements and the related accuracy has to be further investigated. When selecting an ECP core one also has to take into account, for example, that not all configurations listed in Table 3 are of equal importance for chemical problems.

Transition metals are more complicated than main group elements, since their $(n-1)$d and *ns* valence orbitals have two different main quantum numbers and thus also a different radial extension. Figure 9 shows that the Ti 3d radial density maximum is located roughly at the positions of those of the closed-shell 3s and 3p semicore orbitals. Although these have a considerably lower orbital energy, see Figure 10, they have to be included in the valence shell to avoid large frozen core errors. Note that a change of the Ti 3d occupation by one electron changes the effective nuclear charge for the more diffuse Ti 4s orbital also by roughly one unit. To a lesser extent also the 3s and 3p shells feel a change of the effective nuclear charge. Thus, when performing the core−valence separation on the basis of energetic criteria (orbital energies) and freezing the 3s and 3p shells, that is, treating Ti as a four-valence electron system, one observes FC errors which depend on the 3d occupation number. Table 4 shows that the FC errors can amount to more than 1 eV. However, when using spatial criteria (radial orbital and core densities) one is led to include the 3s and 3p shells in the valence space, that is, to treat Ti as a 12-valence electron system. The corresponding FC errors are now at most 0.02 eV, which is acceptable for most chemical investigations. Besides the Ar and Ne cores a Mg core is also included, since corresponding core definition are sometimes also used,[157,207−210] see sections 6.4,

dx.doi.org/10.1021/cr2001383 |*Chem. Rev.* 2012, 112, 403–480

Table 4. Relative Dirac−Hartree−Fock (DHF) Energies (eV), Obtained with the Dirac−Coulomb (DC) Hamiltonian, of the 2*J* + 1-Weighted Average of All *J* Levels Belonging to a Nonrelativistic Configuration[198] with Respect to the Value for the Ti [Ar] $3d^2$ $4s^2$ Ground State Configuration[a]

			FCE		
		DHF/DC	4ve	10ve	12ve
Ti^{4+}		86.261	3.320	0.393	0.021
	s^1	53.741	2.498	0.248	0.001
	s^2	30.370	1.972	0.172	0.001
d^1		44.064	0.702	0.063	0.000
d^1	s^1	22.131	0.474	0.043	0.000
d^1	s^2	8.319	0.357	0.037	0.000
d^2		18.558	0.018	0.002	0.000
d^2	s^1	5.838	0.003	0.000	0.000
d^2	s^2	0.000	0.000	0.000	0.000
d^3		6.952	0.152	0.037	0.000
d^3	s^1	1.743	0.116	0.022	0.000
d^4		5.477	0.206	0.045	0.000
m.a.e.			0.893	0.097	0.002

[a] The frozen-core errors (FCE; eV) in the relative energies are given for 4, 10, and 12 valence electron (ve) systems. The frozen core was taken from the neutral atom in the ground state configuration. The mean absolute errors (m.a.e.) are listed in the last line. The DHF/DC results for $4s^2$ and $3d^2$, relativistic contribution, and FC errors were interchanged in the original publication.[198]

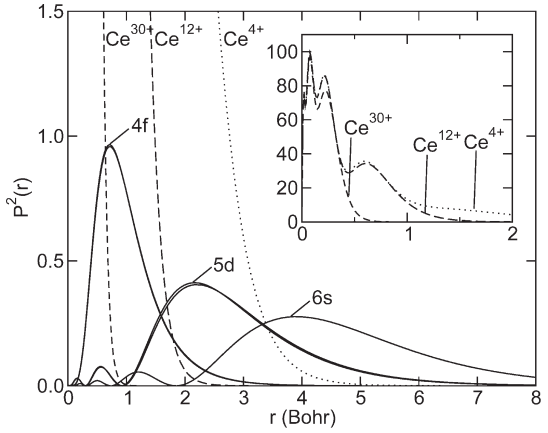

Figure 11. Orbital densities for Ce ([Xe] $4f^1$ $5d^1$ $6s^2$) from multiconfiguration Dirac−Hartree−Fock calculations with the Dirac−Coulomb Hamiltonian using the program GRASP.[83] The Ce^{30+} (small-core ECPs), Ce^{12+} (large-core ECPs), and Ce^{4+} densities are also plotted. For reasons of clarity the 4s, 4p, 4d (maxima near the 4f maximum), and 5s, 5p (maxima near the 5d maximum) densities have been omitted.

7.1, and 7.2. Although a Mg core is significantly more accurate than the Ar core, errors of a few tenths of an electronvolt have to be expected.

The most complex systems to model are lanthanides and actinides. Here the $(n-2)$f, $(n-1)$d, and ns valence shells have three different main quantum numbers and radial density maxima at different distances from the nucleus. Figure 10 implies that one could try to treat Ce as a four-valence electron atom, whereas Figure 11 reveals that this will not lead to an accurate approximation. On the basis of energetic criteria only 4f, 5d, and 6s are the valence orbitals of Ce, that is, the explicit treatment of only four valence electrons in accord with chemical intuition is implied. Table 5 however shows that FC errors of up to several eV render this approach quite useless. Figure 11 shows for the Ce $4f^1$ $5d^1$ $6s^2$ ground state configuration that the open 4f shell is buried deeply inside a Ce^{12+} core, whereas the open 5d shell is still more compact than the Ce^{4+} core. The closed 5s and 5p semicore shells have their maxima close to the one of 5d and at larger distances from the nucleus than 4f, whereas the 4s, 4p, and 4d shells have their maxima near the one of 4f. Using the same arguments as applied for Ti above, changes of the 4f occupation number modify the effective charges for 5s, 5p, 5d, and 6s but also to a lesser extent for 4s, 4p, and 4d. In addition, changes of the 5d occupation number alters the effective charge for 6s but also to a lesser extent for 5s and 5p. As a result the FC errors for a Ce^{4+} core depend on the 4f occupation, and to a lesser extent also on the 5d occupation. For a Ce^{12+} the dependency on the 4f occupation is still noticeable, whereas the one on the 5d occupation is of minor importance. Finally a high accuracy with negligible FC errors below 0.01 eV is reached for a small Ce^{30+} core, that is, when all shells with $n \geq 4$ are considered in the valence space. A similar situation is present for actinides, see, for example, corresponding tabulations for Th[29] or U.[30] It is thus strongly advocated to motivate the core−valence separation in ECP methods on the basis of spatial rather than energetic criteria.

Table 5 also shows that the errors of energy differences between configurations with the same Ce 4f occupation are relatively small. This was the motivation to derive PPs for lanthanides and actinides including the open f shell into the core. These unusual PPs will be discussed in section 6.1.3 in more detail. Table 4 suggests that PPs for transition metals including the open d shell into the core could also be considered. In fact such PPs were used to model the environment of finite cluster calculations of, for example, for Ni^{2+} $3d^8$ in NiO.[211]

5.3. Pseudopotentials

In the following sections, the basic ideas and equations underlying the pseudopotential (PP) approach and the commonly used analytical forms of the PP valence-only (VO) model Hamiltonian will be briefly reviewed. The methods of PP parametrization for those PP approaches which are still actively used by a wider community or which are currently further developed will be discussed in section 6. Several points discussed here for PPs also apply to the model potential (MP) approach, which is described in sections 5.4 and 7.

5.3.1. Generalized Phillips−Kleinman Equation. One of the first PPs was proposed by Hellmann already in 1935 for a semiempirical treatment of the valence electron of potassium.[73] A rigorous theoretical foundation of PPs was provided only more than 20 years later by Phillips and Kleinman in 1959, who derived within an effective one-electron framework for the calculation of wave functions of crystals and molecules the so-called Phillips−Kleinman (PK) equation.[200] Another decade later Weeks and Rice presented in 1968 the generalized PK (GPK) equation,[3,212] which provides a first general prescription for the construction of a PP from an (effective) Hamiltonian and its eigenfunctions. Although the use of the (original) PK and GPK formalisms leads in practice not to accurate PPs and the analytical forms of modern PPs do not have much in

dx.doi.org/10.1021/cr2001383 |*Chem. Rev.* 2012, 112, 403–480

Table 5. Relative Dirac−Hartree−Fock (DHF) Energies (eV), Obtained with the Dirac−Coulomb (DC) Hamiltonian, of the 2*J* + 1-Weighted Average of All *J* Levels Belonging to a Nonrelativistic Configuration[29] with Respect to the Value for the Ce $4f^1\ 5d^1\ 6s^2$ Ground State Configuration[a]

			FCE							FCE		
		DHF/DC	4ve	12ve	30ve				DHF/DC	4ve	12ve	30ve
Ce^{4+}		68.115	5.037	0.466	0.002	f^1			33.273	0.416	0.001	0.000
	s^1	42.873	3.872	0.427	0.002	f^1		s^1	16.313	0.198	0.000	0.000
	s^2	24.654	3.104	0.400	0.002	f^1		s^2	5.592	0.094	0.000	0.000
d^1		38.662	2.911	0.408	0.002	f^1	d^1		14.981	0.046	0.000	0.000
d^1	s^1	21.087	2.312	0.385	0.002	f^1	d^1	s^1	4.767	0.007	0.000	0.000
d^1	s^2	9.909	1.965	0.371	0.002	f^1	d^1	s^2	0.000	0.000	0.000	0.000
d^2		18.900	1.648	0.381	0.002	f^1	d^2		5.107	0.039	0.001	0.000
d^2	s^1	8.254	1.420	0.370	0.002	f^1	d^2	s^1	0.661	0.037	0.000	0.000
d^2	s^2	3.231	1.330	0.364	0.002							
d^3		7.881	1.034	0.376	0.002	f^1	d^3		2.210	0.104	0.001	0.000
d^3	s^1	3.234	1.013	0.372	0.002							
d^4		4.322	0.845	0.384	0.002	m.a.e.			0.000	1.306	0.224	0.001

[a] The frozen-core errors (FCE; eV) in the relative energies are given for 4, 12, and 30 valence electron (ve) systems. The frozen core was taken from the neutral atom in the ground state configuration. The mean absolute errors (m.a.e.) are also listed.

common with the PK or GPK PPs, it is instructive to review these in order to rationalize the assumptions and approximations underlying the PP schemes.

We start with an (effective) one-electron Hamiltonian $\hat{H}_{\text{eff}}$, and imagine that there is only one upper energy eigenfunction $|\varphi_v\rangle$, which we will call the valence (v) eigenfunction, and several lower energy eigenfunctions $|\varphi_c\rangle$, which we will call core (c) eigenfunctions

$$\hat{H}_{\text{eff}}|\varphi_a\rangle = \varepsilon_a|\varphi_a\rangle\,, a \in \{v,c\} \tag{61}$$

We further assume that all eigenfunctions are orthonormal, that is,

$$\langle\varphi_a|\varphi_{a'}\rangle = \delta_{aa'},\ a,a' \in \{v,c\} \tag{62}$$

Now one may define an arbitrary, normalized function $|\varphi_p\rangle$, which is later called a pseudovalence orbital, as a linear combination of the valence and core eigenfunctions

$$|\varphi_p\rangle = N_p(|\varphi_v\rangle + \sum_c a_c|\varphi_c\rangle) \tag{63}$$

Using the orthogonality constraints eq 62 between the $|\varphi_c\rangle$ and $|\varphi_v\rangle$ we can evaluate the coefficients a_c as

$$a_c = {N_p}^{-1}\langle\varphi_c|\varphi_p\rangle \tag{64}$$

Solving eq 63 for $|\varphi_v\rangle$, using eq 64 to replace the coefficients a_c and substituting with the resulting expression $|\varphi_v\rangle$ in eq 61 yields after multiplying with the normalization factor N_p

$$\hat{H}_{\text{eff}}|\varphi_p\rangle - \sum_c \varepsilon_c|\varphi_c\rangle\langle\varphi_c|\varphi_p\rangle = \varepsilon_v[|\varphi_p\rangle - \sum_c |\varphi_c\rangle\langle\varphi_c|\varphi_p\rangle] \tag{65}$$

Introducing the so-called Phillips−Kleinman (PK) "potential" $\hat{V}^{\text{PK}}$

$$\hat{V}^{\text{PK}} = \sum_c(\varepsilon_v - \varepsilon_c)|\varphi_c\rangle\langle\varphi_c| \tag{66}$$

one can rewrite eq 65 with this expression to give the so-called Phillips−Kleinman equation[200]

$$(\hat{H}_{\text{eff}} + \hat{V}^{\text{PK}})|\varphi_p\rangle = \varepsilon_v|\varphi_p\rangle \tag{67}$$

Equations 67 and 63 imply that without changing the eigenvalue ε_v the form of pseudovalence orbital $|\varphi_p\rangle$ is not unique and may be chosen quite freely. Note that for n_c core orbitals used in eq 66, the ground state solution of eq 67 with energy ε_v is $(n_c + 1)$-fold degenerate.

Since $\hat{V}^{\text{PK}}$ is not a usual potential, that is, a function depending on the position $\vec{r}$, it is called a pseudopotential (PP). We note that operators we will call later PPs in addition model Coulomb and exchange operators included in $\hat{H}_{\text{eff}}$ in eq 67. It is also important to note that the operator $\hat{V}^{\text{PK}}$ is energy-dependent because it depends on ε_v and all ε_c, and it is nonlocal because it depends on all $|\varphi_c\rangle$. Note that the PK Hamiltonian implicitly takes care of core−valence orthogonality conditions and that one can use any arbitrary trial wave function $|\tilde{\varphi}_p\rangle$ in a variational procedure to approach ε_v from above, without danger to collapse to the core energy levels. The linear combination eq 63 may be used to eliminate from $|\varphi_v\rangle$ the radial nodal structure arising from core−valence orthogonality constraints, yielding a smooth and nodeless pseudovalence function $|\varphi_p\rangle$ with low basis set requirements. We prefer to use for $|\varphi_p\rangle$ the term pseudovalence orbital, instead of the frequently used term valence pseudo-orbital, since $|\varphi_p\rangle$ fulfills all requirements for a legitimate orbital. Unfortunately, the construction of the PK potential requires the knowledge of $|\varphi_c\rangle$ and ε_a $(a \in v,c)$, that is, the full problem still has to be solved and thus no computational savings arise so far.

In 1968, Weeks and Rice generalized the PK PP formalism to cases where more than one valence electron is present.[3,212] Moreover, in their formalism, only $|\varphi_v\rangle$ is required to be an eigenfunction of the (effective) one-electron Hamiltonian $\hat{H}_{\text{eff}}$, whereas the $|\varphi_c\rangle$ are not. As a start one may assume eq 61 only to hold for a valence orbital $|\varphi_v\rangle$ and act from left with a projector $\hat{P}_c$ on the orthogonal core orbitals

$$\hat{P}_c = \sum_c |\varphi_c\rangle\langle\varphi_c| \tag{68}$$

dx.doi.org/10.1021/cr2001383 |*Chem. Rev.* 2012, 112, 403–480

leading to

$$(1-\hat{P}_c)\hat{H}_{eff}|\varphi_v\rangle = \varepsilon_v|\varphi_v\rangle \quad (69)$$

Expressing the original valence orbital $|\varphi_v\rangle$ in terms of its pseudovalence counterpart $|\varphi_p\rangle$ eq 63, that is,

$$|\varphi_v\rangle = N_p^{-1}(1-\hat{P}_c)|\varphi_p\rangle \quad (70)$$

one obtains from eq 61 a pseudo eigenvalue problem for the pseudovalence orbital $|\varphi_p\rangle$:

$$(1-\hat{P}_c)\hat{H}_{eff}(1-\hat{P}_c)|\varphi_p\rangle = \varepsilon_v(1-\hat{P}_c)|\varphi_p\rangle \quad (71)$$

Defining the so-called generalized PK (GPK) PP $\hat{V}^{GPK}$ as the following nonlocal, energy-dependent effective one-electron operator

$$\hat{V}^{GPK} = -\hat{H}_{eff}\hat{P}_c - \hat{P}_c\hat{H}_{eff} + \hat{P}_c\hat{H}_{eff}\hat{P}_c + \varepsilon_v\hat{P}_c \quad (72)$$

the GPK eigenvalue equation for a pseudovalence orbital is obtained

$$(\hat{H}_{eff} + \hat{V}^{GPK})|\varphi_p\rangle = \varepsilon_v|\varphi_p\rangle \quad (73)$$

In case that the $|\varphi_c\rangle$ are also eigenfunctions of $\hat{H}_{eff}$, $\hat{V}^{GPK}$ reduces to $\hat{V}^{PK}$. Equations 66 and 67 or eqs 72 and 73 do not bring about any computational savings compared to eq 61, but rather consist of a rewriting of the original AE problem in a quite complicated form. Thus, the PK and GPK equations prove that in principle one can get the same answer as from an AE calculation by working with a suitable effective valence-only Hamiltonian and pseudovalence orbitals with simplified radial nodal structure. The importance of the PK and GPK approaches does not result so much from the explicit prescriptions they provide for performing valence-only calculations, but rather from the ideas and suggestions they imply for setting up computationally more efficient as well as also more accurate ab initio valence-only approaches.

As already stated by Cohen and Heine in 1961, neither the pseudovalence orbitals constructed according to eq 63 nor the corresponding pseudopotentials are unique.[213] At this point essentially two approaches to eliminate the nonuniqueness originate. One possibility is to choose a potential with a physically reasonable analytical form and to optimize the free parameters in this potential so as to fit experimental or AE ab initio reference data. A typical early example is the Hellmann PP.[73] Also the energy-consistent PP approach described in section 6.1 follows this strategy. Another possibility is to construct by some prescription some appropriately smooth pseudovalence orbital $|\varphi_p\rangle$ and to generate the corresponding (local) potential. This strategy is followed by the shape-consistent PP approaches summarized in section 6.2. Still, following this variant requires to eliminate the nonuniqueness of eq 63 by adding constraints. Cohen and Heine suggested several criteria to obtain unique and smooth pseudovalence orbitals, among them the minimization of the kinetic energy. Goddard and co-workers based their PPs on the nodeless and unique valence orbitals obtained with the G1 generalized valence-bond (GVB) approach.[214−216] Later the so-called coreless HF (CHF) PP approach was advocated.[217,218] The linear combination of HF orbitals $|\varphi_a\rangle$ ($a \in v,c$) in eq 63 were fitted to a suitable Slater orbital using a weighting factor $1/r^2$ in order to emphasize the fit in the core region. CHF PPs have been generated for K through Zn in 1978,[219] however at that time the exact obedience of the PK prescription eq 63 was already shown to lead to errors.[194,220−222] For a recent attempt to explicitly apply PK theory as well as additional references to previous work in this field we refer the reader to articles by Schwartz and co-workers.[223,224]

So far, the derivation and subsequent application of the PPs could be carried out on a grid. However, in order to become computationally efficient also for molecular calculations the PPs have to be cast in some analytical form, which can be handled by standard quantum chemistry codes using, for example, Gaussian basis sets.[216,217] The analytical form used nowadays, that is, the semilocal ansatz (vide infra), has only little in common with the original PK and GPK PPs. It was pointed out already by Weeks and Rice that the advantage of the PP formalism lies not so much in the formally exact solution of the problem but rather in the physical insights it provides and the models it suggests.[212] The main result is that it is possible in principle to find a potential that, when added to a Hamiltonian acting only on the valence electrons, allows the variational solution of the corresponding Schrödinger equation without variational collapse to core-like solutions. Moreover, the pseudovalence wave function in this formalism does not need to take into account explicit orthogonality requirements to the core-part of the original wave function and thus can be described with smaller basis sets.

5.3.2. Analytical Form of Pseudopotentials. *Nonrelativistic and Scalar-Relativistic Pseudopotentials.* In 1935, Hellmann proposed in a one page letter to treat potassium as a one-valence electron atom in quantum chemical calculations by using a simple (local) potential acting on the valence electron,[73] that is,

$$\hat{V}_{cv}(\vec{r}) \cong V_{PP}(r) = -\frac{1}{r} + \frac{2.74}{r}e^{-1.16r} \quad (74)$$

Hellmann used $\Psi \approx \exp(-0.29r)$ as an approximate corresponding eigenfunction and adjusted the free parameters to the valence energy of the K $4s^1\ ^2S$ ground state. Further, using the Heitler−London ansatz[225] Hellmann performed the first molecular PP calculations. He obtained for K_2 a bond length of 4 Å (exp. 3.9 Å) and recovered 37% of the experimental binding energy. However, soon it was found that simple r-dependent spherical PPs are not accurate enough for atoms containing valence orbitals of various angular symmetries,[226,227] for example, one can prove that the experimentally[228] observed ordering of the $(n-1)d^1\ ^2D$ states below the $np^1\ ^2P$ states of alkaline earth ions Ca^+, Sr^+, and Ba^+ cannot be obtained with a local PP ansatz.

Starting with the work of Abarenkov and Heine in 1964/5[229,230] in the framework of semiempirical semilocal energy-dependent (model) PPs for solid state physics applications an increasing number of researchers took besides the r-dependency also a l-dependency into account, that is, a dependency of the PP on the angular momentum quantum number l. Such a r- and l-dependency is already suggested in the PK pseudopotential eq 66, for example, when core orbitals of different l are present. The idea of Abarenkov and Heine was a few years later introduced to quantum chemistry by Schwarz[188] as well as Kahn and Goddard.[231] Assuming a superposition of PPs as indicated in eq 60 the so-called semilocal PP ansatz for a core λ may be written as

$$\Delta\hat{V}_{cv}^{\lambda}(i) \cong \Delta\hat{V}_{PP}^{\lambda}(i) = \sum_{l=0}^{l=\infty} V_l^{\lambda}(r_{i\lambda})\hat{P}_l^{\lambda}(i) \quad (75)$$

dx.doi.org/10.1021/cr2001383 |Chem. Rev. 2012, 112, 403–480

with the angular momentum projection operator based on spherical harmonics $|lm,\lambda\rangle$ with respect to core l

$$\hat{P}_l^\lambda(i) = \sum_{m=-l}^{m=l} |lm,\lambda\rangle\langle lm,\lambda| \quad (76)$$

For $l \geq L$, where typically $(L-1)$ is the largest angular momentum used by the core orbitals on center λ, the PPs $V_l^\lambda(r_{i\lambda})$ are only slightly different,[216] that is,

$$V_l^\lambda(r_{i\lambda}) \cong V_L^\lambda(r_{i\lambda}) \text{ for } l \geq L \quad (77)$$

In general, if we assume $V_l^\lambda(r_{i\lambda}) = V_L^\lambda(r_{i\lambda})$ for $l \geq L$, we can use the closure property of the projection operators to write the expression[216]

$$\Delta\hat{V}_{\mathrm{PP}}^\lambda(i) = V_L^\lambda(r_{i\lambda}) + \sum_{l=0}^{L-1} [V_l^\lambda(r_{i\lambda}) - V_L^\lambda(r_{i\lambda})]\hat{P}_l^\lambda(i) \quad (78)$$

The operator $\Delta\hat{V}_{\mathrm{PP}}^\lambda$ in eq 78 is a so-called semilocal PP, that is, it mainly consists of a sum of local potentials $V_l^\lambda(r_{i\lambda})$ acting on each angular momentum symmetry $0 \leq l \leq L-1$ separately up to a maximum angular momentum $L-1$ present in the core λ, beyond which a common local potential $V_L^\lambda(r_{i\lambda})$ acts on all angular momentum symmetries $l \geq L$.

Relativistic Pseudopotentials. Relativistic effects have not been considered in the above description of the PP approach so far. The preferred pseudovalence orbitals have by construction no oscillations and only low function values in the spatial core region. Therefore, in contrast to MPs, it is not possible to generate accurately direct relativistic contributions by relativistic AE operators, which are mainly acting in the core region,[159,162] and modified relativistic operators have to be constructed. However, indirect relativistic effects cause a modification of the effective potential seen by the valence orbitals, an effect which easily can be accommodated by the ansatz used in the nonrelativistic case so far. Luckily, the same is true for the direct scalar-relativistic contributions, and thus PPs taking only into account scalar-relativistic effects can be constructed and used essentially along the same lines as in the nonrelativistic case, merely requiring a change of the AE reference data used for their construction. Kahn, Hay, and Cowan described, in 1978, the first derivation of a scalar-relativistic ab initio PP for the U atom[232] based on atomic CG HF AE calculations.[85]

The inclusion of SO interaction makes some modifications of the analytical form of the PPs necessary. The basic concept used today in most relativistic ab initio PP approaches was already formulated in the work of Animalu in 1966, who extended the semiempirical semilocal energy-dependent (model) PP approach of Abarenkov and Heine[229,230] to a corresponding two-component formalism for investigations in solid state physics.[233] In quantum chemistry relativistic, that is, two-component, PPs were first published at the same time by Hafner and Schwarz[234] at the semiempirical level and independently by Lee, Ermler and Pitzer[235] at the ab initio level. The analytical form of such relativistic PPs will be described in the following.

In a description of an atom at the nonrelativistic Hartree–Fock level (HF) all orbitals belonging to a shell with main quantum number n and angular momentum quantum number l are degenerate, thus leading to a semilocal PP with a l-dependence by means of a projection operator $\hat{P}_l^\lambda$ based on spherical harmonics. At the relativistic Dirac–Hartree–Fock (DHF) level the degeneracy is reduced and depends in addition to n and l also on the total angular momentum j of the orbital (or spinor), implying a semilocal PP with a lj-dependence

$$\Delta\hat{V}_{\mathrm{cV}}^\lambda(i) \cong \Delta\hat{V}_{\mathrm{PP}}^\lambda(i) = \sum_{l=0}^{l=\infty} \sum_{j=|l-1/2|}^{j=l+1/2} V_{lj}^\lambda(r_{i\lambda})\hat{P}_{lj}^\lambda(i) \quad (79)$$

by means of the projection operators $\hat{P}_{lj}^\lambda$ set up with spinor spherical harmonics $|ljm,\lambda\rangle$ with respect to core λ

$$\hat{P}_{lj}^\lambda(i) = \sum_{m=-j}^{m=j} |ljm,\lambda\rangle\langle ljm,\lambda| \quad (80)$$

Similar to the nonrelativistic case $\Delta V_{\mathrm{PP}}^\lambda$ may be approximately written as

$$\Delta\hat{V}_{\mathrm{PP}}^\lambda(i) = V_{LJ}^\lambda + \sum_{l=0}^{l=L-1} \sum_{j=|l-1/2|}^{j=l+1/2} V_{lj}^\lambda(r_{i\lambda}) - V_{LJ}^\lambda(r_{i\lambda})\hat{P}_{lj}^\lambda(i) \quad (81)$$

Note that

$$\hat{P}_l^\lambda(i) = \sum_j \hat{P}_{lj}^\lambda(i) = \hat{P}_{l,|l-1/2|}^\lambda(i) + \hat{P}_{l,l+1/2}^\lambda(i) \quad (82)$$

and

$$V_l^\lambda(r_{i\lambda}) = \frac{1}{2l+1}[lV_{l,|l-1/2|}^\lambda(r_{i\lambda}) + (l+1)V_{l,l+1/2}^\lambda(r_{i\lambda})] \quad (83)$$

The relativistic PP in eq 81 may thus be rewritten as the sum of a spin-free averaged (av) and a spin-dependent (so) term[236]

$$\Delta\hat{V}_{\mathrm{PP}}^\lambda(i) = \Delta\hat{V}_{\mathrm{PP,av}}^\lambda(i) + \Delta\hat{V}_{\mathrm{PP,so}}^\lambda(i) \quad (84)$$

where

$$\Delta\hat{V}_{\mathrm{PP,so}}^\lambda(i) = \sum_{l=1}^{L-1} \frac{\Delta V_l^\lambda(r_{i\lambda})}{2l+1}[l\hat{P}_{l,l+1/2}^\lambda(i) - (l+1)\hat{P}_{l,l-1/2}^\lambda(i)] \quad (85)$$

Here ΔV_l^λ is the difference between the corresponding relativistic PPs

$$\Delta V_l^\lambda(r_{i\lambda}) = V_{l,l+1/2}^\lambda(r_{i\lambda}) - V_{l,|l-1/2|}^\lambda(r_{i\lambda}) \quad (86)$$

$\Delta\hat{V}_{\mathrm{PP,av}}^\lambda$ is a scalar-relativistic PP, that is, without inclusion of SO coupling, and it corresponds to $\Delta\hat{V}_{\mathrm{PP}}^\lambda$ defined in eq 78 if the difference between $V_{LJ}^\lambda(r_{i\lambda})$ and $V_L^\lambda(r_{i\lambda})$ is neglected.[236] The $\Delta\hat{V}_{\mathrm{PP,so}}^\lambda$ is called a SO PP. A simpler form especially suited for use in SO configuration interaction (CI) calculations following a scalar-relativistic HF solution was derived by Pitzer and Winter[237]

$$\Delta\hat{V}_{\mathrm{PP,so}}^\lambda(i) = \sum_{l=1}^{L-1} \frac{2\Delta V_l^\lambda(r_{i\lambda})}{2l+1} \hat{P}_l^\lambda(i)\hat{\vec{l}}_{\lambda i}\cdot\hat{\vec{s}}\hat{P}_l^\lambda(i) \quad (87)$$

Here $\hat{\vec{l}}_{\lambda i} = \hat{\vec{r}}_{\lambda i} \times \hat{\vec{p}}_i$ and $\hat{\vec{s}}$ stand for the operators of orbital angular momentum with respect to core λ and spin, respectively. Actually only one of the $\hat{P}_l^\lambda(i)$ is needed because $\hat{P}_l^\lambda(i)$ commutes with $\hat{\vec{l}}_{\lambda i}\cdot\hat{\vec{s}}_i$ and is idempotent.[237] We note here in passing that relativistic (two-component) PPs can be averaged and thus also used in scalar-relativistic (one-component) calculations, whereas the usage of a scalar-relativistic small-core PP together with a large-core SO term, that is, a SO operator optimized only for the valence orbitals and not for the semicore orbitals, in fully variational two-component calculations usually leads to errors. Although the usage of the same core definition for the

dx.doi.org/10.1021/cr2001383 |Chem. Rev. 2012, 112, 403–480

scalar-relativistic PP and the SO term is a natural choice avoiding such difficulties, the usage of different core definitions may be computationally attractive, for example, one can maintain a high accuracy by using a small-core PP approach at the scalar-relativistic level, whereas a computationally simple perturbative treatment with a large-core SO term can be applied to derive multiplet splittings arising from open valence shells.

A simple although often sufficiently accurate alternative approach to include SO coupling is the use of a scaled AE Pauli-type SO operator

$$\hat{V}_{\mathrm{SO}}(i) = \frac{\alpha^2}{2}\sum_{\lambda}\left(\frac{Z^{\mathrm{eff}}_{\lambda,l}}{r^3_{\lambda i}}\right)\hat{\vec{l}}_{\lambda i}\cdot\hat{\vec{s}}_i \tag{88}$$

which was originally proposed by Cohen et al.[238] The operator eq 88 is not variationally stable, and thus its application has to be restricted to perturbation theory based on solutions from a scalar-relativistic calculation. The approach was used successfully in calculations applying scalar-relativistic PPs by Wadt,[137] Koseki and co-workers,[138−140] and Heinemann et al.[239]

Gaussian Expansion of Radial Pseudopotentials. To facilitate calculations using Gaussian basis sets the potentials $V^{\lambda}_{l}(r_{i\lambda}) - V^{\lambda}_{L}(r_{i\lambda})$, $V^{\lambda}_{L}(r_{i\lambda})$ in the nonrelativistic and scalar-relativistic case, and $V^{\lambda}_{lj}(r_{i\lambda}) - V^{\lambda}_{LJ}(r_{i\lambda})$, $V^{\lambda}_{LJ}(r_{i\lambda})$ in the relativistic case are usually represented by linear combinations of radial Gaussian functions multiplied by powers of the electron−core distance $r_{i\lambda}$,[194]

$$V^{\lambda}_{m}(r_{i\lambda}) = \sum_{k} A^{\lambda}_{km} r^{n_{km}}_{i\lambda} e^{-a^{\lambda}_{km} r^2_{i\lambda}} \text{ with } m = l, L, lj, LJ \tag{89}$$

As a consequence a similar expansion results for the difference potential $\Delta V^{\lambda}_{l}(r_{i\lambda})$ in the SO term. The choice was made mainly because of computational convenience and efficiency for the further calculations, that is, the matrix elements over the PP operators may then be readily evaluated in a Cartesian Gaussian basis.[194,237,240−242] This topic will be discussed in section 8.2. The powers n_{km} of the electron−core distance $r_{i\lambda}$ were restricted to the values −2, −1, and 0, because these values were found to adequately cover the behavior of $\Delta\hat{V}^{\lambda}_{\mathrm{PP}}$ at the origin.[194] Note that $n_{km} \geq -2$ is also required to maintain integrability when evaluating matrix elements.

5.4. Model Potentials

The model potential (MP) approach used for replacing atomic cores is another important variant of the ECP method.[16,18,24] In contrast to the PP approaches discussed so far the MP approach aims at keeping the correct nodal structure of the valence orbitals, that is, no formal transformation to pseudovalence orbitals is performed. Thus, conceptually the MP approach is more accurate than the PP approach. Besides the advantage that untransformed operators, also when acting in the spatial core region, can in principle be applied to the valence orbitals in the MP approach, there is the disadvantage that MP basis sets have to be larger than the PP basis sets, in some cases reaching nearly of the size of AE basis sets, in order to describe the shape of the valence orbitals also in the core region correctly. Since the use of large basis sets is not always desirable, in some older MP approaches radial nodes were sometimes eliminated, at the same time giving up the use of untransformed operators. It is fair to say that the MP approach for atoms is considerably less popular than the PP approach. Nevertheless it represents an important link between the full AE calculation and the PP calculations, and thus it is also discussed here. Moreover, the MP approach has a wider scope than the PP approach, that is, it is not restricted to construct a model valence-only Hamiltonian for an atom exploiting its spherical symmetry, but it can also be used to construct a corresponding model Hamiltonian for an active part of an essentially arbitrary system, replacing its chemically inactive subunits by a MP.[16] This aspect of the MP approach is exploited, for example, in the work of Seijo and Barandiarán, who on one hand use MPs to replace the core electron system of heavy atoms, and on the other hand use a similar formalism to model the surroundings when embedding the heavy atom/ion in a crystalline environment.[24] In the following, we will focus only on the first aspect of the method.

5.4.1. Huzinaga−Cantu Equation. The MP method was originally proposed by Bonifacic and Huzinaga[243] and later improved by Sakai and Huzinaga.[244,245] The main goal is to model as exact as possible a Fock-type AE operator for the valence orbitals. The method originated from the so-called Huzinaga−Cantu equation[199,246]

$$\hat{H}_{\mathrm{eff}} + \sum_{c}(-2\varepsilon_c)|\varphi_{\mathrm{c}}\rangle\langle\varphi_{\mathrm{c}}||\varphi_{\mathrm{a}}\rangle = \varepsilon_a|\varphi_{\mathrm{a}}\rangle, a \in \{v, c\} \tag{90}$$

In this equation $\hat{H}_{\mathrm{eff}}$ stands for an (effective) one-electron Hamiltonian, for example, a Fock operator, and the subscripts denote valence (v) and core (c) orbitals. The valence orbital $|\varphi_{\mathrm{v}}\rangle$ and the core orbitals $|\varphi_{\mathrm{c}}\rangle$ are eigenfunctions of $\hat{H}_{\mathrm{eff}}$ as assumed in eq 61 and fulfill the orthogonality constraints eq 62. In contrast to eq 61 the sum over projection operators onto core orbitals $|\varphi_{\mathrm{c}}\rangle$ added to $\hat{H}_{\mathrm{eff}}$ guarantees that the eigenvalues of the core orbitals $|\varphi_{\mathrm{c}}\rangle$ appear at an energy $-\varepsilon_c > 0$ in the spectrum, that is, at higher energies than the valence orbital eigenvalues ε_{v} which remain at their original position. The Huzinaga−Cantu equation resembles the Phillips−Kleinman equation, eq 67 with eq 66, however the lowest energy pseudovalence orbital $|\varphi_{\mathrm{p}}\rangle$ in the latter equation does not necessarily have radial nodes, whereas the valence orbital $|\varphi_{\mathrm{v}}\rangle$ in the Huzinaga−Cantu equation keeps the correct nodal structure of the corresponding AE valence orbital.

5.4.2. Analytical Form of Model Potentials. For the VO model Hamiltonian eq 60, assuming the molecular potential as a superposition of atomic contributions, a MP consisting of three terms may be considered for an atom λ

$$\Delta\hat{V}^{\lambda}_{\mathrm{cv}}(i) \cong \Delta\hat{V}^{\lambda}_{\mathrm{MP}}(i) = \Delta\hat{V}^{\lambda}_{\mathrm{C}}(i) + \Delta\hat{V}^{\lambda}_{\mathrm{X}}(i) + \hat{P}^{\lambda}_{\mathrm{S}}(i) \tag{91}$$

Here $\Delta\hat{V}^{\lambda}_{\mathrm{C}}$ is the Coulomb (C) interaction between the core λ and the valence electrons

$$\Delta\hat{V}^{\lambda}_{\mathrm{C}}(i) = -\frac{n^{\lambda}_{\mathrm{c}}}{r_{i\lambda}} + 2\sum_{c}\hat{J}^{\lambda}_{\mathrm{c}}(i) \tag{92}$$

Note that for the core λ the number of core electrons n^{λ}_{c} and the core charge Q_λ add to the nuclear charge Z_λ, that is, $n^{\lambda}_{\mathrm{c}} + Q_\lambda = Z_\lambda$, so that the correct AE core−electron interaction is kept in the VO model Hamiltonian. $\Delta\hat{V}^{\lambda}_{\mathrm{X}}$ represents the core−valence exchange (X) interaction

$$\Delta\hat{V}^{\lambda}_{\mathrm{X}}(i) = -\sum_{c}\hat{K}^{\lambda}_{\mathrm{c}}(i) \tag{93}$$

$\hat{J}^{\lambda}_{\mathrm{c}}$ and $\hat{K}^{\lambda}_{\mathrm{c}}$ stand for the usual Coulomb and exchange operators related to the core orbital $|\varphi^{\lambda}_{\mathrm{c}}\rangle$ and the sums in eqs 92 and 93 run over all occupied core orbitals. To prevent the valence electrons from collapsing into the core a shift (S) operator $\hat{P}^{\lambda}_{\mathrm{S}}$ constructed

dx.doi.org/10.1021/cr2001383 |Chem. Rev. 2012, 112, 403–480

from core orbitals centered on core λ has to be included in the VO model Hamiltonian eq 60

$$\hat{P}_S^{\lambda}(i) = \sum_c (-2\varepsilon_c^{\lambda})|\varphi_c^{\lambda}(i)\rangle\langle\varphi_c^{\lambda}(i)| \quad (94)$$

The value of $-2\varepsilon_c^{\lambda}$ for the energy shift can be motivated for atoms,[247] and is usually transferred to molecules as well.

For calculations using Gaussian basis sets a basis set expansion is used to represent the $|\varphi_c^{\lambda}\rangle$ in eq 94. The modeling of the Coulomb and exchange terms differs, that is, whereas in the ab initio model potential (AIMP) approach (see section 7.1) an expansion in Gaussian functions times powers of r and a spectral representation in a large atom centered basis set are used for the local Coulomb (eq 92) and nonlocal exchange (eq 93) parts, respectively, the model core potential (MCP) approach (see section 7.2) only uses the expansion in Gaussian functions times powers of r. Relativistic effects, including the SO effects, are treated by the two approaches using a spectral representation of the WB SO term and an effective Pauli-type SO operator, respectively.

5.5. Corrections to the Frozen-Core Approximation

The formal derivations of the PP and MP VO model Hamiltonians discussed so far assumed the core−valence separation and the frozen-core (FC) approximation. Thus electron correlation effects, i.e., core−core correlation and especially core−valence correlation, also called dynamic core polarization, as well as static core polarization were not taken into account. The notion that core-polarization plays an important role in, for example, the atomic spectroscopy of the heavy alkaline elements, when these are treated as one valence electron systems, is essentially as old as quantum mechanics. Born and Heisenberg, following the classical treatment, found that for large radial distances the interaction energy between the valence electron and the core is $-(1/2)\alpha/r^4$, where α is the core dipole polarizability.[248] A major problem of this expression is the singularity at the nucleus, which was avoided in later work by implementing suitable cutoff functions. Corresponding references are given in an article by Meyer and co-workers.[178] First applications of core-polarization terms in molecules were reported in 1970 in the context of ECP calculations by Bardsley.[4,249] A simple superposition of atomic terms, leading to an overestimation of the effects, was used. A systematic derivation of atomic interactions for many-valence-electron one- and two-center systems was performed by Bottcher and Dalgarno, including also higher multipole polarizability contributions as well as nonadiabatic terms connected with the frequency dependence of the polarizabilities.[250]

The leading contribution for core−valence correlation in an AE CI treatment would be single excitations from the core orbitals coupled to single excitations from the occupied valence orbitals to the virtual orbital space. If we suppose that the (spherically symmetric) core of an atom will not be affected when the atom bonds to other atoms, that is, the FC approximation is valid, one can just take the PPs determined separately for each atom in the system (see sections 6 and 7) to construct the molecular PP by means of their superposition (see eq 58). Contributions arising from the deformation of the atomic cores under the field of the other cores and all valence electrons in the system, that is, static core-polarization effects, are thus neglected. The induced error may become especially significant for systems with large, easily polarizable cores and only a few valence electrons, for example, for large-core PPs in case of group 1 and 2 or 11 and 12 elements. At the AE level, starting with spherical mutually orthogonalized cores, the static core-polarization could be accounted for in a CI treatment by single excitations from the core orbitals to the virtual ones. An approximate perturbative treatment based on such a picture of core-polarization effects has been developed by Jeung, Malrieu and Daudey[251] and was applied in PP calculations to alkaline atoms and some of their compounds.[251,252]

Since in the ECP approximation the core electrons have been removed from the system, the above-mentioned single excitations from the core cannot be performed explicitly. However they can be taken into account in form of an effective operator acting on the valence electrons. Therefore, a so-called core-polarization potential (CPP) $\hat{V}_{\mathrm{cpp}}$ is frequently added to the valence electron model Hamiltonian eqs 54 and 60. The $\hat{V}_{\mathrm{cpp}}$ accounts for both static core-polarization, that is, polarization of the core at the HF level, as well as dynamic core polarization, that is, core−valence correlation. The method outlined below was first developed by Meyer and co-workers in the framework of AE calculations for alkaline elements[178,179] and adapted to energy-consistent large-core PPs by Fuentealba and co-workers.[195] It has been demonstrated in PP calculations that by including the dipole polarization of the core charge density one can also take care of the largest part of the core−valence correlation contributions.[195]

The electric field $\hat{\vec{f}}_\lambda$ generated at a core λ by all other cores/nuclei μ, as well as all valence electrons i in the system is given as

$$\hat{\vec{f}}_\lambda = -\sum_i \frac{\vec{r}_{i\lambda}}{r_{i\lambda}^3} + \sum_{\mu\neq\lambda} Q_\mu \frac{\vec{r}_{\mu\lambda}}{r_{\mu\lambda}^3} \quad (95)$$

For a polarizable core λ the dipole moment $\hat{\vec{\mu}}_\lambda$ induced by an external electric field $\hat{\vec{f}}_\lambda$ is

$$\hat{\vec{\mu}}_\lambda = \alpha_\lambda \hat{\vec{f}}_\lambda \quad (96)$$

where α_λ denotes the dipole polarizability of the core λ. We note here in passing that according to eq 96 the application of a CPP will also contribute to the dipole moment as well as to oscillator strengths of a system. Of course, the core dipole polarizabilities contribute to the overall static dipole polarizability of the system.

Figure 12 schematically shows contributions to the induced dipole moment arising in a polyatomic molecule: the coupling of (1) an electronic and nuclear contribution, (2) two electronic contributions, and (3) two nuclear contributions. The interaction of such induced dipoles with the external electric field yields an expression for the CPP

$$\hat{V}_{\mathrm{cpp}} = -\frac{1}{2}\sum_\lambda \hat{\vec{\mu}}_\lambda \cdot \hat{\vec{f}}_\lambda = -\frac{1}{2}\sum_\lambda \alpha_\lambda \hat{\vec{f}}_\lambda^2 \quad (97)$$

It is obvious from eq 97 that the energetic contribution of a CPP is not simply a sum over one-electron and one-nucleus contributions. For a two-valence electron atom like Be one could assume that due to their Coulomb repulsion the electrons prefer to stay at opposite sides of the core, that is, one could assume that the angle between $\vec{r}_1$ and $\vec{r}_2$ would be π, leading to a cancellation of the one-electron contributions by the two-electron contribution. This simple picture demonstrates that the superposition of one-electron terms might lead to an overestimation. However, it has been shown by Gill and co-workers[253] by analyzing the so-called angle intracule that the two valence electrons in Be actually have a preferred angle of $\pi/2$. Thus the average CPP contribution

dx.doi.org/10.1021/cr2001383 |Chem. Rev. 2012, 112, 403–480

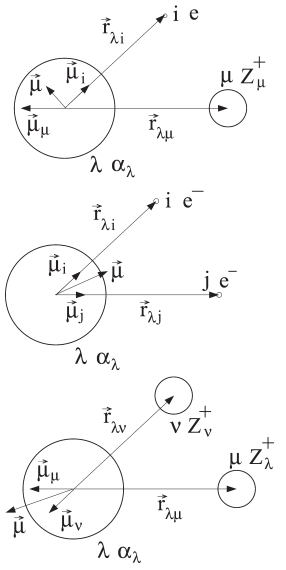

Figure 12. Schematic representation of an induced dipole moment $\vec{\mu}$ at core λ arising from contributions of (1) one electron and one nucleus/core (adapted from Fuentealba et al.[195]), (2) two electrons, and (3) two nuclei.

would be smaller than obtained from the superposition of one-electron terms, but would not vanish completely.

Equation 95 strictly applies only to large distances of the polarizing charges from the polarized cores and even diverges in the limit of vanishing distances. Therefore Meyer and co-workers[178,179] have suggested to multiply the field $\hat{\vec{f}}_\lambda$ with a cutoff function F removing the singularities. The field at a core λ then reads as

$$\hat{\vec{f}}_\lambda = -\sum_i \frac{\vec{r}_{i\lambda}}{r_{i\lambda}^3} F(r_{i\lambda}, \delta_e^\lambda) + \sum_{\mu \neq \lambda} Q_\mu \frac{\vec{r}_{\mu\lambda}}{r_{\mu\lambda}^3} F(r_{\mu\lambda}, \delta_c^\lambda) \quad (98)$$

where the cutoff functions can be chosen, for example, as follows:

$$F(r_{i\lambda}, \delta_e^\lambda) = (1 - e^{-\delta_e^\lambda r_{i\lambda}^2})^{n_e} \quad (99)$$

$$F(r_{\mu\lambda}, \delta_c^\lambda) = (1 - e^{-\delta_c^\lambda r_{\mu\lambda}^2})^{n_c} \quad (100)$$

The exponents n_e and n_c for the electronic and nuclear contributions are usually 1 or 2, and the corresponding cutoff parameters δ_e^λ and δ_e^λ can be used for the adjustment to suitable reference data. CPPs of the type described here often accompany large-core PPs for main group elements[254,255] as well as group 11 and 12 transition metals.[256,257] For the latter systems quadrupole corrections have also been developed.[258]

The CPP ansatz of Meyer and co-workers was later also adapted by Christiansen for the shape-consistent PP approach.[196] Daudey and co-workers extended the CPP ansatz by using l-dependent cutoff factors, which accounts for the finding that the core−valence correlation, for example, for an alkaline atom, depends on the symmetry of the valence orbital.[197] The uniform cutoff function eq 99 is replaced by

$$F(r_{i\lambda}, \delta_e^\lambda) \rightarrow \sum_{l=0}^{l_{max}} F_l(r_{i\lambda}, \rho_l^\lambda) \hat{P}_l^\lambda \quad (101)$$

where $\hat{P}_l^\lambda$ is the projection operator eq 76 with respect to the spherical harmonics centered at core λ. For Rb and Cs the sum was truncated at $l_{max} = 3$ and a step function defined as

$$F_l(r_{i\lambda}, \rho_l^\lambda) = \begin{cases} 0 & \text{for} \quad r < \rho_l^\lambda \\ 1 & \text{for} \quad r \geq \rho_l^\lambda \end{cases} \quad (102)$$

was used for the cutoff. The parameter ρ_l^λ was adjusted to the experimental total valence energies of the lowest state in each symmetry l. Formulas for the corresponding integrals over Cartesian Gaussian functions were also provided. The method was successfully applied, for example, to Rb_2 and Cs_2 in connection with one-valence-electron PPs for Rb and Cs.[197]

5.6. Corrections to the Point-Charge Repulsion Model

In cases where the atomic cores are relatively compact as compared to the valence shells, for example, the typical bond lengths formed between a pair of atoms are so large that the corresponding core densities do not significantly overlap, the point-charge repulsion model is a good approximation for the core−core interaction V_{cc} and eq 59 can be truncated after the first term. However, if large cores are used the core−core repulsion (CCRC) correction for "overlapping" or "mutually penetrating" cores becomes significant, that is, the second term in eq 59, must be included. A similar core−nucleus repulsion correction (CNRC) has to be applied for the interaction between nuclei of atoms treated without PPs and centers with large-core PPs. A Born-Mayer-type ansatz proved to be quite successful to model the pairwise repulsive correction in both cases[256,257]

$$\Delta V_{cc}^{\lambda\mu}(r_{\lambda\mu}) = B_{\lambda\mu} e^{-b_{\lambda\mu} r_{\lambda\mu}} \quad (103)$$

The parameters can be derived, for example, directly from FC HF calculations on pairs of atomic cores. In case of the interaction between a core and a nucleus the parameters of $\Delta V_{cc}^{\lambda\mu}$ can be obtained by fitting directly to the electronic contribution to the electrostatic potential $U(r) + Q/r$ of the PP core multiplied by the charge Z of the interacting nucleus. The electrostatic potential $U(r)$ of the core with charge Q bearing the PP is readily accessible from atomic finite difference calculations.[83] Figure 13 demonstrates that the exponential decay is valid in the valence region and also shows, that the correction is needed when alkaline atoms are treated as one-valence-electron systems, whereas it becomes negligible if the semicore orbitals are included in the valence space.

6. PSEUDOPOTENTIAL PARAMETRIZATION

There are essentially two methods for the adjustment of PPs to atomic reference data in current use, that is, the adjustment of parameters of a suitable model Hamiltonian to total AE valence energies simultaneously for a multitude of many-electron states leading to energy-consistent PPs and the derivation of the PPs from quantities defined within an effective one-electron picture, that is, orbital energies and the shape of valence orbitals in the spatial valence region for a specific reference state, leading to shape-consistent PPs. In the following both schemes will be described in some detail, whereas some other alternative approaches will only be briefly mentioned. The analytical form of energy-consistent PPs is essentially identical to the one of most shape-consistent PPs. Therefore both types of PPs can be used in most standard quantum chemical program packages (e.g., CFOUR,[259] COLUMBUS,[260] GAUSSIAN,[261] GAMESS,[262] MAGIC,[263] MOLCAS,[264] MOLPRO,[265] NWCHEM,[266]

dx.doi.org/10.1021/cr2001383 |Chem. Rev. 2012, 112, 403–480

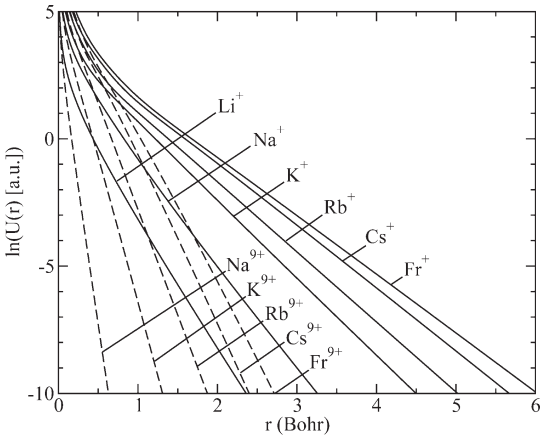

Figure 13. Logarithmic electronic contribution to the electrostatic potential $ln(U(r) + Q/r)$ of alkaline cations M^+ ($Q = 1$) and M^{9+} ($Q = 9$). The electrostatic potential $U(r)$ was evaluated with the GRASP code[83] at the DHF/DC level. The linear part approximated by eq 103 and multiplied by Z can be used as a core-nucleus repulsion correction for a nucleus with charge Z penetrating the alkaline core, that is, $\Delta V_{cc} \approx ZU(r)$.

TURBOMOLE,[267] Q-CHEM[268]), program packages designed for Quantum Monte Carlo calculations (e.g., CASINO,[269] CHAMP,[270] Quantum MagiC[271]), as well as polymer or solid state codes using Gaussian basis sets (e.g., CRYSTAL[272]),

Although the valence basis sets are tightly connected to the specific PPs and are therefore mentioned in the corresponding sections, a separate section on valence basis sets tries to summarize some aspects common to all PP approaches, see section 8.1.

6.1. Energy-Consistent Pseudopotentials

The energy-consistent ab initio PPs in use today developed during the last three decades from the semiempirical PP approach. In the latter, the free PP parameters were adjusted to reproduce (the relevant parts of) the experimental atomic spectrum, similar to the classic work of Hellmann in 1935.[73] Various difficulties where encountered when trying to extend the semiempirical approach to all elements of the periodic table and led to a switch to ab initio PPs, but still keeping the energy-adjustment. A justification for the energy-adjustment scheme is provided by the finding of Topp and Hopfield in 1973, that if the eigenvalues for the ground state and excited states for any given angular momentum agree, the logarithmic derivatives of the wave functions at any point on or outside a core radius will also be correct[273] (see also eqs 138 and 139 in section 6.5.5). This finding is related to a theorem probably going back to Kramers in 1938 which even states that if a potential gives the ground- and excited-state energies of a given symmetry in agreement with experiment, it will give the correct wave function in the tail region as well (see ref 16 in the article of Topp and Hopfield[273]). Thus the shape-consistency of energy-consistent PPs is guaranteed.

6.1.1. Semiempirical Pseudopotentials. In principle experimental atomic spectra would indeed be the best reference data for an energy-adjustment of PPs. However, such an adjustment to experimental reference energies in practice has some severe limitations. For atoms/ions with more than one valence electron the valence correlation effects usually cannot be taken into account with sufficiently high accuracy in ab initio calculations to guarantee a systematic derivation of the PPs. The generated PPs would implicitly correct for errors in the treatment of the valence electron system in the atomic reference states. These atomic corrections are usually not transferable, for example, from atoms to molecules, and thus relatively large errors might result. Therefore the semiempirical PP energy-adjustment is restricted essentially to one-valence electron systems, where valence correlation is absent and the Schrödinger equation for the valence-only model Hamiltonian can be solved exactly using either finite difference methods or very large basis sets.

Prototype examples for semiempirical PPs are the alkaline atoms,[274,275] but such PPs have also been proposed for, e.g., the first- and second-row main group elements.[276] Core−core and core−valence correlation as well as relativistic effects are present in the experimental reference data and are thus accounted for implicitly. In case of core−valence correlation this was found to lead to too short bond lengths in molecules (e.g., K_2 calcd 3.85 Å, exp 3.93 Å), whereas a corresponding adjustment to uncorrelated ab initio HF data lead to too long bond distances (K_2 calcd 4.13 Å). The reason is that core−valence correlation contributions determined for a single valence electron are simply treated additively in the many-valence-electron Hamiltonian and thus are overestimated. A more successful way to account for core−valence correlation, i.e., dynamic core polarization, together with nonfrozen core effects, that is, static core polarization, is provided by core-polarization potentials (CPPs) in operational form as devised by for AE calculations by Meyer and co-workers[178,179] and implemented for PPs by Fuentealba et al.[195] Quite good results have been obtained using this ansatz for alkaline and alkaline-earth systems,[180,195] at least for atoms.

Semiempirical PPs and corresponding CPPs were generated by Igel et al. for most of the main group elements by fitting the spectra of the one-valence electron ions for PP and CPP, and requiring the pure PP result for the one-valence electron ion ground state to agree with, for example, DHF/DC data.[254] These PPs and CPPs were successfully applied to various molecules.[255] Similar PPs and CPPs were developed and applied for heavy elements such as Br, I, Tl, and Pb by Schwerdtfeger and co-workers.[277−279]

Even when supplemented by CPPs the semiempirical PP approach is bound to fail when trying to achieve high accuracy. Since the many-electron Schrödinger equation cannot be solved sufficiently accurate for a general atom, one is tied to perform a one-electron adjustment of the PP and CPP, where a correlated treatment of the valence shell is avoided. Since especially for d and f transition metals, but also for post-d main group elements, the choice of a small core is a prerequisite for accurate, highly transferable PPs, the necessary one-electron adjustment has to be performed for highly charged cores. However, because of the limited validity of the frozen-core approximation when going from a highly charged one-valence electron ion to a neutral atom or nearly neutral ion, large errors result. Note that because of the partial screening of the nuclear charge by the valence shells and the higher electron−electron repulsion an atomic core in a neutral atom is more diffuse than in a highly charged ion. An additional drawback of the semiempirical PP approach is that in many cases accurate experimental atomic reference data is missing or incomplete. Finally, recent calibration studies of, for example, alkaline and alkaline earth as well as post-d elements exhibited, that also for these cases for accurate molecular calculations a small-core approach is needed.[280−282] Thus, except for the cases where large-core PPs can safely be applied, for

dx.doi.org/10.1021/cr2001383 |Chem. Rev. 2012, 112, 403–480

Table 6. Energy-Consistent WB-Adjusted Relativistic Effective Core Potentials and Valence Basis Sets[a]

elements	core	n_c	n_v	basis set	ref
^{5}B−^{9}F	^{2}He	2	3−7	(4s4p)/[2s2p], seg., HF	148
^{10}Ne	^{2}He	2	8	(7s7p)/[4s4p], seg., HF; +1d; +3d1f	298
^{13}Al−^{17}Cl	^{10}Ne	10	3−7	(4s4p)/[2s2p], seg., HF	148
^{18}Ar	^{10}Ne	10	8	(7s7p)/[4s4p], seg., HF; +1d; +3d1f	298
^{19}K, ^{20}Ca	^{10}Ne	10	9−10	(7s6p)/[5s4p], (6s6p5d)/[4s4p2d]	299
^{21}Sc−^{30}Zn	^{10}Ne	10	11−20	(8s7p6d)/[6s5p3d], seg., HF; +1f	283
^{31}Ga−^{35}Br	^{18}Ar 3d^{10}	28	3−7	(4s4p)/[2s2p], seg., HF	148
				cc-pVXZ (X = T,Q), seg., ANO	300
^{36}Kr	^{18}Ar 3d^{10}	28	8	(7s7p)/[4s4p], seg., HF; +1d; +3d1f	298
^{37}Rb, ^{38}Sr	^{18}Ar 3d^{10}	28	9−10	(7s6p)/[5s4p], (6s6p5d)/[4s4p2d)	281, 299
				def-SVP, def-TZVP, seg.	301
^{39}Y−^{48}Cd	^{18}Ar 3d^{10}	28	11−20	(8s7p6d)/[6s5p3d], seg., HF; +1f	147
				cc-pVXZ (X = T,Q), seg., ANO	300
^{49}In−^{53}I	^{36}Kr 4d^{10}	46	3−7	(4s4p)/[2s2p], seg., HF	148
				cc-pVXZ (X = T,Q), seg., ANO	300
				def-SVP, def-TZVP, seg.	301
^{54}Xe	^{36}Kr 4d^{10}	46	8	(7s7p)/[4s4p], seg., HF; +1d; +3d1f	298
^{55}Cs, ^{56}Ba	^{36}Kr 4d^{10}	46	9−10	(7s6p)/[5s4p], (6s6p5d1f)/[4s4p2d]	281, 299
				def-SVP, def-TZVP, seg.	301
^{57}La−^{71}Lu	^{18}Ar 3d^{10}	28	29−43	(14s13p10d8f6g)/[6s6p5d4f3g]	145, 302
				p-VQZ reducible to p-VTZ, p-VDZ	
				(14s13p10d8f6g)/[10s8p5d4f3g], seg., ANO	303
^{72}Hf−^{80}Hg	^{36}Kr 4d^{10}4f^{14}	60	12−20	(8s7p6d)/[6s5p3d], seg., HF; +1f	147
				cc-pVXZ (X = T,Q), seg., ANO	300
^{81}Tl−^{86}Rn	^{54}Xe 4f^{14}5d^{10}	78	3−8	(4s4p), HF; +1d	144
				def-SVP, def-TZVP, seg.	301
^{89}Ac−^{103}Lr	^{36}Kr 4d^{10} 4f^{14}	60	29−43	(12s11p10d8f)/[8s7p6d4f], seg., HF	149, 304
				(14s13p10d8f6g)/[6s6p5d4f3g], gen., ANO	304
				p-VQZ reducible to p-VTZ, p-VDZ	
				(14s13p10d8f6g)/[10s9p5d4f3g]	305

[a] The PPs for Sc−Zn are HF-adjusted and contain a first-order relativistic correction from DHF/DC.

example, for weakly bounded systems as metal clusters, the semiempirical adjustment does not lead to an accurate approach.

6.1.2. Wood−Boring- and Dirac−Hartree−Fock-Adjusted Ab Initio Pseudopotentials. Despite the problems associated with semiempirical pseudopotentials the idea to construct an effective valence-only Hamiltonian by avoiding reference to quantities which are merely defined in an independent-particle approximation, that is, orbitals and orbital energies, is quite attractive. If instead of experimental total valence energies corresponding (relativistic) ab initio AE values are used, it is in principle possible to go beyond the HF approach in the adjustment. On one hand static correlation effects could be included at the multiconfiguration HF (MCHF) level, on the other hand an intermediate coupling scheme instead of pure LS or *jj* coupling can be used. Moreover, both AE reference and PP adjustment calculations can be carried out using a finite difference approach, thus avoiding that any basis set incompleteness errors to affect the PP parameters. Finally, relatively small effects which are typically only handled by quasidegenerate perturbation theory at the post-MCDHF AE level, for example, the Breit interaction or quantum electrodynamic contributions, can be directly adjusted into the PP provided that the same configuration space is used at the AE and PP levels. It is thus not surprising that the energy-adjustment of PPs regained attention in the ab initio framework.[283] To emphasize the difference to semiempirical energy-adjusted PPs the term energy-consistent was coined for these PPs.

The free parameters of a given valence-only model Hamiltonian are chosen in such a way that the value of the functional

$$S = \sum_I w_I (E_I^{\mathrm{PP}} - E_I^{\mathrm{AE}} + \Delta E_{\mathrm{shift}})^2 := \min \qquad (104)$$

becomes a minimum. Here, depending on the Hamiltonian and the type of PP to adjust, the sum runs over configurations, LS states or *J* levels. E_I^{AE} and E_I^{PP} denote the total valence energies, calculated with respect to the total energy of the core systems, for the *I*th reference configuration, LS state or *J* level from AE and PP calculations, respectively. The weight factors w_I are usually chosen to give every nonrelativistic configuration independent from the number of underlying LS states or *J* levels the same weight, for example, for each of the ^{3}P, ^{1}D, and ^{1}S states arising from a p^2 configuration a weight $w_I = 1/3$ is chosen to fit a scalar-relativistic PP, whereas for each of the corresponding five *J* levels 0, 1, 2, 2, and 0 a weight $w_I = 1/5$ is used for fitting a relativistic PP. The global shift $\Delta E_{\mathrm{shift}}$ used in recent adjustments typically amounts to less than 1% of the total ground state valence energy, but allows a significantly better fit. It relaxes the requirement that the PP and AE total valence energies E_I^{PP} and E_I^{AE} agree in a

dx.doi.org/10.1021/cr2001383 |Chem. Rev. 2012, 112, 403–480

Table 7. Energy-Consistent DHF/DC+B-Adjusted Relativistic Effective Core Potentials and Valence Basis Sets

elements	core	n_c	n_v	basis set	ref
^{19}K, ^{20}Ca	^{10}Ne	10	9−10	(11s11p5d3f),(12s1p7d)	292, 293
^{21}Sc−^{28}Ni	^{10}Ne	10	11−18		285
^{29}Cu, ^{30}Zn	^{10}Ne	10	19−20	(12s12p9d3f2g)/[6s6p4d3f2g]	291
				aug-cc-pwCVXZ (X = D,T,Q,5), gen., ANO	204
^{31}Ga−^{36}Kr	^{10}Ne	10	21−26	(12s12p9d3f2g)/[6s6p4d3f2g], gen.	174
^{37}Rb−^{38}Sr	^{18}Ar 3d^{10}	28	9−10	(13s10p5d3f1g),(14s11p5d4f1g)	292, 293
				aug-cc-pVXZ (X = D,T,Q,5), gen., ANO	306, 307
				dhf-XVP(−2c) X = S,TZ,QZ	308−310
^{39}Y−^{46}Pd	^{18}Ar 3d^{10}	28	11−18	aug-cc-pwCVXZ (X = D,T,Q,5), gen., ANO	294
				dhf-XVP(−2c) X = S,TZ,QZ	308−310
^{47}Ag, ^{48}Cd	^{18}Ar 3d^{10}	28	19−20	(12s12p9d3f2g)/[6s6p4d3f2g]	291
				aug-cc-pwCVXZ (X = D,T,Q,5), gen., ANO	204
				dhf-XVP(−2c) X = S,TZ,QZ	308−310
^{49}In−^{54}Xe	^{18}Ar 3d^{10}	28	21−26	(12s12p9d3f2g)/[6s6p4d3f2g], gen.	174, 307
				aug-cc-pVXZ (X = D,T,Q,5), gen., ANO	306, 307
				dhf-XVP(−2c) X = S,TZ,QZ	308−310
^{55}Cs, ^{56}Ba	^{36}Kr 4d^{10}	46	9−10	(12s11p5d3f2g),(13s12p6d4f2g)	292, 293
				aug-cc-pVXZ (X = D,T,Q,5), gen., ANO	306, 307
				dhf-XVP(−2c) X = S,TZ,QZ	308−310
^{72}Hf−^{78}Pt	^{36}Kr 4d^{10}4f^{14}	60	12−18	aug-cc-pwCVXZ (X = D,T,Q,5), gen., ANO	295
				dhf-XVP(−2c) X=S,TZ,QZ	308−310
^{79}Au, ^{80}Hg	^{36}Kr 4d^{10}4f^{14}	60	19−20	(12s12p9d3f2g)/[6s6p4d3f2g)	291
				aug-cc-pwCVXZ (X = D,T,Q,5), gen., ANO	204
				dhf-XVP(−2c) X=S,TZ,QZ	308−310
^{81}Tl−^{86}Rn	^{36}Kr 4d^{10}4f^{14}	60	21−26	(12s12p9d3f2g)/[6s6p4d3f2g], gen.	173, 174
				aug-cc-pVXZ (X = D,T,Q,5), gen., ANO	306, 307
				dhf-XVP(−2c) X = S,TZ,QZ	308−310
^{87}Fr, ^{88}Ra	^{54}Xe 4f^{14}5d^{10}	78	9−10	(14s13p8d5f3g),(15s14p8d4f3g)	292, 293
				aug-cc-pVXZ (X = D,T,Q,5), gen., ANO	306, 307
^{111}Eka-Au, ^{112}Eka-Hg	^{54}Xe 4f^{14}5d^{10}5f^{14}	92	19−20	[9s7p7d4f], [10s7p7d4f]	290,311
^{119}Eka-Fr	^{86}Rn 5f^{14}6d^{10}	110	9	(17s16p13d6f5g)	292

least-squares sense, for example, the sums of all n ionization potentials from PP and AE calculations may deviate by about ΔE_{shift}. If one assumes that the energy shift equals the difference of the total valence energies of the highest energy configurations, LS states or J levels included in eq 104, $\Delta E_{shift} = E_0^{AE} - E_0^{PP}$, one obtains

$$S = \sum_I w_I[(E_I^{PP} - E_0^{PP}) - (E_I^{AE} - E_0^{AE})]^2 := \min \quad (105)$$

Thus, when including an energy shift only the total valence energies calculated with respect to the highest energy configuration, LS state or J level included in eq 104 are required to agree in a least-squares sense. Energy differences such as excitation energies, ionization potentials, and the electron affinity are still indirectly required to show good agreement with those of the AE reference data, however now excluding those involving the core energy.

The formalism described here to derive energy-consistent pseudopotentials can be used for one-, two-, and four-component PPs at any desired level of relativity (nonrelativistic Schrödinger, or relativistic Wood−Boring, Douglas−Kroll−Hess, Dirac−Coulomb or Dirac−Coulomb−Breit Hamiltonian; implicit or explicit treatment of relativity in the valence shell) and electron correlation (single- or multiconfigurational wave functions). Mainly two approaches were used in the past three decades. Scalar-relativistic PPs, frequently supplemented by SO operators suitable for use in perturbation theory, were adjusted to WB scalar-relativistic AE HF reference data,[145,146] see Table 6. More recently, relativistic PPs suitable also for variational two-component calculations were adjusted to MCDHF/DC+B reference data,[284] see Table 7.

Figures 14−16 and Figures 17 and 18 show the radial potentials of a MCDHF/DC+B-adjusted small-core PP for Ti and the corresponding valence orbitals, respectively. They are compared to corresponding curves for shape-consistent PPs (section 6.2) and a QMC-adapted energy-consistent PP (section 6.4) to be discussed later. It is seen that the shape of the potentials differs significantly in the core-region, reflecting the nonuniqueness of the PPs.[213] When comparing the radial potentials for small r values it has to be noted that the MCDHF/DC+B-adjusted PP contains only pure Gaussian functions as radial potentials, whereas the other PPs also have terms with factors $1/r$ and/or $1/r^2$ times Gaussian functions. However, the 4d and 3d pseudovalence orbitals of all three standard PPs agree excellently with the (averaged) large components of an AE DHF/DC calculation in the valence region and exhibit only small differences near the core. Similar findings resulted from a detailed study of various large-core PPs for In.[280]

dx.doi.org/10.1021/cr2001383 |Chem. Rev. 2012, 112, 403–480

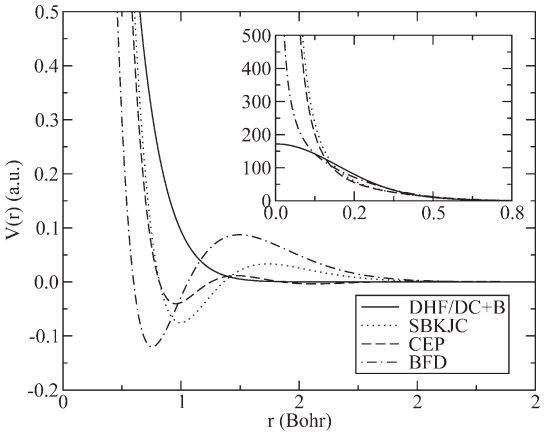

Figure 14. Radial pseudopotentials for $l = 0$ for various small-core Ti PPs: relativistic MCDHF/DC+B-adjusted energy-consistent PP (DHF/DC+B),[285] shape-consistent DHF/DC-adjusted PPs of Stevens et al. (SBKJC)[286] and Christiansen and co-workers (CEP),[287] and WB-adjusted QMC-adapted energy-consistent PP of Burkatzki et al. (BFD).[154]

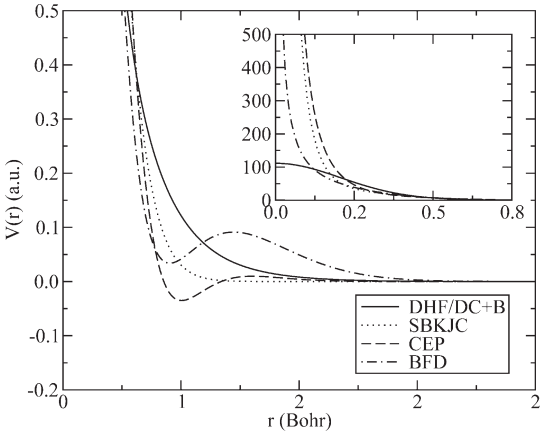

Figure 15. Same as Figure 14, but for $l = 1$.

The freedom to go beyond the independent-electron approximation was thus exploited by the present fitting procedures only to a small extent, that is, by the use of an intermediate coupling scheme for the MCDHF/DC+B-adjusted PPs. One may think about possible extensions such as including states of special importance at different levels of correlation treatment into the reference data, or even carrying out the adjustment using highly correlated wave functions, for example, a (full-)CI or CC. The difficulty here is of course the choice of the one-particle basis sets, which have to be exactly of the same quality for the all-electron and the valence-only calculation. Because of the pseudovalence orbital transformation this might not be achievable, except maybe when the basis sets are saturated up to a maximum angular quantum number. Clearly, the computational effort of such a procedure will be much larger than of the present one. Another interesting aspect arises from pseudopotentials which incorporate corrections for basis set incompleteness and deficiencies in the correlation treatment, cf. also section 6.3.

Parameters of energy-consistent ab initio pseudopotentials and corresponding valence basis sets are available for almost all elements of the periodic table.[144−149,169,173,174,283,284,288−295]

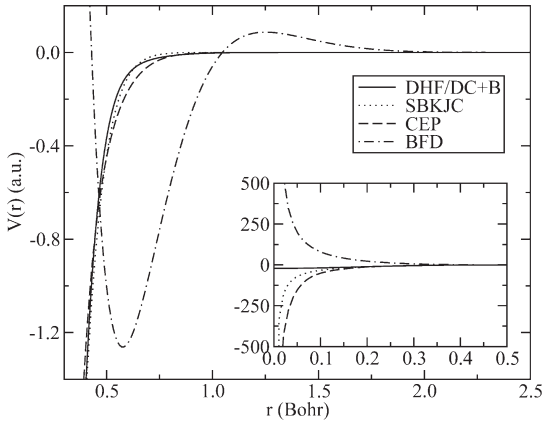

Figure 16. Same as Figure 14, but for $l = 2$.

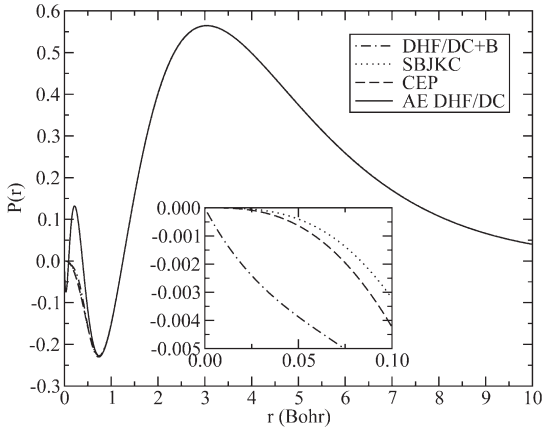

Figure 17. Radial 4s functions for various small-core Ti PPs in comparison to the large component from AE DHF/DC calculations: relativistic MCDHF/DC+B-adjusted energy-consistent PP (DHF/DC+B),[285] and shape-consistent DHF/DC-adjusted PPs of Stevens et al. (SBKJC)[286] and Christiansen and co-workers (CEP).[287]

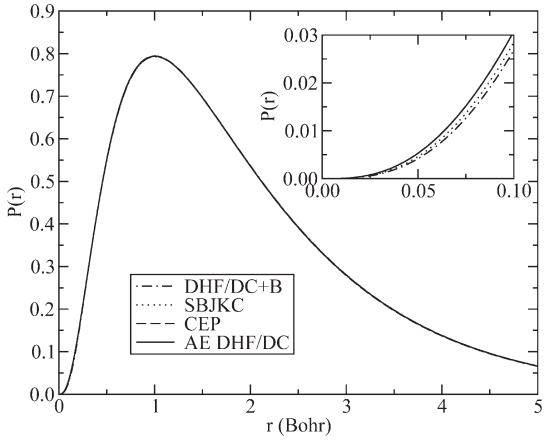

Figure 18. Same as Figure 17, but for 3d.

A compilation of PP parameters together with corresponding optimized valence basis sets is available from the EMSL database[296] (acronyms SDD for Stuttgart−Dresden, SBK for Stuttgart−Bonn−Köln) and the Cologne PP webpages.[297]

dx.doi.org/10.1021/cr2001383 |*Chem. Rev.* 2012, 112, 403–480

Special care has to be taken when spin−orbit coupling is planned to be included in calculations with small-core PPs: some SO operators are constructed (similar to the large-core case) for a fully variational two-component treatment, whereas in some cases effective valence SO operators are defined. The latter have to be applied in SO−CI calculations for the valence electrons, in which the semicore shells (outside the PP core) are frozen in their scalar-relativistic form.

The Stuttgart−Cologne PPs have been supplemented by various high quality valence basis sets, in addition to the basis sets published together with the PPs. For the WB-adjusted energy-consistent large-core PPs Sundermann and Martin published segmented contracted cc-pVTZ and cc-pVQZ basis sets for the heavy p-block elements Ga− Kr and In− Xe and performed extensive molecular tests.[296,297,300] Ahlrichs and co-workers developed basis sets of split-valence/valence double-ζ (def-SVP) and valence triple-ζ quality (def-TZVP) for the elements Rb− At, except the lanthanides.[301,312] In the same publication auxiliary basis sets for applying the resolution of the identity approach to the Coulomb interaction (RI-J) within DFT were presented and applied in geometry optimizations of systems with up to 300 atoms and/or 2500 basis functions.

For the newer MCDHF/DC+B-adjusted energy-consistent small-core PPs Peterson and collaborators constructed general contracted cc-pVXZ-PP (X = D,T,Q,5) basis sets for all p- and d-elements beyond Kr.[204,294−297,306,307,313,314] These basis sets allow a systematic extrapolation of correlation energies to the basis set limit. For the inclusion of core−valence correlation cc-pwCVXZ-PP (X = D,T,Q,5) basis sets were developed for 4d and 5d transition elements as well as the post-d main group elements Ga−Rn.[294−297,313,314] Extensive tests for atoms and molecules were reported. Results of explicitly correlated CCSD(T)-F12 calculations using orbital-pair specific Slater-type geminals were recently reported;[315] however, the applied cc-pVXZ-F12-PP basis sets of Peterson and Hill have not been published yet. Weigend and collaborators optimized segmented-contracted error-balanced basis sets of split-valence/valence double-ζ to valence quadruple-ζ quality (def2-SV(P), def2-TZP, def2-QZP and def2-SVP, def2-TZPP, def2-QZPP for a smaller and larger set of polarization functions, respectively) for 5p and 6p elements,[296,308,312] as well as for 4d, 5d, 5s, and 6s elements.[296,310,312] The basis sets were systematically tested for 80 5s-5d and 40 5p-6p compounds. At the DFT/BP86 level it was found that the differences between WB- and MCDHF/DC+B-adjusted are usually small for atomization energies, bond lengths and HOMO−LUMO-gaps.[310]

When using these basis sets in two-component calculations including SO terms it was found that the expansions for the semicore orbitals were not flexible enough to account for the radial differences of the spinors with $j = l \pm 1/2$. To solve the problem Armbruster et al. added sets with steep functions, that is, (2s1d)/[1p1d] for In−I, (2p)/[1p] for Au and Hg, (5p1d)/[3p1d] for Tl−At, to the def2-XVP (X = S, TZ, QZ) basis sets, yielding def2-XVP-2c basis sets.[312,316] Weigend and Baldes optimized def2-XVP and def2-XVP-2c basis sets for the 5s−6s and 4d−5d elements and relabeled them as dhf-XVP and dhf-XVP-2c, respectively.[310,312] When comparing results of one- and two-component DFT/BP86 calculations it was found that SO effects are mainly relevant for the 6p elements, concerning the HOMO−LUMO-gaps also for the 5p and 5d elements. The basis sets were found to keep a good balance of errors between s, p, and d elements. Typical errors in binding energies are 1, 5, and 20 kJ/mol for dhf-QZVP, dhf-TZVP, and dhf-SVP, respectively.

6.1.3. Lanthanide and Actinide f-in-Core Pseudopotentials. Energy-consistent WB-adjusted PPs for lanthanides and actinides attributing the open f shell to the PP core have been published and were quite successfully applied during the last two decades in quantum chemical studies.[20,29,30,317] Guided by AE FC results as discussed in section 5.2 for Ce, compare Table 5, the 5s, 5p, 5d, and 6s orbitals of the lanthanides, as well as the 6s, 6p, 6d, and 7s orbitals of the actinides were included in the valence space. The PPs describe lanthanide or actinide atoms with a fixed valency, corresponding to a fixed f occupation modeled by the PP core. The PPs are suited to perform electronic structure calculations for a superconfiguration, that is, an average over all electronic states with a given f occupation, a corresponding average over all f substates, and a specific valence substate coupled to them in all possible ways. The underlying superconfiguration concept was advocated by Field to rationalize the extremely complex electronic spectra of lanthanide diatomics.[318] For example the electronic structure of CeO can be modeled as arising from an ionic Ce^{2+} $4f^1 6s^1$ O^{2-} system. In $C_{\infty v}$, eight electronic states $^{1,3}\Sigma,\Pi,\Delta,\Phi$ belong to the $4f^1\sigma^1$ superconfiguration. Because of the core-like character of the Ce 4f shell these eight states have very similar bond distances and vibrational frequencies, which can on average be calculated using a 4f-in-core PP for a trivalent Ce with a $4f^1$ subconfiguration.[288,319] Energy differences between molecular states arising from different superconfigurations can be estimated by setting the atomic energy differences at the dissociation limit to the experimental or a suitable theoretical value.[320−322] Although this may seem to be a crude procedure, it has the advantage that the large differential correlation contributions arising mainly from the change of the f occupation number do not have to be calculated explicitly, which is quite difficult.[29,317] The lanthanide and actinide f-in-core PPs are available for the most common valencies and were supplemented with valence basis sets of varying size, mainly pVDZ, pVTZ, and pVQZ quality. In addition basis sets without diffuse functions and suitable for solid state calculations are available. The available PPs and valence basis sets are listed in Table 8. The parameters for PPs and basis sets are also available from the Cologne PP webpage.[297]

6.2. Shape-Consistent Pseudopotentials

More widely used than energy-consistent PPs are shape-consistent ones. Historically these were developed starting from pseudovalence orbitals constructed according to the original prescription of Phillips and Kleinman eq 63,[200] which was later relaxed and thus improved. Instead of quantum mechanical observables as in the energy-consistent PP approach the shape-consistent PPs are extracted from quantities defined within an effective one-electron picture, that is, AE valence orbitals and orbital energies from (relativistic) HF or DHF calculations for a specific electronic reference state.[220−222,240,325,326]

6.2.1. Non-Shape-Consistent Prescription of Kahn, Baybutt, and Truhlar. In 1976, Kahn, Baybutt, and Truhlar[194] proposed a first prescription for obtaining PPs from finite-difference HF atomic orbitals, which does not lead to shape-consistent PPs, but paved the way toward an ab initio construction of PPs, contrasting the various semiempirical approaches used so far. Taking advantage of the spherical symmetry of an

dx.doi.org/10.1021/cr2001383 |Chem. Rev. 2012, 112, 403–480

Table 8. Energy-Consistent WB-Adjusted f-in-Core Relativistic Effective Core Potentials and Valence Basis Sets[a]

elements	core	n_c	n_v	basis set	ref
^{57}La−^{71}Lu	1s−4f^n	46−60	11	(7s6p5d)/[5s4p3d]; seg., HF; +1f/+2f	146, 288, 323
				(8s7p6d)/[6s5p5d,5s4p4d],	324
				(7s6p5d)/[6s5p4d,5s4p4d], seg., HF; sol.	
^{57}La−^{70}Yb	1s−4f^{n+1}	47−60	10	(7s6p5d)/[5s4p3d]; seg., HF; +1f/+2f	146,288,323
^{58}Ce−^{60}Nd,	1s−4f^{n-1}	45−48,	12	(6s5p4d,7s6p5d)/p-VXZ,	155
^{65}Tb,^{66}Dy		53,54		X = D,T,Q, seg., HF; +2f1g; sol.	
^{89}Ac−^{103}Lr	1s−5f^n	78−92	11	(6s5p4d,7s6p5d,8s7p6d)/p-VXZ,	150
				X = D,T,Q, seg., HF; +2f1g; sol.	
^{94}Pu−^{102}No	1s−5f^{n+1}	84−92	10	(6s5p4d,7s6p5d)/p-VXZ,	151
				X = D,T,Q, seg., HF; +2f1g; sol.	
^{90}Th−^{98}Cf	1s−5f^{n-1}	78−86	12	(6s5p4d,7s6p5d)/p-VXZ,	151
				X = D,T,Q, seg., HF; +2f1g; sol.	

[a] In some cases reduced basis sets for use in solid state calculations are available (sol.).

atom the orbitals appearing in eq 63 can be factorized in a radial part and an angular part

$$\langle \vec{r} | \varphi_a \rangle = R_{nl}(r) Y_{lm}(\theta, \phi) = \frac{1}{r} P_{nl}(r) Y_{lm}(\theta, \phi) \text{ with } a \in \{c, v, p\} \quad (106)$$

which are treated at the finite difference level and analytically, respectively. Note that P_{nl} is normalized to unity, whereas R_{nl} is not. In the following we will switch between P_{nl} and R_{nl} for convenience. The basic idea is to construct according to eq 63 a pseudovalence orbital $|\varphi_p\rangle$ for each angular symmetry l as a linear combination of the AE valence and core orbitals, to plug it in the radial Fock equation together with the appropriate orbital energy ε_v

$$\left[-\frac{1}{2}\frac{d^2}{dr^2} + \frac{l(l+1)}{2r^2} + V_l^{PP}(r) + \hat{W}_{l,p}(\{|\varphi_{n'l',p}\rangle\}) \right] P_{p,nl}(r) = \varepsilon_{v,nl} P_{p,nl}(r) \quad (107)$$

and to solve the resulting expression for the unknown potential $V_l^{PP}(r)$

$$V_l^{PP}(r) = \varepsilon_{v,nl} - \frac{l(l+1)}{2r^2} + \frac{\left(\frac{1}{2}\frac{d^2}{dr^2} - \hat{W}_{p,l}(\{|\varphi_{p',n'l'}\rangle\}) \right) P_{p,nl}(r)}{P_{p,nl}(r)} \quad (108)$$

Here $\hat{W}_{l,p}$ denotes the Coulomb and exchange potential evaluated with the pseudovalence orbitals $|\varphi_p\rangle$. Here and in the following we keep the main quantum number n of the original valence orbital also for the pseudovalence orbital, although it might not have $(n - l - 1)$ radial nodes.

Three conditions were imposed in addition to eq 63 on the pseudovalence orbital $|\varphi_p\rangle$: (1) The (energetically lowest) pseudovalence orbital $|\varphi_p\rangle$ (in each angular symmetry) should have no radial nodes (a node or zero at $r = 0$ is not considered a radial node). (2) The pseudovalence orbital $|\varphi_p\rangle$ should be as close as possible to the original valence orbital $|\varphi_v\rangle$. (3) The pseudovalence orbital $|\varphi_p\rangle$ should have a minimal number of spatial undulations.

These conditions mainly arise from the wish that the basis set used to represent the pseudovalence orbital $|\varphi_p\rangle$ can be reduced comparing to the original basis set used to describe the true valence orbital $|\varphi_v\rangle$. To impose these conditions in practice, Kahn et al. constructed a functional which had to be minimized with respect to the core orbital expansion coefficients a_c in eq 63

$$S = (1+\lambda)^{-1} \left[\sum_{m=1}^{n-1} \left(\int_0^\infty P_{c,ml} P_{p,nl} dr \right)^2 + \lambda \int_0^\infty \left[\frac{d}{dr} \left(\frac{R_{p,nl}}{r^l} \right) \right]^2 dr \right] \quad (109)$$

The parameter λ allows to weigh the importance of the two terms, which are designed to favor the fulfillment of the conditions (2) and (1,3), respectively. The minimization is subject to the constraint

$$\lim_{r\to\infty} \left(\frac{R_{p,nl}}{r^l} \right) = 0 \quad (110)$$

The potentials $\Delta V_l(r) = V_l(r) + Q/r$ and $\Delta V_L(r) = V_L(r) + Q/r$ were generated on a grid and then fitted according to eq 89 in a least-squares sense by a linear combination of radial Gaussian type functions multiplied by powers of the electron−core distance r.

6.2.2. Shape-Consistent and Norm-Conserving Prescriptions. The development of the shape-consistent PP approach resulted from the finding that the sole admixture of core orbitals to valence orbitals according to eq 63 leads to pseudovalence orbitals which are too compact, for example, exhibit too low amplitudes in the spatial valence region. This deficiency leads to unsatisfactory molecular results such as too short bond lengths and too large bond energies.[194,327]

The defect was actually already noticed and overcome in 1974 by the work of Durand and Barthelat,[220,221] who extended eq 63 by a (formal) admixture of virtual orbitals. However, in practice these are less readily available from finite difference atomic HF or DHF calculations and incomplete for corresponding calculations using finite basis sets. Thus explicit reference to virtual (and core) orbitals was avoided. Thereafter, Christiansen, Lee, and Pitzer[325] in quantum chemistry and Hamann et al.[328] in solid state physics also presented prescriptions to construct improved pseudovalence orbitals leading to the shape-consistent and norm-conserving PP approaches, respectively.

dx.doi.org/10.1021/cr2001383 |Chem. Rev. 2012, 112, 403–480

To arrive at a practical approach one abandons the explicit admixture of core and virtual orbitals to the valence orbitals and rather requires the pseudovalence orbital $|\varphi_p\rangle$ to retain the correct radial distribution of charge given by the AE valence orbital $|\varphi_v\rangle$ in the spatial valence region outside a critical radius r_c. In addition the corresponding PP pseudovalence orbital energy ε_p is set equal to the AE valence orbital energy ε_v, that is, for a given l in the nonrelativistic and scalar-relativistic case or a given lj in the relativistic case one requires that

$$R_{p,nlj}(r) = \begin{cases} R_{v,nlj}(r) & \text{for} \quad r \geq r_c \\ f_{lj}(r) & \text{for} \quad r < r_c \end{cases} \text{ and } \varepsilon_{p,lj} = \varepsilon_{v,lj} \tag{111}$$

For one- and two-component AE HF reference calculations the radial part of $|\varphi_v\rangle$ can be used directly, whereas in the four-component case usually the radial part of the (renormalized) upper (large) components of the DHF spinors are used for $|\varphi_v\rangle$. The auxiliary function $f_{lj}(r)$ is required to be radially nodeless and smooth in the core region ($r < r_c$). Except for the normalization and continuity conditions for $|\varphi_p\rangle$ the choice of the core radius r_c, as well as the smoothing function $f_{lj}(r)$ is in certain limits arbitrary and may differ for the existing approaches.[325,326,329,330] Usually r_c is required to be located somewhere between the outermost radial node and the outermost (density) maximum of $|\varphi_v\rangle$. Especially in solid state physics, where plane-wave basis sets are used, larger values of r_c leading to smoother PPs are desired, since these exhibit a rapid convergence of the total energy and other system properties with respect to an increase of the plane-wave basis set. However, larger r_c values also lead to a decreased transferability of the PPs. In solid state physics shape-consistent PPs are often referred to as norm-conserving PPs,[328] since the second condition in eq 111 is replaced by the evaluation of a normalization integral implicitly imposing a condition on $f_{lj}(r)$, that is,

$$R_{p,nlj}(r) = R_{v,nlj}(r) \text{ for } r \geq r_c \tag{112}$$

and

$$\int_0^r |P_{p,nlj}(r)|^2 dr = \int_0^r |P_{v,nlj}(r)|^2 dr \text{ for } r \geq r_c \tag{113}$$

have to be fulfilled.

Once $|\varphi_p\rangle$ defined in eq 111 has been obtained a PP $\Delta\hat{V}_{cv}$ has to be constructed which, when inserted into the valence Hamiltonian $\hat{H}_v$, eq 60, should yield $|\varphi_{p,lj}\rangle$ as HF orbital for the atomic reference state under consideration. When using semi-local PPs defined in eq 79, that is, restricting $\Delta\hat{V}_{cv}$ to the form of a radially multiplicative potential $V_{lj}(r)$ for each lj-set, a radial Fock equation can be set up

$$\left[-\frac{1}{2}\frac{d^2}{dr^2} + \frac{l(l+1)}{2r^2} + V_{lj}^{PP}(r) + \hat{W}_{p,lj}(\{|\varphi_{p',n'l'j'}\rangle\})\right] P_{p,nlj}(r) = \varepsilon_{v,nlj} P_{p,nlj}(r) \tag{114}$$

The first two terms in parentheses are the radial kinetic energy operator and $\hat{W}_{p,lj}$ stands for an effective valence Coulomb and exchange potential for $|\varphi_{p,lj}\rangle$. With a given $|\varphi_{p,lj}\rangle$ and $\varepsilon_{v,lj}$, the PP V_{lj}^{PP} can be determined pointwise by inversion of eq 114

$$V_{lj}^{PP}(r) = \varepsilon_{v,nlj} - \frac{l(l+1)}{2r^2} + \frac{\left(\frac{1}{2}\frac{d^2}{dr^2} - \hat{W}_{p,lj}(\{|\varphi_{p',n'l'j'}\rangle\})\right) P_{p,nlj}(r)}{P_{p,nlj}(r)} \tag{115}$$

Clearly, difficulties arise when pseudovalence orbitals with radial nodes are inserted, since at the nodes V_{lj}^{PP} becomes singular. Therefore, shape-consistent PPs are usually derived for radially nodeless pseudovalence orbitals. In cases where small PP cores are needed in order to limit frozen core errors, positively charged reference states have to be used. A procedure to allow also pseudovalence orbitals with nodes was developed by Titov and co-workers (see section 6.2.7).[331]

Relativistic effects are implicitly included in V_{lj}^{PP} since the AE reference calculation explicitly describes these effects, which thus enter $|\varphi_p\rangle$ and ε_v. The resulting potentials $\Delta V_{lj}^{PP} = V_{lj}^{PP} + Q/r$ and $\Delta V_{LJ}^{PP} = V_{LJ}^{PP} + Q/r$ are tabulated on a grid and are then usually fitted by means of a least-squares criterion to a linear combination of radial Gaussian functions. Repeating this procedure for each lj set one arrives at the final semilocal form of the shape-consistent PP acting on the ith electron

$$\hat{\hat{V}}^{PP}(i) = -\frac{Q}{r_i} + \sum_{lj}\left(\sum_k A_{lj,k} r_i^{n_{lj,k}-2} e^{-\alpha_{lj,k} r_i^2}\right)\hat{P}_{lj}(i) \tag{116}$$

The separation of $\hat{\hat{V}}^{PP}$ into a scalar-relativistic spin-averaged part $\Delta\hat{V}_{cv,av}$ and a spin−orbit (SO) part $\Delta\hat{V}_{cv,so}$ according to eq 84 is the same as has been discussed in section 5.3.2.

An extension of the shape-consistent approach has been proposed by Rappé et al., who generated shape- and Hamiltonian-consistent PPs by requiring that in addition to shape-consistency also the average valence−valence interactions for pseudovalence orbitals are the same as for AE valence orbitals.[332]

6.2.3. (Averaged) Relativistic Effective Potentials of Christiansen, Ermler and Co-workers. Shape-consistent spin-averaged PPs (averaged relativistic potentials, AREP) and corresponding SO operators based on single-configuration Dirac−Hartree−Fock (DHF) AE calculations using the Dirac−Coulomb (DC) Hamiltonian have been generated for all elements from Li (Z = 3) to Eka-Rn (Z= 118) by Christiansen, Ermler and co-workers.[287,333−341] The PPs are based on the two-component formalism of Lee, Ermler and Pitzer[235] and an improved shape-consistency requirement according to Christiansen, Lee and Ermler.[325] In eq 111 the function $f_{lj}(r)$ was chosen as

$$f_{lj}(r) = r^b g_{lj}(r) = r^{l+2}\sum_{k=0}^{4} a_{lj,k} r^k \tag{117}$$

The coefficients $a_{lj,k}$ were determined by matching at r_c for $R_{v,nlj}$ and $f_{lj}(r)$ the function values and the first three derivatives, as well as by the normalization condition for the resulting $|\varphi_p\rangle$. The reference orbitals $|\varphi_v\rangle$ were the large components of the DHF/DC solutions, see Figure 3. In many cases PPs for two alternative choices of the core were derived. The PPs are accompanied by (partly) energy-optimized valence basis sets, where the expansion coefficients for all exponents are usually provided for the

dx.doi.org/10.1021/cr2001383 |Chem. Rev. 2012, 112, 403–480

Table 9. Shape-Consistent DHF/DC-Adjusted Relativistic Effective Core Potentials and Valence Basis Sets of Christiansen, Ermler, and Co-workers

elements	core	n_c	n_v	basis set	ref
^{3}Li−^{4}Be	[^{2}He]	2	1−2	(4s4p)	333
				(4s4p)/[2s2p]	343
^{5}B−^{10}Ne	[^{2}He]	2	1−8	(4s4p)	333
				(4s4p1d)/[2s2p1d]	343
				(5s5p)/[3s3p]	344
^{11}Na−^{12} Mg	[^{2}He]	2	9−10	(6s4p)	333
				(6s6p)/[3s3p]	343
^{13}Al−^{18}Ar	[^{10}Ne]	10	3−8	(4s4p)	333
				(4s4p1d)/[2s2p1d]	343
				(5s5p)/[3s3p]	344
^{19}K−^{20}Ca	[^{10}Ne]	10	9−10	(5s4p)	287
				(6s6p4d)/[3s3p2d]	345
^{21}Sc−^{30}Zn	[^{10}Ne]	10	11−20	(7s6p5d)	287
^{21}Sc−^{30}Zn	[^{18}Ar]	18	3−12	(4s5p)	287
^{31}Ga−^{36}Kr	[^{18}Ar]	18	13−18	(3s3p4d)	287
				(5s5p)/[3s3p]	344
				(6sd4p1f)/[4sd3p1f]	345
^{31}Ga−^{36}Kr	[^{18}Ar] 3d^{10}	28	3−8	(3s3p)	287
^{37}Rb, ^{38}Sr	[^{18}Ar] 3d^{10}	28	9−10	(5s5p)	334
^{39}Y−^{48}Cd	[^{18}Ar] 3d^{10}	28	11−20	(5s5p4d)	334
^{39}Y−^{48}Cd	[^{36}Kr]	36	3−12	(3s3p4d)	334
^{49}In−^{54}Xe	[^{36}Kr]	36	13−18	(3s3p4d)	334
^{49}In−^{54}Xe	[^{36}Kr] 4d^{10}	46	3−8	(3s3p)	334
^{55}Cs−^{57}La	[^{36}Kr] 4d^{10}	46	9−11	(5s5p5d)	335, 336
^{57}La	[^{54}Xe]	54	3	(3s3p4d)	335,336
^{58}Ce−^{71}Lu	[^{54}Xe]	54	4−17	(6s6p6d6f)	337
^{72}Hf−^{80}Hg	[^{36}Kr] 4d^{10}4f^{14}	60	12−20	(5s5p4d)	335, 336
^{72}Hf−^{80}Hg	[^{54}Xe] 4f^{14}	68	4−12	(3s3p4d)	335, 336
^{81}Tl−^{86}Rn	[^{54}Xe] 4f^{14}	68	13−18	(3s3p4d)	335, 336
^{81}Tl−^{86}Rn	[^{54}Xe] 4f^{14}5d^{10}	78	3−8	(3s3p)	335, 336
^{87}Fr−^{88}Ra	[^{54}Xe] 4f^{14}5d^{10}	78	9−10	(5s5p4d)	338
^{89}Ac−^{94}Pu	[^{54}Xe] 4f^{14}5d^{10}	78	11−16	(5s5p4d4f)	338
^{81}Tl−^{86}Rn	[^{54}Xe] 4f^{14}	68	13−18	(...)/[4s4p4d1f]	339
^{95}Am−^{118}Eka-Rn	[^{54}Xe] 4f^{14}5d^{10}	78	17−40	(6s7p6d5f)	340, 341
^{104}Rf−^{118}Eka-Rn	[^{54}Xe] 4f^{14}5d^{10}5f^{14}	92	12−40	(6s7p6d5f)	340, 341

atomic ground state. In case of the superheavy elements Cartesian Gaussian basis sets with 3s- and 3d-type, as well as 4p- and 4f-type, functions sharing the same exponents were published, whereas for all other elements the usual spherical Gaussian basis sets with 1s-, 2p-, 3d-, and 4f-type functions are provided.

An overview of the available PPs and accompanying basis sets of these groups is given in Table 9. Orbital (contraction) coefficients were provided for all original basis set exponents published together with the PPs. Parameters for PPs and valence basis sets are available in electronic form from the EMSL database[296] (acronym CEP for Christansen, Ermler, Pitzer) and the homepage of the Christiansen group.[342]

The shape-consistent PPs of Christiansen, Ermler and collaborators can be used in scalar-relativistic calculations (AREP), followed by a perturbative (e.g., based on HF or CI wave functions) or variational (spin−orbit configuration interaction[346]) SO treatment, or after converting to the two-component form (REP) also in quasi-relativistic HF and subsequent correlation calculations. As judged from the underlying reference data they should be more accurate than those of other groups based on, for example, CG or WB scalar-relativistic HF reference data. However, for heavy and superheavy elements the neglected contributions of the Breit interaction might become apparent. A procedure to consider the Breit interaction after reconstructing the correct nodal structure of the valence orbitals was discussed in the first paper of the series,[333] but has never been applied to our knowledge.

Figures 14−16 and Figures 17 and 18 compare the radial potentials and pseudovalence orbitals of a small-core shape-consistent AREP for Ti to corresponding curves obtained for other approaches. The shape-consistency, which was actually required for the Ti^{2+} ion with an empty 4s shell is maintained also for the neutral atom.

In the original papers,[287,334−336] atomic small-core (11−20 valence electrons) AREP $s^2d^n \rightarrow s^1d^{n+1}$ excitation energies for all three transition metals rows are compared to scalar-relativistic

dx.doi.org/10.1021/cr2001383 |Chem. Rev. 2012, 112, 403–480

AE GC results of Martin and Hay.[158] The deviations usually are well below 0.1 eV (mean absolute errors 0.04, 0.03, and 0.05 eV for the 3d, 4d and 5d elements, respectively), except for Tc and Re where the AREP values are by 0.13 and 0.12 eV larger than the AE GC values. Of course it has to be noted that the GC HF scheme is an approximation to spin-free DHF/DC calculations and as such is also affected by errors which may amount up to a few 0.01 eV for elements as heavy as Au.

For the large-core AREPs of the 3d elements the corresponding deviations were reported by Pacios to amount to about 0.15 and 0.5 eV for $s^2d^n \rightarrow s^1d^{n+1}$ and $s^2d^n \rightarrow d^{n+2}$ excitation energies, respectively.[347] Walker et al. analyzed the partitioning of the valence orbitals into the part in the core region, which is smoothed for the pseudovalence orbitals, and the unchanged part in the valence region. It was shown that when the matching point moves closer toward the nucleus, the 4s pseudovalence orbital still remains nodeless, but exhibits a bump, which is reminiscent of a corresponding minimum of the original 4s valence orbital near the outermost maximum of the 3s valence orbital. The so-called 3s bump results from the normalization requirement for the 4s pseudovalence orbital. Walker et al. showed for Sc, Ti, Fe, and Co that the errors in the above energy differences can be considerably reduced to less than 0.15 eV, when the 4s pseudovalence orbital is not smooth, but rather has a 3s bump in the core region.[348] As mentioned by Walker et al. such large-core PPs may be useful for studying large transition metal clusters or for quantum Monte Carlo studies, however neither the probably enhanced requirements for basis sets able to describe the bumps nor the effects of the bumps on electron correlation energies have been studied so far. To our knowledge the corresponding PP parameters were not made public.

Pacios demonstrated that an averaging of standard AREPs derived from different configurations can also reduce these deviations considerably, whereby a weighted average of AREPs derived for s^2d^n and d^{n+2} for Sc−Ni and for s^2d^9 and s^1d^{10} for Cu yielded the best overall results with m.a.e. of 0.05 and 0.16 eV for the $s^2d^n \rightarrow s^1d^{n+1}$ and $s^2d^n \rightarrow d^{n+2}$ excitation energies, respectively.[347,349] These results compare favorably to the corresponding small-core AREP m.a.e. of 0.04 and 0.07 eV.[287]

A similar comparison of excitation energies and ionization potentials was provided for Yb and Lu, however, no results for cases where the 4f occupation changes were given.[337] In view of the very large cores used for the lanthanide AREPs, quite large FC errors are to be expected.[29] No corresponding results were published for the actinides and superheavy elements, for which a more reliable smaller core was used.[338,340]

Most of the original papers also provide some results for SO splittings of atoms and their ions obtained with both REPs in two-component HF calculations and AREPs by first-order perturbation theory using the SO term derived from the difference of REPs and AREPs. In comparison to AE DHF/DC reference data for the lighter elements Li−Mg, which exhibit small splittings, relatively large errors of up to 33% arise in some cases, whereas for Al to Ar the errors remain below 10%.[333] REP and AREP+SO results are quite similar, indicating small orbital relaxation under the SO term. It was pointed out that the basis sets need sufficient flexibility in the core region, especially for the 2p shells, where the REP and consequently the SO term was generated directly from the large components of the AE DHF solution and thus exhibits a $1/r^3$ behavior.[333] For the heavier main group and transition elements the REP results are usually more reliable than the AREP+SO ones. For the cases reported the REP errors are usually clearly below 10%, with some exceptions in the 3d series (Sc $3d^1$ $4s^2$,17.8%; Cu $3d^9$ $4s^2$, 12.2%; Zn^+ $3d^9$ $4s^2$, 11.3%).[287,334−336] For many cases the AREP+SO approach performs quite well with errors of less than 15%, but a few very large deviations are observed (e.g., almost +40% for Y and La d^1 s^2). For lanthanides[337] and actinides[338] mostly p^1, d^1, and f^1 splittings were reported for up to 5-fold positive ions. Very large errors of up to 50% arise for the lanthanide REP d^1 splittings, whereas those for p^1 and f^1 are below 7% and 5%, respectively. The AREP+SO errors are usually larger. For the light actinides the REP d^1, p^1, and f^1 splittings have errors below 20%, 9%, and 5%, respectively. No corresponding results are available for the heavier actinides and the superheavy elements.[340] Since the above-mentioned results for excitation energies, ionization potentials, and SO splittings were obtained with finite basis sets, it is quite difficult to judge if errors are mainly because of the PPs or to the finite basis sets.

After the small-core PPs for Tl−Rn[335,336] were found to lead to too long bond distances in molecular calculations, a revised set with an improved representation of the 5f pseudovalence spinors was published and shown to lead to good agreement with AE results.[339] The more favorable results of the corresponding large-core PPs[335,336] were found to be due to a fortuitous error cancellation.

In addition to the basis sets originally published with the PPs, see Table 9, more extended basis sets have been published for some elements. Wallace et al. presented pVDZ basis sets for Li to Ar.[343] Pacios and Gomez optimized split-valence 311G basis sets for B−Ne, Al−Ar, and Ga−Kr and tested them in correlated molecular calculations.[344] Blaudeau and Curtiss devised correlation-consistent basis sets slightly larger than pVDZ quality for K, Ca, and Ga−Kr.[345] A corresponding pVDZ basis set for O was derived by Zhang et al.[350] Finally, Blaudeau et al. published correlation-consistent pVDZ and pVTZ basis sets for Cl and a corresponding pVDZ set for U. To better describe the pseudovalence orbitals near the nucleus and to avoid the coalescence of two exponents with nearly coefficients of nearly equal magnitude, but opposite sign, Cartesian Gaussian sd sets with 6 primitives were partly used.

The shape-consistent PPs of Christiansen, Ermler, and collaborators were extensively used by Balasubramanian to investigate the electronic structure of diatomic and small polyatomic molecules.[351,352] A number of review articles focusing on this PP approach and its applications is available in the literature.[10−12,22,353]

6.2.4. Effective Core Potentials of Hay and Wadt. A very popular PP set for main group and transition elements published by Hay and Wadt[326,354,355] is based on scalar-relativistic Cowan−Griffin (CG) AE calculations.[85] These PPs are especially attractive, since they are supplemented by quite compact valence basis sets. It should be noted that the large-core PPs for the 3d transition metals were adjusted to nonrelativistic HF AE data to be able to make a comparison to corresponding AE results. Corresponding scalar-relativistic PPs are also available for U, Np, and Pu.[356,357] Table 10 lists the available PPs and valence basis sets. Orbital (contraction) coefficients are provided for all original basis set exponents published together with the PPs. The parameters for PPs and basis sets are also available in electronic form from the EMSL database[296] (acronym LANL for Los Alamos National Laboratory; LANL1 and LANL2 for large and small-core transition metals PPs, respectively).

dx.doi.org/10.1021/cr2001383 |Chem. Rev. 2012, 112, 403–480

In the PP derivation of Hay and Wadt r_c in eq 111 is chosen to be near the outermost maximum of the AE valence orbital $\varphi_{v,l}$. The smooth radial function $f_l(r)$ adopted for $r < r_c$ is chosen similar to Christiansen et al.[325] as

$$f_l(r) = r^b g_l(r) = r^b \sum_{k=0}^{n} a_{l,k} r^k \quad (118)$$

with g_l being a fourth degree polynomial $(n = 4)$ and $b = l + 3$ in the nonrelativistic case. In the scalar-relativistic case $b = \lambda + 2$ was chosen, with

$$\lambda + 1 = \frac{1}{2}(1 - \delta_{0,l}) + \sqrt{l(l+1) + \frac{1}{4}(1 + \delta_{l,0})^2 + (\alpha Z)^2} \quad (119)$$

Here α denotes the fine structure constant. For relativistic s orbitals however the choice of $b = \lambda + 3$ and g_l being a fifth degree polynomial $(n = 5)$ has been found to lead to smoother pseudovalence orbitals. The five coefficients $a_{l,k}$ occurring for $l > 0$ in eq 118 are determined by requiring that $f_l(r)$ and its first 3 derivatives match the AE valence orbital $R_{v,nl}$ and its first 3 derivatives at r_c, and the pseudovalence orbital $|\varphi_P\rangle$ remains normalized. For the six coefficients $a_{0,l}$ in case $l = 0$ the necessary additional condition is that $f_l(r)$ and $R_{v,nl}$ also match at a neighboring point to r_c. With an appropriate choice of r_c and the above conditions it can be achieved that $R_{P,l}(r)$ is nodeless, has only two inflection points $(R''_{P,l}(r) = 0)$ and its second derivative has only three extrema $(R'''_{P,l}(r) = 0)$. Using the derived shape-consistent pseudovalence orbital the radial Fock eq 114 can be solved for the radial pseudopotential V_l^{PP} for each l value separately according to eq 108 in accord with the prescription of Kahn, Baybutt, and Truhlar.[194] A linear combination of radial Gaussian functions times powers of r according to eq 89 is then fitted with a least-squares procedure to the numerical potentials $\Delta V_l = V_l + Q/r$.

For the large-core transition metal PPs[326] Hay and Wadt compared HF $s^2d^n \rightarrow s^1d^{n+1}$ and $s^2d^n \rightarrow d^{n+2}$ excitation energies calculated with the Gaussian basis sets listed in Table 10 to AE finite difference HF (3d metals) and CG (4d and 5d metals) results. The PPs predict the ordering of the states correctly, however the $s^2d^n \rightarrow s^1d^{n+1}$ excitation energies are by 0.12 to 0.57 eV too low, except for V where a 0.08 eV too high value is obtained. The errors in the $s^2d^n \rightarrow d^{n+2}$ excitation energies are less systematic and range from −0.42 to 0.34 eV. Besides errors of the PPs, the small basis sets probably also cause the deviations. Based on results of AE FC calculations, see Table 4 for Ti, one would expect a better performance for the corresponding small-core PPs,[354] however neither for these nor for the main group PPs[355] a corresponding systematic comparison is available. At the finite difference HF level the small-core PP $s^2d^6 \rightarrow s^1d^7$ and $s^2d^6 \rightarrow d^8$ excitation energies of Ru deviate from WB AE HF reference data by only −0.06 and −0.13 eV, respectively,[147] however the corresponding errors for the heavier homologue Os are significantly larger. A corresponding comparison of various three-valence electron PPs for In gave a mean absolute error in excitation energies and ionization potentials of 0.18 eV for the Hay−Wadt PP.[280]

The GC-based PPs of Hay and Wadt are scalar-relativistic. Cohen et al.[238] and Wadt[137] proposed to account for spin−orbit (SO) effects using perturbation theory and an effective one-center one-electron operator adapted from AE calculations according to eq 88. Since the pseudovalence orbitals do not have the correct radial dependence in the spatial core region, the parameter Z^{eff} cannot be interpreted as an effective nuclear charge seen by an electron in a valence orbital. It rather has to be adjusted to reproduce atomic SO splittings and can attain very large values. In cases where the SO interaction does not lead to too large differences in the radial shapes of the $j = l - 1/2$ and $j = l + 1/2$ spinors, the application of this simple operator in first-order perturbation theory based on a scalar-relativistic PP calculation leads to reasonable, albeit not highly accurate multiplet splittings. Similar effective SO operators were proposed and tested for the main group and transition metal PPs of Stevens, Krauss, and collaborators by Koseki et al.[138−140] and Heinemann et al.[239]

For subsequent usage in molecular valence-only calculations compact valence basis sets were generated, see Table 10. In some cases the pseudovalence orbitals were fitted by using a nonlinear least-squares procedure, similar to the one for fitting the potentials, to a linear combination of Gaussian functions. In other cases an energy-optimization was performed for the ground state. Orbital expansion coefficients for the occupied shells are available for all exponents[326,354,355] and various contraction patterns can be generated. The basis sets and PPs are available from many databases with keywords beginning with LANL (Los Alamos National Laboratory). Mostly used are the HF contracted basis sets contracted of double-ζ quality, which are labeled LANL2DZ.[296]

Many authors supplemented the basis sets of Hay and Wadt with diffuse or polarization functions. In the present review we cannot report all work done on individual atoms, but rather restrict ourselves to sets of functions derived for a larger number of elements. A set of f polarization/correlation functions was optimized by Frenking and co-workers[358] for the small-core transition metal PPs[354] in CISD calculations for the lowest states of the $d^{n+1}s^1$ configurations. The contraction patterns used for

Table 10. Shape-Consistent GC-Adjusted Relativistic Effective Core Potentials of Hay and Wadt[a]

elements	core	n_c	n_v	basis set	ref
^{11}Na−^{18}Ar	[^{10}Ne]	10	1−8	(3s3p)	355
^{19}K, ^{20}Ca	[^{18}Ar]	18	1−2	(3s3p)	355
^{19}K−^{20}Ca	[^{10}Ne]	10	9−10	(5s5p)	354
^{21}Sc−^{30}Zn	[^{18}Ar]	18	3−12	(3s2p5d)	326
^{21}Sc−^{30}Zn	[^{10}Ne]	10	11−20	(5s5p5d)	354
^{31}Ga−^{36}Kr	[^{18}Ar] 3d^{10}	28	3−8	(3s3p)	355
^{37}Rb, ^{38}Sr	[^{36}Kr]	36	1−2	(3s3p)	355
^{37}Rb−^{38}Sr	[^{18}Ar] 3d^{10}	28	9−10	(5s5p)	354
^{39}Y−^{48}Cd	[^{36}Kr]	46	3−12	(3s3p4d)	326
^{39}Y−^{48}Cd	[^{18}Ar] 3d^{10}	28	11−20	(5s5p4d)	354
^{49}In−^{54}Xe	[^{36}Kr] 4d^{10}	46	3−8	(3s3p)	355
^{55}Cs−^{56}Ba	[^{36}Kr] 4d^{10}	46	9−10	(5s5p)	354
^{55}Cs, ^{56}Ba	[^{54}Xe]	54	1−2	(3s3p)	355
^{57}La	[^{54}Xe]	54	3	(3s3p3d)	326
^{57}La	[^{36}Kr] 4d^{10}	46	11	(5s5p3d)	354
^{72}Hf−^{80}Hg	[^{54}Xe] 4f^{14}	68	4−12	(3s3p3d)	326
^{72}Hf−^{80}Hg	[^{36}Kr] 4d^{10}4f^{14}	60	12−20	(5s5p3d)	354
^{81}Tl−^{83}Bi	[^{54}Xe] 4f^{14}5d^{10}	78	3−5	(3s3p)	355
^{81}Tl	[^{54}Xe] 4f^{14}	68	13	(3s3p3d)	355
^{92}U−^{94}Pu	[^{54}Xe] 4f^{14}5d^{10}	78	14−16		356, 357

[a] A nonrelativistic parametrization was used for the 3d transition metals.

dx.doi.org/10.1021/cr2001383 |Chem. Rev. 2012, 112, 403–480

the (5s5p5d), (5s5p4d), and (5s5p3d) primitive sets were (441/2111/41), (441/2111/31), and (441/2111/21) for the 3d, 4d, and 5d elements, respectively. In a related article Frenking and co-workers[359] optimized f polarization/correlation functions for large-core PPs of Zn, Cd, and Hg.[326] For the (3s2p5d), (3s3p4d), and (3s3p3d) primitive sets, the contraction patterns (21/11/41), (21/21/31), and (21/21/21) were used for Zn, Cd, and Hg, respectively. In the same publication, optimized d polarization/correlation functions for the group 13 to 18 main group elements PPs of Al to Bi[355] were presented. The (3s3p) primitive set was contracted as (21/21). Finally, for the alkaline and alkaline earth elements K, Ca, Rb, Sr, Cs and Ba d polarization/correlation functions were optimized for the (5s5p) primitive sets using a (441/2111) contraction pattern. It was found that the optimized exponents are not too different from those of AE basis sets, thus implying that polarization/correlation functions of AE basis sets could also be used for ECPs. Sunderlin and co-workers[360] published (d) polarization and (p) diffuse basis functions for the group 14−17 main group element PPs[355] for DFT/B3LYP, as well as MP2 calculations. Recommended values for the exponents were published and found to be similar to values obtained, for example, by Frenking and co-workers[359] for d polarization functions for the Wadt and Hay PPs or by Martin and Sundermann[300] for energy-consistent PPs. The addition of polarization and diffuse basis functions to the Hay and Wadt basis sets was found to lead to substantially improved results for electron affinities, bond lengths and energies, as well as vibrational frequencies.[360] Hu and Huang reported (d) polarization and (p) diffuse basis functions for rare gas elements.[361]

Recently, Roy, Hay and Martin proposed revised basis sets for the Hay and Wadt PPs,[354,355] which are especially suited for density functional calculations.[362] For the small-core transition metal PPs the (5s5p5d), (5s5p4d) and (5s5p3d) primitive basis sets were contracted to [5s5p3d], [4s4p3d], and [4s4p3d] for the first, second, and third transition metal series, respectively, and bear the name LANL2TZ. In case of the second and third row, one of two nearly linear dependent p exponents had to be eliminated. Diffuse d functions were proposed for the first transition metal series leading to the LANL2TZ+ basis sets. For the main group elements the use of the uncontracted original primitive sets, labeled as LANL08, was recommended. The addition of polarization functions[358−360] then leads to LANL2TZ(f) and LANL08(d) sets for transition metals and main group elements, respectively. The revised DFT-adapted basis sets have successfully been tested for some transition metal carbonyls and organometallic compounds[362] and are available from the EMSL basis set compilation.[296]

6.2.5. Pseudopotentials of Barthelat, Durand, and Co-workers. Durand and Barthelat pioneered the shape-consistent PP approach. In 1974, they required the pseudovalence orbitals to coincide at best with the true valence orbitals in the atomic valence region,[220] and in 1975, they formulated pseudovalence orbitals as a linear combination of the original valence orbital, core orbitals and, at variance with the PK prescription eq 63, also virtual orbitals.[221] The pseudovalence orbitals $|\varphi_p\rangle$ were determined from the AE valence orbitals $|\varphi_v\rangle$ by minimizing the functional

$$S = \langle \varphi_p - \varphi_v | \varphi_p - \varphi_v \rangle_{r_c} \text{ with } \langle \varphi_p | \varphi_p \rangle = 1 \qquad (120)$$

The subscript r_c denotes that the above integral is to be evaluated for $r \geq r_c$, where r_c is the radius at which the radial parts of the valence orbital and outermost core orbital of the same symmetry intersect. Initially, Barthelat and Durand determined their pseudovalence orbitals $|\varphi_p\rangle$ as linear combinations of AE Slater orbitals $|\chi_i\rangle$, that is

$$|\varphi_p\rangle = \sum_{i=1}^{n} C_i |\chi_i\rangle \qquad (121)$$

The constraint minimization of eq 120, taking eq 121 into account, leads to a system of linear equations

$$\sum_{j=1}^{n} [\langle \chi_i | \chi_j \rangle_{r_c} - \lambda \langle \chi_i | \chi_j \rangle] C_j = \langle \chi_i | \varphi_p \rangle_{r_c} \qquad (122)$$

which is solved iteratively.[221] Here λ denotes a Lagrangian multiplier. From the generated pseudovalence orbitals the radial PPs can be obtained by inverting the radial Fock equation. The approach was later extended to account for relativistic effects, including SO effects.[222] The corresponding reference data was obtained by algebraic calculations using a second-order Dirac equation.[86]

To arrive at compact Gaussian expansions for $\hat{\tilde{V}}^{PP}$ Durand and Barthelat proposed a quite useful overlap-energy criterion,[221,240] that is, the minimization of the following operator norm

$$||\hat{\mathcal{O}}|| = \langle \varphi_p | \hat{\mathcal{O}}^2 | \varphi_p \rangle^{1/2} \text{ with}$$
$$\hat{\mathcal{O}} = \tilde{\varepsilon}_v |\tilde{\varphi}_p\rangle\langle\tilde{\varphi}_p| - \varepsilon_v |\varphi_p\rangle\langle\varphi_p| \qquad (123)$$

The prescription can be applied for the *l*- as well as for the *lj*-dependent case. The quantities without tilde are obtained with the exact V_l^{PP} or V_{lj}^{PP} from a radial Fock equation such as eq 114, whereas those with tilde are calculated with an analytical potential $\tilde{V}_l^{PP}$ or $\tilde{V}_{lj}^{PP}$. Nonrelativistic PPs for Li to Ar[221] and for Li to Kr as well as for I[240] were generated according to this scheme. In the more recent work only one or two Gaussian terms per *l* value were needed to have an operator norm $||\hat{\mathcal{O}}||$ below 7×10^{-3} for all cases. The PPs were tested for halogen dimers X_2 (X = F, Cl, Br, I),[363] as well as for the transition metal compounds ScH_3, TiH_3F, $MnO4^-$, $Zn(CH_3)_2$, and $Pd(CO)_4$.[364] The construction of a Cu PP for usage with minimal basis sets was investigated and tested for Cu_2 and CuF.[365]

Revised PPs as well as 31G[366] and 21G[367] double-ζ basis sets were derived for Li−Ca and Ga−Kr. The PPs and basis sets were successfully tested for 30 small molecules, where good agreement of the PP 31G results with AE 6-31G reference data for geometries, atomization energies, force constants, and dipole moments was found. The PPs and 21G basis sets were also tested for periodic Hartree−Fock calculations of various solids. A relativistic extension of the method was based on a relativistic analytical SCF procedure for atoms based on the second-order Dirac equation, which was developed by Barthelat, Pélissier and Durand.[86] Corresponding scalar-relativistic PP calculations for InH_n, TlH_n (n = 1,3) and SnH_n, Pb_n (n = 2,4) were mentioned and results for corresponding calculations on Sc, Cr, Cu, and CrH, CuH were reported.[368] PPs parameters of this type as well as a valence basis set were published for F.[369] In case of I both a scalar-relativistic PP and a corresponding SO operator were derived[370] and tested in SO CI calculations with the CIPSO method[371] for ground and excited states of CH_3I[370] and I_2.[372] Maron and Teichteil derived PPs for the halogen atoms from relativistic AE DHF/DC calculations.[373] In this work it was also attempted to include a part of the core polarization effects into

dx.doi.org/10.1021/cr2001383 |Chem. Rev. 2012, 112, 403–480

the PPs. Unfortunately no larger sets of relativistic PPs and valence basis sets were generated by the Toulouse group. However, the overlap-energy criterion eq 123 developed by Durand and Barthelat[221,240] was later very successfully applied by Stevens and co-workers[286,374,375] to generate DHF/DC based scalar-relativistic PPs for the elements Li to Rn, which are described below in section 6.2.6. The criterion was also used by Lester and co-workers to derive PPs for QMC calculations,[376,377] which are described in section 6.4.

Barthelat, Illas and co-workers generated a Pt one-electron PP modeling a Pt^+ core with a fixed d^9 configuration.[378] The PP was, supplemented by a *l*-dependent CPP and a core−core/nucleus repulsion correction, relatively successfully applied in HF, MP2 and FCI calculations of PtH, Pt_2 and PtH_2. The results indicate that it might be a useful tool for modeling Pt surfaces, e.g., for studies of heterogeneous catalysis. A simple model consisting of five quadrupoles, one for each d-shell, multiplied by an occupancy was proposed by Sellers and Ove to account for the anisotropy of such an open d shell core in such PP or MP calculations.[379]

6.2.6. Relativistic Compact Effective Potentials of Krauss, Stevens, and Co-workers. A relatively complete set of compact shape-consistent PPs using a prescription analogous to Christiansen et al.[325] for the construction of nodeless pseudovalence spinors from HF or DHF/DC AE reference calculations and analogous to the one given by Barthelat et al.[240] for the generation of compact expansions of the PPs as linear combination of Gaussian functions has been published by Stevens and co-workers.[286,374,375] Whereas the PPs for the first- and second-row elements were parametrized nonrelativistically,[374] those for the third, fourth, and fifth row elements[286] and the lanthanides[375] were parametrized relativistically. A relativistic PP for U was also reported and applied in calculations on diatomics such as UH, UO or UF.[380,381] Table 11 summarizes the available PPs and valence basis sets. Orbital (contraction) coefficients are provided for all original basis set exponents published together with the PPs. The PP and basis set parameters are also available in electronic form from the EMSL database[296] (acronym SBKJC for Stevens, Basch, Krauss, Jasien, Cundari). A review of early applications of the PPs was published by Krauss and Stevens.[9]

The procedure of Stevens et al.[286] to generate nodeless pseudovalence spinors from results of DHF/DC AE[80] valence spinors is similar to the prescription by Christiansen et al.,[325] with a few small modifications. The large components of the valence j-dependent spinors were used to construct nodeless pseudovalence spinors. The r_c was chosen as close as possible to the outermost radial density maximum of the DHF valence spinor, and the smooth radial function $f_{lj}(r)$ had a leading cubic term for s, p, and d, as well as a leading quartic term for f spinors. The pseudovalence spinors were generated on the same grid as used in the AE calculations and expanded in a large even-tempered basis set. Relativistic PPs were obtained by inverting the radial Fock equation eq 114 in this basis set and then averaged according to eq 82. As usual atomic ions had to be used in some cases in order to avoid nodes in pseudovalence orbitals and corresponding singularities in the PPs. The resulting averaged PPs, as well as the averaged pseudovalence spinors and the corresponding spinor energies were considered to be exact and used as reference data. The proposal to use an optimization procedure based on an energy-overlap functional of Durand and Barthelat[221,240] was followed to generate compact expansions of the radial PPs in Gaussian functions. Using the same even-tempered basis set as above the atomic radial HF problem was solved for an approximate PP in analytical form, whereas the Coulomb and exchange operators $\hat{W}$ were constructed from the exact pseudovalence orbitals. Then eq 123 was minimized with respect to the parameters in the analytical ansatz for the PP. In contrast to Christiansen et al. or Hay and Wadt, who used a least-squares fit of Gaussian functions to the PP tabulated on a grid and often ended up with six or more Gaussians per *l*-value, no more than three Gaussians per *l*-value were needed for the resulting relativistic compact effective potentials (RCEPs). The overlap between exact and approximate pseudovalence orbitals was larger than 0.99999 and the difference between exact and approximate eigenvalues was less than 0.001 hartree.

Table 11. Shape-Consistent DHF/DC-Adjusted Relativistic Effective Core Potentials of Stevens and Co-workers[a]

elements	core	n_c	n_v	basis set	ref
^{3}Li−^{10}Ne	[^{2}He]	2	1−8	(4sp)/[2sp]	374
^{11}Na−^{18}Ar	[^{10}Ne]	10	1−8	(4sp)/[2sp]	374
^{19}K, ^{20}Ca	[^{18}Ar]	18	1−2	(4sp)/[2sp]	286
^{21}Sc−^{30}Zn	[^{10}Ne]	10	11−20	(8sp6d)/[3sp3d]	286
^{31}Ga	[^{10}Ne]	10	21	(8sp6d)/[4sp3d]	286
^{31}Ga−^{36}Kr	[^{18}Ar] 3d^{10}	28	3−8	(5sp)/[2sp]	286
^{37}Rb, ^{38}Sr	[^{36}Kr]	36	1−2	(4sp)/[2sp]	286
^{39}Y−^{48}Cd	[^{18}Ar] 3d^{10}	28	11−20	(8sp5d)/[3sp3d]	286
^{49}In	[^{18}Ar] 3d^{10}	28	21	(8sp5d)/[4sp3d]	286
^{50}Sn−^{54}Xe	[^{36}Kr] 4d^{10}	46	4−8	(5sp)/[2sp]	286
^{55}Cs, ^{56}Ba	[^{54}Xe]	54	1−2	(4sp)/[2sp]	286
^{57}La	[^{36}Kr] 4d^{10}	46	11	(9sp5d)/[3sp3d]	286
^{58}Ce−^{71}Lu	[^{36}Kr] 4d^{10}	46	12−25	(6sp3d7f)/[4sp2d2f]	375
^{72}Hf−^{80}Hg	[^{36}Kr] 4d^{10}4f^{14}	60	12−20	(7sp5d)/[4sp3d]	286
^{81}Tl	[^{36}Kr] 4d^{10}4f^{14}	60	21	(8sp5d)/[4sp3d]	286
^{82}Pb−^{86}Rn	[^{54}Xe] 4f^{14}5d^{10}	78	4−8	(5sp)/[2sp]	286

[a] A nonrelativistic HF-adjustment was performed for Li−Ar.

Large cores were used for the alkaline and alkaline earth elements Li−Cs and Be−Ba, which were treated as one- and two-valence electron systems, respectively.[286,374] Parameters for an effective CPP eq 97 to 99 of the type proposed by Meyer and co-workers[178,179] were adapted to experimental data.[286] The authors note, however, that these large-core PPs have to be used with care in cases of strong ionic bonding, since the exchange repulsion between the metal cation core modeled by the PP and the ligand electrons is underestimated for small metal−ligand distances.[286] This finding agrees with results of other authors.[281,354]

Large cores were also used for the group 13 to 18 main group elements, except for the group 13 post-d elements, where the small-core definition of the transition metals was recommended.[286] The small-core choice for the group 13 post-d elements is also shared by other researchers.[280,282] Small cores were also chosen for the transition metals, in analogy to the PPs derived by other groups.[147,283,287,334−336,354] In case of the lanthanides Ce−Lu an intermediate core was applied, that is, the 4f, 5s, 5p, 5d, and 6s shells were assigned to the valence shell.[375]

Figures 14−16 and Figures 17 and 18 compare the radial potentials and pseudovalence orbitals of a small-core shape-consistent RECP for Ti to corresponding curves obtained for other approaches.

dx.doi.org/10.1021/cr2001383 |*Chem. Rev.* 2012, 112, 403–480

Basis sets of double-ζ quality with equal exponents for s and p expansions, and triple-ζ quality for the d expansions were optimized for the main group and transition metal PPs.[286] For lanthanides a quadruple-ζ contraction of the common s and p exponents, as well as a double-ζ contraction of the d and f exponents was recommended.[375] It was found that a relatively large number of six, seven, and eight Gaussians was needed to describe the 4f shell of the early, middle and late lanthanides. As a compromise contractions based on seven Gaussians were generated.

Atomic tests were published for transition metal atoms, that is, energy differences between the lowest LS states of the neutral atom $d^n s^2$, $d^{n+1} s^1$, and cation d^{n+1} configurations (group 3−10), neutral atom $d^9 s^2$, $d^{10} s^1$ and cation $d^9 s^1$, d^{10} configurations (group 11), as well as neutral atom $d^{10} s^2$ and cation $d^9 s^2$ configurations (group 12) were evaluated using the PPs and optimized valence basis sets. The errors compared to the AE CG data of Martin and Hay[158] are for most cases less than 0.1 eV and amount to at most 0.17 eV,[286] proving the good quality of the derived compact PPs. For the lanthanides Ln^{2+} $4f^n 5d^1 \rightarrow Ln^{3+}$ $4f^n$ ionization energies calculated with the PPs and corresponding valence basis sets exhibit errors between 0.04 eV (Ce) and 0.19 eV (Lu) in comparison to finite difference AE DHF/DC reference data.[375] In view of the small FC errors for this process, see Table 4, one might expect that the errors partly also arise from the applied valence basis sets.

The PPs of Stevens and co-workers are scalar-relativistic. The authors recommend to treat SO effects using the effective one-electron AE SO term eq 88 as proposed by Wadt.[137] Parameters for the effective nuclear charges Z_{eff} were derived by Koseki et al.[138] for main group elements by adapting to experimental fine structure splittings of Π states of diatomic hydrides. The SO terms were tested for over 120 diatomics in perturbation theory using a MCSCF wave function. The comparison to corresponding AE results is quite favorable, whereas with respect to the available experimental data for 61 cases errors of 10% or less were observed. For other 25 cases the errors were 30% or less and for 26 cases they amounted to more than 30%. Corresponding parameter sets were also reported for the 3d, 4d and 5d transition metal atoms[139] and calibrated against results obtained with the full Breit−Pauli Hamiltonian.[140] Work using an effective one-electron AE SO term was also published by Heinemann et al. for the Pt atom.[239]

The usage of SO terms as suggested, for example, by Lee et al.[235] or by Hafner and Schwarz,[234] was investigated for C and Si by Stevens and Krauss,[382] but obviously not further pursued. Whereas the p SO term for C represented the usual $1/r^3$ radial behavior moderated by two-electron screening terms, the corresponding p SO term of Si looked very different, depending on how the pseudovalence orbital was constructed.

6.2.7. Generalized Relativistic Effective Core Potentials of Titov, Mosyagin, and Co-workers. Small cores have to be used in case of transition metals, lanthanides and actinides in order to keep FC errors in PP calculations below a required threshold. For small cores, however, more than a single occupied pseudovalence orbital of the same *lj* combination may be present in suitable reference states, that is, states for not too highly charged ions. Therefore one or more pseudovalence orbitals may have a radial node, which would lead to singularities in the PP, if it is determined by inversion of the Fock equation eq 114. Most shape-consistent PPs are therefore derived for positive ions, which are chosen in such a way that this problem does not occur. However, if the ions are highly charged, frozen-core (FC) errors arise for the derived PP when it is transferred from the ions to the neutral atoms or molecules. A solution to this problem is attempted in the so-called generalized relativistic ECP (GRECP) approach of Titov, Mosyagin, and co-workers,[331,383−385] where the PP is interpolated in a vicinity of the pseudospinor node.[331] If more than one pseudospinor per *lj* is available, more than one radial PP for this *lj* combination can be derived. The GRECP approach therefore employs the idea of separating the orbital space of a heavy atom into three regions: inner core, outer core, and valence, which are treated differently. The idea to partition into these three regions appeared already in 1985 in work of Andzelm et al.[386] on MPs of the Huzinaga type; however, the approach is currently not further pursued.

The GRECP operator to be used in atomic calculations is written in the form[331]

$$\begin{aligned}\Delta V_{\mathrm{GRECP}}(i) &= V_{n_v LJ}(r_i) + \sum_{l=0}^{L} \sum_{j=|l-1/2|}^{l+1/2} [V_{n_v lj}(r_i) - V_{n_v LJ}(r_i)] \hat{P}_{lj}(i) \\ &+ \sum_{n_{oc}} \sum_{l=0}^{L} \sum_{j=|l-1/2|}^{l+1/2} [[V_{n_{oc},lj}(r_i) - V_{n_v,lj}(r_i)]\, \hat{\tilde{P}}_{n_{oc},lj}(i) \\ &+ \hat{\tilde{P}}_{n_{oc},lj}(i)[V_{n_{oc},lj}(r_i) - V_{n_v,lj}(r_i)]] \\ &- \sum_{n_{oc},n'_{oc}} \sum_{l=0}^{L} \sum_{j=|l-1/2|}^{l+1/2} \hat{\tilde{P}}_{n_{oc},lj}(i) \left[\frac{V_{n_{oc},lj}(r_i) + V_{n'_{oc},lj}(r_i)}{2} \right. \\ &\left. - V_{n_v,lj}(r_i) \right] \hat{\tilde{P}}_{n'_{oc},lj}(i) \end{aligned} \tag{124}$$

Here n_v and n_{oc} are the principal quantum numbers for valence and outer core orbitals, respectively. The maximum J and L quantum numbers are related by $J = L + 1/2$. $\hat{P}_{lj}$ is the projector on the spinor spherical harmonics $|ljm\rangle$

$$\hat{P}_{lj}(i) = \sum_{m=-j}^{m=j} |ljm\rangle\langle ljm| \tag{125}$$

where as $\hat{\tilde{P}}_{n_{oc},lj}$ is the projector on the outer core pseudospinors

$$\hat{\tilde{P}}_{n_{oc},lj}(i) = \sum_{m=-j}^{m=j} |\widetilde{n_{oc},ljm}\rangle\langle\widetilde{n_{oc},ljm}| \tag{126}$$

The GRECPs combine the standard semilocal form of the PPs with additional nonlocal terms to take into account the difference between the effective potentials acting on the outer core and valence electrons with the same *l* and *j* quantum numbers.

For application of the GRECP to molecular calculations the GRECP operator is often rewritten as a sum over spin-free (averaged) and spin-dependent parts.[331] A number of GRECPs accounting also for contributions of the Breit interaction have been published recently for U, Pu, and the superheavy elements 112, 113, 114.[103,175] An extension of the method is the self-consistent GRECP approach, which aims to reduce the d- or f-occupation number dependence of the errors by mixing GRECPs adjusted for two different configurations depending on the occupation number of the d or f shell under consideration.[103,331,384] An occupation number dependence to reduce errors in large-core transition metal PPs was also discussed previously in 1974 by Schwarz and co-workers.[191] Another correction to be applied for fine structure splittings, the term splitting correction, corrects the one- and two-electron

dx.doi.org/10.1021/cr2001383 |Chem. Rev. 2012, 112, 403–480

integrals of a shell between pseudovalence spinors under consideration by using the corresponding integrals evaluated at the AE level.[103,331] The basic idea to replace integrals over pseudovalence orbitals by their AE counterparts was also used earlier by Marian and Wahlgren[142] and Schimmelpfennig et al.[143]

The parametrized form of the GRECPs contains a relatively large number of parameters, which easily can exceed 100 for heavier elements. Parametrizations are available for a few heavy elements (Ba, Yb, Au−Rn, Th, U, Cn, Eka-Tl−Eka-Bi) on the webpages of the Titov group.[387] If this more complex valence-only model Hamiltonian also leads to higher accuracy compared to the usual semilocal ansatz has to be carefully investigated. Since the GRECP ansatz is at present not supported by most of the standard quantum chemistry codes, such tests and applications of GRECPs are still scarce and were performed mainly by the authors of the method.[103,388−392] Some limited investigation for U and Pu suggests that the GRECP ansatz is quite accurate, but still suffers from f occupation number dependent errors of up to ∼0.1 eV in energy differences (excitation energies, ionization potentials) when the 5f occupation is changed,[103] which might result from the single reference state used to extract the GRECP and is not present, for example, when more reference states are used as in the energy-consistent PP scheme.[31,393]

6.3. Pseudopotentials Including Implicitly Correlation Contributions

Initially pseudopotentials were adjusted to reproduce experimental data, see, for example, Hellmann.[73] In a 1981 publication of shape- and Hamiltonian-consistent PPs Goddard and co-workers stated that the usage of PPs is "*charmingly seductive, not unlike the sirens of Greek mythology*".[332] From time to time researchers are actually seduced to include more than the modeling of a HF core and the implicit inclusion of relativistic effects into the PP approach. Clearly, all semiempirically adjusted PPs, for example, the one derived by Hellmann for K in 1935,[73] contain implicitly core−valence correlation effects. These are however overestimated, if more than one valence electron is treated with such an empirical PP,[195] and should better be treated with CPPs described in section 5.5. In the following, we, therefore, focus on the modification of ab initio PPs to account implicitly also for (some) correlation contributions.

In the 1970s, Goddard and co-workers, mainly motivated by the lack of sufficient computer power to evaluate differential correlation contributions in transition metals systems at the ab initio level, proposed modified effective (core) potentials (MEPs) for Ni (and Fe), which are ab initio PPs supplemented by additional terms accounting for intra-atomic electron correlation effects.[394−396] Although several applications to molecules, that is, NiO, NiCO, and Ni_2, were reported, the details of the approach were not published. Basch and Osman followed the ideas of Goddard and co-workers and adjusted an Ar-core MEP for Cu, by adding semilocal terms adjusted so that the energy separations between low-lying states of Cu, Cu^+ and Cu^{2+} with differing 3d and 4s occupations agree better with experimental data[397] compared to the original compact effective (core) potential (CEP).[219]

The Toulouse group reported also some work, where the usual PP approach was modified to include additional contributions. Mahé and Barthelat proposed as hybrid shape-consistent/energy-consistent PP adjustment procedure, using scalar-relativistic reference data, and applied it to Cu.[398] The pseudovalence orbitals were derived for a single reference state similar to the method described above, and the scalar-relativistic HF energy differences between the $3d^9 4s^2\ ^2D$, $3d^{10}4s^1\ ^1S$, $3d^9 4s^1 4p^1\ ^4P$, and $3d^8 4s^2\ ^3F$ states were fitted using a modification of the original scheme of Durand and Barthelat.[221] In the same work Cu PPs are discussed which account for a part of the atomic dynamic correlation energy, that is, correlation of the 3s and 3p shells, at the CI or MP2 level. The hybrid PP and the correlation corrected PPs were successfully applied to Cu excitation and ionization energies as well as to CuH, Cu_2, Cu_2^+, CuF, and CuCl. The CuX and Cu_2X series (X = O, S, Se, Te, Po) were also investigated.[399]

6.4. Pseudopotentials for Quantum Monte Carlo Calculations

Quantum Monte Carlo (QMC) methods[400,401] use random walks to sample the Schrödinger equation. In the fixed-node pure diffusion QMC approach an approximate solution of the Schrödinger equation is simulated by constructing a random walk which generates distributions weighted by a known trial wave function $\Psi_T(\vec{R})$. Here $\vec{R}$ is a $3n$ dimensional vector representing the electronic coordinates in real space. Within the fixed-node constraint the distribution evolving for very long imaginary time is exact. The expectation value of the Hamiltonian $\hat{H}$ is obtained during the QMC process as a statistical average of the local energy $E_{local} = \hat{H}\Psi_T(\vec{R})/\Psi_T(\vec{R})$.

Since about two decades PPs in semilocal form are also frequently applied in QMC calculations,[402−407] mainly since they reduce the number of electrons to be dealt with, as well as the fluctuations of the local energy E_{local} in the core region, thus enhancing the computational efficiency. A scheme to use PPs with a nonlocal form in variational QMC for solids was developed by Fahy et al.[408−410] The computational effort of a QMC calculation for an n-electron system scales approximately as $O(n^3)$. For the additional Z^x scaling of the computational effort with nuclear charge Z the exponent is reduced from $x \approx 5.5$ — 6.5 to $x \approx 3.4$ when the atomic cores are replaced by PPs.[402] Especially suited are so-called soft PPs which avoid $1/r$ and $1/r^2$ singularities at the core in the effective one-electron potential. In view of the evaluation of the energy by sampling the local energy it is also desired to keep the PPs as local as possible, that is, to keep L in eq 78 as small as possible and the corresponding radial potentials eq 89 as compact as possible. In addition the number of Gaussians in the expansion should be kept as small as possible. There is also evidence that HF- or DHF-adjusted PPs give better results in diffusion QMC calculations than DFT/LDA-based PPs.[376]

6.4.1. Pseudopotentials of Lester and Co-workers.

Nonrelativistic PPs meeting these requirements have been derived a decade ago using the shape-consistent approach for Be to Ne and Al to Ar by the group of Lester.[376,377] The part $f_l(r)$ of the radial part $R_{p,l}$ of the pseudovalence orbital $|\varphi_{p,l}\rangle$ in the core region $r < r_c$ in eq 111 is taken as

$$f_l(r) = r^l \sum_{k=0}^{4} a_k r^{2k} \tag{127}$$

The five parameters a_k are used to satisfy the normalization constraint and to match the AE valence orbital $\varphi_{v,l}$ and its first three derivatives at r_c. Because of the choice of only even powers in eq 127 and a leading power of 0, there is no singularity of the kinetic energy at $r = 0$ and the corresponding PP is finite and

dx.doi.org/10.1021/cr2001383 |Chem. Rev. 2012, 112, 403–480

smooth. In order to compensate the $-Q/r$ Coulomb potential the analytic PP for L in eq 78

$$V_L(r_i) = r_i^{-2} \sum_k A_{L,k} r_i^{n_{L,k}} e^{-a_{L,k} r_i^2} \quad (128)$$

has to have parameters $A_{L,1} = Q$, $n_{L,1} = 1$, $A_{L,2} = Qa_{L,1}$, $n_{L,2} = 3$, and $a_{L,2} = a_{L,1}$. The first term cancels the Coulomb singularity within some distance from the nucleus controlled by $a_{L,1}$, which remains as a free parameter. The second term is included to cancel the cusp of $-Q/r + V_L(r)$ at $r = 0$. Only a semilocal s term was used, e.g., $L = 1$ was chosen. Lester and co-workers used, with a slight modification, the overlap-energy criterion eq 123 proposed by Durand and Barthelat[221,240] to determine the remaining free PP parameters. In atomic test calculations AE HF ionization potentials and electron affinities were reproduced with mean absolute errors (m.a.e.) of 0.017 and 0.015 eV, respectively. For the DHF/DC adjusted shape-consistent PPs of Stevens and co-workers[286] the m.a.e. were 0.022 and 0.010 eV, whereas for the energy-consistent WB adjusted PPs of Bergner et al.[148] the m.a.e. amounted to 0.011 and 0.016 eV.[377] A small bias might arise from the comparison of nonrelativistic and relativistic results.

6.4.2. Pseudopotentials of Trail and Needs. Nondivergent shape-consistent DHF/DC averaged relativistic PPs and corresponding SO terms, for H to Ba and Lu to Hg were generated by Trail and Needs.[411,207] The shape-consistent prescription eq 111 was slightly modified, that is,

$$R_{p,lj}(r) = \begin{cases} [G_{v,lj}(r)^2 + F_{v,lj}(r)^2]^{1/2} & \text{for } r \geq r_c \\ f_{lj}(r) & \text{for } r < r_c \end{cases} \quad \text{and } \varepsilon_{p,lj} = \varepsilon_{v,lj} \quad (129)$$

where $G_{v,lj}$ and $F_{v,lj}$ denote the upper and lower radial components of the DHF spinor $|\varphi_{v,lj}\rangle$. Equation 129 preserves exactly the valence charge density outside of the core region. Trail and Needs report that the core radius r_c was usually chosen to be $r_c = r_n + 0.9(r_m - r_n)$, where r_n and r_m denote the position of the outermost node and the outermost maximum (of probably $G_{v,lj}$), respectively. The smoothing function $f_{lj}(r)$ was chosen according to the Troullier–Martins scheme[330] as

$$f_{lj}(r) = r^{l+1} \exp\left(\sum_{m=0}^{6} c_{2m} r^{2m} \right) \quad (130)$$

The factor r^{l+1} ensures that no $1/r^2$ singularity occurs in the PP, whereas $c_1 = 0$ ensures that no $1/r$ singularity is present. Terms with r^{2m+1} in the sum have been excluded to prevent the appearance of a cusp of any order at the origin. The seven coefficients were determined by the norm-conservation within r_c, continuity of $R_{p,lj}$ and its four derivatives at r_c, as well as a zero curvature of the resulting potential at the origin.

Instead of simply inverting the radial Fock equation, Trail and Needs applied a more refined procedure,[411] which also eliminates long-range nonlocal contributions due to the HF or DHF nonlocal exchange interaction, that is, generates a potential which is nonlocal only close to the core. The analytical PPs were finally obtained by applying an extended overlap-energy criterion eq 123, that is,

$$\Sigma = \sum_p \langle \varphi_p | \hat{\mathcal{O}}^2 | \varphi_p \rangle \text{ with}$$
$$\hat{\mathcal{O}} = \tilde{\varepsilon}_v |\tilde{\varphi}_p\rangle\langle\tilde{\varphi}_p| - \varepsilon_v |\varphi_p\rangle\langle\varphi_p| \quad (131)$$

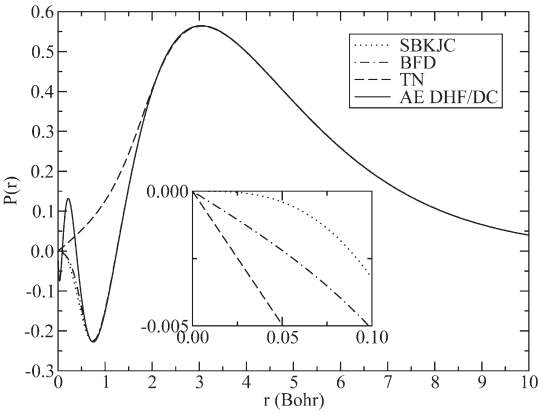

Figure 19. Radial 4s functions for various small-core Ti PPs in comparison to the large component from AE DHF/DC calculations: standard shape-consistent DHF/DC-adjusted PPs of Stevens et al. (SBKJC),[286] and QMC-adapted shape-consistent DHF/DC-adjusted PP of Trail and Needs (TN)[207] and WB-adjusted energy-consistent PP of Burkatzki et al. (BFD).[154]

In contrast to the original formulation of Durand and Barthelat[221,240] Trail and Needs use a sum over all pseudovalence orbitals in the minimized functional Σ, instead of separate optimizations for each pseudovalence orbital. Still the expansions are relatively long and contain 16 terms each for the local PP as well as the semilocal s and p PPs. The fact that the d-projector was taken to be local might lead to inaccuracies especially for wave function-based correlated calculations of the heavier d transition elements.

The Ti small-core PP of Trail and Needs was not included into the comparison of the PPs in Figures 14–16, since its core definition ([Mg]) does not match the one of the other PPs ([Ne]). The 3d and 4s pseudovalence orbitals however can be compared, see Figures 19 and 20. The nodeless 4s pseudovalence orbital of the Trail and Needs PP deviates inside $r \approx 2$ Bohr from the AE DHF large component, whereas this is the case only inside $r \approx 0.7$ Bohr for the other PPs using the Ne-core. Both QMC-adapted PPs deviate for 3d inside $r \approx 1.3$ Bohr from the AE reference, whereas the agreement for the standard PP of Stevens et al. is essentially perfect. The lack of shape-consistency occurring for shape-consistent QMC-adapted PPs as well as also for the corresponding energy-consistent PPs described in the following section can be attributed in this case to the requirements imposed to eliminate the Coulomb singularity at the nucleus. Accuracy is thus sacrificed to computational efficiency.

Valence basis sets for the Trail–Needs PPs were not reported to our knowledge. The PPs are available from the CASINO QMC code homepage.[412] On this page also PPs with smaller cores are provided, for example, for the transition elements, and a relatively large amount of atomic calibration data is provided for every PP.

6.4.3. Pseudopotentials of Burkatzki, Filippi, and Dolg. Finally energy-consistent scalar-relativistic WB adjusted PPs for main group and 3d transition metals were published by Burkatzki et al.[152,154] The $1/r$ singularity at the origin was removed and the local PP was restricted to be finite and behave quadratically for small r

$$V_L(r_i) = \frac{Q}{r_i} e^{-a_{L,1} r_i^2} + Q a_{L,1} r_i e^{-a_{L,2} r_i^2} + A_{L,3} e^{-a_{L,3} r_i^2} \quad (132)$$

dx.doi.org/10.1021/cr2001383 |Chem. Rev. 2012, 112, 403–480

see also Figures 14−16. Including the semilocal part, the PP is given by

$$\Delta V_{\mathrm{PP}}(i) = V_L(r_i) + \sum_{l=0}^{L-1} A_l e^{-a_l r_i^2} \hat{P}_l(i) \qquad (133)$$

where $L = 1$ and $L = 2$ was used for first-row and second-row, as well as 3d transition metals, respectively. The semilocal s and p potentials were required to have a negative curvature at the origin by optimizing the parameters according to eq 104 under the additional nonlinear constraint $A_{L,3}a_{L,3} + A_l a_l > 0$ for each $l \leq L - 1$. The large difference of the d potential causes the significant deviations of the 3d PP orbital from the AE reference, cf. Figure 20.

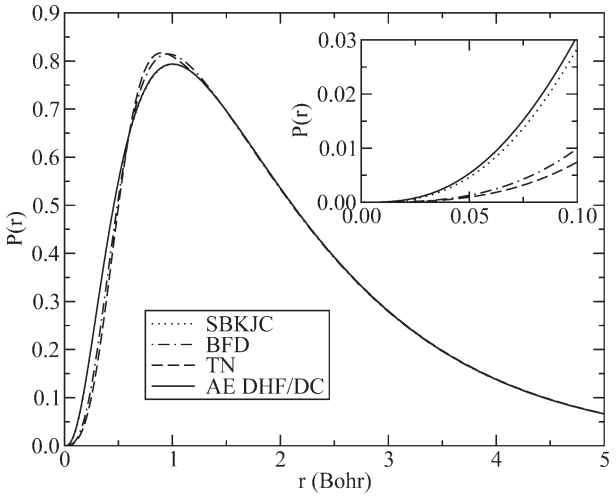

Figure 20. Same as Figure 19, but for 3d.

In contrast to the set of Trail and Needs,[207] who use a large-core definition for all of their PPs, a more reliable small-core option was used for the 3d transition metals and the number of adjustable parameters is significantly smaller.

The PPs are supplemented with correlation-consistent valence basis sets of pVDZ to pV5Z quality for the first and second row main group elements, pVDZ and pVTZ quality for the third to fifth row main group elements as well as pVTZ and pVQZ quality for the 3d transition metals. The PPs are also available from the Internet.[413]

Overview and Atomic Test. An overview of PPs constructed especially for QMC is provided by Table 12. These PPs might also be used in standard quantum chemical calculations. However, due to the additional restrictions for their analytical form made to suit the needs of the QMC approach, their accuracy is probably not as good as the one of standard PPs. This is illustrated in Table 13 for Ti, where atomic energy differences for configurational averages with respect to the Ti $3d^2 4s^2$ ground state configuration are listed for finite difference AE DHF/DC calculations performed with the program GRASP,[83] together with errors for PP of various groups. It is obvious that the shape-consistent Ar-core PPs of Trail and Needs[207] and Christiansen and co-workers[287] perform about equally bad, with mean absolute errors of 0.90 and 0.94 eV, respectively. A comparison to Table 4 reveals that the errors follow the behavior of the FC errors at the AE DHF/DC level for the Ar-core. The Needs group developed also a 10 valence electron PP (Mg core),[412] which performs significantly better, but still exhibits a m.a.e. of 0.15 eV. This m.a.e. corresponds roughly to the m.a.e. of 0.10 eV observed in corresponding AE DHF/DC FC calculations. A better performance with a m.a.e. of only 0.039 eV yields the energy-consistent PP of Burkatzki et al.[154]

Table 12. PPs and Corresponding Valence Basis Sets Constructed for Usage in QMC Calculations[a]

elements	core	n_c	n_v	basis set	ref
^{4}Be−^{10}Ne	^{2}He	2	2−8		377
^{13}Al−^{18}Ar	^{10}Ne	10	3−8		377
^{1}H−^{2}He		0	1−2		207
^{3}Li−^{10}Ne	^{2}He	2	1−8		207
^{11}Na−^{18}Ar	^{10}Ne	10	1−8		207
^{19}K−^{30}Zn	^{18}Ar	18	1−12		207
^{31}Ga−^{36}Kr	^{18}Ar $3d^{10}$	28	3−8		207
^{37}Rb−^{48}Cd	^{36}Kr	36	1−12		207
^{49}In−^{54}Xe	^{36}Kr $4d^{10}$	46	3−8		207
^{55}Cs, ^{56}Ba	^{54}Xe	54	1−2		207
^{71}Lu−^{80}Hg	^{54}Xe $4f^{14}$	68	3−12		207
^{1}H−^{2}He		0	1−2	cc-pVXZ (X = D,T,Q,5), seg., ANO	152
^{3}Li−^{10}Ne	^{2}He	2	1−8	cc-pVXZ (X =D,T,Q,5), seg., ANO	152
^{11}Na−^{18}Ar	^{10}Ne	10	1−8	cc-pVXZ (X = D,T,Q,5), seg., ANO	152
^{19}K, ^{20}Ca	^{18}Ar	18	1−2	cc-pVXZ (X = D,T), seg., ANO	152
^{21}Sc−^{30}Zn	^{10}Ne	10	11−20	cc-pVXZ (X = T,Q), gen., ANO	154
^{31}Ga−^{36}Kr	^{18}Ar $3d^{10}$	28	3−8	cc-pVXZ (X = D,T), seg., ANO	152
^{37}Rb, ^{38}Sr	^{36}Kr	36	1−2	cc-pVXZ (X = D,T), seg., ANO	152
^{49}In−^{54}Xe	^{36}Kr $4d^{10}$	46	3−8	cc-pVXZ (X = D,T), seg., ANO	152
^{55}Cs, ^{56}Ba	^{54}Xe	54	1−2	cc-pVXZ (X = D,T), seg., ANO	152
^{81}Tl−^{86}Rn	^{54}Xe $4f^{14}5d^{10}$	78	3−8	cc-pVXZ (X = D,T), seg., ANO	152

[a] The three groups refer to the shape-consistent nonrelativistic PPs of Lester and co-workers,[377] the shape-consistent relativistic PPs of Trail and Needs[207] and the energy-consistent PPs of Burkatzki et al.[152,154] No basis sets were published for the PPs of the first two groups.

dx.doi.org/10.1021/cr2001383 |*Chem. Rev.* 2012, 112, 403–480

Table 13. Relative Dirac−Hartree−Fock (DHF) Energies (eV) for the Dirac−Coulomb−Hamiltonian of the $2J + 1$-Weighted Average of All J Levels Belonging to a Nonrelativistic Configuration[198] with Respect to the Value for the Ti $3d^2\ 4s^2$ Ground State Configuration[a]

			PPs for QMC			standard PPs			
		AE	TN		BFD	CEP		SBKJC	D
		DHF/DC	4ve	10ve	12ve	4ve	12ve	12ve	12ve
core		86.261	2.692	−0.255	0.007	2.580	0.193	0.012	0.027
	s^1	53.741	2.488	0.141	0.106	2.731	0.161	0.033	0.023
	s^2	30.370	2.491	0.537	0.164	2.883	0.143	0.052	0.023
d^1		44.064	0.413	−0.156	0.009	0.362	0.069	−0.011	0.000
d^1	s^1	22.131	0.410	0.035	0.045	0.435	0.060	0.010	0.003
d^1	s^2	8.319	0.454	0.183	0.060	0.503	0.057	−0.007	0.006
d^2		18.558	0.031	0.002	−0.010	0.036	−0.006	−0.021	−0.005
d^2	s^1	5.838	0.011	0.002	−0.001	0.009	−0.003	−0.007	−0.002
d^2	s^2	0.000	0.000	0.000	0.000	0.000	0.000	0.000	0.000
d^3		6.952	0.307	0.144	0.004	0.317	−0.048	−0.036	−0.015
d^3	s^1	1.743	0.207	0.049	0.001	0.180	−0.041	−0.022	−0.014
d^4		5.477	0.351	0.161	0.026	0.319	−0.060	−0.050	−0.031
m.a.e.		0.000	0.896	0.151	0.039	0.941	0.077	0.025	0.013

[a] Errors of corresponding finite-difference calculations are listed for the scalar-relativistic QMC-adapted nonsingular PPs of Trail and Needs (TN),[207] and Burkatzki et al.,[154] as well as for the standard singular PPs of Christiansen and co-workers (CEP),[287] Stevens et al. (SBKJC),[286] and Dolg (D).[285] The number of valence electrons (ve) is listed for each PP. The 10ve PP of the Needs group was taken from the CASINO homepage.[412] The mean absolute errors (m.a.e.) are given in the last line.

The small-core shape-consistent PP Christiansen and co-workers[287] exhibits a m.a.e. of 0.077 eV. A better accuracy is obtained with the small-core shape-consistent PP of Stevens et al.,[286] as well as with the energy-consistent PP of Dolg,[285] which yield m.a.e. of 0.025 and 0.013 eV, respectively. It should be noted that the first two PPs were adjusted to DHF/DC reference data, whereas the latter one used DHF/DC+B reference data. The Breit interaction leads to a mean absolute deviation from the DHF/DC data of 0.012 eV and the deviations roughly parallel the deviations of the energy-consistent PP from the DHF/DC data.[198] The m.a.e. calculated with respect to the DHF/DC+B reference data is therefore reduced to 0.006 eV. Although the results presented here for Ti are just a single case, we think that they are representative for the situation: the large-core PPs desired for QMC studies exhibit too large FC errors to be of use for accurate calculations. Moreover, at least for the energy-consistent case tests suggest that removing the $1/r$ singularity in the PP leads to a worse fit and thus less accurate PPs. Except for this practical finding the statement of Greeff and Lester is true, that there is no reason in principle why the PP should be singular at the nucleus.[376]

6.5. Pseudopotentials for Use in Density Functional Theory

6.5.1. Use of Hartree−Fock Pseudopotentials in Density Functional Theory. The ab initio PPs presented so far are almost routinely also used by quantum chemists in density functional theory (DFT)[49,50] calculations applying Gaussian basis sets. In contrast to the solid state physics community, where it is quite common to have separate PPs generated for each density functional and especially adapted to plane-wave basis sets, quantum chemists almost exclusively use PPs derived at the ab initio CG HF, WB HF or DHF/DC(+B) level. Some justification for this approach exists, for example, from a PP DFT study by Russo et al. on selected 3d transition metal compounds.[414] PPs derived from atomic HF calculations were found to be applicable also in DFT calculations with only little loss of accuracy, provided that not the (small) PP HF basis sets but the more flexible AE basis sets are also used at the PP level.[414] For the test molecules ScF_3, TiF_4, VF_5, TiO, CuF, and $Ni(CO)_4$ the mean absolute deviation (m.a.d.) between AE and PP results was 0.001, 0.001, and 0.001 Å at the HF, DFT/S-VWN and DFT/B-LYP level, respectively. The corresponding results for the binding energies were 0.5, 0.4, and 0.6 kcal/mol. The transferability of the PPs from HF to DFT seems to be especially good for small-core PPs, whereas for large cores it may be an issue. An example was given by de Jong et al., who investigated the performance of various large- and small-core U PPs for uranyl UO_2^{2+}.[415] A HF/CG-adjusted large-core PP of Hay and Martin[357] falsely yielded a bent equilibrium structure, whereas a corresponding PP adjusted in the framework of DFT/LDA yielded more reasonable results, although as the other investigated large-core PPs it was found not to perform as well as the small-core PP.

The use of small-core transition metal PPs was also investigated for various first- and second-row transition metal carbonyls.[416] The PP calculations were found to be able to reproduce well structures and binding energies obtained in AE DFT calculations. A more recent study compared results for the halogen atoms Br, I and At as well as for their homonuclear dimers at the DFT/BP86 and B3LYP level for energy-consistent small-core PPs[307] and the DKH6 approach in one- and two-component calculations.[417] For the best basis sets the m.a.d. in the atomic ionization potentials and electron affinities were ≤ 0.02 and ≤ 0.03 eV for the one- and two-component results, respectively. For the bond lengths, vibrational constants and binding energies the m.a.d. were at most 0.003 Å, 1 cm^{-1} and 0.03 eV at the scalar-relativistic level and 0.011 Å, 2 cm^{-1} and 0.05 eV when including SO coupling. Several examples were also provided for

dx.doi.org/10.1021/cr2001383 |Chem. Rev. 2012, 112, 403–480

the actinide series.[415,418,419] Russo et al. pointed out, however, that highly erratic results were obtained when the HF optimized PP basis sets were used in DFT studies.[414] Roy et al. therefore suggested to recontract the LANL PP basis sets for use in DFT calculations and obtained for the Hay−Wadt small-core PPs[354] quite good results for test systems containing first- to third-row transition metal elements.[362]

6.5.2. Pseudopotentials in Solid-State Physics. DFT was already quite popular in solid-state physics before quantum chemists discovered it as a very useful tool. The same is true for PPs,[200] despite the early applications to molecules by Hellmann[73] and later by Preuss.[274] For crystalline solids a plane-wave basis approach in connection with a DFT scheme is mathematically and numerically among the simplest and most natural formalisms for a quantum mechanical description. However, it turns out to be extremely inefficient to expand quite compact core orbitals or the oscillatory core part of valence orbitals into plane-waves. Therefore, especially in combination with PPs the plane-wave basis DFT approach became one of the most popular methods for first-principles electronic structure calculations in solid state physics.[15,17] Since the current review is focused on molecular quantum chemistry rather than on theoretical solid state physics, we will not review all developments in the latter field, but rather focus on a few very popular PP approaches in current use.

6.5.3. Nonlinear Core Correction. In solid state physics, where the use of DFT in connection with DFT-adjusted large-core PPs is a standard approach (vide infra), the lack of transferability of the PPs was traced to the linearization of the energy expression when separating the core from the (pseudo)valence density, which is a critical approximation especially for the exchange and correlation contributions in cases of a significant mutual penetration of the two densities. Louie et al. therefore proposed to add the core density, or at least a model (partial) core density

$$\rho_c^{\text{partial}} = \begin{cases} A \sin(Br)/r & \text{for} \quad r < r_d \\ \rho_c^{AE} & \text{for} \quad r \geq r_d \end{cases} \tag{134}$$

to the (pseudo)valence density for the evaluation of the exchange-correlation potential.[420] Here r_d is an adjustable parameter, which is usually chosen to be the radius at which the core density is 1 to 2 times larger than the valence density. The spherical Bessel function used for the inner part was chosen for numerical convenience, especially in view of plane-wave basis sets. The nonlinear core correction was proven to lead to a significantly improved PP transferability and also to a better description of magnetic systems in solid state physics, but except for the work of Delley[421] is not used in molecular quantum chemistry.

6.5.4. Density Functional Semicore Pseudopotentials of Delley. Despite these encouraging findings, PPs of course were also derived from DFT reference data. Delley presented so-called density functional semicore PPs (DSPP) for all elements from H to Am for use with local orbital methods.[421] The DSPPs are based on a minimization of errors with respect to the norm conservation conditions for two to three relevant bound atomic configurations of the atom. The target function D to be minimized consists mainly of

$$D_0 = \frac{1}{2n-1}\sum_i [(\varepsilon_{p,i} - \varepsilon_{v,i})^2 + (\varphi_{p,i}(r_b) - \varphi_{v,i}(r_b))^2] \tag{135}$$

which makes the pseudovalence and valence orbital eigenvalues agree at best and relates to the charge conservation. n denotes the number of orbital-eigenvalue pairs considered. r_b denotes a sufficiently large radius chosen at or larger than the radius of the outermost turning point of the orbital of interest. D_0 is supplemented by three penalty functions

$$D = D_0 + \sum_{i=1}^{3}\sum_l D_{i,l} \tag{136}$$

which for each l-dependent radial PP control the core radius r_c, keep the PPs within certain limits, and limit the number of turning points in these to at most two, thus avoiding wiggles. For a completed optimization of D the contribution of the penalty functions usually vanishes and $D \approx D_0$. The requirement to fulfill the norm-conservation conditions for different (ionic) configurations of an atom amounts to seeking hardness-conserving PPs.[422] Hardness is defined to be one-half the second derivative of the total energy of a chemical system with respect to the number of electrons, and thus is an important property for the correct prediction of electron transfer. The l-dependent radial potentials were expanded in four even Legendre polynomials for $r \leq r_c$ and were required to match the bare potential $-Q/r$ up to the third derivative for $r > r_c$.

The primary density functional used to define the AE reference data was the Perdew−Burke−Ernzerhof (PBE) gradient-corrected functional, but DSPPs were also optimized for both the PBE functional as well as the local density approximation (LDA) using the Perdew−Wang local correlation functional and local exchange. Since the DSPPs are intended to be used in local orbital methods the semicore orbitals were usually kept in the valence space. In addition, following the work of Louie et al.,[420] to improve the numerical stability and transferability a model core density is added to the valence density whenever the exchange and correlation energy or potential is computed. Outside the core density matching radius r_d the core model density is defined as

$$\log[\rho_c(r)] = \sum_{i=1}^{n} c_i \left(\frac{r}{r_d}\right)^{2-i} \quad \text{for } r > r_d \tag{137}$$

whereas for $r \leq r_d$ an even polynomial determined from the matching conditions up to the third derivative was used. The coefficients c_i are determined by a least-squares fit to the core density of an AE calculation.

Delley performed test calculations on the 148 molecules of the so-called G2 set and obtained similar errors as in AE calculations. The performance of the DSPPs was hereby better than the one of the PPs of Troullier and Martins,[330] probably due to the larger r_c values used for the latter, which limit their transferability in cases of short molecular bonds. Additional tests were performed for simple monoelemental solids, zinc blende type semiconductors and rock salt type ionic crystals. Delley finally concluded that the PP approximation is clearly less severe than the DFT approximation, however, he also points out that the PP approximation is significantly more severe than numerical approximations and truncations inherent in his local orbital AE method.

6.5.5. Norm-Conserving Pseudopotentials of Bachelet, Hamann, Schlüter, and Chiang. The development of first-principles norm-conserving PPs by Hamann, Schlüter, and Chiang[328] in 1979 devised a way to accurate calculations of solid state properties within a PP DFT approach. Based on this work Bachelet, Hamann and Schlüter published in 1982 a set of

dx.doi.org/10.1021/cr2001383 |Chem. Rev. 2012, 112, 403–480

relativistic PPs for H to Pu[423,424] for use in local density approximation (LDA) DFT studies, which found widespread use in the physics community. The formal nonrelativistic treatment of relativistic effects within PP approaches in solid-state physics is based on work of Kleinman.[425] On the basis of a relativistic LDA calculation for an atom in a suitable reference state, for example, the ground state, the following requirements are made for the PP calculation:[328] (1) The valence and pseudovalence orbital eigenvalues agree. (2) The valence and pseudovalence orbitals agree outside a chosen core radius, that is, for $r > r_c$. (3) The integrals of the valence and pseudovalence charge densities from 0 to r agree for $r > r_c$. (4) The logarithmic derivatives of the valence and pseudovalence functions and their first energy derivatives agree for $r > r_c$. The second requirement is known as the shape-consistency condition in quantum chemistry,[325] whereas the third one is known as the norm-conservation condition[328] in solid state physics. From the third condition in the framework of LDA it is clear that the PP and the full AE potential are identical for $r > r_c$. The fourth requirement guarantees that the error for the scattering property of the full AE potential inside r_c at the eigenvalue energy and for the particular angular momentum is minimized by the PP. Provided the first two conditions are fulfilled, it is sufficient to require the last two conditions to be fulfilled at $r = r_c$. Hamann et al.[328] noted that these two requirements can be related by an identity derived by Topp and Hopfield[273]

$$-2\pi\left[(rR_{\varepsilon lj})^2\frac{\mathrm{d}}{\mathrm{d}\varepsilon}\frac{\mathrm{d}}{\mathrm{d}r}\ln(R_{\varepsilon lj})\right]_{r_c,\varepsilon} = 4\pi\int_0^{r_c} R_{\varepsilon lj}{}^2 r^2\mathrm{d}r \quad (138)$$

where the radial logarithmic derivative of $R_{\varepsilon lj}$ is related to the scattering phase shift. The identity of $R_{\varepsilon lj}$ and its first derivative implies the identity of the logarithmic derivative

$$\frac{\mathrm{d}}{\mathrm{d}r}\ln(R_{\varepsilon lj})|_{r_0} = \frac{1}{R_{\varepsilon lj}}\frac{\mathrm{d}R_{\varepsilon lj}}{\mathrm{d}r}|_{r_0} \quad (139)$$

The requirements guarantee the transferability of the PPs from the atom to other situations where the external potential has changed, that is, other atomic states, molecules, and solids.

The PPs of Bachelet et al.[424] were constructed as follows. The initial Dirac−Kohn−Sham (DKS) calculation within the framework of LDA, using an exchange and correlation functional based on the Perdew−Zunger parametrization of the Ceperly and Alder[400] QMC free electron gas results and relativistic corrections to it according to MacDonald and Vosko, yields the necessary reference data. The PP generation can be performed for each lj quantum number separately. A first intermediate pseudopotential PP $V_{lj}^{(1)}$ was constructed from the full AE potential V_{lj}, that is, the nucleus-electron Coulomb potential and the LDA potential, by cutting off the singularity at the nucleus with a suitable smooth cutoff function $f(r/r_{c,lj})$

$$V_{lj}^{(1)} = V_{lj}\left[1 - f\left(\frac{r}{r_{c,lj}}\right)\right] + c_{lj}f\left(\frac{r}{r_{c,lj}}\right) \text{ with}$$

$$f\left(\frac{r}{r_{c,lj}}\right) = \exp[-(r/r_{c,lj})^{\lambda}] \quad (140)$$

An optimum value $\lambda = 3.5$ was used, whereas the parameter $r_{c,lj}$ decides the range over which the AE and intermediate PP are allowed to deviate from each other. Finally, c_{lj} is adjusted so that the lowest nodeless solution $|\varphi_{p,lj}^{(1)}\rangle$ of the Schrödinger equation containing $V_{lj}^{(1)}$ yields the correct valence eigenvalue $\varepsilon_{p,lj}^{(1)} = \varepsilon_{v,lj}$. Note that here and in the following paragraphs the superscripts (1) and (2) are used to denote the various potentials, orbitals, and orbital energies occurring in the derivation.

In a next step the initial pseudovalence orbital $|\varphi_{p,lj}^{(1)}\rangle$ is modified at short-range to yield a normalized pseudovalence orbital $|\varphi_{p,lj}^{(2)}\rangle$, which agrees with the full core AE valence orbital for $r > r_c$

$$R_{p,lj}^{(2)} = \gamma_{lj}\left[R_{p,lj}^{(1)} + \delta_{lj}r^{l+1}f\left(\frac{r}{r_{c,lj}}\right)\right] \quad (141)$$

δ_{lj} is obtained as the smallest solution from the normalization condition for $R_{p,lj}^{(2)}$, where typically the norm correction $\gamma_{lj}{}^2 - 1$ is found to be small ($\sim 10^{-2}$−10^{-3}). Although the existence of a solution δ_{lj} is guaranteed, unphysical results can occur for weakly bound and extended excited states. These can be avoided by basing the derivation on appropriately ionized configuration. The final screened PP $V_{lj}^{(2)}$ producing the nodeless eigenfunction $|\varphi_{p,lj}^{(2)}\rangle$ at the correct eigenvalue $\varepsilon_{p,lj}^{(2)} = \varepsilon_{v,lj}$ is obtained by inverting the radial Schrödinger equation, which can be done analytically knowing $V_{lj}^{(1)}$ and $|\varphi_{p,lj}^{(2)}\rangle$,

$$V_{lj}^{(2)} = V_{lj}^{(1)} + \frac{\delta_{lj}r^{l+1}f}{2R_{p,lj}^{(2)}}[A(r) - 2\varepsilon_{v,lj} - 2V_{lj}^{(1)}] \quad (142)$$

with the auxiliary function

$$A(r) = r^{-2}\left[\lambda^2\left(\frac{r}{r_{c,lj}}\right)^{2\lambda} - (2\lambda l - \lambda(\lambda+1))\left(\frac{r}{r_{c,lj}}\right)^{\lambda}\right] \quad (143)$$

Finally, the unscreened PP is obtained using the nodeless pseudovalence orbital $|\varphi_{p,lj}^{(2)}\rangle$ and its radial density ρ_v as

$$V_{lj}^{\mathrm{ion}}(r) = V_{lj}^{(2)}(r) - \int\frac{\rho_v(r')}{|r-r'|}\mathrm{d}r' - \frac{\delta E_{xc}[\rho_v]}{\delta\rho_v(r)} \quad (144)$$

The radial PPs can then be averaged and differenced as shown in eq 79 to 85 to yield a scalar-relativistic PP and a SO term.

To facilitate tabulation and use, a fit to a few analytical functions was performed for the PPs so far tabulated on a grid. The scalar-relativistic PP was split into a long-range Coulomb-type part V_{core} and a short-range l-dependent part ΔV_l,

$$V_l^{\mathrm{ion}}(r) = V_{\mathrm{core}} + \Delta V_l \quad (145)$$

with the Coulomb-type part smoothly approaching a finite value for $r \to 0$

$$V_{\mathrm{core}} = -\frac{Q}{r}\left[\sum_{i=1}^{2} c_i\,\mathrm{erf}[\alpha_i^{1/2}r]\right] \quad (146)$$

Here Q denotes the charge of the core, and the restriction $c_1 + c_2 = 1$ applies. Both the l-dependent part ΔV_l, as well as the difference potential in the SO term are expanded in Gaussian-type functions according to eq 89. The choice of the error function and Gaussian-type functions was made to enable an efficient PP integral evaluation in plane-wave, Gaussian and mixed plane-wave Gaussian basis sets. The free parameters in the analytical ansatz were obtained by least-squares fitting the PP matrix elements.

The PP tabulation of Bachelet et al.[424] typically comprises large core PPs, with the notable exception of the lanthanides,

dx.doi.org/10.1021/cr2001383 |Chem. Rev. 2012, 112, 403–480

that is, main group elements are considered with 1 to 8 valence electrons (group 1, 2, and 13−18), d-transition metals with 3−12 electrons (group 3−12), and the actinides Ac to Pu with 3−8 electrons. For the lanthanides the 5s and 5p shells were included in the valence space for the reasons detailed in section 5.2. The authors report that the error in 4f−5d excitations is hereby decreased from 1.7 to 0.2 eV. For Zn, Cd, and Hg alternative PPs with a two-valence-electron approximation are also offered.

6.5.6. Pseudopotentials of Troullier and Martins. About a decade after the work of Hamann, Schlüter, and Chiang,[328] Troullier and Martins[330] proposed a more simple procedure to generate relativistic smooth nonsingular norm-conserving PPs. Their strategy is closer to the one adapted in quantum chemistry, that is, as a first step a smooth pseudovalence orbital is generated from an AE valence orbital, and as a second step the corresponding KS equation for the pseudovalence orbital is solved for the screened effective potential, from which the Hartree potential, as well as the exchange and correlation potentials are then subtracted, to get the PP for the ionic atom core. Following an idea of Kerker,[329] Troullier and Martins modified the shape-consistency prescription eq 111 to avoid the singularity at the nucleus, that is, instead of a polynomial eq 118 as used by Christiansen et al.[325] or Hay and Wadt,[326] an exponential of a sixth-order polynomial in r^2 is used

$$f_l(r) = r^l \exp[p(r)] \text{ with } p(r) = \sum_{i=0}^{6} c_{2i} r^{2i} \tag{147}$$

The seven coefficients c_{2i} are determined by the norm-conservation condition eq 113 for $r = r_c$, the continuity of the pseudovalence orbital and its first four derivatives ar r_c, and the zero curvature of the screened effective potential at the origin. After descreening the screened effective potential, smooth PPs were obtained for all elements up to Hf, as well as for a few heavier ones. The authors report applications to solids and a detailed comparison to the norm-conserving PPs of Kerker[329] and Hamann et al.,[328] as well as the non-norm-conserving ones of Vanderbilt.[426] They could convincingly demonstrate that the required energy cutoff for the plane-wave basis set could be considerably reduced compared to the PPs of Bachelet at al., for example, for Zn the cutoff energy could be reduced from ∼900 Ry (Rydberg) to ∼70 Ry, reducing the number of plane-waves from ∼140 000 to ∼3000 for zinc blende.

6.5.7. Separable Form of Pseudopotentials. For computational efficiency the semilocal part of the PPs derived by Bachelet et al.[424] or Troullier and Martins[330] can be converted to a nonlocal or separable form proposed by Kleinman and Bylander[427] and generalized by Blöchl.[428] For an energy band calculation the number of integrals is thus reduced from $mn(n+1)/2$ to mn for each l, when n is the number of plane-waves and m the number of points in the Brioullin zone at which the calculation is performed. The two contributions to the atomic PP given in eq 78 are a local part and a semilocal part, which are abbreviated in the following by $\hat{V}_{\text{loc}}$ and $\hat{V}_{n\text{loc}}$, respectively. Given a complete but otherwise arbitrary set of functions $|\varphi_i\rangle$, for example, atomic orbitals, the semilocal part can be exactly transformed to the nonlocal form

$$\hat{V}_{n\text{loc}} = \sum_i \sum_j A_{ij} |\hat{V}_{n\text{loc}}\varphi_i\rangle\langle\hat{V}_{n\text{loc}}\varphi_j| \tag{148}$$

where the matrix A satisfies the condition

$$\sum_j A_{ij}\langle\varphi_j|\hat{V}_{n\text{loc}}|\varphi_k\rangle = \delta_{ik} \tag{149}$$

The validity of eqs 148 and 149 can be proven by acting with $\hat{V}_{n\text{loc}}$ on an arbitrary function, which is expanded into the functions $|\varphi_i\rangle$. A transformation to a new set of functions $|\overline{\varphi}_i\rangle$, for which the matrix $\langle\overline{\varphi}_j|\hat{V}_{n\text{loc}}|\overline{\varphi}_k\rangle$ and hence also the matrix $\overline{A}$ is diagonal, leads to the general form of a separable potential

$$\hat{V}_{n\text{loc}} = \sum_i \overline{A}_i |\hat{V}_{n\text{loc}}\varphi_i\rangle\langle\hat{V}_{n\text{loc}}\varphi_i| \tag{150}$$

Here the $\overline{A}_i$ denote the diagonal elements of the matrix $\overline{A}$. Clearly, it is straightforward to generate the functions $|\hat{V}_{n\text{loc}}\varphi_i\rangle$ when a semilocal PP has been constructed previously. Blöchl[428] and Vanderbilt[426] demonstrated that, in the framework of DFT, it is also possible to avoid the construction of a semilocal PP and generate the nonlocal PP directly from AE reference data by using

$$|\hat{V}_{n\text{loc}}\varphi_i\rangle = \left[\varepsilon_i - \left(-\frac{1}{2}\hat{\nabla}_i^2 + \hat{V}_{\text{loc}}\right)\right]|\varphi_i\rangle \tag{151}$$

Here $|\varphi_i\rangle$ belongs to a set of rather arbitrarily chosen pseudovalence orbitals which match the AE orbital at a set of energies ε_i outside some radius. $\hat{V}_{\text{loc}}$ denotes a local potential which matches the true atomic potential outside the same radius, but is otherwise rather arbitrary. In practice the set of the functions $|\varphi_i\rangle$ is not complete, which might lead to errors.[428] A corresponding transformation from semilocal to nonlocal respectively separable form was proposed by Pélissier et al.[429] in quantum chemistry, to facilitate, for example, the evaluations of energy gradients, see section 8.2.1.

A computer code able to generate scalar-relativistic PPs of the type proposed by Hamann et al.[328] and Troullier and Martins[330] for a number of popular gradient-corrected density functionals was published by Fuchs and Scheffler.[430]

6.5.8. Separable Dual-Space Pseudopotentials of Hartwigsen, Goedecker, and Hutter. Hartwigsen, Goedecker, and Hutter[431] presented relativistic separable dual-space PPs for H to Rn in the context of LDA, extending earlier corresponding nonrelativistic work for the first two rows of the periodic table.[432] The dual-space PPs have an analytic form involving Gaussians multiplied by a polynomial in real space and reciprocal space, thus allowing analytical integration in both cases. The PP parameters were determined by minimizing the differences between the eigenvalues and the charges within an atomic sphere of the AE atom and the PP atom, where the radius of the sphere was usually taken to be the covalent radius of the atom. In order to ensure transferability also unoccupied orbitals with the same angular momentum as occupied in the core, as well as with higher angular momentum were included in an generalized norm-conservation condition. The calculations did not exceed $l = 3$, which might become problematic for heavier elements. In order to include virtual orbitals the atomic calculations were performed in an external parabolic confining potential. The parameters are fitted directly to the AE eigenvalues and charges, rather than fitting analytical or numerical potentials which reproduce for the correct eigenvalues pseudovalence wave functions, constructed from the AE solutions. Since in contrast to the method applied by Bachelet et al.[424] or Troullier and Martins[330] the best overall representation for the eigenvalues and charges of several orbitals was required, rather than exactly obeying the norm-conservation

dx.doi.org/10.1021/cr2001383 |Chem. Rev. 2012, 112, 403–480

conditions for a single state, a smaller number of adjustable parameters was found to suffice. Hartwigsen et al.[431] presented results of plane-wave PP LDA calculations for about 100 small molecules containing atoms from H to Bi and found a favorable agreement with corresponding AE results. Corresponding PPs optimized for several gradient-corrected density functionals were derived by for H to Kr by Krack.[433]

6.5.9. Ultrasoft Self-Consistent Pseudopotentials of Vanderbilt. In 1990, Vanderbilt[426] proposed soft self-consistent (ultrasoft) PPs, for which the norm-conservation constraint does not apply and which have to be used in the framework of a generalized eigenvalue problem

$$\left[-\frac{1}{2}\hat{\vec{\nabla}}_i^2 + \hat{V}_{\mathrm{loc}} + \hat{V}_{n\mathrm{loc}}\right]|\varphi_i\rangle = \varepsilon_i \hat{S}|\varphi_i\rangle \qquad (152)$$

Here $\hat{S}$ denotes a nonlocal overlap operator. $\hat{V}_{\mathrm{loc}}$ stands for the sum of the core−electron Coulomb potential and the valence electron−electron Coulomb, exchange and correlation potentials. $\hat{V}_{n\mathrm{loc}}$ has a form similar to eq 148; however, the parameters A_{ij} now depend on the valence electron density, that is, on the solutions $|\varphi_i\rangle$. Thus $\hat{V}_{n\mathrm{loc}}$ has to be updated together with $\hat{V}_{\mathrm{loc}}$ during the SCF iterations.

One advantage of the ultrasoft PPs is, that now for valence orbitals without radial nodes, that is, 2p, 3d or 4f, smooth pseudovalence orbitals still can be constructed and difficulties to describe these compact orbitals by plane-wave basis sets are thus avoided. The PPs can be constructed directly in nonlocal form eq 148 and converted to separable form eq 150, avoiding the (intermediate) construction of semilocal PPs. A tabulation of ultrasoft PPs for many elements of the periodic table, as well as a generation code, can be found on the homepage of the Vanderbilt group.[434]

6.6. Pseudopotentials with Explicit Relativistic Hamiltonian

Some work considered an explicitly relativistic valence-only model Hamiltonian. Whereas the concomitant gain of computational accuracy is not convincing if present at all, the computational effort turns out to be significantly higher compared for the commonly used implicit treatment of relativity. Datta et al.[435] used a PK-type PP in a four-component study of PbO. Ishikawa and Malli[181] investigated the usage of semilocal PPs in four-component atomic finite difference DHF calculations. Dolg[182] performed four-component atomic and molecular DHF calculations and subsequent CI calculations on alkaline atoms and their monohydrides using four-component energy-adjusted PPs and CPPs. Pyper[436,437] derived quite complicated expressions for $\hat{V}_{\mathrm{cv}}$ by applying the Foldy−Wouthuysen transformation[130,131] to a four-component PP Hamiltonian and tested the approach in atomic calculations.[438] The usage of PPs in four-component calculations might still be of some use, for example, to reduce the effort for the treatment of heavy atoms in the neighborhood of a center treated accurately at the AE level. The above work however indicates that the direct relativistic contributions are very small for pseudovalence orbitals, and thus, it is probably sufficiently accurate to apply the parameters of standard PPs with an implicit treatment of relativity in such calculations, that is, the adjustment of sets of four-component PPs is probably not needed. The same may also hold for approximate relativistic Hamiltonians. This situation is at variance with the MP method, where because of the correct nodal structure of the valence orbitals explicitly calculated relativistic contributions are expected to be larger, see also section 7.4.

7. MODEL POTENTIAL PARAMETRIZATION

There is a considerably smaller variety of MP approaches than PP approaches. Because of the different choices of the analytical form of $\Delta\hat{V}^{\lambda}_{\mathrm{MP}}$ in eq 91 there are mainly two versions of the MP approach in current use which differ by the approximation of the Coulomb and exchange terms, as well as by the implicit treatment of relativistic effects including SO coupling.[439,24] Both versions are ab initio in character and originate from the pioneering work of Huzinaga.[243]

7.1. Ab Initio Model Potentials of Huzinaga, Seijo, Barandiáran, and Co-workers

Probably the so far most successful and widely used MP variant originating from the method developed by Huzinaga[243] are the ab initio model potentials (AIMP) of Huzinaga, Seijo, Barandiarán, and co-workers.[440,24] The available relativistic CG-adjusted AIMPs and corresponding valence basis sets are listed in Table 14. The AIMP and basis set parameters are also available in electronic form from the homepage of the Seijo group.[441] A review of the approach, stressing its capability not only to model atomic cores but also the environment in embedded cluster calculations, was published by Seijo and Barandiarán.[24]

In the AIMP approach the core shifting operator $\hat{P}^{\lambda}_{\mathrm{S}}$ is kept as it stands in eq 94. For practical calculations the core orbitals $|\varphi^{\lambda}_{\mathrm{c}}\rangle$ are represented by sufficiently large (AE) basis sets. The operator for Coulomb core−valence interaction eq 92 is represented by a linear combination of radial Gaussians with prefactors $1/r$, that is, a local spherically symmetric model potential

$$\Delta\hat{V}^{\lambda}_{\mathrm{C}}(i) = \frac{1}{r_{\lambda i}}\sum_k C^{\lambda}_k e^{-\alpha^{\lambda}_k r^2_{\lambda i}} \qquad (153)$$

The exponents α^{λ}_k and coefficients C^{λ}_k are adjusted to the all-electron (AE) potential in a least-squares sense under the constraint that $\Sigma_k C^{\lambda}_k = Z_{\lambda} - Q_{\lambda} = -n^{\lambda}_{\mathrm{c}}$ to enforce the correct asymptotic behavior of the AIMP. Since the evaluation of integrals over such a local potential is not costly, essentially any desired accuracy can be easily achieved by using a sufficiently long expansion.

The nonlocal exchange part $\Delta\hat{V}^{\lambda}_{\mathrm{X}}$ eq 93 is finally substituted by its spectral representation in the space defined by a set of functions $|\chi^{\lambda}_p\rangle$ centered on core λ

$$\Delta\hat{V}^{\lambda}_{\mathrm{X}}(i) = \sum_{p,q}|\chi^{\lambda}_p(i)\rangle A^{\lambda}_{pq}\langle\chi^{\lambda}_q(i)| \qquad (154)$$

It should be noted that this AIMP operator yields the same one-center integrals as the true AE core-exchange operator as long as the basis functions can be represented by the set of the $|\chi^{\lambda}_p\rangle$. Two- and three-center integrals are approximated. Since, in contrast to the Coulomb part, the exchange part is short-ranged, only a moderate number of functions $|\chi^{\lambda}_p\rangle$ is needed and the applied one-center approximation is expected to be very good, at least for not too large cores. In practical applications the basis used in the spectral representation is chosen to be identical to the primitive functions of the valence basis set used for the atom under consideration and the A^{λ}_{pq} are calculated during the input processing of each AIMP calculation.

Following ideas of Katsuki and Huzinaga[16,120,442,443] toward the development of a variationally stable relativistic AE and also VO Hamiltonian based on a spectral representation of the CG Hamiltonian, Seijo, Barandiaran and Huzinaga developed a corresponding AIMP variant.[444] Instead of taking core orbitals

dx.doi.org/10.1021/cr2001383 |Chem. Rev. 2012, 112, 403–480

Table 14. Ab Initio Model Potentials for Li to Lr of Seijo, Barandiarán, and Co-workers Derived from Scalar-Relativistic CG AE Data, as well as Accompanying Valence Basis Sets[a]

elements	core	n_c	n_v	basis set	ref
^{3}Li, ^{4}Be	[^{2}He]	2	1-2	(5s)/[2s]	208
^{5}B−^{10}Ne	[^{2}He]	2	3-8	(5s5p)/[2s1p]	156, 157, 208
^{11}Na−^{12}Mg	[^{10}Ne]	10	1−2	(7s)/[3s]	157, 208
	[^{4}Be]	4	7−8	(7s5p)/[3s1p]	157, 208
^{13}Al−^{18}Ar	[^{10}Ne]	10	3−8	(7s6p)/[3s2p]	156, 157, 208
^{19}K−^{20}Ca	[^{18}Ar]	18	1−2	(9s)/[4s]	157, 208
	[^{12}Mg]	12	7−8	(9s6p)/[4s2p]	157, 208
^{21}Sc−^{30}Zn	[^{12}Mg]	12	9−18	(9s5p5d)/[4s2p1d]	157, 208, 209
^{31}Ga−^{36}Kr	[^{18}Ar] 3d^{10}	28	3−8	(9s8p)/[4s3p]	156, 157, 208
^{37}Rb−^{38}Sr	[^{36}Kr]	36	1−2	(11s)/[5s]	157, 208
	[^{30}Zn]	30	7−8	(11s8p)/[5s3p]	157, 208
^{39}Y−^{48}Cd	[^{30}Zn]	36	9−18	(11s7p6d)/[5s3p2d]	157, 444
^{49}In−^{54}Xe	[^{36}Kr] 4d^{10}	46	3−8	(11s10p)/[5s4p]	156, 157, 208, 446
^{55}Cs−^{56}Ba	[^{54}Xe]	46	1−2	(13s)/[6s]	157, 208
	[^{48}Cd]	48	7−8	(13s10p)/[6s4p]	157, 208
^{57}La	[^{54}Xe]	54	3	(13s7d)/[6s3d]	157, 208
	[^{48}Cd]	48	9	(13s10p7d)/[6s4p3d]	157, 208
				(13s10p9d5f)[3s3p4d2f]	447
	[^{48}Cd]	48	11	(13s9p7d)[1s1p1d]	447
				(13s10p8d1f)[3s3p3d1f]	447
^{58}Ce−^{71}Lu	[^{36}Kr] 4d^{10}	46	12−25	(14s10p9d8f)/[2s1p1d1f]	448
				(14s10p9d8f)/[6s5p5d4f]	448
^{72}Hf−^{80}Hg	[^{48}Cd] 4f^{14}	62	10−18	(13s9p8d)[1s1p1d]	447, 449
				(13s10p9d5f)[3s3p4d2f]	447
^{81}Tl−^{86}Rn	[^{54}Xe] 4f^{14}	68	13−18	(13s12p8d5f)/[3s4p4d2f]	156, 446
^{90}Th−^{103}Lr	[^{54}Xe] 4f^{14} 5d^{10}	78	12−25	(14s10p11d9f)/[2s1p1d1f]	448
				(14s10p11d9f)/[6s5p5d4f]	448

[a] WB-based spin-orbit operators and valence basis sets suitable to evaluate spin-orbit splittings are available for the valence orbitals of B to Lr. The minimal basis sets published for most elements can be decontracted to add flexibility.

entering eq 94 and eq 153 from nonrelativistic finite difference HF calculations, they were now determined by corresponding scalar-relativistic GC calculations.[85] For use in eq 94 suitable linear combinations of Gaussian functions were determined using a maximum overlap criterion. Once a basis set for an atomic or molecular calculation is chosen, the mass-velocity and Darwin terms of the CG Hamiltonian are cast into a spectral representation eq 154, together with the nonlocal exchange part. Therefore indirect relativistic effects on the valence orbitals originating from the core are accounted for by the core orbital shift operator eq 94, the local approximate Coulomb operator eq 153 and the spectral representation of the exchange operator eq 154, whereas the direct effects on the valence orbitals enter implicitly by a modification of the latter.

Seijo also developed a scheme to account for SO coupling within the AIMP approach by adding a one-electron SO operator,[156,24] which has a similar form as the PP SO operator in eq 86 suggested by Pitzer and Winter,[445] but is a representation of the AE WB SO operator[84]

$$\Delta\hat{V}^{\lambda}_{\mathrm{cv,so}}(i) = \sum_{l}\left(\sum_{k}\frac{B^{\lambda}_{lk}}{r^{2}_{\lambda i}}e^{-\beta^{\lambda}_{lk}r^{2}_{\lambda i}}\right)\hat{P}^{\lambda}_{l}(i)\hat{\vec{l}}_{\lambda,i}\cdot\hat{\vec{s}}_{i}\hat{P}^{\lambda}_{l}(i) \qquad (155)$$

Here $\hat{\vec{l}}_{\lambda,i} = \hat{\vec{r}}_{\lambda,i}\times\hat{\vec{p}}_{i}$ and $\hat{\vec{s}}$ denote the operators of orbital angular momentum and spin, respectively. $\hat{P}^{\lambda}_{l}$ stands for the projection operator onto the subspace of angular quantum number l with respect to core λ. The coefficients B^{λ}_{lk} and exponents β^{λ}_{lk} are determined by means of a least-squares fit to the radial components of the WB SO term. The two-component WB-AIMP method[156] can be viewed as an extension of the scalar-relativistic CG-AIMP approach,[444] which results from the addition of a representation of the WB one-electron SO operator to the GC-adjusted AIMP.

The AIMP approach makes use of valence orbitals with the correct nodal structure. In contrast to, e.g., the shape-consistent PP approach, the atomic core MPs can be directly constructed from the AE operators they represent and no reference has to be made to the valence orbitals during the adjustment. This feature allows to derive MPs replacing atomic anions, which do not have bound states for an additional electron, and is especially useful for modeling crystal lattices in solid state calculations.[24,201] Since the operators appearing in the AIMP are explicit representations of the core Coulomb and exchange operators as well as of the CG/WB relativistic operators, it is possible to analyze the physical effects associated with these terms to a certain extent individually. Some limitations in doing this exist of course, for example, relativistic changes of the core also enter the model core Coulomb and exchange operators. A further advantage is, that the design and optimization of valence basis sets follows closely the procedures outlined for AE basis sets.

dx.doi.org/10.1021/cr2001383 |Chem. Rev. 2012, 112, 403–480

Table 15. Model Core Potentials of Klobukowski and Co-workers Derived from Nonrelativistic HF and Scalar-Relativistic CG, RESC, and DK (DKH3) AE Reference Data

elements	fit	core	n_c	n_v	ref
^{3}Li, ^{4}Be	HF	[^{2}He]	2	1−2	210, 457
^{5}B−^{10}Ne	HF,DKH3	[^{2}He]	2	3−8	210, 457, 461
^{11}Na, ^{12} Mg	HF	[^{4}Be]	4	7−8	210, 457
^{13}Al	DKH3	[^{2}He]	2	11	461
^{13}Al−^{18}Ar	HF	[^{10}Ne]	10	3−8	210, 457
^{14}Si−^{18}Ar	DKH3	[^{4}Be]	4	10−14	461
^{19}K, ^{20}Ca	HF	[^{12}Mg]	12	7−8	210, 457
^{21}Sc−^{30}Zn	HF	[^{18}Ar]	18	3−12	452
	HF	[^{10}Ne]	10	11−20	454
^{31}Ga	DKH3	[^{10}Ne]	10	21	461
^{31}Ga−^{36}Kr	HF	[^{18}Ar] 3d^{10}	28	3−8	210
	CG,RESC	[^{18}Ar]	18	13−18	457, 458
^{32}Ge−^{36}Kr	DKH3	[^{12}Mg]	12	20−24	461
^{39}Y−^{48}Cd	CG	[^{36}Kr]	36	3−12	452
	CG	[^{18}Ar] 3d^{10}	28	11−20	455
^{37}Rb, ^{38}Sr	CG	[^{20}Ca] 3d^{10}	28	7−8	210
	RESC	[^{20}Ca] 3d^{10}	28	7−8	457
^{49}In	DKH3	[^{18}Ar] 3d^{10}	18	21	461
^{49}In−^{54}Xe	CG	[^{36}Kr] 4d^{10}	46	3−8	210
	CG,RESC	[^{36}Kr]	36	13−18	457, 458
^{50}Sn−^{54}Xe	DKH3	[^{18}Ar] 3d^{10} 4s^{2}	30	20−24	461
^{55}Cs, ^{56}Ba	CG	[^{48}Cd]	48	7−8	210
	RESC	[^{48}Cd]	48	7−8	457
^{57}La−^{71}Hg	CG	[^{36}Kr] 4d^{10}	46	11−25	460
^{71}Lu−^{80}Hg	CG	[^{54}Kr] 4^{f14}	68	3−12	452
	CG	[^{36}Kr] 4d^{10} 4f^{14}	60	11−20	456
^{79}Au	DKH3	[^{36}Kr] 4d^{10} 4f^{14}	60	19	462
^{81}Tl	DKH3	[^{36}Kr] 4d^{10} 4f^{14}	60	21	461
^{81}Tl−^{86}Rn	CG	[^{54}Kr] 4f^{14} 5d^{10}	78	3−8	210
	CG,RESC	[^{54}Kr] 4f^{14}	68	13−18	457, 458
^{82}Pb−^{86}Rn	DKH3	[^{36}Kr] 4d^{10} 4f^{14} 5s^{2}	62	20−24	463

Nonrelativistic AIMPs and corresponding valence basis sets were published for the main group and 3d and 4d transition metals from Li to Xe.[440,444,450] Relativistic CG-adjusted AIMPs accompanied by valence basis sets were published for Li to La, for the alkaline M^{+} and alkaline M^{2+} ions, and for the halogen anions X^{-}.[208,444] Corresponding AIMPs augmented by WB-derived SO operators as well as suitable valence basis sets are available for the 5d transition metals,[447] as well as for the lanthanides and actinides.[448] WB-adjusted SO operators for B to Ba together with basis sets modified to properly account for SO effects were also made available.[156,157,209,449] The modified basis sets essentially result from the original scalar-relativistically optimized basis sets by recontracting the most tight primitive with the fixed linear combination of the rest of the primitives, followed by a normalization, so that finite difference one-electron SO splittings are reproduced.[156,157] The core definitions used by Seijo and co-workers often differ from the ones which are used in the PP approaches, for example, for the transition metals the $(n-1)$s shell is attributed to the core, whereas the $(n-1)$p shell, together with the $(n-1)$d and ns shell, is included in the valence. Although in contrast to the PP approach because of the correct nodal structure of the radial parts of the MP valence orbitals no difficulties with respect to the correlation treatment arise from a modified shape or the orbitals, the frozen-core errors still may be significantly larger compared to cases where the (n-1)s shell is also treated as valence shell. Table 4 provides some evidence for the Ti atom by comparing the treatments as 10 and 12 valence electron atom. The choice of the core in MP calculations has also been discussed by Zeng and Klobukowski,[462] see sections 7.2 and 9.5.

7.2. Model Core Potentials of Huzinaga, Sakai, Klobukowski, and Co-workers

Like the AIMP approach of Seijo, Baradiáran, and co-workers the model core potential (MCP) approach advocated by Klobukowski and collaborators[439] originated from the MP theory proposed by Huzinaga and co-workers.[243−245] The scalar-relativistic MCP approach was pioneered in 1983 by Klobukowski,[451] who based his derivation of a Ag MCP on the scalar-relativistic CG HF formalism.[85] The MCP approach uses a somewhat simpler form of the MP in eq 91, that is, in the atomic and molecular ECPs eq 57 and eq 58. The first two terms modeling Coulomb and exchange interaction are combined in a local term, which has a slightly different form from the local term used by Seijo, Barandiáran, and co-workers, that is

$$\Delta V_{\mathrm{C}}^{\lambda}(i) + \Delta V_{\mathrm{X}}^{\lambda}(i) = -\frac{Q_{\lambda}}{r_{\lambda i}} \sum_{k} A_{k}^{\lambda} r_{\lambda i}^{n_{k}^{\lambda}} e^{-\alpha_{k}^{\lambda} r_{\lambda i}^{2}} \qquad (156)$$

dx.doi.org/10.1021/cr2001383 |Chem. Rev. 2012, 112, 403–480

In newer publications the sum on the right-hand side runs over three terms for $n_k^\lambda = 0$ and $n_k^\lambda = 1$ each. The shift operator P_S^λ corresponds to the one given in eq 94 and the scalar-relativistic AE HF core orbitals used to construct it are least-squares fitted using (a small number of) Gaussian basis functions. Several sets of nonrelativistic and relativistic MCPs using different core definitions were developed during the last three decades by Huzinaga, Sakai, Klobukowski, Miyoshi and collaborators. An overview is given in Table 15.

Nonrelativistic (Sc−Zn) and relativistic (Y−Cd, Lu−Hg) MCPs with a large-core approximation treating only the *ns* and $(n-1)$d shell in the valence were derived for the first, second and third transition metal series.[452] Whereas $(n-1)\mathrm{d}^n ns^2 \rightarrow (n-1)\mathrm{d}^{n+1} ns^1$ HF excitation energies between the lowest LS states exhibit errors of up to 0.3 eV when compared to corresponding AE reference data, much larger errors of up to 0.7 eV are present for $(n-1)\mathrm{d}^n ns^2 \rightarrow (n-1)\mathrm{d}^{n+2}$ excitations between the lowest LS states. It is unclear to which extent the results were influenced by the finite basis sets used; however, it is clear that a significant part of the errors corresponds to FC errors. A corresponding set of MCPs includes also the $(n-1)$p semicore orbitals, but not the $(n-1)$s semicore orbitals, in the valence space.[453] Unfortunately no results for atomic excitations energies obtained with these pdsMCPs were given in the original paper;[453] however, from more recent work,[454−456] one can find errors of up to 0.7 eV in $(n-1)\mathrm{d}^n ns^2 \rightarrow (n-1)\mathrm{d}^{n+1} ns^1$ excitation energies, that is, the performance of the pdsMCPs is actually worse than the one of the dsMCPs.

For main group elements nonrelativistic and, for elements heavier than Ar, scalar-relativistic CG-based MCPs were derived.[210] For the heavier s-block atoms so-called psMCPs treating besides the ns also the $(n-1)$p shell in the valence were developed, whereas for Li and Be sMCPs treating only the 2s shell in the valence were proposed.[210] For the p-block elements the ns and np shells were attributed to the valence shell, i.e., the corresponding spMCPs adopt a large-core definition.[210] Instead of numerical radial functions the construction of well-tempered MCPs (wtMCPs) for the main group elements Li− Rn by Mane and Klobukowski used well-tempered AE basis sets for the reference calculations.[457] A nonrelativistic parametrization was provided for all atoms, and a scalar-relativistic one based on the elimination of small components (RESC) formalism[92] for those heavier than Ar. For the 12 post-*nd* (n = 3, 4, 5) dimers of groups 14− 17, the mean absolute errors for bond lengths and vibrational frequencies were 0.008 Å and 0.4 cm^{-1}, respectively, when compared to scalar-relativistic RESC AE calculations.

Scalar-relativistic GC adjusted MCPs for main group elements including the $(n-1)$d shell, besides the *ns* and *np* shells in the valence space, that is, dspMCs, have been derived for the fourth (Ga−Kr), fifth (In−Xe), and sixth (Tl−Rn) main group elements.[458] The MCPs treat these elements with 13−20 valence electrons. Miyoshi et al. proposed compact basis sets for main group elements from Li to Rn.[459] Their MCP-dzp, MCP-tzp and MCP-qzp sets are designed to have comparable quality to corresponding Dunning-type AE correlation consistent basis sets, that is, cc-pVDZ, cc-pVTZ, and cc-pVQZ. For the lanthanides La−Lu corresponding MCPs with 11−25 valence electrons were presented.[460] GC AE HF energy differences of low-lying LS states of Pr to Pr^{3+} with $4f^3$ or $4f^2$ occupation are reproduced with errors of 0.2 eV or less, whereas the error for a $4f^1\ 5d^1\ ^3\mathrm{H}$ state of Pr^{3+} amounts to 1.7 eV.

Recently, improved MCPs based on the CG[85] scalar-relativistic HF approach were presented for the three transition metal series Sc−Zn, Y−Cd, and Lu−Hg.[454−456] The MCPs treat these elements with 11−20 valence electrons, that is, they correspond to a small core approach including, in addition to the *ns*, $(n-1)$d shells, also the $(n-1)$s and $(n-1)$p semicore shells in the valence space. Atomic $(n-1)\mathrm{d}^n ns^2 \rightarrow (n-1)\mathrm{d}^{n+1} ns^1$ HF excitation energies between the lowest LS states calculated with these so-called spdsMCPs agree within 0.1 eV with finite difference CG AE reference data. This accuracy is similar to the one obtained with PPs, both shape- and energy-consistent, when the same core definition is adopted.

Quite recently in 2009, Zeng and Klobukowski investigated various core definitions (pdsMCP, spdsMCP, fpdsMCP, sfpdsMCP), as well as an adjustment to third-order Douglas−Kroll−Hess (DKH3) reference data for the Au atom.[462] The small-core approach with 1s−4f in the core (60 core electrons) and 5s, 5p, 5d, and 6s in the valence (19 valence electrons) turned out to be most accurate and efficient. The same small-core approach, which can be motivated by the spatial extension of the core and valence orbitals, is also successfully used for PPs since at least two decades.[147,335,336,354]

Klobukowski and co-workers also tested the performance of the Breit−Pauli (BP) and Douglas−Kroll−Hess (DKH) spin−orbit (SO) Hamiltonians (see section 3.2) for their MCPs. It was found that for light elements the BP SO Hamiltonian including one- and two-electron terms (eqs 36) works quite well (errors of 3% and less for P, As and Sb atoms, diatomic hydrides and homonuclear diatomic cations),[464] whereas larger deviations from experimental values arise for heavier elements.[465] When analyzing the one-electron spin−orbit contributions for DKH3-adjusted MCPs for Pb and Bi it turned out that the DKH SO Hamiltonian (eq 38) leads to smaller and more accurate splitting than the BP SO Hamiltonian.[466] Both SO Hamiltonians are closely related as described in section 3.2. The kinematic factor $\hat{B}$ eq 37 in the one-electron DKH SO term damps the high momentum orbital contributions in the underlying BP term and thus corrects the overestimation.

However, when applying the DKH SO Hamiltonian to the MCP scheme it was also found that minute errors in the radial parts of the valence orbitals lead to large errors in the SO splittings. Thus it became necessary to fit also the MCP $\hat{B}r^{-3}\hat{B}$ matrix elements to the corresponding AE reference values. For this purpose Zeng et al.[466] proposed to minimize a functional Δ_{total} containing a spin-free (SF) and a SO contribution, that is,

$$\Delta_{\mathrm{total}} = \Delta_{\mathrm{SF}} + \Delta_{\mathrm{SO}} \tag{157}$$

The SF part consists of an orbital energy deviation Δ_ν^ε and an orbital radial deviation $\Delta_\nu^{\mathrm{rad}}$ which are associated with weighting factors w_ν^ε and w_ν^{rad}, and summed over all valence orbitals ν

$$\Delta_{\mathrm{SF}} = \sum_\nu (w_\nu^\varepsilon \Delta_\nu^\varepsilon + w_\nu^{\mathrm{rad}} \Delta_\nu^{\mathrm{rad}}) \tag{158}$$

with

$$\Delta_\nu^\varepsilon = |\varepsilon_\nu^{\mathrm{MCP}} - \varepsilon_\nu^{\mathrm{AE}}| \text{ and}$$

$$\Delta_\nu^{\mathrm{rad}} = \sqrt{\frac{1}{n}\sum_{k=1}^{n} [r_k R_\nu^{\mathrm{MCP}}(r_k) - r_k R_\nu^{\mathrm{MCP}}(r_k)]^2} \tag{159}$$

Here the sum in the latter expression runs over n grid points, where more weight was given to small r values. Finally, one

dx.doi.org/10.1021/cr2001383 |*Chem. Rev.* 2012, 112, 403–480

relevant SO integral is fitted with a weight factor w_{SO} as

$$\Delta_{SO} = w_{SO}\left|\frac{X^{MCP} - X^{AE}}{X^{AE}}\right| \text{ with } X = \langle \hat{B} r^{-3} \hat{B}\rangle \quad (160)$$

In case of the tested elements Pb and Bi the SO fit was only performed for the 6p valence orbital.

Similar DKH3-adjusted MPs were generated for the p-block elements B−Tl.[461,463] For the first row the valence space had to be 2s2p (spMCP), whereas for the second row it was 2s2p3s3p for group 13 (spspMCP) and 2p3s3p for groups 14−18 (pspMCP). Starting from the third row the underlying (n-1)s, (n-1)p and (n-1)d orbitals were included in the valence space for group 13 (spdspMCP), whereas only $(n-1)$p and $(n-1)$d were included for groups 14−18 (pdspMCP). Again, the smaller cores as compared to previous MCPs resulted in significantly lower errors when compared to AE results, i.e., for excitations in the ground state configuration of X and X^+ (X = P, As, Sb) the deviations usually stay below 0.1 eV. However, since the comparison was performed at the correlated (MBQDPT) level and no configuration changes were considered, it is quite difficult to judge the MCP errors. The optimized valence basis sets were (21s14p5d) contracted to [7p7p5d] for B−Ne, (21s17p5d) contracted to [8s8p5d] for Al and [7s8p5d] for Si−Ar, (27s21p16d) contracted to [8s8p6d] for Ga and [7s8p6d] for Ge− Kr, (29s24p19d) contracted to [11s12p9d] for In, [10s11p10d] for Sn and Sb, and [11s11p9d] for Te− Xe, as well as (29s25p20d) contracted to [11s12p8d] for Tl and [10s11p9d5f3g] for Pb−Rn. (4f3g)/[4f3g] and (5s3g)/[5f3g] correlation/polarization sets were added to all basis sets for B−Tl and Pb−Rn, respectively. Despite the large basis sets the computational savings at the CI level range from 52% for O and 87% for Te.[461]

The DKH3 MCPs and the corresponding DKH SO formalism will certainly undergo further development in the near future, for example, for transition metals, as well as lanthanides and actinides, it will be necessary to optimize the SO matrix elements of more than just one shell. In addition, for heavier elements the Breit interaction has to be included also in the scalar-relativistic MP formalism.

7.3. Model Potentials for Use in Density Functional Theory

The nonrelativistic MP approach was first used by Katsuki and co-workers in the framework of Hartree−Fock−Slater (HFS) X_α calculations.[467,468] A DFT-based MP method using the local-spin density (LSD) approach with the VWN local correlation functional was developed by Andzelm, Radzio and Salahub.[469] Starting from the Kohn−Sham (KS) equation for a spin-polarized system with n_v valence electrons and assuming orthogonality between the valence $|\varphi_v^\sigma\rangle$ and core orbitals $|\varphi_c^\sigma\rangle$ of spin σ (σ = +, −) the Huzinaga−Cantu eq 90 can be rewritten as

$$\hat{H}_{eff}^\sigma + \sum_c (-2\varepsilon_c^\sigma)|\varphi_c^\sigma\rangle\langle\varphi_c^\sigma||\varphi_v^\sigma\rangle = \varepsilon_v^\sigma|\varphi_v^\sigma\rangle \quad (161)$$

The effective one-electron operator $\hat{H}_{eff}^\sigma$ and the shift operator in eq 161 can be split up into a valence part $\hat{H}_{eff,v}^\sigma$ and a model potential $\Delta\hat{V}_{MP}^\sigma$, that is,

$$\hat{H}_{eff}^\sigma + \sum_c (-2\varepsilon_c^\sigma)|\varphi_c^\sigma\rangle\langle\varphi_c^\sigma| = \hat{H}_{eff,v}^\sigma + \Delta\hat{V}_{MP}^\sigma \quad (162)$$

with

$$\hat{H}_{eff,v}^\sigma = -\frac{1}{2}\hat{\vec{\nabla}}^2 - \sum_\lambda \frac{Q_\lambda}{r_\lambda} + \int \frac{\rho_v(\vec{r}\,')\,d\vec{r}\,'}{|\vec{r} - \vec{r}\,'|} + v_{xc}[\rho_{+,v}, \rho_{-,v}] \quad (163)$$

Here Q_λ stands for the charge of core λ and v_{xc} represents the exchange-correlation potential. $\rho_{+,v}$ and $\rho_{-,v}$ denote the spin-up and spin-down valence densities, respectively, which are defined in terms of the valence orbitals φ_i^σ and their occupation numbers f_i^σ

$$\rho_{\sigma,v}(\vec{r}) = \sum_i^{n_v} f_i^\sigma |\varphi_i^\sigma(\vec{r})|^2 \quad (164)$$

If one assumes that FC approximation is valid, that is, the core orbitals of the atoms do not overlap with each other and cross terms in the exchange and correlation potential can be neglected, $\Delta\hat{V}_{MP}^\sigma$ can be written as a sum over atomic MPs $\Delta\hat{V}_{MP}^{\lambda,\sigma}$ centered at cores λ

$$\Delta\hat{V}_{MP}^\sigma = \sum_\lambda \Delta\hat{V}_{MP}^{\lambda,\sigma} \quad (165)$$

Similar to eq 91 the MP is split into a Coulomb potential $\Delta\hat{V}_C^{\lambda,\sigma}$, an exchange and correlation potential $\Delta\hat{V}_{Xc}^{\lambda,\sigma}$ and the core shift operator P_S^λ

$$\Delta\hat{V}_{MP}^{\lambda,\sigma} = \Delta\hat{V}_C^{\lambda,\sigma} + \Delta\hat{V}_{Xc}^{\lambda,\sigma} + P_S^\lambda \quad (166)$$

with

$$\Delta\hat{V}_C^{\lambda,\sigma} = -\frac{n_c^\lambda}{r_\lambda} + \int \frac{\rho_c^\lambda(\vec{r}\,')\,d\vec{r}\,'}{|\vec{r} - \vec{r}\,'|} \quad (167)$$

$$\Delta\hat{V}_{Xc}^{\lambda,\sigma} = v_{xc}[\rho_{+,c}^\lambda, \rho_{-,c}^\lambda] \quad (168)$$

and

$$\hat{P}_S^\lambda = \sum_c (-2\varepsilon_c^{\lambda,\sigma})|\varphi_c^{\lambda,\sigma}\rangle\langle\varphi_c^{\lambda,\sigma}| \quad (169)$$

Here n_c^λ and ρ_c^λ stand for the number of electrons included in the core λ and the corresponding core electron density, respectively. $\rho_{+,c}^\lambda$ and $\rho_{-,c}^\lambda$ are the corresponding spin-up and spin-down densities, respectively, which can be evaluated from the core orbitals analogous to eq 164 used for the valence densities.

For practical calculations the Coulomb and exchange-correlation potentials are approximated as a linear combination of radial Gaussian functions divided by r

$$\Delta\hat{V}_C^{\lambda,\sigma}(i) + \Delta\hat{V}_{Xc}^{\lambda,\sigma}(i) = \frac{1}{r_{i\lambda}}\sum_k A_k^\lambda e^{-\alpha_k^\lambda r_{i\lambda}^2} \quad (170)$$

Similar to the AIMP approach of Seijo and co-workers the constraint $\Sigma_k A_k^\lambda = Z^\lambda - Q^\lambda = -n_c^\lambda$ is imposed to obtain the correct asymptotic behavior, where n_c^λ denotes the number of core electrons of core λ. The core orbitals used in the shift operator $\hat{P}_S^\lambda$ are approximated by a linear combination of Gaussian functions determined with a least-squares fit procedure. Similar to the work of Seijo and co-workers the reference atomic orbitals were obtained from CG/WB-type LSD VWN finite-difference atomic AE calculations.[85,84]

7.4. Model Potentials with Explicit Relativistic Hamiltonians

It is well-known that direct relativistic contributions originate mainly in the vicinity of the nucleus. Those MPs, which keep the

dx.doi.org/10.1021/cr2001383 |Chem. Rev. 2012, 112, 403–480

correct nodal structure of the valence orbitals, are therefore much more suited for an explicit inclusion of relativistic effects than PPs, for which the radial nodal structure of the pseudovalence orbitals has been simplified, or some older MPs were due to economic reasons nodal structure is not fully kept. Various approximate relativistic AE schemes were combined with the MP approach during the last two decades. Although the reported results are generally very good, the usage of these approaches in applications is rather scarce.

Wittborn and Wahlgren presented in 1995 relativistic AIMPs for third-row transition metals where indirect relativistic effects of the core on the valence orbitals were incorporated in the potential, whereas the direct relativistic effects were treated explicitly using the scalar-relativistic second-order DKH (DKH2) Hamiltonian.[183] The AIMP included the 4s, 4p, 4d, 5s, 5p, 5d, and 6s orbitals in the valence space, but not the 4f orbitals. The basis sets compared to AE reference calculations could be significantly reduced. Atomic $s^2d^n-s^1d^{n+1}$ HF energy differences between the lowest LS states exhibited mean absolute errors of 0.05 and 0.07 eV with respect to AE DKH2 results and the finite difference CG results of Martin and Hay.[158] In case of the monohydrides the AE and AIMP DKH2 differ typically by 1 or 2 kcal/mol for HF, MCPF and PCI80 binding energies. Whereas the AE and AIMP DKH2 bond lengths of HfH to OsH agree within 0.01 Å, deviations of up to 0.04 Å are found for LaH, IrH and PtH, with the AIMP yielding the longer bonds.

Similar scalar-relativistic AIMPs to be used with the second-order DKH (DKH2) Hamiltonian were presented for the first-, second- and third-row transition metals by Rakowitz et al. using a $(n-1)$p $(n-1)$d ns valence space,[184] as well as a $(n-1)$s $(n-1)$p $(n-1)$d ns valence space.[185] In test calculations for the group 5 and group 10 transition metal oxides (VO, NbO, TaO; NiO, PdO, PtO) the second choice was found to yield superior results, especially it leads to a decrease of the dissociation energies of the early transition metal oxides bringing them to better agreement with the AE DKH values. This finding coincides with experience from PP calculations.[147,335,336,354]

For lanthanides[186] and actinides,[187] scalar-relativistic AIMPs to be used with the third-order DKH (DKH3) Hamiltonian were derived by Seijo, Hirao and co-workers. The 4f, 5s, 5p, 5d, and 6s shells of the lanthanides were treated explicitly in the valence space (46 core electrons, $[^{36}Kr]$ $4d^{10}$ core), whereas for the actinides a 5f, 6s, 6p, 6d, and 7s valence space (78 core electrons, $[^{54}Xe]$ $4f^{14}$ $5d^{10}$ core), as well as a 5d, 5f, 6s, 6p, 6d, and 7s valence space (68 core electrons, $[^{54}Xe]$ $4f^{14}$ core), were applied. For the actinides it was concluded that the larger core, which is analogous to the one used for the lanthanides, is sufficiently accurate. The accuracy of the approach was established by comparing AE and MP orbital energies and radial expectation values as well as by molecular calculations on CeO and ThO. It should be noted, however, that changes of the f occupation number were not considered in these tests. FC errors for Ce and Th treated at the AE MCDHF/DC level amount to up to 0.44 and 0.27 eV, respectively.[29] A SO treatment using the DKH-type atomic mean-field approximation in a state-interaction method was also proposed.[470]

The relativistic scheme by eliminating the small components (RESC) of the Dirac equation advocated by Nakajima and Hirao[92] was also combined with the AIMP approach for Pt, Au and Hg using a 5p, 5d, 6s valence space.[471]

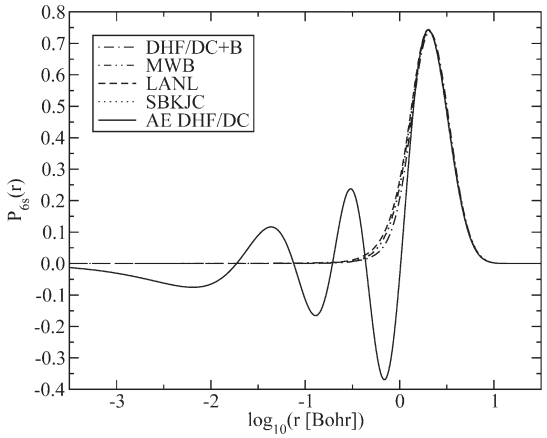

Figure 21. 6s pseudovalence orbitals of Pb in the $6s^2$ $6p^2$ ground state configuration for MCDHF/DC[174] and WB[148] energy-consistent and LANL[355] and SBKJC[286] shape-consistent four-valence-electron PPs in comparison to the 6s large component from a multiconfiguration Dirac–Hartree–Fock calculation with the Dirac–Coulomb Hamiltonian using the program GRASP.[83]

8. COMPUTATIONAL DETAILS

8.1. Valence Basis Sets for Pseudopotentials

The optimization of reliable valence basis sets is as important as the PP parametrization itself. Since the valence basis sets are connected to the PPs for which they were optimized, we described the available basis sets together with the corresponding PP approaches in section 6. In this section, we will briefly discuss some features common to all types of PPs. Several reviews on basis sets appeared, some of them address also basis sets for modern PPs.[472−474]

In most ab initio electronic structure calculations atom-centered one-particle basis sets of Gaussian-type are used to construct the molecular orbitals as a linear combination.[58,59] One important motivation for the usage of PPs is to reduce the number of primitive basis functions in the integral evaluation in comparison to AE calculations. Because of the simplified radial nodal structure of the pseudovalence orbitals one might also expect smaller basis set superposition errors, at least at the HF level. Some of these advantages are usually lost when large unoptimized basis sets, for example, even-tempered basis sets or also AE basis sets, are applied in PP calculations. Because of the completely different radial shape of AE valence orbitals and PP pseudovalence orbitals in the core region, contracted AE sets are usually not suitable for the PP case. Even uncontracted AE sets yield sometimes higher total energies than smaller sets optimized for the PP.

Because the non-uniqueness of the pseudovalence orbitals discussed in section 5.3.1, these exhibit different radial shapes in the spatial core region for the different PPs of a specific element, despite equal core–valence separation, that is, despite an equal choice of the core. Examples are provided in Figures 21 and 22 for the $6s^2$ $6p^2$ ground state configuration of Pb. Although the four PPs of different origin show a similarly good agreement with the large components of the 6s and averaged 6p spinors of a state-averaged MCDHF/DC calculation[83] in the valence region, they differ substantially in the core region. Therefore only the usage of valence basis sets optimized for the PP under consideration will provide a reliable description, whereas the usage of basis sets optimized for other PPs, even for the same core definition,

dx.doi.org/10.1021/cr2001383 |Chem. Rev. 2012, 112, 403–480

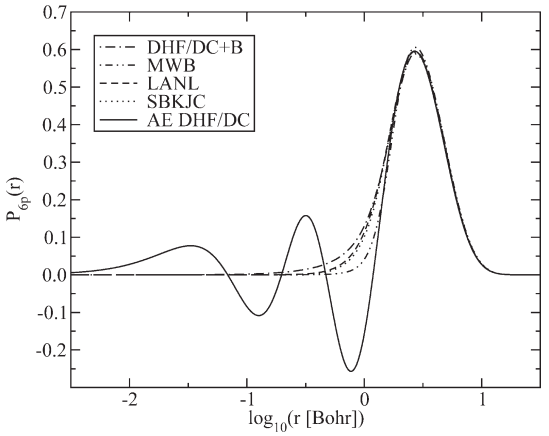

Figure 22. Same as Figure 21, but for the 6p pseudovalence orbitals. The AE 6p valence orbital is a $2j + 1$-weighted average of the $6p_{1/2}$ and $6p_{3/2}$ spinors.

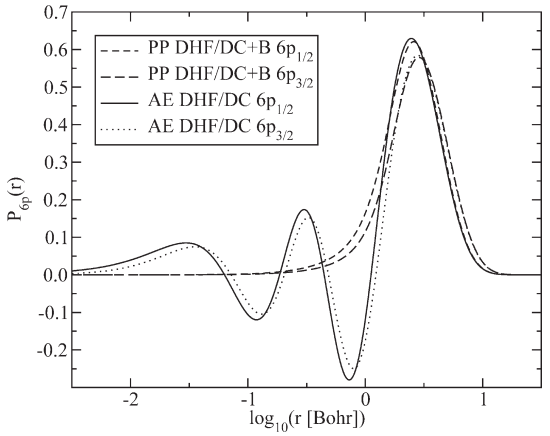

Figure 23. Same as Figure 21, but for the $6p_{1/2}$ and $6p_{3/2}$ pseudovalence spinors.

frequently leads to relatively large errors in the total valence energy.[27] If a more extended basis set than provided for a specific PP is desired, it is thus recommended to optimize and contract a new primitive set, or if this is not desired to augment the original basis sets coming with the PP.

It was pointed out by Christiansen, that care has to be taken when augmenting small contracted basis sets with diffuse functions.[475] Pseudovalence orbitals have a fundamentally different shape compared to AE valence orbitals in the core region. For the shape-consistent approach this follows from their construction according to eq 111 and the conditions imposed on the function f_{lj}. Whereas nonrelativistic AE s orbitals have nonzero amplitudes at the origin, p orbitals have nonzero first derivatives, etc., the corresponding pseudovalence orbitals have zero values in each case. Primitive Gaussian s functions, however, have their maximum at the origin, where the PPs are usually most repulsive for angular momenta present in the core. One therefore frequently observes during basis set optimizations that two exponents become nearly equal and the coefficients attain a similar magnitude, but are of different sign. To avoid such problems some researchers used Cartesian Gaussian basis sets instead of spherical ones,[476] for example, of the 6 and 10 Cartesian Gaussian primitives arising for $i + j + k = 2$ and 3 in $x^i y^j z^k \exp(-\alpha r^2)$ the linear combinations corresponding to one 3s and three 4p functions were kept in the basis in addition to the usual five 3d and seven 4f functions, respectively. However, as was pointed out by Christiansen, the problem is more complex and besides one-center effects also two-center effects have to be considered.[475]

A nodeless s pseudovalence orbital described by a contraction of Gaussian functions is often made more flexible by either freeing the most diffuse s function from the contraction or by adding a diffuse s function. In both cases, although the HF energy remains the same or gets somewhat lower, the gain in the correlation energy may be quite limited. The reason is that when freeing the most diffuse s function from the contraction the lower (occupied) orbital will have coefficients such that the amplitude near the nucleus becomes nearly zero, whereas this is not possible for the higher (virtual) orbital. This therefore experiences the strong repulsion of the PP at the origin and gets a quite high orbital energy. When adding a diffuse s function to an existing contraction, which already has coefficients such that the amplitude near the nucleus is nearly zero, no function is available to compensate the nonzero amplitude of the added diffuse function at the origin. Thus, again a high orbital energy results. In both cases the virtual orbital is unfavorable for electron correlation calculations. One solution is to use two primitives $|\chi_m\rangle$ and $|\chi_{m-1}\rangle$, and contract them so that the amplitude at the origin is zero, that, to use a so-called augmented primitive

$$|\chi_m\rangle - (\alpha_m/\alpha_{m-1})^{(2l+3)/4}|\chi_{m-1}\rangle \text{ with } \alpha_{m-1} > \alpha_m \qquad (171)$$

Here α_m and α_{m-1} denote the primitive exponents. This prescription solves the atomic case, however in case of a molecule diffuse orbitals on a neighboring center may have nonnegligible s contributions on the PP center. If for the PP center only contractions and augmented contractions with zero amplitude at the origin are used, these cannot cancel the nonzero amplitude of the diffuse orbitals on neighbor atoms. Therefore, Christiansen advocated for s type basis functions on PP centers not to use augmented primitives, but rather a diffuse primitive and an additional tight primitive in uncontracted fashion. The two-center effect described here is less strong for p shells than for s shells. For p Christiansen therefore favored the addition of an augmented primitive, whereas for higher angular momenta the diffuse functions can be selected as in AE work. Thus, according to Christiansen at least a basis set with three s functions (contraction, tight function and diffuse function) and two p functions (contraction, augmented diffuse primitive) is needed for a large-core PP description. The CI and MP2 correlation energies of H_2O and HI increased by 3−7% compared to those obtained for an addition of single diffuse functions.[475] We note that the analysis is valid for small contracted basis sets, since in most larger basis sets there are enough uncontracted functions to achieve zero or near-zero amplitudes at the PP origin.

A related topic to the nonuniqueness of the pseudovalence orbitals and the nontransferability of (contracted) scalar-relativistic valence basis sets from one PP to another, is the usage of such basis sets in calculations with SO coupling. It can be seen from a comparison of Figure 23 with Figures 21 and 22 that the Pb $6p_{1/2}$ and $6p_{3/2}$ pseudovalence spinors differ radially as much from each other, as well as from their scalar-relativistic 6p counterpart, as the scalar-relativistic 6s or 6p pseudovalence orbitals of different PPs do. Therefore similar problems are expected when using a scalar-relativistically contracted basis set in a two-component PP calculation for cases where the

dx.doi.org/10.1021/cr2001383 |*Chem. Rev.* 2012, 112, 403–480

differences in the radial shapes of spinors are significant. It was therefore suggested to use separate contractions for $j = l - 1/2$ and $j = l + 1/2$ spinors.[27] The problem was also discussed by Armbruster et al.,[309] who added steep functions to their scalar-relativistic PP valence basis sets.

8.2. Integrals over Ab Initio Pseudopotentials

To use a valence-only model Hamiltonian $\hat{H}_v$ with ECPs in standard quantum chemical calculations one needs to evaluate the corresponding integrals over (Cartesian) Gaussian basis functions. The integrals for semilocal PPs are more involved than those for MPs, where only a local potential and in case of AIMPs a nonlocal representation of the exchange has to be considered.

The one- and two-electron integrals over Cartesian Gaussian basis functions[60] commonly encountered in quantum chemistry can be evaluated, e.g., according to the formalism developed by McMurchie and Davidson.[477] Early computer codes for the corresponding PP integral evaluation at the scalar-relativistic level were developed by Kahn et al. (LPPOLY),[194] Barthelat et al. (PSIBMOL),[240] Kolar (PSEPOT),[241] and McMurchie and Davidson (MELDPS).[242] The latter approach was improved and extended to calculate the integrals over SO PPs by Pitzer and Winter.[445] An implementation of the McMurchie–Davidson scheme for scalar-relativistic cases using partly quadrature instead of analytical integration was reported by Skylaris et al.[478] Possible numerical instabilities occurring for exponents of unusual size were discussed by van Wüllen.[479] First and second derivatives with respect to nuclear coordinates were reported for scalar-relativistic PPs, for example, by Kitaura et al.[480] and Cui et al.,[481] respectively, and for two-component PPs by van Wüllen and Langermann.[482] For atom-centered PPs and basis functions the derivatives of the PPs can be formulated in terms of derivatives of basis functions,[480] which are for Cartesian Gaussians linear combinations of (other) Cartesian Gaussians. Therefore gradient contributions of PP integrals, both one- and two-component, can be evaluated using a modified PP integral code.

To simplify the integral evaluation Pélissier et al. transformed the semilocal PPs into nonlocal form, so that the integral evaluation consists only of the evaluation of overlap integrals.[429] This approach works well if the PP is only represented by Gaussian functions, but is less accurate when prefactors as $1/r$ or $1/r^2$ are present as in some shape-consistent PPs and fails for terms with $1/r^4$ occurring in CPPs.

Integral formulas over the CPP with cutoff functions of Meyer and co-workers were derived for Cartesian Gaussian functions by Schwerdtfeger and Silberbach using a Laplace transformation.[483,484] Smit later also applied the method of McMurchie and Davidson and presented formulas to evaluate CPP integrals,[485] however a corresponding implementation was not performed to our knowledge.[485] Integrals for CPPs with a l-dependent step cutoff function were elaborated by Foucrault et al.[197]

Some older work was performed with Gaussian lobe functions.[61] The corresponding integrals over scalar-relativistic and spin–orbit PPs are available from work of Chang et al.[191] and Hafner and Schwarz,[234] respectively, and those over CPPs were given by Schwerdtfeger et al.[277] A detailed review of the methods of computation of the ECP and CPP integrals is beyond the scope of the present review. In the following sections, we just try to illustrate a few basic steps and refer for details to the original articles.

8.2.1. Integrals Using a Nonlocal Representation.

The approach of Pélissier et al.[429] uses a transformation of the atomic semilocal part $V_l\hat{P}_l$ of the PP in eqs 75 and 78 into a nonlocal form

$$\hat{\tilde{V}}_l = \sum_i \sum_j A_{ij} |g_i\rangle\langle g_j| \tag{172}$$

where the $|g_i\rangle$ are orthonormalized linear combinations of Cartesian Gaussian functions

$$\langle \vec{r}\,|g_i\rangle = \sum_k B_{ik} x^{l_{ix}} y^{l_{iy}} z^{l_{iz}} e^{-b_{ik} r^2} \text{ with } l_{ix} + l_{iy} + l_{iz} = l \tag{173}$$

The parameters in eq 173 are determined by minimizing the sum S of squared differences of matrix elements over $\hat{\tilde{V}}_i$ and V_l for a large atom centered basis set $\{|\chi_i\rangle\}$ of appropriate angular symmetry l

$$S = \sum_{ij} (\langle\chi_i|\hat{\tilde{V}}_l|\chi_j\rangle - \langle\chi_i|V_l\hat{P}_l|\chi_j\rangle)^2 \tag{174}$$

For applications the nonlocal operator $\hat{\tilde{V}}_l$ is cast in simpler form by diagonalizing the matrix of the coefficients A_{ij}

$$\hat{\tilde{V}}_l = \sum_i \bar{A}_i |\bar{g}_i\rangle\langle\bar{g}_i| \tag{175}$$

where $\bar{A}_i$ and $|\bar{g}_i\rangle$ are the resulting eigenvalues and eigenvectors of the $[A_{ij}]$ matrix in the original $\{|g_i\rangle\}$ basis. The integral evaluation in molecular calculations is thus reduced to the calculation of overlap integrals between the molecular basis and the expansion basis $\{|\bar{g}\rangle\}$. Similarly the evaluation of derivatives of PP matrix elements with respect to the nuclear coordinates which are needed in energy gradients for geometry optimizations involves only the computation of derivatives of these overlap integrals.[429] The approach of Pélissier et al. is closely related to the separable form of PPs developed in theoretical solid state physics for usage with plane-wave basis sets,[426−428] which is also useful for Car–Parrinello dynamics,[486] see section 6.5.7.

8.2.2. Integrals over Scalar-Relativistic Pseudopotentials.

Considering unnormalized Cartesian Gaussian functions on center A

$$\langle \vec{r}\,|\phi(n,l,m,\alpha_A,A)\rangle = x_A^{i_A} y_A^{j_A} z_A^{k_A} e^{-\alpha_A r_A^2} \tag{176}$$

with

$$\vec{r}_A = (x_A, y_A, z_A) = \vec{r} - \vec{A} \tag{177}$$

and analogously on B, and the semilocal PP eq 78 on center C, one ends up after applying the expansion eq 89 with two basic types of integrals to be solved, that , type 1 for the local part without projector on C

$$\chi_{AB} = \langle\phi_A|r_C^n \exp(-ar_C^2)|\phi_B\rangle \tag{178}$$

and type 2 for the semilocal part with projector on spherical harmonics centered on C

$$\gamma_{AB} = \sum_{m=-l}^{+l} \int_0^\infty \langle\phi_A|lm,C\rangle r_C^{n+2} \exp(-ar_C^2)\langle lm,C|\phi_B\rangle \, dr_C \tag{179}$$

Here the following abbreviation is used for the function resulting from the angular integration of the product of the basis function

dx.doi.org/10.1021/cr2001383 |Chem. Rev. 2012, 112, 403–480

ϕ_A with the (real) spherical harmonics Y_{lm}:

$$\langle \phi_A | lm, C \rangle = \int \phi_A(\Omega_A, r_A) Y_{lm}(\Omega_C) \mathrm{d}\Omega_C \quad (180)$$

The basic steps for the evaluation of the type 1 integrals χ_{AB} according to McMurchie and Davidson[242] are (1) the transformation of the exponential parts of $|\phi_A\rangle$ and $|\phi_B\rangle$ to the center C, (2) the transformation of x_A^{iA}, etc., to center C, and (3) the expansion of the nonspherically symmetric part of the resulting integrand in products of spherical harmonics and modified spherical Bessel functions of the first kind. After separating the angular from the radial variables of integration one ends up with multiple sums over products of angular and radial integrals. The angular integrals are of the type

$$\Omega_\lambda^{IJK} = \sum_{\mu=-\lambda}^{+\lambda} Y_{\lambda\mu}(\Omega_k) \int \hat{x}^I \hat{y}^J \hat{z}^K Y_{\lambda\mu}(\Omega) \mathrm{d}\Omega \quad (181)$$

with Ω_k being determined by the positions and exponents of the basis functions at A and B, λ being the running index for the expansion used in step (3) above, and $\hat{x} = x/r$. The radial integral is of the type

$$Q_\lambda^N(k, \alpha) = \int_0^\infty r^N \exp(-\alpha r^2) M_\lambda(kr)\, \mathrm{d}r \quad (182)$$

with k being determined by the positions and exponents of the basis functions at A and B, α the sum of exponential parameters of the basis functions at A and B and the PP term at C, and M_λ a modified spherical Bessel function of the first kind.

The type 2 integrals γ_{AB} are also reduced to multiple sums over products of angular and radial integrals using the above-mentioned three steps. Because of the presence of the projection operator on center C, the resulting angular and radial integrals are slightly more involved, since the expansion of step (3) has to be applied twice, that is,

$$\Omega_{\lambda,lm}^{IJK} = (4\pi)^{-1} \sum_{\mu=-\lambda}^{+\lambda} Y_{\lambda\mu}(\Omega_k) \int \hat{x}^I \hat{y}^J \hat{z}^K Y_{\lambda\mu}(\Omega) Y_{lm}(\Omega) \mathrm{d}\Omega \quad (183)$$

and

$$Q_{\lambda,\lambda}{}^N(k, \alpha) = \int_0^\infty r^N \exp(-\alpha r^2) M_\lambda(k_A r) M_\lambda(k_B r)\, \mathrm{d}r \quad (184)$$

McMurchie and Davidson showed that the angular integrals can be readily evaluated in analytical form by expanding the $Y_{\lambda\mu}$ in terms of $\hat{x}$, $\hat{y}$, and $\hat{z}$. The evaluation of the type 1 radial integral Ω_λ^{IJK} is relatively straightforward and leads to a product of a ratio of gamma functions and a hypergeometric function. Using a recursion relation for the modified spherical Bessel functions McMurchie and Davidson could also derive a number of useful recursion relations for the type 1 radial integrals. An additional recursion relation was given by Pitzer and Winter.[445] There is no integration scheme suitable for all cases of the more difficult type 2 integrals $Q_{\lambda,\lambda}^N$. McMurchie and Davidson proposed three schemes[242] and a fourth one was suggested by Pitzer and Winter.[445] Besides Gauss–Hermite quadrature, McMurchie and Davidson used in their code a power series expansion of one of the two modified spherical Bessel functions leading to a reduction to a sum over type 1 radial integrals. Another variant using power series expansions for both modified spherical Bessel functions leading to a sum over hypergeometric functions was also proposed. Pitzer and Winter were able to express the integrals as a finite double sum over all positive contributions containing Bessel functions. The corresponding integral codes select for each case the integration scheme which is suitable in terms of accuracy and computational speed, and of course make use of recursion relations whenever it is possible. Skylaris et al. proposed to evaluate eq 180 analytically on a radial grid and then to apply quadrature to compute eq 179 directly without further analytical manipulations.[478]

8.2.3. Integrals over Spin–Orbit Pseudopotentials. The integrals over the spin–orbit operator can be factored into space and spin parts. The choice of Pitzer and Winter was the evaluation of the three components of the spatial part separated from the spin part,[445] which has to be generated later, e.g., in the spin–orbit CI code.[346] In the currently applied formalism based on eqs 84 and 87 type 1 SO integrals do not occur. The spatial part of the type 2 integrals is of the form

$$\nu_{AB} = \sum_{m=-l}^{l} \sum_{m'=-l}^{l} i^{-1} \int_0^\infty r_C{}^n e^{-br_C{}^2} \langle \phi_A | lm \rangle \langle lm | \hat{\vec{l}} | lm' \rangle \langle lm' | \phi_B \rangle \mathrm{d}r \quad (185)$$

Here a factor $-i$ was inserted to make the integral real (note that $\hat{\vec{l}} = -i\,\vec{r} \times \hat{\vec{\nabla}}$). The double sum over m and m' contains a maximum of $(2l - 1)$ terms, because many of the matrix elements $\langle lm | \hat{\vec{l}} | lm' \rangle$ are zero. Using the strategy of McMurchie and Davidson,[242] the integral can be reduced to a multiple sum over products of angular and radial integrals, corresponding to eq 181 and eq 182, respectively. To the three methods proposed by McMurchie and Davidson for the evaluation of the radial integrals, Pitzer and Winter added as a fourth method the rewriting as a finite double sum over all positive terms containing Bessel functions.[445] Since this method is also not applicable to all cases, Pitzer and Winter used also the expansion of one Bessel function as a power series and the quadrature proposed by McMurchie and Davidson, as well as a recursion relation involving no differencing.

8.2.4. Integrals over Core Polarization Potentials. To evaluate the matrix elements over the core polarization potential V_{cpp} eqs 97–100, one has to recognize that the two-electron integrals can be traced to a product of two one-electron integrals. The one-electron integrals are of the following two basic types:

$$\omega_{AB}^1 = \langle \phi_A | \frac{1}{r_C{}^4} F^2(r_C, \delta) | \phi_B \rangle \text{ and}$$
$$\omega_{AB}^2 = \langle \phi_A | \frac{x_C}{r_C{}^3} F(r_C, \delta) | \phi_B \rangle \quad (186)$$

with F denoting the cutoff function. Despite the absence of projection operators the evaluation of CPP integrals is considerably more complex than the one over the scalar-relativistic PPs and SO PPs outlined in the last two sections. In 1988, Schwerdtfeger and Silberbach succeeded in finding analytical expressions for the above integrals by using a Laplace transformation[483,484] and generated a working code available in the MOLPRO program system. About a decade later Smit[485] showed that these integrals can also be calculated using the formalism of McMurchie and Davidson,[242] when a slight modification by Jensen et al.[487] is used.

The product of two Gaussians $|\phi_A\rangle$ and $|\phi_B\rangle$ centered at points A and B, respectively, is first written as a new Gaussian $|\phi_P\rangle$ with

dx.doi.org/10.1021/cr2001383 |Chem. Rev. 2012, 112, 403–480

exponent $\alpha_P = \alpha_A + \alpha_B$ centered at point P, with $\alpha_P\vec{P} = \alpha_A\vec{A} + \alpha_B\vec{B}$. Similar to the scheme of McMurchie and Davidson $|\phi_P\rangle$ is then expanded with respect to point C. According to Jensen et al. the integral over an arbitrary (local) potential $V(r_C)$ can be written for s-type Gaussian function $|\phi_P\rangle$ as[487]

$$\omega^s_{AB} = E_{AB}2\pi e^{-\alpha_p|\overrightarrow{CP}|^2}\int_0^\infty V(r_C)r_C^2 \times e^{-\alpha_P r_C^2} \times \left(\int_{-1}^{1} e^{2\alpha_P|\overrightarrow{CP}|r_C u}du\right)dr_C \quad (187)$$

with E_{AB} being a constant depending on the exponents and positions of $|\phi_A\rangle$ and $|\phi_B\rangle$. Smit gave corresponding analytical solutions for the integrals $\omega^{s,1}_{AB}$ and $\omega^{s,2}_{AB}$ involving the error function. The integrals for Cartesian Gaussian functions with $l > 0$ can be written as a linear combination of the partial derivatives of these integrals with respect to CP_x, CP_y, and CP_z.[485]

8.2.5. Derivatives of Pseudopotential Integrals. Morokuma and co-workers pointed out that integrals over derivatives of ECPs may be complicated, but nevertheless they can be easily evaluated when the translational invariance of the matrix elements is exploited.[480] For instance, the translational invariance in x-direction requires that the first derivatives of an ECP matrix element with respect to the x-coordinates of the nuclei D sum up to zero

$$\sum_D \frac{\partial}{\partial x_D}\langle\phi_A|\hat{V}_C|\phi_B\rangle = 0 \quad (188)$$

from which the expression

$$\left\langle \phi_A\left|\frac{\partial\hat{V}_C}{\partial x_C}\right|\phi_B\right\rangle = -\left(\left\langle\frac{\partial\phi_A}{\partial x_A}|\hat{V}_C|\phi_B\right\rangle + \left\langle\phi_A|\hat{V}_C|\frac{\partial\phi_B}{\partial x_B}\right\rangle\right) \quad (189)$$

can be derived. In case of Cartesian Gaussian functions the derivatives occurring on the right side are just linear combinations of other Cartesian Gaussian functions, for example, for eq 176 one obtains

$$\frac{\partial}{\partial x}\langle\vec{r}\,|\phi(n,l,m,\alpha_A,A)\rangle = (1-\delta_{i_A,0})x_A^{i_A-1}y_A^{j_A}z_A^{k_A}e^{-\alpha_A r_A^2} - 2\alpha_A x_A^{i_A+1}y_A^{j_A}z_A^{k_A}e^{-\alpha_A r_A^2} \quad (190)$$

A similar strategy can be used to evaluate higher derivatives.[481] Contributions of ECPs to gradients of the total energy can thus be readily evaluated with a modified ECP integral code.

8.3. Computational Schemes

Figure 24 shows schematically the major sequences (I−IV) of computational steps in relativistic ab initio electronic structure calculations. Hereby it is assumed that a relativistic and correlated calculation is to be performed, the result of which can be compared to experimental data. In Figure 24, the entry configuration interaction stands for a wave function-based correlated calculation such as CI (configuration interaction), CC (coupled cluster), or many-body perturbation theory (MBPT). Similarly, the entries Dirac−Hartree−Fock and Hartree−Fock also stand for their multiconfiguration analogues. The most rigorous strategy (IV) are 4-component AE DHF calculations followed by CI, CC, or MBPT in the basis of the spinors corresponding to the electronic one-particle states. Although 4-component ECPs can be derived and applied in corresponding calculations with an explicit treatment of relativistic contributions,[181] and even CI calculations have been performed,[182] a much more efficient modeling of the AE case is the usage of 2-component ECPs with an implicit treatment of relativistic contributions (III). Such an approach was early advocated by Hafner, Schwarz, and Esser,[234,488−490] who developed and implemented a GUGA-based MRCI code. The code was later extended to perform, e.g., ACPF calculations.[311] Implementations of several electron correlation schemes based on Kramers-restricted (KR)[491] and Kramers-unrestricted (KU)[492] HF solutions were developed by Lee and co-workers, that is, KRMP2,[493] KUMP2,[492] KRCI,[494] KRCCSD and KRCCSD(T),[495] as well as KRCASSCF.[496,497] These implementations partly made use of the infrastructure provided by the MOLFDIR relativistic AE package.[93] A two-component HF SCF[417] and energy-gradient[482] code was reported by van Wüllen and co-workers. An efficient DFT version suitable for the treatment of larger systems was also described.[498] Recently, an implementation of MP2 using two-component $f(r_{12})$-dependent wave functions (SO-MP2-F12) starting from a two-component HF SCF solution[499] was reported by Bischoff and Klopper.[500]

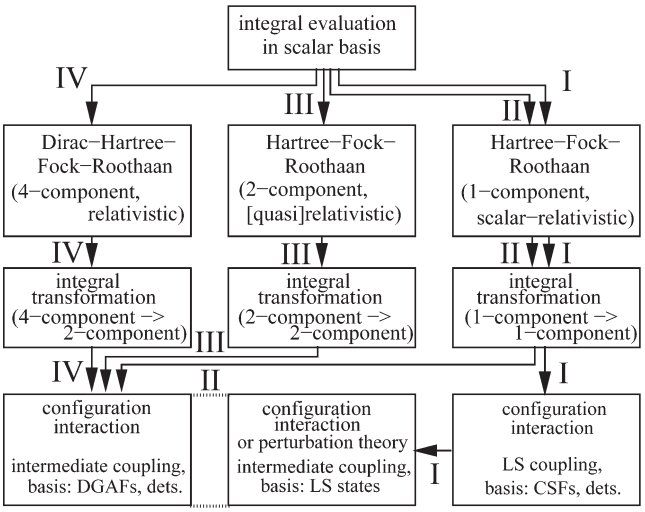

Figure 24. Schematic overview of relativistic quantum chemical ab initio approaches accounting also for spin−orbit coupling. Four major sequences (I−IV) of calculation steps exist, which lead to an increasing accuracy, but also require an increasing computational effort.

Although the computational effort of the final correlation step is the same for both the AE and ECP case, provided an identical number of electrons is correlated in an identical number of orbitals, large computational savings arise in ECP schemes at the three earlier stages of the calculation, i.e., integral evaluation, HF step and integral transformation. In addition, in particular in PP approaches effective one-particle operators are used instead of the AE operators, which might consist of or include two-particle terms (e.g., the Breit interaction). The requirements for the correlation are therefore actually smaller than in the corresponding AE case, thus leading also here to computational savings. Since for the cases IV and III the SO interaction is already treated at the HF level, the wave function has a high flexibility and can accurately take into account the relaxation of the orbitals under the influence of SO effects. The approaches are especially useful for heavy and superheavy elements, where SO effects are very large and potentially more important than electron correlation effects.

dx.doi.org/10.1021/cr2001383 |Chem. Rev. 2012, 112, 403–480

The computationally cheapest approach on the contrary assumes only very small SO effects, which essentially do not lead to a relaxation of the orbitals and only cause small energetic changes. Scalar-relativistic HF calculations are followed by CI, CC or MBPT in the LS or ΛS coupling scheme using a basis of determinants (dets.) or configuration state functions (CSFs). If SO contributions are of interest these are either evaluated by (quasi-degenerate) first-order perturbation theory using the correlated wave function(s) as zeroth-order wave function(s) or in a usually small SOCI in the basis of the correlated many-electron LS or ΛS states (I). This approach, which can be routinely performed today with most standard quantum chemical ab initio packages, assumes that electron correlation is much more important than SO interaction. The basic principles for such calculations using PPs were written down by Ermler et al.[236] and applied to TlH.[501] Shortly thereafter the CIPSO approach of Teichteil and co-workers, based on the efficient selecting CI approach CIPSI, was designed, implemented and applied.[371,502] Since orbital relaxation in presence of the SO terms may not be sufficiently accounted for in the CIPSO approach, Vallet et al. presented the EPCISO approach as an extension which includes also all single excitations in the many-electron basis set.[503]

For cases intermediate between I and III Chang and Pitzer[346] suggested to treat SO effects and electron correlation on equal footing by diagonalizing in a double group CI (DGCI) a large Hamiltonian matrix including the SO terms (II) in a determinant basis (dets.) or, better, in a basis of double-group adapted (many-electron) functions (DGAFs). Seijo and co-workers formulated and implemented a spin-free state shifted (SFSS) effective Hamiltonian version, which can exploit results from large-scale scalar-relativistic calculations.[209] A parallel version of the DGCI code increasing the capabilities of the original code by about 3 orders of magnitude was reported by Tilson et al.[504] A GUGA-based variant allowing significantly longer CI expansions was developed by Yabushita and collaborators.[505] An efficient implementation of a determinant-based CI including SO contributions was also reported by Sjøvoll, Gropen and Olsen.[506] The approach II was found to be useful and sufficiently accurate for most heavier elements of the periodic table up to the actinides. Especially for open f shells with more than one electron or hole the large number of LS or ΛS states to be correlated prior to the SOCI in the more efficient scheme I may exceed the computational capabilities, and scheme II might become advantageous.

It has to be noted that when all possible states and excitations are taken into account the CIPSO, DGCI and KRCI approaches will yield the same result, that is, for ECPs with an implicit treatment of relativistic contributions the paths I, II, and III lead to the same answer; however, in very expensive calculations. For practical calculations the three different paths allow to neglect unimportant contributions at different stages of the calculation and thus may gain efficiency compared to others if applied to a suitable problem.

For DFT approaches Figure 24 could be truncated after the HF steps, which would then be replaced by corresponding KS calculations, resulting in three major computational schemes, i.e., scalar-relativistic KS (I,II), [quasi]relativistic KS (III) and relativistic DKS (IV). ECPs could be used in all three schemes in principle, however, the scalar-relativistic ECP KS approach is by far the most popular and a standard approach of computational chemistry. However, the development of quasirelativistic ECP KS approaches has recently received more attention.[498,499]

When applying the above schemes in connection with ECPs it is important to check if the chosen approach is compatible with the available SO operator. In many cases ECPs are supplemented by SO operators which are suitable only for usage in first-order perturbation theory or should act only on certain (valence) shells.[137−140] Such operators should be applied only for path I in the framework of a first-order perturbative treatment of the SO effects or a small SOCI. Marian and Wahlgren[142] and Schimmelpfennig et al.[143] devised a scheme which allows to replace PP by AE SO integrals in the framework of an effective one-electron (mean-field) SO Hamiltonian, which might be helpful if no PP SO term is available or if it is considered not to be accurate enough.

Despite the increased availability of codes that are able to include SO effects, the by far majority of ECP and AE studies neglects these and stays at the scalar-relativistic (or even non-relativistic) level, for which all computational first-principles approaches of nonrelativistic quantum chemistry can be applied.

9. ACCURACY AND CALIBRATION

ECPs are usually adjusted for atoms, mostly in the framework of the independent-particle approximation. Calibration of ECPs in atomic and molecular calculations going beyond the independent-particle level are necessary to check the transferability of the ECPs and to estimate possible errors in subsequent applications. For calibration studies a major problem is to distinguish between errors of the Hamiltonian used (e.g., variants of relativistic AE or ECP approaches), the applied computational method (e.g., HF as well a variants of CI, CC, MBPT, or DFT), and the applied basis sets used to cast the equations to be solved into matrix form. Comparison to experimental data is informative, but because of the necessary incompleteness of the applied basis sets and the usually only approximate treatment of electron interactions it does not allow to conclude unambiguously about the quality of the applied ECP. In addition, especially for actinides and of course for superheavy elements, suitable accurate experimental data is often missing or incomplete. Therefore, although for applications it is good to know that a specific combination of ECPs, basis sets and computational method yields results in good agreement to experimental data, for the development of accurate ECPs it is often more helpful to compare to AE reference data. In view of Figure 1 it is important for an unbiased comparison of two approaches to ensure that the calculations correspond to the nearby points in the planes defined by the Hamiltonians. This may be achieved by using, for example, corresponding correlation-consistent basis sets and the same correlation method at the ECP and AE level. Unfortunately, for most of the ECPs only a very limited choice of suitable basis sets exists and the checking of basis set completeness errors is therefore quite difficult. Ideally the AE Hamiltonian used to produce the reference data for the ECP calibration should correspond to the one used to generate the reference data for the adjustment, since otherwise errors due to the ECP and differences between the AE Hamiltonians cannot be separated. In some cases this is not possible, since the AE Hamiltonian used for the atomic adjustment cannot be applied in corresponding molecular calculations, and thus the comparison has to be made to data obtained with another Hamiltonian aiming to describe the same effects. For example the CG and WB Hamiltonians can only be used to generate atomic relativistic HF

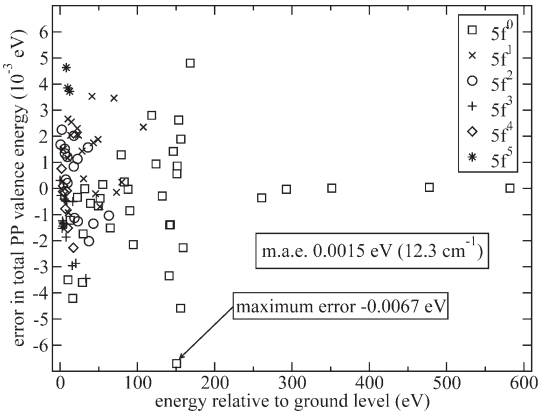

Figure 25. Errors (eV) in total valence energies of 100 nonrelativistic configurations for the multiconfiguration Dirac−Hartree−Fock/Dirac−Coulomb−Breit Fermi nucleus adjusted small-core pseudopotential for uranium of Cao and Dolg.[393]

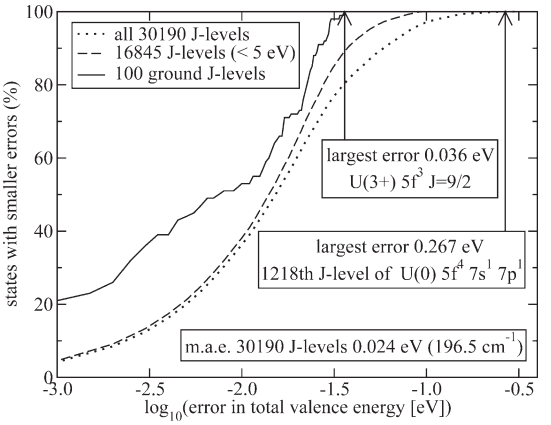

Figure 26. Percentage (%) of *J* levels with errors in the total valence energies below the threshold (eV) indicated on the abscissa for the multiconfiguration Dirac−Hartree−Fock/Dirac−Coulomb−Breit Fermi nucleus adjusted small-core pseudopotential for uranium of Cao and Dolg.[393]

reference data, and molecular calibration of the ECPs has to be with respect to (spin−orbit averaged) results for the DC Hamiltonian, or an approximation to it as the DKH Hamiltonian.

In the following sections we try to establish the present limitations of accuracy of ECPs using the U atom as an example, discuss briefly available computational schemes to perform correlated atomic and molecular calculations including SO effects, and report on the accuracy of valence correlation energies in ECP approaches. We then summarize a few recent calibration studies for main group and transition elements demonstrating the accuracy of modern ECPs.

9.1. Limitations of Accuracy

Before using ECPs in molecules or solids it is important to know how well the chosen approach can reproduce atomic AE results, especially how accurate was the adjustment to the atomic AE reference data. The requirements concerning the accuracy of ECPs changed drastically during the last decades, with a clear trend toward higher accuracy by using more elaborate relativistic Hamiltonians to generate the reference data, smaller ECP cores to avoid FC errors, and also larger parameter sets in order to obtain a good fit. Therefore it is important to investigate which effects are large enough at the AE level to be included in the ECP adjustment.

A recent example for the accuracy which can be achieved by an ECP is provided by an energy-consistent small-core 32-valence-electron PP for U adjusted to MCDHF reference data obtained with the Dirac−Coulomb−Breit (DCB) Hamiltonian.[102,507] U is chosen since both correlation and relativistic effects, including SO effects, are large and because of the extension of the valence shells over three main quantum numbers (5f, 6d, 7s) an accurate adjustment is not trivial. The PP discussed here has an accuracy which is probably at the border of what can be reached with a semilocal ansatz for U. Shape-consistent PPs, based on DCB AE calculations, which aim to reach a similar accuracy were derived by Titov and co-workers.[103] Other PPs and MPs for U do not include the Breit interaction or even use Hamiltonians which merely approximate the DC Hamiltonian, and use larger and less accurate cores.[30]

A detailed description of the energy-consistent fitting procedure used for U was recently published[31] and only a brief summary will be given here. The small core (60 core electrons)

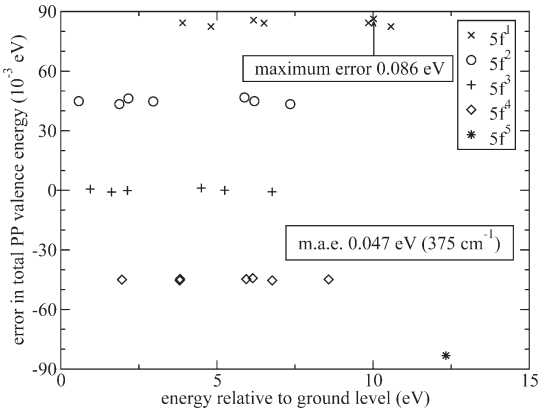

Figure 27. Errors (eV) in total valence energies of 29 nonrelativistic configurations for the Fermi nucleus small-core Dirac−Coulomb−Breit-adjusted generalized effective core potential for uranium of Mosyagin et al.[103]

was motivated by frozen-core AE calculations using various core definitions. When 5f and 6d occupation number changes are considered, only this small-core definition leads to errors in energy differences of less than 0.01 eV.[30,31] The reference data, MCDHF total valence energies calculated with the finite Fermi nucleus DC Hamiltonian and the Breit term in first-order quasidegenerate perturbation theory, was obtained for 100 nonrelativistic configurations for the neutral U atom to the 7-fold charged U^{7+} cation. These corresponded to 30190 J levels stretched over an energy interval of about 600 eV. Using 56 adjustable parameters the accuracy of the fit measured by the mean root square error was 300 cm^{-1} (0.037 eV) for the individual J levels and 16 cm^{-1} (0.002 eV) for the averages corresponding to nonrelativistic configurations.[102,507] These errors are of similar magnitude as corresponding FC errors in AE DHF/DC+B calculations.[31] A pictorial summary of the accuracy of the fit is provided by Figures 25 and 26 for the configurational averages and the individual J levels, respectively. Figure 25 can be compared with corresponding data for 29 nonrelativistic configurations for the shape-consistent GRECP

dx.doi.org/10.1021/cr2001383 |*Chem. Rev.* 2012, 112, 403–480

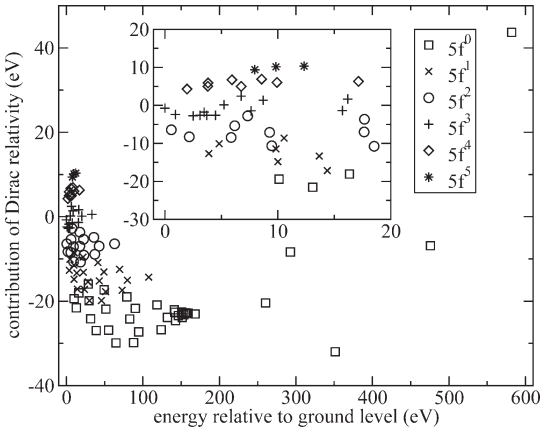

Figure 28. Effect of (Dirac and Breit) relativity on the average energies of 100 configurations of U to U^{7+} with respect to the U $5f^3$ $6d^1$ $7s^2$ configuration at the MCDHF level calculated with the program GRASP.[83]

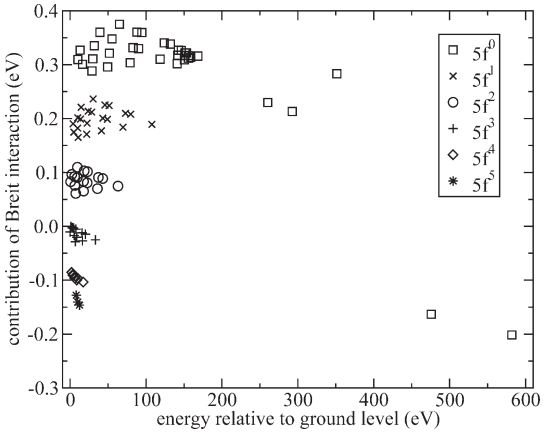

Figure 29. Effect of the Breit interaction on the average energies of 100 configurations of U to U^{7+} with respect to the U $5f^3$ $6d^1$ $7s^2$ configuration at the MCDHF/Fermi-type nucleus level calculated with the program GRASP.[83]

published by Mosyagin et al.,[103] which shows despite the use of a small core significantly larger errors depending very systematically on the 5f occupancy, see Figure 27.

Figure 28 clearly shows that the relativistic effects in the spectrum of U are about 4 orders of magnitude larger than the errors of the PP fit displayed in Figure 25. The relativistic contributions were evaluated as the difference of results from DHF/DC+B calculations and corresponding calculations achieving the nonrelativistic limit by multiplying the velocity of light with a factor of 10^6. It is seen that relativistic contributions fall into groups depending on the 5f occupation, with $5f^3$ cases near zero, since the energies were calculated relative to the $5f^3$ $6d^1$ $7s^2$ ground state configuration. Cases with higher and lower 5f occupation are destabilized and stabilized by relativity, respectively. Note that even for low-energy excitations and ionizations the relativistic contributions may exceed the value of interest itself and thus cannot be neglected for a realistic modeling of U.

The contributions of the Breit (two-particle) interaction shown in Figure 29 are about 2 orders of magnitude less important than the Dirac (one-particle) contributions but are certainly necessary for an accurate description of U. Since they

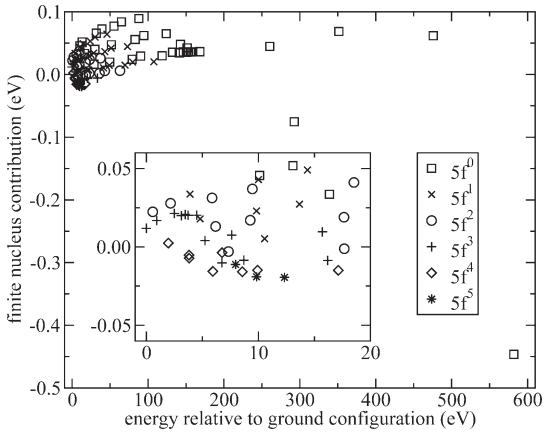

Figure 30. Effect of a finite Fermi-type nuclear charge distribution on the energies of the lowest *J*-levels of 100 configurations of U to U^{7+} with respect to the U $5f^3$ $6d^1$ $7s^2$ configuration at the MCDHF/DC+B level calculated with the program GRASP.[83]

are still about 2 orders of magnitude larger than the errors of the PP fit, they can be safely included.[103,393] Again, the Breit contributions fall into groups depending on the 5f occupation, with $5f^3$ cases near zero. In contrast to the Dirac (one-particle) contributions dominating in Figure 28, the cases with higher and lower 5f occupation are stabilized and destabilized, respectively, by the Breit (two-particle) contributions. It is obvious that ECPs perfectly adjusted to (approximate) DC reference data will exhibit errors in excitation energies and ionization potentials of roughly 0.1 eV for every change of the 5f occupation by one unit. The same is of course true for AE Hamiltonians omitting the Breit term. These differences should be considered when comparing the performance of ECPs which are based on different relativistic AE models. This detail is important for an unbiased comparison, but is sometimes overlooked.[103]

Finally, the contributions of a finite nuclear charge distribution displayed in Figure 30 exceed for not too highly ionized cases the errors of the PP fit still by about 1 order of magnitude. For all cases of chemical interest the contributions stay below 0.05 eV. This order of magnitude roughly corresponds to the accuracy of modern ECPs, which consequently also include finite nucleus contributions in the reference data.[103,393]

9.2. Scope of Applications

ECPs are usually adjusted to atomic reference data and later used in molecular calculations. A basic requirement for a good ECP is certainly that it is transferable and yields accurate energetic and structural data for the molecular case. Beyond this one may ask which properties, except the total valence energy and its derivatives with respect to nuclear coordinates, one can calculate with an ECP. It is clear, that due to the elimination of the core electron system ECPs cannot yield answers for properties which depend on the presence of the core. An example is the topological analysis of the electron density according to Bader,[508] in which large-core PPs (and most likely also MPs) may fail to yield bond critical points.[509,510] It was pointed out by Frenking and co-workers that small-core PPs perform well and that the erratic behavior of large-core PPs can be corrected by simply adding core electron densities obtained from atomic calculations, or by adding a core-like density obtained from core orbitals orthogonalized to the pseudovalence orbitals.[510] The addition of core or model core densities to obtain good energetics but also

dx.doi.org/10.1021/cr2001383 |*Chem. Rev.* 2012, 112, 403–480

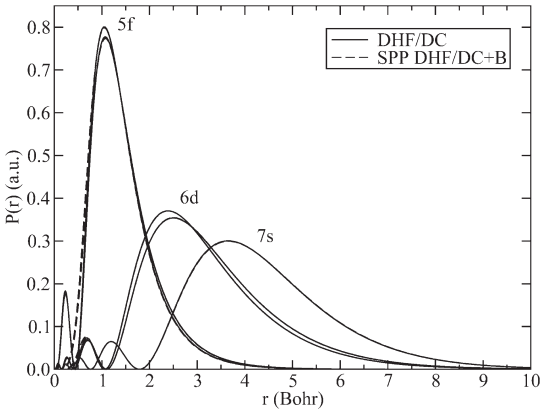

Figure 31. Radial orbital densities of uranium in the [Rn] $5f^3 6d^1 7s^2$ ground state configuration from state-averaged multiconfiguration Dirac–Hartree–Fock/Dirac–Coulomb calculations[83] in comparison to pseudovalence functions obtained from corresponding valence-only calculations with a two-component Dirac–Hartree–Fock/Dirac–Coulomb–Breit adjusted small-core pseudopotential.[393]

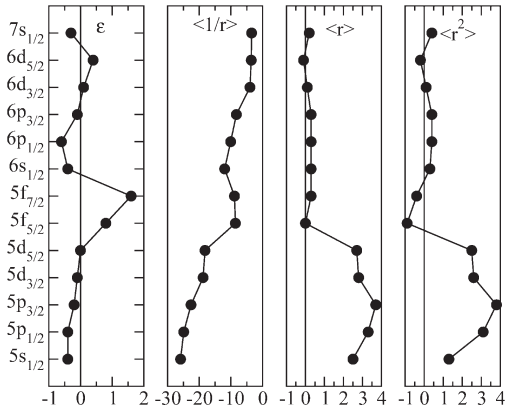

Figure 32. Errors (%) of orbital energies, $\langle 1/r \rangle$-, $\langle r \rangle$-, and $\langle r^2 \rangle$-expectation values for U from two-component calculations with a Dirac–Hartree–Fock/Dirac–Coulomb–Breit adjusted small-core pseudopotential[393] in comparison to values from state-averaged multiconfiguration Dirac–Hartree–Fock/Dirac–Coulomb calculations.[83]

reasonable properties with DFT-based large-core PPs in solid state physics applications was also discussed by Louie et al.[420] It was also observed that large-core PPs may lead to unreasonable Mulliken charges of atoms, whereas the results for small-core PPs correspond more to the common expectations.[509]

There are also other cases where core orbitals exhibit non-negligible contributions to properties. For example, it was pointed out recently by Schwerdtfeger and co-workers that core contributions cannot be neglected in quadrupole moments of heavy elements such as Au and their compounds such as AuF.[511] The multipole moment operator is given as[512]

$$M_{nml} = \sum_i q_i x_i^n y_i^m z_i^l \qquad (191)$$

The expectation value has to be evaluated by summing over all charges in the system, i.e., electrons and nuclei. Schwerdtfeger et al. compared AE DKH2 data to energy-consistent[291] and shape-consistent[286,354] small-core PP results for HF, MP2 and various density functionals. In case of AuH maximum deviations of 2%, 11%, 6% and 2% were observed for the HF dipole moment μ_z, quadrupole moment Q_{zz}, octupole moment O_{zzz} and hexadecupole moment H_{zzzz} tensor components, respectively. Similar errors were observed for magnetizabilities. In contrast to the work of Schwerdtfeger and co-workers excellent results for dipole and quadrupole polarizabilities were obtained for the rare gas atoms Ne, Ar, Kr, and Xe with large-core PPs and CPPs by Nicklass et al.[298] The failure observed for the quadrupole moment of Au was mainly attributed by Schwerdtfeger et al. to the $[^{36}Kr]4d^{10}4f^{14}$ core, which contributes with 15% to the final result at the AE level, and to a lesser extent from the use of pseudovalence orbitals. CPPs have been shown to improve ionization potentials and excitation energies even for the not very polarizable Ne-core used in small-core 3d transition metal PPs,[285] and one might thus wonder if the inclusion of quadrupole corrections in the CPP used by Stoll and co-workers successfully for Cu and Ag one-valence-electron PPs[258] might help also in case of the Au small-core PPs. Dipole moments, as well as static dipole polarizabilities, are routinely calculated with ECPs, possibly supplemented by CPPs, and for sufficiently large basis sets usually reliable results are obtained.[180,292,298,513]

For properties that depend essentially only on the valence orbitals and their shape no difficulties should arise for MPs, which keep the correct radial nodal structure of the orbitals. For example, Krause and Klobukowski reported an agreement within 1% for $\langle r^n \rangle$ ($n = -3, -2, -1, 1, 2$) expectation values from AE and MP calculations.[514] Therefore operators taken directly from the AE framework, for example, effective SO operators with a $1/r^3$ singularity, can be applied. In case of PPs, a formal transformation to pseudovalence orbitals with a simplified nodal structure in the spatial core region is performed, thus requiring in principle also the use of accordingly transformed operators, for example, the effective SO operators with a Gaussian-type radial behavior. Figure 31 compares for U the radial densities of the original AE valence orbitals/spinors and the PP pseudovalence orbitals/spinors for an energy-consistent small-core MCDHF/DC+B-adjusted PP.[393] Although only total valence energy data entered the fit the radial shape of the original AE orbitals/spinors and the PP pseudovalence orbitals/spinors is nearly identical in the chemically relevant spatial valence region. A similar performance is generally observed for shape-consistent PPs, which are adjusted to reproduce the correct radial shape of the original AE orbitals/spinors in the valence region for a selected reference state. Operators that sample essentially the valence region usually give reasonable results even without transformation, whereas those which sample the core region will not.

The accurate long-range shape of the pseudovalence orbitals is reflected by the $\langle r \rangle$- and $\langle r^2 \rangle$-expectation values, which in case of the U small-core MCDHF/DC+B-adjusted PP deviate by less than 1% from the AE reference values, see Figure 32. The deviations for the semicore shells 5s, 5p and 5d are with up to 4% somewhat larger. Pseudovalence orbital energies are determined by the long-range shape of the orbitals and due to their accuracy exhibit errors of less than 2%. The correct shape of the pseudovalence orbitals in the valence region, their accurate orbital energies as well as the accuracy of the total valence energies for various atomic states leads to a high transferability of the PPs from atoms to molecules, and molecular properties, such as bond distances and angles, binding energies, and vibrational frequencies, are very well reproduced.

In contrast very large deviations are observed for $\langle r^n \rangle$ ($n < 0$) expectation values in PP approaches. These expectation values

dx.doi.org/10.1021/cr2001383 |Chem. Rev. 2012, 112, 403–480

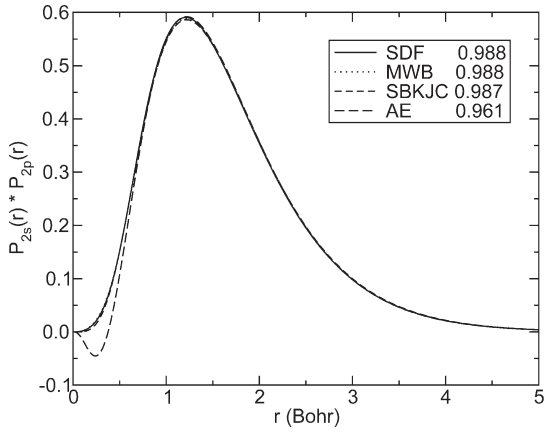

Figure 33. 2s*2p product of radial functions for C in the $2s^2$ $2p^2$ ground state configuration. Results for the DHF/DC (SDF)[254] and WB[148] energy-consistent and SBKJC[286] shape-consistent PPs are compared to AE DHF/DC results obtained with the program GRASP.[83] The numbers in the legend are the radial overlap of the 2s and 2p radial functions.

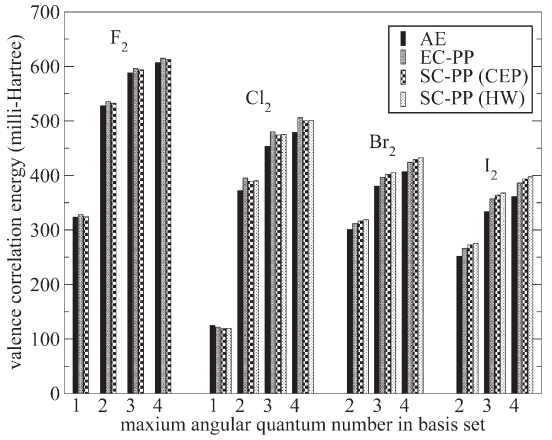

Figure 34. Total valence correlation energies of halogen dimers X_2 (X = F, Cl, Br, I) from AE and PP CCSD(T) calculations using large uncontracted basis sets.[531]

have large contributions from the region near the nucleus, where the nodes of the AE valence orbitals were removed to obtain the pseudovalence orbitals, see Figure 32 for $\langle 1/r \rangle$. An example is the SO operator, where in PP approaches either an effective nuclear charge has to be used to correct the wrong $\langle 1/r^3 \rangle$ values,[137−140] or effective (transformed) operators are constructed.[234,235] Similarly, the removal of the inner nodes causes large deviations of PP expectation values of derivatives $\langle d^m/dr^m \rangle$, for example, the (nonrelativistic) virial theorem $\langle \hat{V} \rangle = -2\langle \hat{T} \rangle$ does not hold in PP calculations. In general expectation values $\langle r^n d^m/dr^m \rangle$ from PP calculations are meaningful only for $(n - m) \geq 0$, whereas for $(n - m) < 0$ either effective (transformed) operators have to be developed or the original radial structures of the valence orbitals have to be (approximately) reconstructed.[515−517]

Although core-like properties related to a specific core/nucleus cannot be calculated when a PP is used for this center, it is still possible to calculate such properties for other centers with light nuclei treated at the AE level, and account for the influence of heavy atoms in the vicinity with relativistic PPs (or MPs). Such an approach was pioneered for nuclear magnetic resonance (NMR) shielding factors and chemical shifts in the framework of DFT by Kaupp and co-workers,[518−523] who evaluated ^{1}H, ^{13}C, ^{17}O, ^{19}F, and ^{31}P chemical shifts using scalar-relativistic PPs for other heavy nuclei. Later the approach was refined by including SO effects via PP SO operators.[524] In some studies of uranium complexes small-core PPs were found to yield more reliable results than large-core PPs.[523,525]

Whereas in NMR shielding tensors and corresponding chemical shifts one looks at the interaction of a nuclear magnetic moment with an external magnetic field, it is the spin magnetic moment interacting with an external magnetic field that is considered for the evaluation of electron spin resonance (ESR) *g* tensors and corresponding *g* shifts. The conceptual relationship and the valence nature of these properties is discussed in an overview by Schreckenbach and Ziegler.[526] Similar to their use in the calculation of NMR chemical shifts ECPs including SO terms can also be used to evaluate ESR *g* shifts, which was first demonstrated in DFT calculations by Malkina et al.[527] Finally, hyperfine coupling tensors describing the interaction of the nuclear magnetic moment with the spin magnetic moment can be evaluated for light atoms treated at the AE level, whereas the effect of heavy nuclei in the neighborhood is described by relativistic ECPs and SO terms.[528,529]

9.3. Valence Correlation Energies

A quite long-standing question is the overestimation of exchange integrals, and as a consequence of correlation energies as well as multiplet splittings due to the use of pseudovalence orbitals in PP calculations. The problem was detected independently by Pittel and Schwarz[530] and Teichteil et al.[363] It seems to be especially severe when exchange integrals between pseudovalence orbitals and unchanged valence orbitals are evaluated, for example, for the 2s and 2p orbitals of the first-row main group elements. In case of a He-core, one radial node is removed from the 2s AE valence orbital to yield a nodeless 2s pseudovalence orbital, whereas the nodeless 2p AE valence orbital is essentially identical to the one used in the PP calculation. In exchange integrals products of the 2s and 2p orbitals appear. Since at the AE level, 2s has both positive and negative contributions, the resulting part of the integrand has too, whereas this is not the case at the PP level. Figure 33 compares the 2s*2p product of radial functions for C of AE and various PP calculations. The classical example found by Pittel and Schwarz is F^{5+}, for which the valence correlation energy is overestimated in PP studies by approximately 20%.[530] However, already Teichteil et al. found in their correlated PP calculations of the halogen dimers X_2 (X = F, Cl, Br, I) that although the valence correlation energies are overestimated by about 10%, the AE correlation effects on the bond lengths, force constants, and dissociation energies are perfectly mimicked in the PP approach.

Systematic studies of the first-row main group elements Li−Ne, as well as the halogens F−I indicate that for modern PPs[148,287,333,334,355] applied to neutral atoms in ground and low-lying excited states, anions and monocations as well as to homonuclear dimers the resulting errors in the total valence correlation energies are at most 9%. Moreover, for energy differences these errors often cancel, so that for excitation energies, electron affinities, ionization potentials and binding energies errors of less than 0.1 eV arise.[531,532] An example is illustrated in Figures 34 and 35 for the total valence correlation energies and the correlation contributions to the binding

dx.doi.org/10.1021/cr2001383 |*Chem. Rev.* 2012, 112, 403–480

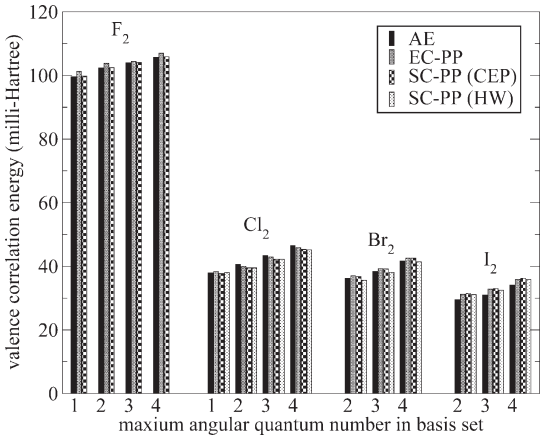

Figure 35. Correlation contributions to the binding energy D_e of halogen dimers X_2 (X = F, Cl, Br, I) from AE and PP CCSD(T) calculations using large uncontracted basis sets.[531]

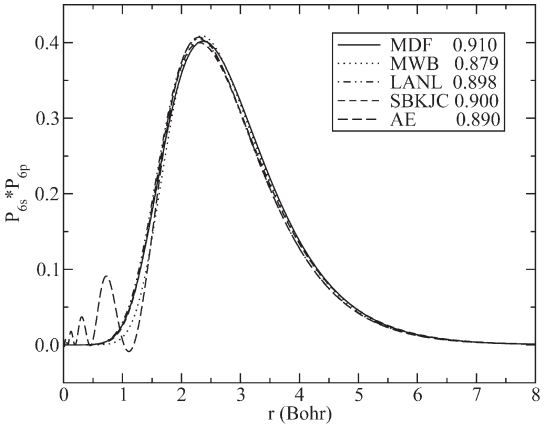

Figure 36. 6s*6p product of radial functions for Pb in the $6s^2$ $6p^2$ ground state configuration. Results for MCDHF/DC[174] and WB[148] energy-consistent and LANL[355] and SBKJC[286] shape-consistent PPs are compared to AE DHF/DC results obtained with the program GRASP.[83] The numbers in the legends are the radial overlap of the 6s and 6p radial functions.

energies for the halogen dimers X_2 (X = F, Cl, Br, I), respectively.[531] The comparison of PP and AE values is made at the CCSD(T) level using large uncontracted sp, spd, spdf, and spdfg basis sets.

The errors found in PP studies are similar in magnitude to those found in corresponding MP calculations.[533,534] Whereas the pseudovalence orbital transformation used in the PP approach mixes core orbital character to both the valence orbitals and the virtual orbitals, the MP approach shifts the core orbitals in their entirety to the virtual space and also uses these in wave function-based correlation calculations. This most likely also leads to a slight overestimation of valence correlation energies, for example, MP calculations using AE basis sets were found to overestimate the correlation energies of P_2, As_2, and Sb_2 by 2.8 (4), 4.8 (6), and 7.6 (11) mH at the CISD (MP2) level, corresponding to a maximum deviation of 4.8(6.0)%.[514] The significant errors in total valence correlation energies in PP calculations of up to 25% found by Klobukowski[533] and discussed by Seijo and Barandiarán[534] could be shown to be due to a truncation of the virtual space.[531,532]

Table 16. HF Bond Lengths R_e (Å), Vibrational Constants ω_e (cm^{-1}), and Binding Energies D_e (eV) of the Halogen Hydrides HX (X = F, Cl, Br, I, At) Obtained from AIMP CG Calculations with *nsnp* (F, Cl, Br) and $(n-1)$*dnsnp* (I, At) Valence Space[156] in Comparison to Scalar-Relativistic AE DKH2 Reference Data[537a]

	R_e		ω_e		D_e	
HX	AIMP	DKH2	AIMP	DKH2	AIMP	DKH2
HF	0.896	0.897	4526	4477	4.32	4.40
HCl	1.275	1.264	3097	3139	3.33	3.54
HBr	1.414	1.404	2745	2789	2.85	2.98
HI	1.603	1.599	2439	2451	2.35	2.47
HAt	1.692	1.682	2259	2297	2.09	2.15
m.a.e.	0.007		39		0.12	

[a] Data taken from Seijo[156] and Dolg.[537] Mean absolute errors are listed in the last line. The AIMP basis sets are of pVTZ quality, whereas large uncontracted basis sets were used for the AE DKH2 reference calculations.

It should be noted that for modern energy-consistent PPs multiplet splittings, and thus indirectly also exchange integrals, enter into the reference data, which avoids severe overestimations. Moreover, for heavier elements often exchange integrals are evaluated between two pseudovalence orbitals leading to smaller deviations from the AE case. This is obvious from a comparison of the 6s*6p product of radial functions for Pb displayed in Figure 36 with Figure 33 for the 2s*2p product of radial functions for C. In addition, modern PPs use small cores, that is, they leave some radial nodes in the pseudovalence orbitals, which also reduces the errors in the exchange integrals. This is supported by the observation of Rohlfing et al. that small-core PPs for Ni, Pd, and Pt allow a more consistent treatment of correlation than the corresponding large-core ones.[535] Although further detailed investigations, for example, for transition metals, as well as lanthanides and actinides, are still missing, one may expect that the overestimation of valence correlation energies in PP approaches frequently mentioned in the introduction of MP publications[454−456,459] are not as severe as initially expected.

9.4. Calibration: Main Group Elements

ECPs are routinely used in electronic structure calculations for main group and transition metal compounds and a very large number of applications exists.[19,351,353,536] The reliability of the ECPs is manifested in most of these studies simply by comparison of the results to available experimental data. Instead of selecting some of these studies as examples, we focus on a few calibration studies. Whereas for every set of ECPs calibrations with respect to AE or experimental reference data have been performed, studies with a direct comparison of different ECPs are quite scarce.[172,280,282,531] In order to arrive at a comparison it is therefore necessary to combine the results from different studies, which certainly bears the risk of a bias because of not completely equivalent applied computational approaches.

Seijo presented results obtained with CG- and WB-adjusted AIMPs for the halogen hydrides at the HF and CIDBG(SD) levels of theory.[156] The HF results for the scalar-relativistic CG-AIMPs using about pVTZ basis sets can be compared to scalar-relativistic AE DKH2 reference data, which was obtained with large uncontracted basis sets.[537] Table 16 lists some of the results for bond lengths R_e, vibrational constants ω_e, and binding

dx.doi.org/10.1021/cr2001383 |Chem. Rev. 2012, 112, 403–480

Table 17. Root Mean Squared Errors for Theoretical Values of Bond Lengths R_e (Å), Vibrational Constants ω_e (cm^{-1}), and Binding Energies D_e (eV) of the Halogen Hydrides HX and Dimers X_2 (X = F, Cl, Br, I) Obtained from Two-Component Calculations with Large-Core Energy-Consistent WB PPs and CPPs[144,148] with Respect to Experimental Data[a]

		R_e		ω_e		D_e	
method	basis	HX	X_2	HX	X_2	HX	X_2
PP+CPP,CCSD(T)+SO	uncontracted	0.006	0.004	22	5	0.01	0.04
PP+CPP,ACPF+SO	uncontracted	0.007	0.004	19	3	0.01	0.09
PP+SO+CPP,CISD	pVTZ	0.005	0.021	39	90	0.14	0.98
PP+SO+CPP,CISD+Q	pVTZ	0.003	0.025	19	8	0.04	0.53
WB AIMP,SO−CIDBG	pVTZ	0.008		55		0.42	
AE,DHF,CISD	(aug-)pVTZ		0.026		97		1.09
AE,DHF,CISD+Q	(aug-)pVTZ	0.006		8		0.22	
AE,DHF,CCSD(T)	(aug-)pVTZ	0.007	0.034	10	11	0.18	0.27

[a] PP+CPP and PP+SO+CPP denote one- and two-component HF calculations using large and small basis sets, respectively. For the one-component large basis set case SO contributions derived from the small basis set correlated calculations were added after the correlation treatment. For comparison AIMP WB results of Seijo[156] and fully-relativistic AE results obtained for the DCG Hamiltonian by Visscher and co-workers[541,538] are included. Data taken from Dolg.[537]

energies D_e, as well as the corresponding mean absolute errors (m.a.e.). The CG-AIMPs reproduce the AE DKH values very well, although the bonding at the AIMP CG level is slightly too weak, that is, the bond lengths are typically slightly too long, whereas the vibrational constants and binding energies are usually somewhat too low.

Although a comparison as compiled in Table 16 already gives a good impression about the accuracy of the tested method, it is not fully satisfactory. On one hand it is not obvious if the remaining errors are due to the limited basis sets used at the AIMP CG level, on the other hand one is also interested in the correlated results and a comparison to experiment. Table 17 provides m.a.e. of AIMP WB results including SO corrections at the CIDBG(SD) level. The m.a.e. in bond lengths is below 0.01 Å and comparable to the one obtained in AE DHF/DC CISD and CCSD(T) calculations,[538] however the ones in the vibrational constants and the binding energies are more significant. Since both the AIMP WB and the AE calculations use basis sets of approximately pVTZ quality, one can not clearly distinguish between the corresponding basis set errors and errors in the AIMP.

Fortunately, with the development of atomic natural orbital (ANO) contracted basis sets by Almlöf and Taylor[539] and correlation-consistent basis sets by Dunning[540] a systematic convergence toward and extrapolation to the complete basis set (CBS) limit became possible. This allows more systematic comparisons between AE and ECP schemes also at the correlated level, and deviations can be assigned more safely to differences in the AE and ECP Hamiltonians. In other words, one knows much better the position on the corresponding Hamiltonian planes in Figure 1. Of course, when comparing to experiment errors with respect to all three axes still have to be considered. In this and the next section we will therefore put emphasis on newer studies which apply large uncontracted basis sets, or correlation-consistent basis sets both for ECP and AE calculations.

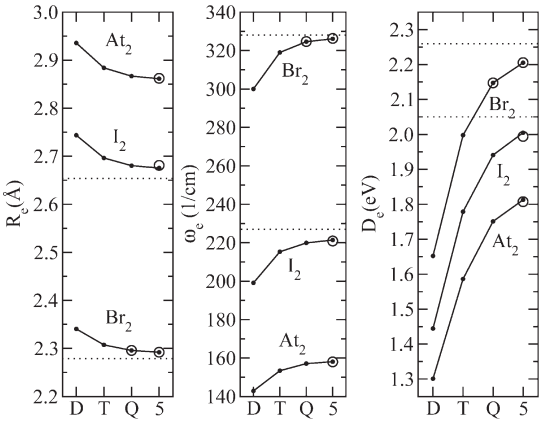

Figure 37. Bond lengths R_e (Å), vibrational constants ω_e (cm^{-1}), and binding energies D_e (eV) of the halogen dimers Br_2, I_2, and At_2 from CCSD(T) calculations using energy-consistent small-core PPs and cc-pVXZ-PP (X = D, T, Q, 5) basis sets (filled circles and solids lines) in comparison to AE DKH2 results obtained with cc-pVXZ-DK (X = Q, 5) basis sets (circles).[307] The experimental values were corrected for SO effects using results from two-component PP calculations[537] and are indicated by a dotted line.

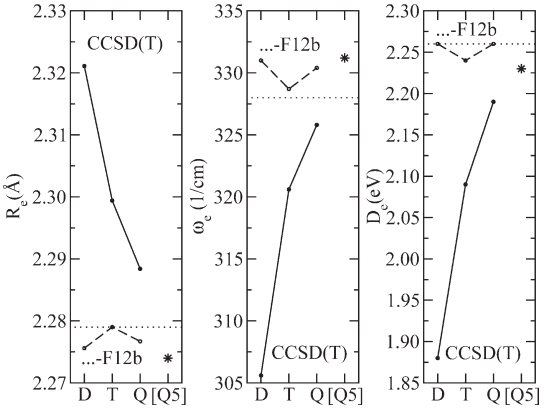

Figure 38. Bond lengths R_e (Å), vibrational constants ω_e (cm^{-1}), and binding energies D_e (eV) of the bromine dimer Br_2 from CCSD(T) and CCSD(T)-F12b calculations using energy-consistent small-core PPs[307] and unpublished cc-pVXZ-F12-PP (X = D, T, Q) basis sets of Peterson. Results of a basis set extrapolation using aug-wCVXZ-PP (X = Q, 5) basis sets are indicated by a star. Data taken from Werner et al.[315] The experimental values are indicated by a dotted line. D_e has been corrected for the experimental atomic SO energy splittings.

Peterson compared scalar-relativistic AE DKH2 and MCDHF/DC+B PP results for the halogen dimers Br_2, I_2 and At_2 at the CCSD(T) level.[307] His results are displayed in Figure 37, together with experimental values, which were corrected for SO effects (0.002, 0.012, 0.135 Å, −3, −12, −41 cm^{-1} and −0.27, −0.49, −1.06 eV for Br_2, I_2, and At_2) taken from two-component large-core PP calculations.[537] It can be seen that the agreement between AE and PP values is excellent. It is also obvious that the theoretical values approach the SO-corrected experimental ones, however, the convergence is very slow and even with quintuple basis sets the deviations from the experimental values are bigger than the difference between the AE and PP values. The situation is especially unpleasant for the binding energies, which are not converged with respect to the basis set.

dx.doi.org/10.1021/cr2001383 |Chem. Rev. 2012, 112, 403–480

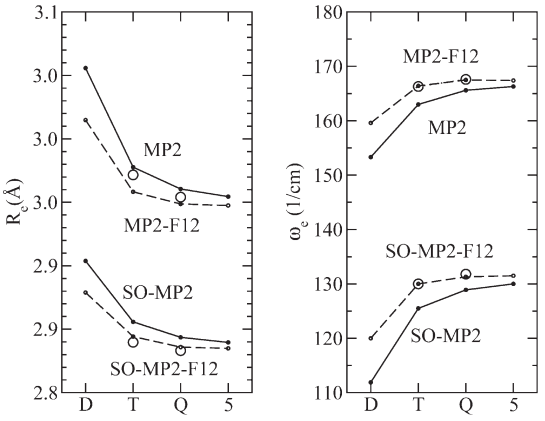

Figure 39. Bond lengths R_e (Å) and vibrational constants ω_e (cm^{-1}) of the astatine dimer At_2 from MP2, MP2-F12, MP2-SO, and MP2-F12-SO calculations using energy-consistent small-core PPs[307] and aug-cc-pVXZ-PP (X = D, T, Q, 5) basis sets (dots connected by solid/dashed lines),[307] as well as def2-XZVPP (X = T, Q) basis sets (circles).[308] Data taken from Bischoff and Klopper.[500]

Very recently explicitly correlated approaches have been extended to include PPs. Werner et al. reported CCSD(T)-F12b calculations of Br_2.[315] Their results are displayed in Figure 38. The same SO corrections as discussed above were applied to the experimental values. It can be seen from 38 that the basis set dependence of the CCSD(T)-F12b results is significantly smaller than of the CCSD(T) results. All CCSD(T)-F12b results are relatively close to values obtained from a basis set extrapolation using aug-wCVXZ-PP (X = Q, 5) basis sets. The deviations from the SO-corrected experimental values are lower than 0.01 Å, 3 cm^{-1}, and 0.03 eV.

Corresponding explicitly correlated two-component calculations including SO effects were recently reported by Bischoff and Klopper.[500] Their results for At_2 are summarized in Figure 39. In comparison to the CCSD(T)-F12b results of Werner et al. for Br_2, the convergence of the MP2-F12 values seems to be slower. Although the absolute values at the MP2 level may not be very accurate, it is interesting to extract SO contributions. These are 0.114 ± 0.002 Å and −36.1 ± 0.3 cm^{-1} for aug-cc-pVXZ-PP (X = T, Q, 5) and def2-XZVPP (X = T, Q) basis sets, whereas for aug-cc-pVDZ-PP values of 0.136 Å and −39.5 cm^{-1} are obtained. The latter values agree well with the corrections mentioned above from large-core PPs.[537] The about 10% smaller corrections for the better basis sets may be due to the small-core definition or the more rigorous AE DHF/DC+B reference data used for the PP[307] applied by Klopper and Bischoff.[500] Another reason might be the inclusion of the CPP, that is, core−valence correlation, in the large core case, which increases SO splittings, whereas for the small-core PP only valence correlation was considered.

Table 17 summarizes errors obtained with the large-core WB adjusted PPs and CPPs[144,148] when used in scalar-relativistic calculations (PP + CPP) with large uncontracted AE basis sets. The agreement with experimental data is excellent, that is, the root-mean-square errors are lower than 0.01 Å for bond lengths of hydrides and dimers, about 20 and 5 cm^{-1} for vibrational constants of hydrides and dimers, respectively, and at most 0.01 and 0.09 eV for binding energies of hydrides and dimers, respectively, at the SO-corrected CCSD(T) and ACPF level (CCSD(T)+SO, ACPF+SO).

Table 18. Electric Dipole Moment μ_z, Static Polarizability $\bar{\alpha}$, Static First-Order and Second-Order Hyperpolarizabilities $\mu_z\bar{\beta}$ and $\bar{\gamma}$, Respectively, from Time-Dependent HF/DHF Calculations Using Large-Core WB PPs,[144,148] the DKH2 Hamiltonian, and the DC Hamiltonian[513a]

HX	method	level	μ_z	$\bar{\alpha}$	$\mu_z\bar{\beta}$	$\bar{\gamma}$
HF	TD-HF	PP	0.7690	4.93	−4.06	257.4
		DKH2	0.7668	4.97	−4.35	276.9
	TD-DHF	DC	0.7667	4.97	−4.35	277.0
HCl	TD-HF	PP	0.4885	16.78	0.49	2117.7
		DKH2	0.4799	16.95	−1.41	2206.4
	TD-DHF	DC	0.4794	16.96	−1.30	2201
HBr	TD-HF	PP	0.3672	23.24	0.77	3571.3
		DKH2	0.3638	23.41	0.01	4214.5
	TD-DHF	DC	0.3610	23.48	−0.07	4257
HI	TD-HF	PP	0.2109	35.69	4.10	12441.3
		PP+SO	0.2015			
		DKH2	0.2114	35.37	3.25	11561.1
		DKH2+SO	0.2020			
	TD-DHF	DC	0.1971	35.52	3.31	9383
HAt	TD-HF	PP	−0.0481	42.50	2.50	18331.9
		PP+SO	0.0439			
		DKH2	−0.0515	41.84	2.16	17126.5
		DKH2+SO	0.0405			
	TD-DHF	DC	0.0621	43.43	−2.92	18652

[a] Data taken from Norman et al.[513] SO corrections (+SO) for the dipole moment were obtained from two-component PP calculations[537] and added to the scalar-relativistic PP and DKH2 values.

Upon using pVTZ basis sets in two-component HF and CISD calculations (PP+SO+CPP) the errors increase, but are of the same magnitude as those of fully relativistic AE DHF and CISD calculations using the DCG Hamiltonian and pVTZ basis sets.[538,541]

We finally turn to time-dependent HF/DHF (TD-HF/DHF) calculations of properties, which were reported by Norman et al. for electric dipole moments, linear polarizabilities, and first- and second-order hyperpolarizabilities using scalar-relativistic energy-consistent large-core PPs,[144,148] the scalar-relativistic DKH2 approach and the fully relativistic DHF/DC method.[513] These properties are defined as follows: the polarization of a molecule at the microscopic level can be expanded as follows in the presence of an external electric field $\vec{F}$

$$\mu_i = \mu_i^0 + \sum_j \alpha_{ij}F_j + \frac{1}{2}\sum_{jk}\beta_{ijk}F_jF_k + \frac{1}{6}\sum_{jkl}\gamma_{ijkl}F_jF_kF_l + \ldots \quad (192)$$

where μ_i^0 is the permanent electric dipole moment component ($i, j, k, l, \ldots = x, y, z$). The experimentally measured quantities refer to a set of laboratory axes which are related to the molecular properties through orientational averaging. The averaged properties are the averaged dipole polarizability

$$\bar{\alpha} = \frac{1}{3}\sum_{i=x,y,z}\alpha_{ii} \quad (193)$$

dx.doi.org/10.1021/cr2001383 |Chem. Rev. 2012, 112, 403–480

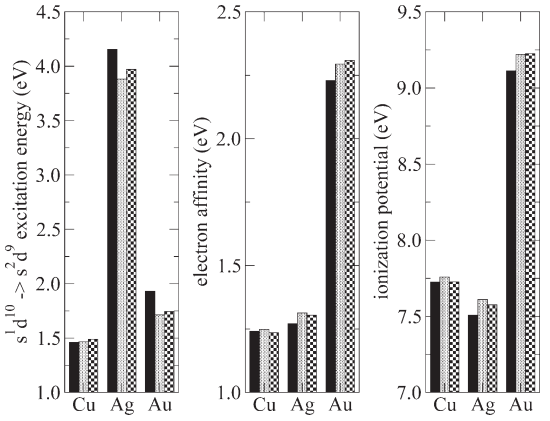

Figure 40. CCSD(T) $s^1d^{10} \rightarrow s^2d^9$ excitation energies, electron affinities and ionization potentials (eV) for Cu, Ag, and Au from energy-consistent MCDHF/DC+B small-core PP calculations without (black bars) and with (dotted bars) correlation of the (n-1)sp semicore orbitals in comparison to experimental data (checked bars). Data taken from Peterson and Puzzarini.[204]

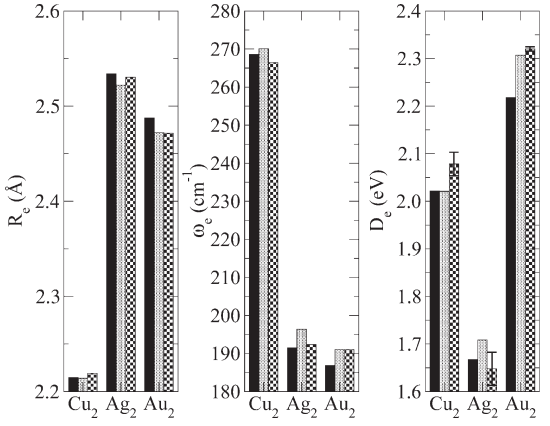

Figure 41. CCSD(T) bond lengths R_e (Å), vibrational constants ω_e (cm^{-1}), and binding energies D_e (eV) of Cu_2, Ag_2, and Au_2 from energy-consistent MCDHF/DC+B small-core PP calculations without (black bars) and with (dotted bars) correlation of the $(n-1)$sp semicore orbitals in comparison to experimental data (checked bars). Data taken from Peterson and Puzzarini.[204]

the first hyperpolarizability (assuming that the molecular z-axis is the dipole axis)

$$\overline{\beta} = \frac{1}{5} \sum_{i=x,y,z} (\beta_{zii} + \beta_{izi} + \beta_{iiz}) \quad (194)$$

and the second hyperpolarizability

$$\overline{\gamma} = \frac{1}{15} \sum_{i,j=x,y,z} (\gamma_{iijj} + \gamma_{ijij} + \gamma_{ijji}) \quad (195)$$

Table 18 summarizes results of Norman et al. using the best basis set for each method. The agreement with the TD-DHF reference data is quite good for TD-HF with the PP and DKH2 Hamiltonians in case of the electric dipole moment and the static polarizability. If SO corrections for the scalar-relativistic PP and DKH2 approaches are included the dipole moment of AtH comes in good agreement with the TD-DHF reference value. The results for the hyperpolarizabilities are less satisfactory, however Norman et al. mention that especially the evaluation of the first-order hyperpolarizability is a notoriously difficult task. It would be interesting to see if two-component small-core PPs would yield more favorable results.

Table 19. Differences in Bond Distances R_e (Å), Vibrational Constants ω_e (cm^{-1}), and Binding Energies D_e (eV) of Cu_2, Ag_2, and Au_2 of CCSD(T) Calculations Using Small-Core Energy-Consistent MCDHF/DC+B PPs[291] with aug-cc-pwCVTZ-PP and the DKH2 Hamiltonian with aug-cc-pwCVTZ-DK Basis Sets[a]

M_2	ΔR_e	$\Delta\omega_e$	ΔD_e
Cu_2	0.002	0.0	−0.004
	0.001	−0.9	−0.007
Ag_2	0.003	−0.3	−0.007
	0.003	−0.9	−0.014
Au_2	−0.002	0.7	0.010
	0.004	−1.3	−0.031

[a] The first line for each molecule corresponds to the results with $(n-1)$dns correlation only, the second to the contributions of correlating the $(n-1)$sp shells. Data taken from Peterson and Puzzarini.[204]

9.5. Calibration: Transition Metals

Schwerdtfeger et al.[160] compared HF, MP2, and CCSD(T) results for the ionization potential, electron affinity and dipole polarizability of Au, and the spectroscopic constants of AuH obtained with seven different scalar-relativistic PPs[147,169,286,326,335,354] to AE DKH and DC data. In agreement with the results of Lee et al.[495] SO contributions were found to be of minor importance for AuH. The authors concluded that for a small-core PP treating 19 valence electron explicitly the variation between AE and PP results is too small to be significant, whereas the large-core PPs with 11 valence electrons show sizable differences.

As a recent example for the performance of MCDHF/DC+B-adjusted PPs for transition metals[291] we consider the work of Peterson and Puzzarini on group 11 and 12 elements and their dimers.[204] Their results for Cu, Ag, and Au are displayed in Figure 40. Correlation of the $(n-1)$sp semicore orbitals improves the results and leads at the CCSD(T) level to errors with respect to SO-averaged experimental data which are below 0.1 eV in all cases, that is, for Cu, Ag, Au, they amount to −0.025, −0.090, −0.031 eV for the $s^1d^{10} \rightarrow s^2d^9$ excitation energies, 0.013, 0.010, 0.015 for the electron affinity, and 0.032, 0.034, and −0.007 eV for the ionization potential. In view of the large differential relativistic effects and correlation effects, see Figure 5 for the excitation energies, these results are quite satisfactory.

Figure 41 summarizes spectroscopic constants for the homonuclear dimers Cu_2, Ag_2, and Au_2. The calculated CCSD(T) bond lengths, vibrational constants and binding energies agree better than 0.01 Å, 4 cm^{-1}, and 0.06 eV with the experimental values. Compared to the differential relativistic effects of Au_2, that is, about −0.31 Å, 54 cm^{-1}, and 0.38 eV in R_e, ω_e, and D_e, respectively,[169] the remaining errors are acceptable.

The comparison between experimental and calculated data depends critically on the chosen correlation method. In order to establish the errors due to the PPs one can compare to AE results obtained with basis sets of comparable size. Table 19 summarizes the differences between PP and DKH2 CCSD(T) results. For all three molecules the deviations are at most 0.004 Å, 1 cm^{-1} and 0.03 eV, demonstrating also the excellent transferability of the PPs.

dx.doi.org/10.1021/cr2001383 |Chem. Rev. 2012, 112, 403–480

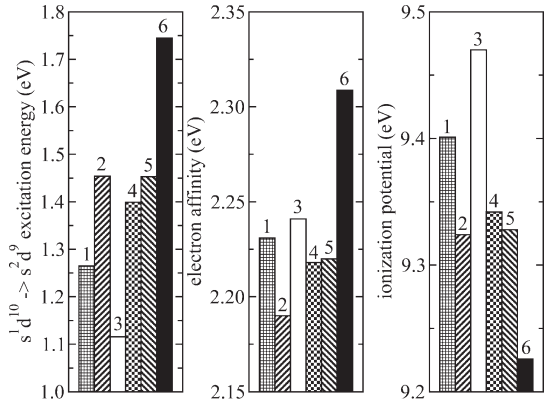

Figure 42. MCQDPT $s^1d^{10} \rightarrow s^2d^9$ excitation energies, electron affinities and ionization potentials (eV) for Au from various MCP calculations in comparison to DKH3 results and experimental data. The bars correspond from left to right to (1) pdsMCP, (2) spdsMCP, (3) fpdsMCP, (4) sfpdsMCP, (5) AE DKH3 results, and (6) experimental data. Data taken from Zeng and Klobukowski.[462]

Table 20. Differences in Bond Distances R_e (Å), Vibrational Constants ω_e (cm^{-1}), and Binding Energies D_e (eV) of Au_2 of CASPT2 Calculations Using Various MCPs[462] and the DKH3 Hamiltonian with a (30s26p18d16f)/[15s14p9d5f] Basis Set[a]

MCP	ΔR_e	$\Delta\omega_e$	ΔD_e
pdsMCP	−0.026	2	0.09
spdsMCP	0.007	0	−0.04
fpdsMCP	−0.045	4	0.14
sfpdsMCP	−0.009	1	0.03

[a] Data taken from Zeng and Klobukowski.[462]

The performance of the small-core energy-consistent MCDHF/DC+B PP for Au[291] summarized in Figures 40 and 41 and Table 19 can be compared to the one of the various DKH3-adjusted MCPs of Zeng and Klobukowski.[462] The authors investigated the core definition for the MCP approach taking the Au atom as an example. Four different MCPs were adjusted including the 5s, 4f, 5p, 5d, and 6s shells or a subset in the valence space. Here the orbitals are ordered according to increasing energy, whereas according to increasing $\langle r \rangle$-values an order 4f, 5s, 5p, 5d, and 6s would result. The four derived MCPs are named pdsMCP, spdsMCP, fpdsMCP, and sfpdsMCP, where the included valence shells are given in energetic order. A main conclusion was that the 4f shell despite its high energy can be attributed to the core, whereas the 5s shell despite the lower energy should be included in the valence space. The spdsMCP, corresponding to a separation of core and valence shells according to their spatial extensions, was found to provide the best accuracy. The slightly inferior performance of the sfpdsMCP was attributed to a less accurate fit, since the same number of parameters was used as for the spdsMCP. The fpdsMCP, corresponding to a separation of core and valence shells according to their energies, performs significantly worse than the spdsMCP, whereas the omittance of 5s from the valence space leads to smaller, but noticeable errors.

Figure 42 displays $s^1d^{10} \rightarrow s^2d^9$ excitation energies, electron affinities and ionization potentials obtained at the multiconfiguration quasidegenerate perturbation theory (MCQDPT) level. The agreement with experimental data is not satisfactory, probably partly because of the lack of g functions in the (30s26p18d16f)/[15s14p9d5f] basis set, as well as the applied correlation method. However, the agreement with the AE DKH3 reference data is quite good. For the preferred spdsMCP the corresponding errors in the excitation energies, electron affinities and ionization potentials are quite small, that is, 0.001, −0.030, and −0.004 eV, respectively.

Table 20 summarizes for the spectroscopic constants of Au_2 the errors of MCP complete active space second-order perturbation theory (CASPT2) values with respect to AE DKH3 results. In case of the preferred choice spdsMCP these are very similar to those of the PP discussed above, which uses the same small core.

10. SELECTED APPLICATIONS

In this final sections, we turn to selected applications for lanthanides and actinides, as well as superheavy elements, that is, fields that are most challenging and also most rewarding for the application of ECPs. In the following sections, we do not provide details of experimental data used for comparison. For a corresponding discussion, as well as the references, we refer the reader to the publications containing the theoretical work discussed here.

10.1. Lanthanides and Actinides

Quantum chemical calculations of lanthanide (Ln) and actinide (An) systems are a very challenging area of computational chemistry.[20,29,317,352,418,542−545] The two major obstacles for accurate electronic structure calculations for f transition metals are the same as for d transition metals, i.e., usually large and often counteracting electron correlation and relativistic effects, cf. Figure 6. Quite frequently applied in atomic and molecular calculations are the shape-consistent large-core lanthanide (46 core electrons) PPs of Cundari and Stevens,[375] and the Stuttgart−Cologne energy-consistent small-core lanthanide[145] and actinide[149] (32 and 60 core electrons) PPs. For the latter, systematic generalized contracted pVXZ (X = D, T,Q) basis sets,[302,304] as well as segmented contracted pVQZ basis sets[303,305] exist. In addition for both lanthanides and actinides f-in-core PPs with valence basis sets for molecular as well as solid-state calculations have been derived.[146,150,151,153,324] With the exception of U, highly accurate MCDHF/DC+B-adjusted PPs are still missing.[393]

On the side of AE calculations ANO basis sets for use in DKH2 calculations have been derived by Roos et al. for lanthanides and actinides.[546,547] These basis sets are certainly useful for investigations at the AE level and, with some care, can also be used for calibration studies, although they are certainly not close to the basis set limit. The same applies to four-component calculations, which are still very scarce for lanthanide and actinide molecules, especially for cases with an open f shell, see a (short) list of available results provided by Styszyński.[548] Another difficulty for theoretical methods is the scarcity or even absence of suitable accurate experimental information, which could be used to calibrate the theoretical models. For example, for the actinide ions essentially only the first ionization potentials have been measured. Higher ionization potentials, which would be ideal to calibrate a method with respect to its ability to accurately describe changes in the 5f occupation number, are still missing (cf. NIST atomic spectra database[228]).

Because of the above situation there are essentially no systematic calibration studies as discussed for the main group and

dx.doi.org/10.1021/cr2001383 |Chem. Rev. 2012, 112, 403–480

Table 21. Selected CCSD(T) Results for IP_3 and IP_4 (in eV) of the Lanthanides[a]

Ln		f	g	h	i	extr.	exp.
La	IP_3	18.81	18.98	19.06	19.09	19.14	19.18
La	IP_4	49.68	49.91	49.99	50.02	50.07	49.95 ± 0.06
Ce	IP_4	34.93	36.11	36.42	36.53	36.74	36.76 ± 0.01
Eu	IP_3	23.79	24.55	24.78	24.89	25.02	24.92 ± 0.10
Gd	IP_4	43.55	44.34	44.59	44.71	44.86	44.40 ± 0.12
Yb	IP_3	23.95	24.58	24.76	24.88	25.00	25.05 ± 0.03
Lu	IP_3	20.78	20.87	20.89	20.90	20.92	20.96
Lu	IP_4	44.26	44.87	45.07	45.21	45.33	45.25 ± 0.03
m.a.e.	a 0.84	0.28	0.17	0.13	0.11		

[a] Large uncontracted basis sets up to the f, g, h, and i symmetry were applied. Extrapolated (extr.) values are compared to experimental (exp.) ones. Data taken from Cao and Dolg.[550]

Table 22. Calculated Term Energies (cm^{-1}) of the J Levels Belonging to the U^{4+} $5f^2$ Configuration[a]

	CG/WB AIMP		DC+B PP	DC+B PP		
	λ = 0.9	AE DC	IHFSCC	IHFSCC	AE DCB	
J	SFSS SOCI	FSCC	std.	unc.	XIHFSCC	exp.
4	0	0	0	0	0	0
2	4062	4084	3959	4233	4202	4161
5	6320	6233	5902	5890	6070	6137
3	8925	9025	8612	8825	8974	8984
4	9276	9585	9196	9264	9404	9434
6	11831	11711	11178	11144	11420	11514
2	17044	16554	15998	16601	16554	16465
4	16581	16929	16181	16221	16630	16656
0	18159	17471	17025	17960	17837	17128
1	21044	20145	19529	20420	20441	19819
6	23278	22581	22594	22441	22534	22276
2	25663	24979	24042	24799	24991	24653
0	43352	46230	43783	45329	45611	43614
m.a.e.	500	403	318	420	357	0
m.a.d.	510	203	567	162	0	357

[a] CG/WB AIMP spin-free state shifted spin-orbit CI,[555] AE/DC Fock-space coupled cluster,[556] energy-consistent MCDHF/DC+B-adjusted PP intermediate Hamiltonian Fock-space coupled cluster (IHFSCC)[507] for standard (std.) and uncontracted (unc.) basis, AE DCB extrapolated extrapolated intermediate Hamiltonian Fock-space coupled cluster (XIHFSCC)[553] results in comparison to experimental data. Mean absolute errors (m.a.e.) refer to the experimental values (last but one line) and AE DCB XIHFSCC results (last line).

transition elements, where the same DFT/WFT approach is used at the PP and AE level. More frequent are studies in which a combination of PP and DFT/WFT approaches are compared to experimental data or to results from relativistic AE calculations using different DFT/WFT approaches.[415] Nevertheless, the quantum chemical investigations of lanthanide and actinide systems is currently a very active and steadily growing field of research, as is manifested by the review articles cited above. A substantial part of the investigations has been carried out with ECPs. The following sections summarize a selection of these studies, where we put the focus mainly on the performance of the ECPs, not so much on the results and insights obtained for the individual systems.

10.1.1. Atoms. The first to fourth ionization potentials (IP_1−IP_4) of lanthanides and actinides have been calculated to test the reliability of the small-core PPs,[145,149] as well as the corresponding valence basis sets.[302−305,549] For lanthanides mean absolute errors (m.a.e.) of less than 0.35 eV compared to experimental data were found at the averaged coupled-pair functional (ACPF) level.[550] The errors are more due to the electron correlation treatment than to the PPs, that is, CCSD(T) calculations for a few single-reference cases led to a significant improvement over the ACPF results with a m.a.e. of ∼0.1 eV,[550] see Table 21. The slow improvement of the m.a.e. with respect to the extension of the basis sets illustrates a major problem of ab initio calculations, especially in view of the presently not feasible molecular calculations, using such large basis sets.

It also has to be noted that experimental data for f elements is not always accurate enough for calibration, for example, the result of 44.86 eV for IP_4 of Gd obtained in the above study[550] differed significantly from the experimental value of 44.0 ± 0.7 eV. A newer experimental value of 44.40 ± 0.12 eV yielding a better agreement was published shortly after the theoretical study.[551] On the basis of the results for lanthanides the accuracy of calculated higher actinides ionization potentials is estimated to be better than ±3%.[549,552] The results obtained with PPs and standard basis sets are for IP_1 of equivalent quality to those from AE calculations using the DKH2 Hamiltonian and ANO basis sets.[546,547]

The most accurate four-component theoretical approach currently available for atoms is the DC(-B) intermediate Hamiltonian Fock-space coupled cluster approach (DC(B)-IHFSCC) [553], which is unique in describing dynamic and nondynamic correlation energies at relatively low computational cost. Unfortunately the applicability is very limited, since at present this approach can only deal with one or two electrons/holes outside/inside a closed shell. By combining it with the newly developed MCDHF+B energy-consistent pseudopotential for uranium, as well as the corresponding standard basis sets, the U^{5+} ($5f^1$ subconfiguration) spin−orbit splitting as well as the fine-structure of the U^{4+} ($5f^2$ subconfiguration) spectrum have been calculated,[554] cf. Table 22 for U^{4+} $5f^2$. The mean absolute deviations (m.a.d.) with respect to experimental data amount to 0 and 318 cm^{-1} for the U^{5+} and the U^{4+} fine-structure levels, respectively. Compared to the AE results obtained by a extrapolated DCB-IHFSCC method with a 32p24d21f12g10h9i basis set and a frozen [Kr]-core[553] the corresponding m.a.d. amount to 13 and 567 cm^{-1},[554] respectively. When the PP is combined with an MRCI approach, which is also suitable for molecular calculations and more general orbital occupations, the m.a.d. are increased to 183 and 918 cm^{-1}, respectively.[554]

Barandiarán and Seijo[555] also calculated the fine-structure of U^{4+} $5f^2$ applying a WB AIMP (1s−5d core), a spin-free state shifted SOCI[209] and a basis set that is also applied for studies of U^{4+} defects in crystals. Comparing to experimental data the m.a.d. of their best result amounts to 180 cm^{-1}. One reason for this very good agreement is, at least in part, a parameter fitting, that is, a scaling factor of 0.9 was applied to the WB SO operator and the ^3P and ^1I states were shifted downward by 1000 cm^{-1}. Without these corrections the m.a.d. amounts to 1284 cm^{-1}, which is quite comparable to the above-discussed PP SOCI result. Including only the empirical scaling of the WB SO operator, but no shifts of LS states, a m.a.e. of 500 cm^{-1} is obtained. In view of the much larger computational effort in the AE DCB XIHFSCC approach and the prospect to use the SFSS SOCI also in larger molecules or for impurities in crystals, this is a very encouraging result.

dx.doi.org/10.1021/cr2001383 |Chem. Rev. 2012, 112, 403–480

Table 23. Bond Lengths R_e (Å), Vibrational Constants ω_e (cm^{-1}), and Binding Energies D_e (eV) of ThO in the $^1\Sigma^+$ Ground State from Energy-Consistent Pseudopotential (PP),[149,304] Model Potential (MP),[561] and Ab Initio Model Potential (AIMP/CG, AIMP/DKH3)[187,448] Calculations in Comparison to Experimental Data[a]

	R_e	ω_e	D_e	D_0	ref
PP(WB,30), SCF	1.829/	943/	6.07/		149
AIMP(CG,12), SCF	1.819/	956/	5.99/		448
AIMP(DKH3,12), SCF	1.833/	945/	5.96/		187
AIMP(DKH3,22), SCF	1.832/	951/	5.96/		187
PP(WB,30), SCF	1.817/1.817	956/955	6.26/6.24		304
MP(DKH2,36), CASSCF	1.928/	847/			561
PP(WB,30), CASSCF	1.882/	876/	8.92/		149
AIMP(CG,12), CASSCF	1.886/	865/	9.15/		448
AIMP(DKH3,12), CASSCF	1.879/	856/	9.14/		187
AIMP(DKH3,22), CASSCF	1.878/	861/	9.14/		187
MP(no-pair,36), MRCI+Q	1.923/	852/	7.85/		561
EC-PP(WB,30), MRCI+Q	1.845/	902/	8.87/	8.45/	149
EC-PP(WB,30), CCSD(T)	1.839/1.845	898/891	9.58/9.38	9.16/8.96	304
Exp.	1.840	896		9.00 ± 0.09	
				8.87 ± 0.15	
				8.79 ± 0.13	

[a] The values are without/with counterpoise correction of the basis set superposition error. The label and number given in parentheses behind the acronyms PP, MP, and AIMP denote the AE method used to derive the reference data and the number of valence electrons for the Th valence-only model Hamiltonian. The zero-point energy and SO contributions were subtracted for the evaluation of the dissociation energy D_0 (eV).

10.1.2. Diatomic Molecules. For many lanthanide diatomics, especially the monoxides, highly accurate spectroscopic data exists. The analysis however is often very difficult for systems with several f electrons due to the extreme complexity of the spectra, as well as of the underlying electronic structure.[318] Here quantum chemical calculations can be very helpful to interpret the experimental results, and on the other hand a sufficient amount of reliable experimental data is highly welcome to calibrate computational methods. For actinide diatomics the situation is much less satisfactory, since experimental data is more scarce.

Spectroscopic and theoretical studies of lanthanide monoxides were recently reviewed by Andrews and co-workers.[557] The assignment for the ground state of YbO to $\Omega = 0^+$ or $\Omega = 0^-$, as well as the configurational assignment to a $4f^{14}\sigma^2\sigma^2\pi^4$ or $4f^{13}\sigma^1\sigma^2\sigma^2\pi^4$ leading (super)configuration is still an open problem for theoreticians.[322] A possible explanation of the observed bond length, which is consistent with $4f^{13}$, and vibrational frequency, which speaks for $4f^{14}$, could be a configurational mixing for the 0^- states of each configuration. It should be noted that the experimentally determined energy difference between the presumably 0^+ ground and 0^- excited state is only ~0.1 eV,[558] whereas the differential relativistic and correlation effects amount to more than 4 and 2 eV, respectively (see ref 558). The entries for IP_3 of Yb, linking Yb^{2+} $4f^{14}$ and Yb^{3+} $4f^{13}$, in Table 21 reveal most likely at least a (MR)CCSD(T) calculation including up to i functions in the Yb basis set and taking SO interactions into account would be required to come to a reliable ab initio answer. Unfortunately, such calculations are currently not feasible. It should be noted that the agreement between experiment and theory applying the same PP and similar correlation methods is excellent for YbH and YbF.[559] Reasonable results in agreement with experiment are also obtained for EuO, where a $4f^7\sigma^1\sigma^2\sigma^2\pi^4$ $^8\Sigma^-$ ground state was found.[321]

In an ionic picture CeO has a ground state superconfiguration Ce^{2+} $4f^1$ $6s^1$ O^{2-}, which gives rise to 8 ΛS states ($^{1,3}\Sigma,\Pi,\Delta,\Phi$) and 16 corresponding Ω levels, which are experimentally well investigated. The system was thus used as a benchmark molecule for, e.g., an energy-consistent small-core Ce PP,[319] a CG-adjusted MP,[460] a CG/WB-adjusted AIMP[560] and a DKH3-adjusted MP.[186] The heavier homologue ThO has a closed shell $^1\Sigma^+$ ground state, that is, no occupied 5f orbital, and was also a target of several studies, cf. Table 23. A DKH2-adjusted Th MP was applied by Marian et al.,[561] whereas WB/CG- and DKH3-adjusted AIMPs were used by Seijo et al.[448] and Tsuchiya et al.,[186] respectively. Hirao and co-workers applied two DKH3-adjusted AIMPs with different core definitions and an explicit treatment of relativity.[470] ThO was also studied with an energy-consistent Th PP by Küchle et al.[149] and Cao and Dolg.[304] For both molecules it is quite difficult to compare the performance of the ECPs, since significant differences exist in the applied basis sets and especially the correlation treatments. At the SCF level all results for ThO agree within ~0.02 Å, ~15 cm^{-1}, and 0.3 eV. At the CASSCF level the bond is significantly lengthened and strengthened. The agreement for the results of the more recent studies is still quite good. Highly correlated calculations were only performed for the energy-consistent PP. At the CCSD(T) level, the calculated values (R_e = 1.845 Å, ω_e = 891 cm^{-1}, D_0 = 8.96 eV)[304] agree very well with experimental data (R_e = 1.840 Å, ω_e = 896 cm^{-1}, $D_0 = 9.00 \pm 0.09$ eV).

A recent study by Averkiev et al. compares small-core energy-consistent PP DFT results to relativistic AE DKH2 CASPT2 and X2C CCSD(T) data for the first and second ionization potential of selected actinide monoxides AnO (An = Th, Pa, U, Np, Pu, Am, Cm).[562] The mean unsigned errors (m.u.e.) of the SO-corrected results with respect to experimental data for all 14 IPs are 0.29 and 0.36 eV at the DKH2 CASPT2 and X2C CCSD(T) level, respectively. Concerning the density functionals used with PPs the M06, M05, B3LYP and MPW3LYP parametrizations worked best with m.u.e. of 0.40, 0.41, 0.42 and 0.44, respectively,

dx.doi.org/10.1021/cr2001383 |Chem. Rev. 2012, 112, 403–480

whereas PW91 exhibited a larger m.u.e. of 0.56 eV. The average of the experimental error bars is 0.39 eV.

For lanthanide fluorides LnF (Ln = Nd, Eu, Gd, Yb) the calculated results by using energy-consistent small-core PPs have shown that the Ln-F bond is of ionic rather than covalent character and that the lanthanide 4f orbitals contribute only little to chemical bonding.[563] Moreover, the calculated spectroscopic constants using PPs combined with DFT calculations were found to be generally in good agreement with the CCSD(T) results.[563] Mosyagin and co-workers performed a GRECP study of the hyperfine, P-odd and P,T-odd constants of YbF in its $^2\Sigma_{1/2}$ ground state and derived an estimate for the effective electric field on the unpaired electron, which is a necessary quantity to link the measured P,T-odd frequency shift with the electric dipole moment of the electron.[564]

For lanthanide and actinide monohydrides, very little experimental information is available. The calculated spectroscopic constants for YbH[563,565] and LuH[565] either using DFT or ab initio methods exhibit errors in comparison to experimental data of at most 0.019 Å for bond distances, 0.06 eV for binding energies, and 7 cm^{-1} for vibrational frequencies. For LaH, EuH, GdH, YbH, LuH and AcH the theoretical results using PPs combined with ab initio methods, that is, CCSD(T) for LaH and LuH, CI for EuH and GdH, agree well with the scalar-relativistic four-component DFT results, except for the binding energies which tend to be larger by up to 1 eV in DFT.[304,565] An MCDHF/DC+B-adjusted small-core PP for U[393] (see also sections 9.1 and 9.2) was applied in a study of the ground and the low-lying excited states of UH. A ^{4} $I_{9/2}$ ground state was predicted and the obtained spectroscopic constants agree very well with results calculated at the AE DKH2 level,[393] see Table 24. The agreement between AE and PP results was found to be slightly improved compared to older studies with a corresponding WB-adjusted PP.[566]

The dimers Ln_2 (Ln = La, Ce, and Pr) were found to have the same valence subconfiguration $\sigma_g^2\pi_u^4$ (with 4f subconfigurations $4f^0$, $4f^1$, $4f^2$ for La, Ce, Pr), forming triple-bonds.[567] For Gd_2 a ground state configuration with 18 unpaired electrons ($4f^7 4f^7\sigma_g^2\sigma_u^1\sigma_g^1\pi_u^2$) was theoretically predicted by using a Gd $4f^7$-in-core PP[568] and later confirmed by an ESR experiment.[569] The molecular constants were subsequently improved in a study of Gd high-spin dimers GdX (X = H, N, O, F, P, S, Cl, Gd), and a $^{19}\Sigma_u^-$ ground state was established.[570] Gd_2 has most likely the highest spin-multiplicity of a diatomic molecule. Because of the stronger destabilization of the 5d orbitals of Lu compared to La the occupation of the π orbitals in Lu_2 is less favorable than in La_2 and thus a $4f^{14}4f^{14}\sigma_g^2\sigma_u^2\pi_u^2$ $^1\Sigma^+$ ground state with only two electrons in π orbitals results. The calculated molecular constants for Ln_2 (Ln = La, Ce, Pr, Gd, Lu)[567] show a satisfactory agreement with experimental data, except for the vibrational frequencies of La_2, Ce_2, and Pr_2, where ~40 cm^{-1} too low values are calculated. The disagreement might at least be partly related to Ar-matrix shifts.

The van der Waals interatomic potentials for YbHe, TmHe, Yb_2, and TmYb were reported by Buchachenko et al. using small-core PPs and large ANO basis sets at the AQCC and CCSD(T) level.[571] The isotropic interactions of Yb and Tm atoms with He are found to be very weak and similar. It was thus suggested that the isotropic interactions are similar for all members of the LnHe family and close to those computed for YbHe. The isotropic interactions of the TmYb and Yb_2 dimers are also very similar. This indicates the possibility of sympathetic cooling of open-shell Ln atoms in an ultracold gas of Yb, if such similarity extends to other LnYb systems.[571]

Table 24. Bond Lengths R_e (Å), Vibrational Constants ω_e (cm^{-1}), and Adiabatic Term Energies T_e (eV) of UH from MRCI Calculations with Spin-Orbit Coupling (State Interaction Approach)[a]

		R_e		ω_e		T_e	
no.	Ω	PP	AE	PP	AE	PP	AE
1	4.5	2.025	2.021	1505	1511	0.000	0.000
2	3.5	2.026	2.021	1499	1504	0.025	0.020
3	2.5	2.024	2.020	1496	1502	0.042	0.039
4	1.5	2.025	2.020	1494	1502	0.054	0.053
5	0.5	2.027	2.021	1494	1500	0.067	0.066

[a] AE DKH2+BP-SO results are compared to small-core energy-consistent PP results.[393]

Besides the calculations with ECPs treating the f shell explicitly, many lanthanide diatomics were studied with 4f-in-core PPs, that is, LnH, LnO, and LnF,[20,320,322,559] Ln_2,[20,323,568] as well as $LnHe^{3+}$.[572] These calculations, which were the first wave function-based correlated calculations on lanthanide systems, provided also the insight, that, for example, for LaO, an ~1 eV increase of the binding energy and a by 0.1 Å shorter bond length results from an active participation of the La 4f orbitals in bonding.[20] Along the lanthanide series the 4f shell becomes more compact and energetically less accessible, so that the active 4f participation in bonding gets weaker. The 4f-in-core approach was also combined with ligand field theory in order to get information about the individual states arising from the open 4f shell.[288]

10.1.3. Polyatomic Compounds. A large number of ECP applications for lanthanides and actinides has been published since the short review of Pyykkö in 1987.[542] We limit the discussion in this section to studies published during the past decade and refer the reader to one of the older previous reviews for a discussion of work performed until 2000.[20,352,418,543,544] Nevertheless the present section can only provide a selection of the available studies.

A quantitative knowledge of lanthanide (Ln^{III}) and actinide (An^{III}) hydration is important for the chemical separation of Ln^{III} and An^{III} in the treatment of nuclear waste, as well as for other problems such as the investigation of the stability of medically applied Ln^{III} complexes such a Gd^{III} or Lu^{III} texaphyrins in aqueous solution (vide infra). The accurate modeling of solvent effects however is a quite difficult task, since explicitly including a larger number solvent molecules may easily exceed the computational resources at hand, whereas using a continuum model to include them implicitly may be too crude. In a 2008 review Schreckenbach and Shamov presented a modified coordinate system of approximations for actinide quantum chemistry, that is, in Figure 1 the axes for one- and many-electron basis were combined to one axis for the chosen model chemistry, which certainly includes besides wave function-based approaches also DFT, the axis for the chosen relativistic approximate Hamiltonian and a new axis for modeling the solvent (condensed phase) effects.[545] In tests of solvation models of the actinyl aquo complexes $[AnO_2(OH_2)_5]^{n+}$ (An = U, Np, Pu and n = 1, 2) Schreckenbach and Shamov found that continuum solvation models are reliable as long as

dx.doi.org/10.1021/cr2001383 |Chem. Rev. 2012, 112, 403–480

the first coordination sphere is included explicitly and that no clear advantage results from the costly explicit treatment of the second coordination sphere. It was also stated that the inclusion of SO effects is necessary to get a correct trend in An(VI)/An(V) reduction potentials. Further it was stressed that a small-core PP approach (e.g., 32 valence electrons for U) is superior to a large-core (e.g., 14 valence electrons for U) approach. The latter view is shared by other researchers,[573,574] but not all. Iché-Tarrat and Marsden agree that, for example, the small-core U PP gives good thermochemical results even when the oxidation state changes; however, they found the large-core U PP still provide good answers for cases where the oxidation state does not change.[575]

A review of computational studies of actinide chemistry in gas phase and solution was published in 2005 by Vallet et al.[573] The authors emphasize that for many cases computationally costly high accuracy is not required, since systematic errors often remain constant and therefore cancel, for example, when comparing geometries of different isomers or when computing reaction energies. Various solvent models, the effects of basis sets and correlation treatment as well as SO coupling found in previous studies of uranyl UO_2^{2+} and related systems are summarized and discussed. The importance to use small-core PPs and to treat the first coordination sphere explicitly was underlined.

Wiebke et al. used An 5f-in-core PPs at the DFT and MP2 level to calculate structures, binding energies, entropies and Gibbs free energies of hydration for An^{III} hydration complexes $An^{III}(OH_2)_h$ (An = Ac−Lr, h = 7, 8, 9) and $An^{III}(OH_2)_{h-1}\cdot H_2O$ (h = 8, 9).[576] The COSMO approach was used to model the bulk water. The Gibbs free energies of hydration for h = 7, 8, and 9 were found to agree with about 60 kJ/mol (∼2%) at the DFT/BP86 level, where a preferred coordination number (CN) of 8 has been found. The well-known tendency of DFT to yield too low CNs is not paralleled at the MP2 level, where preferred CNs of 9 and 8 were obtained for Ac^{III}−Md^{III} and No^{III}−Lr^{III} in closer agreement with experimental evidence. The explicit modeling of H_2O in the second coordination sphere was found to be important to get the An−O distances for H_2O in the first coordination sphere in agreement with experiment. This finding contrasts those of Vallet et al.,[573] as well as Schreckenbach and Shamov,[545] for uranyl and its derivatives.

A corresponding study for Ln^{III} hydration complexes (Ln = La−Lu) was performed by Ciupka et al.,[577] who applied also an improved thermodynamic cycle to evaluate the Gibbs free energies of hydration. Again the CNs obtained at the DFT level are too small, whereas SCS-MP2 yields a preferred CN of 9 for La^{III}−Sm^{III} and 8 for Eu^{III}−Lu^{III} in good agreement with experimental evidence.[578] The m.a.d. of the calculated Gibbs free energies of hydration from two sets of experimental data[579,580] are 36 kJ mol^{-1} (1.1%) and 45 kJ mol^{-1} (1.3%), respectively. Although an agreement with experimental data of ∼1% might appear to be an excellent result, errors of this size are still too large to arrive at reliable answers in quantum chemical investigations of the separation of An^{III} from Ln^{III} in liquid−liquid extraction processes.[581]

For some simple cases energy-consistent f-in-valence PPs were also applied, that is, La^{III},[582,583] Ce^{III},[584] Gd^{III},[585] and Lu^{III},[582,586] where the 4f occupations are 0, 1, 7, and 14, respectively. Similar to the studies mentioned above, it was found for Ce^{III} and Lu^{III} that the explicit inclusion of the second solvation shell improves the structural agreement in comparison to experimental data.[584,586]

The separation of An(III) from Ln(III) by a liquid−liquid extraction process is one of the important steps in the treatment of the nuclear waste produced by nuclear power plants. Purified Cyanex301 (bis(2,4,4-trimethylpentyl)dithiophospinic acid, HBTMPDTP denoted as HL) was found to have very high separation factor for Eu(III) and Am(III)/Cm(III) (>5000).[587] Theoretical studies of this separation with 4f- and 5f-in-core PPs have been reported recently.[581] It was shown that the neutral complexes ML_3, where L acts as a bidentate ligand and the metal cation is coordinated by six S atoms, are most likely stable extraction complexes. Alternative extraction complexes, for example, HML_4, have also been studied. The calculated changes of the Gibbs free energies in the extraction reaction $M^{3+} + 3HL \rightarrow ML_3 + 3H^+$ agree with the experimentally found thermodynamical priority for Am^{3+} and Cm^{3+} over Eu^{3+}. Moreover the ionic metal−ligand dissociation energies of the extraction complexes ML_3 show that, although EuL_3 is the most stable complex in the gas phase, it is the least stable in aqueous solutions.[581]

Complexes of lanthanide(III) ions with texaphyrins, that is, expanded porphyrins with 5 coordinating N atoms, play an important role in medical treatments, for example, X-ray radiation therapy, photodynamic therapy for oncology, photoangioplasty, and the light-based treatment of age-related macular degeneration. Quantum chemical studies for the structure, stability and spectra of these systems were performed with Ln 4f-in-core PPs at the DFT level.[588] Related studies using Ln 4f- and An 5f-in-core PPs of Ln(III) (Ln = La, Gd, Lu) and An(III) (An = Ac, Cm, Lr) motexafins (M-Motex^{2+}, M = Ln, An) have shown that Ac-Motex^{2+} is the most stable complex and should be the best candidate for experimentalists to get stabilization of an An^{3+} ion by motexafin.[589]

The lanthanide trihalides are a popular test set and have been studied with various ECPs, that is, energy-consistent PPs,[590−595] shape-consistent PPs,[590,591,596,594] as well as model core potentials.[597] Good agreement is observed between f-in-core and f-in-valence PP results, when treated at the same level of theory.[593] Tsukamoto and co-workers found that dynamic electron correlation is indispensable for obtaining reliable bond distances, whereas static electron correlation has only little influence.[597] For DyX_3 (X = Cl, Br, I), it has been found that 4f subshell does not influence the geometry of the monomers, but obviously affects their dimers $(DyX_3)_2$ (X = Cl, Br, I).[590,591,594] According to the calculations, DyX_3 (X = Br, I) probably forms both planar and pyramidal DyX_3 units in an inert matrix, leading to the appearance of two symmetric stretching frequencies observed by the experimentalists.[591,594] Similarly, nearby C_{3v} and D_{3h} structures were found for LaF_3 in Ar_n clusters (n = 1−21) at the MP2 level by Lanza[598] using the shape-consistent La PP of Stevens et al.[286]

Figure 43 compares the mean absolute errors in calculated lanthanide halogen distances with respect to two recommended sets of recent PP[592,595] and MP[597] calculations with AE DKH2 data.[592] 4f-in-core energy-consistent PP+CPP[146,288,323,324] results are found overall to be of the same quality as the DKH2 results for both recommended sets of bond distances. The 4f-in-valence energy-consistent PPs[145,302,303] perform also quite well, although the comparison to the other results is not fully justified for the heavier halogens, since in contrast to the 4f-in-core calculations,[595] no PPs were included on the halogen atoms,[592]

dx.doi.org/10.1021/cr2001383 |Chem. Rev. 2012, 112, 403–480

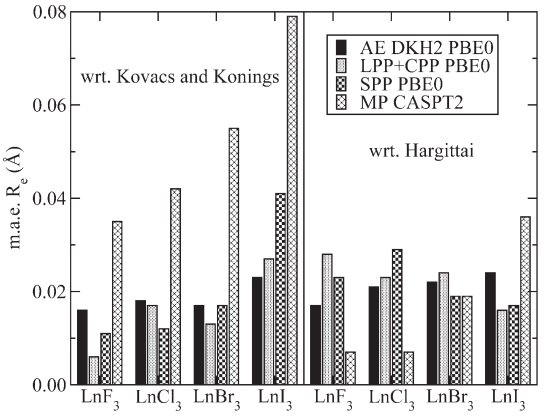

Figure 43. Mean absolute errors in calculated bond lengths of lanthanide trihalides LnX_3 (X=Ce− Lu) from all-electron second-order Douglas−Kroll−Hess (AE DKH2) DFT/PBE0,[592] 4f-in-core pseudopotential and core polarization potential (LPP+CPP) DFT/PBE0,[595] energy-consistent small-core pseudopotential (SPP) DFT/PBE0[592] and model core potential (MCP) CASPT2[597] calculations in comparison to two sets of recommended values (Kovacs and Konings, 2004; Hargittai, 1988).

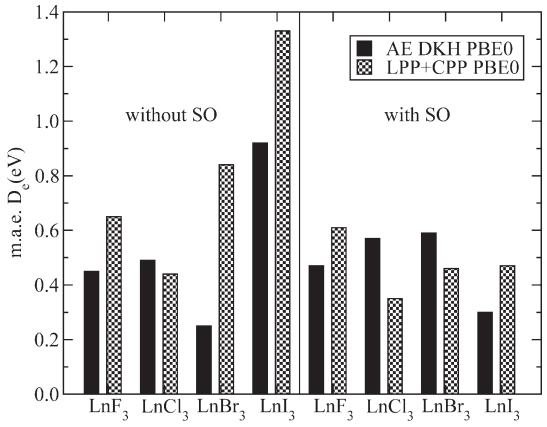

Figure 44. Same as Figure 43, but for atomization energies in comparison to experimental values (Myers, 1977). Atomic spin−orbit corrections for the halogens have been applied for the right half of the graph.

and slightly too long bond lengths result. The MCP CASPT2 results[597] agree much better with the older recommended set of bond lengths, whereas the PPs and AE DKH2 approaches agree well with both sets. We note that the recommended values do not all correspond to gas phase R_e values and thus in a strict sense do not allow a direct comparison to the calculated values. However, an individual discussion of the 56 molecules in the test set is not within the scope of this review.

Figure 44 compares the calculated atomization energies of AE DKH2[592] and 4f-in-core energy-consistent PP[595] calculations to experimental values. It is well-known that SO effects on bond energies are substantial for heavier halogens, and by no means negligible as stated by Pantazis and Neese.[592] Including corresponding atomic corrections from experimental data the results of both AE DKH2 and PP approaches yield roughly the same agreement with the experimental values and a constant quality for all halogens.[595]

A large number ECP studies were reported for small actinide complexes with electronegative ligands, such as halides and pseudohalides. Most of these studies have focused on uranium, that is, AnF_n (An = Pu−No for n = 2; An = Ac−Lr for n = 3, An = Th−Cf for n = 4, An = Pa−Am for n = 5, An = U−Am for n = 6),[150,151,153] AnF_6 (An = Th−Np),[599] $ThF_n^{(4-n)+}$ (n = 1−8),[600] PaX_5 (X = F, Cl),[601] UF_6,[574] UF_n (n = 5, 6),[419] UX_n (X = F, Cl; n = 1−6),[602] UF_n (n = 4, 5, 6),[603] UX_6 and UO_2X_2 (X = F, Cl, Br, I),[604] MF_6, MO_3, MO_2F_2, $MO_2(OH)_2$ (M = U, Np, Pu),[605] UF_4X_2 (X = H, F, Cl, Cl, CN, NC, NCO, OCN, NCS, SCN),[606] and UF_nCl_{6-n} (n = 1−6).[525,523]

Batista et al. investigated structural properties and thermochemistry of UF_6 and UF_5 at the HF and DFT level using the DKH3 AE approach as well as a small-core and a large-core U PP.[419] For the structural properties both large- and small-core PP performed equally well and yielded good agreement with experimental data at the DFT level, but for the $UF_6 \rightarrow UF_5 + F$ bond dissociation energy only the DKH3 AE and the small-core PP approach performed well, whereas the large-core PP results were off by more than 50%. The combination of hybrid density functionals and small-core U PP was recommended for both the evaluation of structural properties and thermochemistry. Using this approach Batista et al. computed for the first time bond dissociation energies for the whole series UX_n (X = F, Cl; n = 1−6) and obtained good agreement with experiment.[602] Using a small-core U PP Pyykkö and co-workers investigated the preference of U to bond to F, O, and Cl rather than to pseudohalides.[606] In this study the U−F bond in UF_6 was found to have some multiple-bond character, approaching at a theoretical limit a bond order of 1.5. Straka and Kaupp,[523] as well as Schreckenbach,[525] demonstrated that a small-core PP for U is able to yield ^{19}F chemical shifts for UF_nCl_{6-n} (n = 1−6) complexes in good agreement with relativistic AE reference data, whereas earlier studies using a large-core U PP failed completely.

Despite the more diffuse actinide 5f shell in comparison to the compact lanthanide 4f shell, and the frequently reported failures of large-core PPs for U treating the 5f shell explicitly (vide supra), the f-in-core PP approach developed for lanthanides two decades ago,[146,155,288,323,324] appears to work also quite well for actinides as long as the actual 5f occupation is consistent with the one modeled by the PP. The 5f-in-core approach is relatively robust if the 5f occupation is slightly higher than the one modeled by the PP, but it breaks down when it is lower.[150,151,153] Interestingly, the approach does even not fail when treating actinocenes, where both 6d and 5f orbitals are involved in metal-ring bonding.[607]

A substantial amount of quantum chemical calculations of actinide systems deals with actinyls, especially the uranyl ion UO_2^{2+}, which is central to the chemistry of uranium.[608] A recent review of Denning summarizes both experimental and theoretical work on actinyls.[609] Here we only report on some more recent studies. Vlaisavljevich, Gagliardi, and Burns have performed calculations to understand the formation of nanoscale cage clusters based on uranyl ions.[610] It was shown that the inherent bending of the configuration, i.e., bending of the $U-O_2-U$ dihedral angle, caused by a covalent interaction along the $U-O_{peroxo}$ bonds encourages curvature and cage cluster formation.[610] Gas phase U^+ and UO_2^+ carbonyl cations have been recently produced and studied.[611] The calculations established the fully coordinated ions are $U(CO)_8^+$ and $UO_2(CO)_5^+$, with D_{4d} square antiprism and D_{5h} pentagonal bipyramid structures.[611] Averkiev et al. compared SO-corrected

dx.doi.org/10.1021/cr2001383 |Chem. Rev. 2012, 112, 403–480

results for the first and second ionization potentials as well as the bond energies of the neutral molecules as well as the mono- and dication for actinide dioxides AnO_2 (An = Th, Pa, U, Np, Pu, Am, Cm) from small-core energy-consistent PP DFT calculations and relativistic AE DKH2 CASPT2 and X2C CCSD(T) calculations.[562] The mean unsigned errors (m.u.e.) for the first and second ionization potentials were 0.53 and 0.65 eV at the AE DKH2 CASPT2 and X2C CCSD(T) level, respectively. In the PP studies the B3LYP, MPW3LYP, PW91, M06 and M05 functionals performed best with errors of 0.52, 0.52, 0.54, 0.55, and 0.56 eV, respectively. The experimental error bars are 0.45 eV on average. Concerning the binding energies m.u.e. of 15 and 13 kcal/mol were found for AE DKH2 CASPT2 and X2C CCSD(T), respectively. The m.u.e. of the best PP results amount to 10, 10, 11, and 12 kcal/mol for B3LYP, MPW3LYP, M06, and M05, respectively, whereas PW91 performs clearly worse with a m.u.e. of 25 kcal/mol.

A major advantage of ECPs is the reduction of computational effort comparing to AE methods, which makes ab initio and DFT studies of more complicated complexes containing f elements feasible. Numerous publications using ECPs for quite complex systems containing f elements have appeared during the last three years.[316,581,610−627] Most of these calculations were performed in cooperation with experimental studies to clarify the structures, spectra as well as reaction mechanisms. For the complexes $[(C_5Me_5)U(\mu\text{-}I)_2]_3N$, $[(C_5Me_5)U(\mu\text{-}I)_2]_3O$, $[(C_5Me_5)_2U(\mu\text{-}N)\text{-}U(\mu\text{-}N_3)(C_5Me_5)_2]_4$, $[(C_5Me_5)_2UN_3(\mu\text{-}N_3)]_3$, $[(C_6F_5)_3BNU\text{-}(N[Me]Ph)_3]$, and $[(C_5Me_5)U(\mu_3\text{-}E)]_8$ with U in a formal oxidation state III or IV the theoretical predictions of the uranium main group element bond distances were found to be very valuable, since from the experimental X-ray data one cannot differentiate main group elements as N from O in the presence of one or more metals as large as uranium.[623] Moreover, all above-mentioned polymetallic uranium complexes are bonded ionically with azide, nitride, or oxide except for $[(C_6F_5)_3BNU(N\text{-}[Me]Ph)_3]$, which is a monouranium complex with uranium in formal oxidation state VI.[623]

Tassell and Kaltsoyannis studied the covalency in $AnCp_4$ (An = Th−Cm).[626] They found that the An−Cp bonding is very ionic. The large 5f contributions to molecular orbitals in compounds of the middle actinides should not be taken as evidence of significant covalency (in the sense of appreciable overlap between metal and ligand orbitals) and the extent of f-based covalency is larger in U complexes than anywhere else in the f block. A similar conclusion was reached by Guillaumont based on the studies on Ln(III) (Ln = La, Ce, Nd) and An(III) (An = U, Pu, Am, and Cm) complexes with tridentate nitrogen ligands. It was found that the direct participation of 5f orbitals in bonding is significant only for U.[628]

10.1.4. Solids. The theoretical studies using methods originating from solids state physics and applying plane-wave expansion are not included here. In the last five years, electronic spectra of f-element ions doped in crystals have attracted a lot of attention of theoreticians.[389,629−643] For lanthanides most studies have focused on La,[641,643] Ce,[629,632,633,636,637] Gd,[641] and Yb.[634,635,638−640,642] For actinides, mainly crystals containing U[389,630,631,633] or Pu[630] were studied. Recently the *ab initio* model potential (AIMP) and embedding method was improved for embedded cluster calculations of ionic solids and applications to three oxides were reported, that is, the cubic perovskite $CeAlO_3$ and the CeO_2 and UO_2 hosts with fluorite structure.[633] The improvement consists of a new calculation of the embedding term that represents the Pauli repulsions between the embedded cluster and its environment, under a criterion of consistency of ground state structures with respect to the size of the embedded clusters.[633]

10.2. Superheavy Elements

The superheavy elements (SHE) are considered to be those that follow the last actinide element 103 (Lawrencium, Lr). The SHE are an ideal playground for heavy-element quantum chemists, since relativistic effects are extremely large and thus their properties may be rather different from their lighter congeners in the same groups. Relativistic effects in SHE have been reviewed by Schwerdtfeger and Seth.[644] Several pioneering high-level ab initio calculations on the electronic structures and properties of compounds of elements 111−114 were performed with PPs.[290,311,645−648] Since it is expected that the top of the island of stability could be located at the nuclide with proton number $Z = 114$ and neutron number $N = 184$, most attention has been paid to elements 112 (E112) and 114 (E114).[290,390,391,649−652] Han and co-workers found first that due to SO effects the bond lengths for E113-H are decreased, but increased for E117-H.[647] Moreover, the single-bond radii of E111−E114 were found to be smaller than of their 6p analogues Au, Hg, Ti, and Pb, whereas the elements E115−E118 are clearly larger than for Bi, Po, At, and Rn.[653] For more applications, the reader is referred to recent review articles published in 2009 and 2010 by Pershina.[651,654]

11. CONCLUSIONS AND OUTLOOK

The effective core potential (ECP) method, invented independently by Hellmann and Gombas around 1935, is almost as old as quantum mechanics. Lines of methodological improvements and applications in molecular quantum chemistry and solid state physics can be traced back to the early work of Preuss in 1955, and Phillips and Kleinman in 1959, respectively. In both fields the ECP approach changed from an initially semiempirical approach to an ab initio or at least first-principles method. Important steps in the ECP development in the quantum chemistry and solid state physics communities were often taken independently, but at similar times, e.g., the development of the shape-consistent and norm-conserving pseudopotential (PP) formalisms.

In solid state physics density functional theory PP calculations performed with plane-wave basis sets are nowadays a routine tool, as evidenced, for example, by the several thousand citations each of the popular PP sets accumulated so far. In quantum chemistry both the model potential (MP) and the PP approach are routinely used, the latter much more frequently. Besides computational savings a major motivation was the simple implicit inclusion of relativistic contributions and the resulting possibility to study relativistic effects in (larger) molecular systems by comparing results obtained with relativistically and nonrelativistically parametrized ECPs. Initially such studies were performed with large-core ECPs and often with quite small basis sets. Because of the lack of competitive alternative approaches the ECP method became a workhorse in relativistic quantum chemistry during the 1980s. By far, more than a thousand applications were performed with the PPs of each of the most popular sets so far. The advances both in computer technology and quantum chemistry codes, the development of more ready to use relativistic all-electron approaches as computational alternative and as tools for calibration, as well as the generation of systematic series of basis sets allowing also extrapolation to the

dx.doi.org/10.1021/cr2001383 |*Chem. Rev.* 2012, 112, 403–480

complete basis set limit, caused in the last two decades a change of preference toward small-core ECPs with significantly improved accuracy. Modern PPs of both the shape-consistent and energy-consistent variety can reach an accuracy which allows to include besides the leading Dirac relativity also small relativistic contributions such as the Breit interaction or the finite nucleus into the adjustment, whereas the development of MPs here has to catch up. The inclusion of contributions from quantum electrodynamics, which are probably already nonnegligible for Au, are as well on the agenda.

One may ask what remains to be done except for filling some gaps of the available ECPs and corresponding basis sets, i.e., what can still be improved concerning the MP and PP methods? Certainly, if an accuracy significantly better than 0.01 eV in energy differences between low-lying electronic states, ionization potentials and electron affinities is the target for PP approaches, the simple formalism with a semilocal (or nonlocal) one-electron valence-only model Hamiltonian and an unchanged Coulomb interaction might not be sufficient. Modified two-electron terms are suggested by the generalized Phillips−Kleinman equation and could be considered in improved valence-only model Hamiltonians. It has to be kept in mind, however, that highly correlated calculations of atoms and diatomics are nowadays not any more the main area of PP applications, but rather the calculations of medium sized to large systems treated with cheap (local) correlation schemes or even density functional theory. On one hand the PP approach should stay computationally simple enough to allow such calculations, including the evaluation of energy gradients, on the other hand the approximate treatments of electron−electron interactions in connection with the limited basis sets applicable for larger systems may lead to errors much larger than those of the existing PPs. Thus one may ask if such higher accuracy is really useful for practical applications. This question is also justified for the further development of MPs, where a modeling of the best available many-electron Hamiltonian, that is, the Dirac−Coulomb−Breit Hamiltonian, is still missing.

(Dirac−)Hartree−Fock-adjusted small-core PPs can also be used in density functional calculations, whereas large-core PPs are frequently found to fail. It would be interesting to see if the situation for quantum chemistry density functional studies can be improved by adding nonlinear core corrections, since these were found to be successful in solid state PP calculations.

Core−valence correlation, described by (*l*- or *lj*-dependent) core-polarization potentials has so far also not been exploited systematically. Especially for small-core ECPs remaining nonnegligible core−valence correlation contributions, for example, 4f correlation contributions for Hg 20-valence-electron ECPs, could be evaluated using core-polarization potentials. However, the use of core-polarization potentials is not common, since the corresponding integral routines are only available in a few quantum chemistry codes and corresponding energy gradients are still missing.

When going beyond the ECP variants discussed here, that is, the PP and MP approaches, the latter is much more advanced when describing the environments consisting of groups of atoms/ions, for example, the environment of embedded clusters investigated in solid state calculations. Although one can imagine to generate also PPs for an ensemble of atoms/ions, a general prescription how to do this in practice has not been given so far.

Summing up, although many scientists who made important contributions to the ECP approach are by now retired (or tired), the ECP approach itself at the age of 75 is still doing well, will continue to be a useful tool for computational chemists for some time and possibly will also undergo further methodological developments to become more accurate and efficient.

AUTHOR INFORMATION

Corresponding Author

*E-mail: m.dolg@uni-koeln.de.

BIOGRAPHIES

Michael Dolg was born in Stuttgart, Germany, in 1958. He obtained his diploma (1985) and doctoral (1989) degrees from the University of Stuttgart, Germany, having worked on pseudopotentials for 3d- and 4f-elements, respectively. In 1994, he became a research group leader at the Max-Planck-Institute for Physics of Complex Systems in Dresden, Germany. From 1999 to 2002, he was a C3 professor at the University of Bonn, Germany, and since 2002, he has been a C4 professor at the University of Cologne, Germany. He has more than 200 scientific articles in theoretical chemistry. In addition to relativistic quantum chemistry for heavy elements, he is also interested in local electron correlation schemes for molecules and solids.

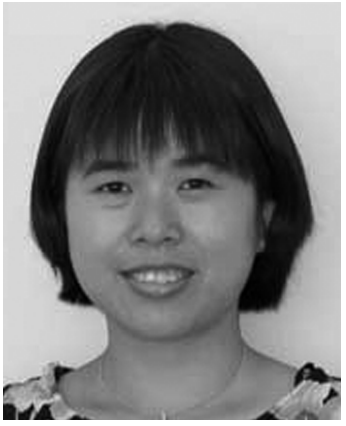

Xiaoyan Cao was born in the Hubei province of China in 1972. She received her B.S. and Ph.D. degrees from Beijing Normal University, Beijing, in physics and quantum chemistry in 1991 and 1996, respectively, for experimental and theoretical research in UV and photoelectron spectroscopy and reaction kinetics. After a postdoctoral stay at the Institute of Chemistry of the Chinese Academy of Sciences (1996−1998), she became

Associate Professor at the Sun Yat-Sen University, Guangzhou, in 1998. In 2000, she moved to the University of Bonn, Germany. Since 2002, she has worked as a senior scientist at the University of Cologne. She has 50 scientific articles in theoretical and physical chemistry. Her main present interests are energy-consistent pseudopotentials and their applications to lanthanides and actinides.

ACKNOWLEDGMENT

The authors are grateful to the German Science Foundation (Deutsche Forschungsgemeinschaft, DFG) for supporting the development of energy-consistent pseudopotentials.

REFERENCES

(1) Pyykkö, P. *Adv. Quantum Chem.* **1978**, *11*, 353.
(2) Pyykkö, P. *Chem. Rev.* **1988**, *88*, 563.
(3) Weeks, J. D.; Hazi, A.; Rice, S. A. *Adv. Quantum Chem.* **1969**, *16*, 283.
(4) Bardsley, J. N. *Case Stud. At. Mol. Phys.* **1974**, *4*, 299.
(5) Dixon, R. N.; Robertson, I. L. *Spec. Period. Rep., Theor. Chem.* **1978**, *3*, 100.
(6) Hibbert, A. *Adv. Atom. Molec. Phys.* **1982**, *18*, 309.
(7) Pitzer, K. S. *Int. J. Quantum Chem.* **1984**, *25*, 131.
(8) Kahn, L. R. *Int. J. Quantum Chem.* **1984**, *25*, 149.
(9) Krauss, M.; Stevens, W. J. *Annu. Rev. Phys. Chem.* **1984**, *35*, 357.
(10) Christiansen, P. A.; Ermler, W. C.; Pitzer, K. S. *Annu. Rev. Phys. Chem.* **1985**, *36*, 407.
(11) Balasubramanian, K.; Pitzer, K. S. *Adv. Chem. Phys.* **1987**, *67*, 287.
(12) Ermler, W. C.; Ross, R. B.; Christiansen, P. A. *Adv. Quantum Chem.* **1988**, *19*, 139.
(13) Laughlin, C.; Victor, G. A. *Adv. At. Mol. Phys.* **1988**, *25*, 163.
(14) Gropen, O. In *Methods in Computational Chemistry*; Plenum: New York, 1988; Vol. 2, p 109.
(15) Pickett, W. E. *Comput. Phys. Rep.* **1989**, *9*, 115.
(16) Huzinaga, S. *J. Mol. Struct. (THEOCHEM)* **1991**, *234*, 51.
(17) Chelikowsky, J. R.; Cohen, M. L. In *Handbook on Semiconductors*; Elsevier: Amsterdam, 1992; Vol. 1, p 59.
(18) Huzinaga, S. *Can. J. Chem.* **1995**, *73*, 619.
(19) Frenking, G.; Antes, I.; Böhme, M.; Dapprich, S.; Ehlers, A. W.; Jonas, V.; Neuhaus, A.; Otto, M.; Stegmann, R.; Veldkamp, A.; Vyboishchikov, S. F. *Rev. Comput. Chem.* **1996**, *8*, 63.
(20) Dolg, M.; Stoll, H. In *Handbook on the Physics and Chemistry of Rare Earths, Vol.* 22; Elsevier: Amsterdam, 1996; p 607.
(21) Cundari, T. R.; Benson, M. T.; Lutz, M. L.; Sommerer, S. O. *Rev. Comput. Chem.* **1996**, *8*, 145.
(22) Balasubramanian, K. In *Encyclopedia of Computational Chemistry*; Wiley: Chichester, U.K., 1998; p 2471.
(23) Pyykkö, P.; Stoll, H. *R.S.C. Spec. Period. Rep., Chem. Modell., Appl. Theory* **2000**, *1*, 239.
(24) Seijo, L.; Barandiarán, Z. In *Computational Chemistry: Reviews of Current Trends*; World Scientific: Singapore, 1999; p 55.
(25) Dolg, M. In *NIC Series*; John Neumann Institute for Computing: Jülich, Germany, 2000; Vol. 3, p 507.
(26) Stoll, H.; Metz, B.; Dolg, M. *J. Comput. Chem.* **2002**, *23*, 767.
(27) Dolg, M. In *Relativistic Electronic Structure Theory, Part 1: Fundamentals*; Elsevier: Amsterdam, 2002; p 793.
(28) Schwerdtfeger, P. In *Progress in Theoretical Chemistry and Physics: Theoretical Chemistry and Physics of Heavy and Superheavy Elements*; Kluwer Academic: Dordrecht, The Netherlands, 2003; p 399.
(29) Dolg, M.; Cao, X. In *Recent Advances in Computational Chemistry*; World Scientific: London, 2004; Vol. 6, p 1.
(30) Cao, X.; Dolg, M. *Coord. Chem. Rev.* **2006**, *250*, 900.
(31) Cao, X.; Dolg, M. In *Relativistic Methods for Chemists. Challenges and Advances in Computational Physics*; Springer: London, 2010; Vol. 10, p 251.
(32) Schwarz, W. H. E. In *Relativistic Methods for Chemists. Challenges and Advances in Computational Physics*, Springer: London, 2010; Vol. 10, p 1.
(33) *Relativistic Effects in Heavy-Element Chemistry and Physics*; Wiley Series in Theoretical Chemistry; Hess, B. A., Ed., Wiley: Chichester, U.K., 2002; Vol. 12.
(34) *Relativistic Electronic Structure Theory. Part 1, Fundamentals. Theoretical and Computational Chemistry*; Schwerdtfeger, P., Ed., Elsevier: Amsterdam, 2002; Vol. 11.
(35) *Relativistic Electronic Structure Theory. Part 2: Applications. Theoretical and Computational Chemistry*; Schwerdtfeger, P., Ed., Elsevier: Amsterdam, 2004; Vol. 14.
(36) *Recent Advances in Relativistic Molecular Theory. Recent Advances in Computational Chemistry*; Hirao, K.; Ishikawa, Y., Eds., World Scientific: London, 2004; Vol. 6.
(37) *Relativistic Methods for Chemists. Challenges and Advances in Computational Physics*; Barysz, M.; Ishikawa, Y., Eds., Springer: London, 2010; Vol. 10.
(38) Dyall, K. G.; K. Faegri, J. *Introduction to Relativistic Quantum Chemistry*; Oxford University Press: Oxford, U.K., 2007.
(39) Grant, I. P. *Relativistic Quantum Theory of Atoms and Molecules. Theory and Computations*; Springer: New York, 2007.
(40) http://rtam.csc.fi/ (accessed Aug 26, 2011).
(41) Pyykkö, P. In *Lecture Notes in Chemistry, Vol.* 41; Spinger: Berlin, 1986.
(42) Pyykkö, P. In *Lecture Notes in Chemistry, Vol.* 60; Spinger: Berlin, 1993.
(43) Pyykkö, P. In *Lecture Notes in Chemistry, Vol.* 76; Spinger: Berlin, 2000.
(44) Szabo, A.; Ostlund,N. S.*Modern Quantum Chemistry: Introduction to Advanced Electronic Structure Theory*; McGraw-Hill: New York, 1989.
(45) Pople, J. A. *J. Chem. Phys.* **1965**, *43*, S229.
(46) Schrödinger, E. *Ann. Phys.* **1926**, *79*, 361.
(47) Born, M.; Oppenheimer, R. *Ann. Phys.* **1927**, *20*, 457.
(48) Schrödinger, E. *Ann. Phys.* **1926**, *79*, 489.
(49) Hohenberg, P.; Kohn, W. *Phys. Rev.* **1964**, *136*, B864.
(50) Kohn, W.; Sham, L. J. *Phys. Rev.* **1965**, *140*, A1133.
(51) Hartree, D. R. *Proc. Camb. Philos. Soc.* **1927**, *24*, 89.
(52) Hartree, D. R. *Proc. Camb. Philos. Soc.* **1927**, *24*, 111.
(53) Slater, J. C. *Phys. Rev.* **1930**, *35*, 210.
(54) Fock, V. *Z. Phys.* **1930**, *61*, 126.
(55) Fock, V. *Z. Phys.* **1930**, *62*, 795.
(56) Pauli, W. *Z. Phys.* **1925**, *31*, 765.
(57) Slater, J. C. *Phys. Rev.* **1929**, *34*, 1293.
(58) Roothaan, C. C. J. *Rev. Mod. Phys.* **1951**, *23*, 69.
(59) Hall, G. G. *Proc. Roy. Soc. London A* **1951**, *205*, 541.
(60) Boys, S. F. *Proc. Roy. Soc. London A* **1950**, *200*, 542.
(61) Preuss, H. *Z. Naturf. A* **1956**, *11*, 823.
(62) Slater, J. C. *Phys. Rev.* **1930**, *36*, 57.
(63) Löwdin, P. O. *Adv. Chem. Phys.* **1959**, *2*, 207.
(64) Das, G.; Wahl, A. C. *J. Chem. Phys.* **1967**, *47*, 2934.
(65) Condon, E. U. *Phys. Rev.* **1930**, *36*, 1121.
(66) Schrödinger, E. *Ann. Phys.* **1926**, *80*, 437.
(67) Møller, C.; Plesset, M. S. *Phys. Rev.* **1934**, *46*, 618.
(68) Coester, F.; Kümmel, H. *Nucl. Phys.* **1960**, *17*, 477.
(69) Foster, J.-M.; Boys, S. F. *Rev. Mod. Phys.* **1960**, *32*, 300.
(70) Edmiston, C.; Ruedenberg, K. *Rev. Mod. Phys.* **1963**, *35*, 457.
(71) Pipek, J.; Mezey, P. G. *J. Chem. Phys.* **1989**, *90*, 4916.
(72) Vleck, J. H. V.; Sherman, A. *Rev. Mod. Phys.* **1935**, *7*, 167.
(73) Hellmann, H. *J. Chem. Phys.* **1935**, *3*, 61.
(74) Gombas, P. *Z. Phys.* **1935**, *94*, 473.
(75) Gombas, P. *Z. Phys.* **1935**, *94*, 687.
(76) Pitzer, K. S. *Acc. Chem. Res.* **1979**, *12*, 271.
(77) Pyykkö, P.; Desclaux, J. P. *Acc. Chem. Res.* **1979**, *12*, 276.
(78) Grant, I. P. *Adv. Phys.* **1970**, *19*, 747.
(79) Desclaux, J. P.; Mayers, D. F.; O'Brien, F. *J. Phys. B: At. Mol. Opt. Phys.* **1971**, *4*, 631.

(80) Desclaux, J. P. *Comput. Phys. Commun.* **1975**, *9*, 31.
(81) Grant, I. P.; McKenzie, B. J.; Norrington, P. H.; Mayers, D. F.; Pyper, N. C. *Comput. Phys. Commun.* **1980**, *21*, 207.
(82) Grant, I. P.; Quiney, H. M. *Adv. At. Mol. Phys.* **1988**, *23*, 37.
(83) Dyall, K. G.; Grant, I. P.; Johnson, C. T.; Parpia, F. A.; Plummer, E. P. *Comput. Phys. Commun.* **1989**, *55*, 425.
(84) Wood, J. H.; Boring, A. M. *Phys. Rev. B* **1978**, *18*, 2701.
(85) Cowan, R. D.; Griffin, D. C. *J. Opt. Soc. Am.* **1976**, *66*, 1010.
(86) Barthelat, J.-C.; Pélissier, M.; Durand, P. *Phys. Rev. A* **1980**, *21*, 1773.
(87) Hess, B. A. *Phys. Rev. A* **1986**, *33*, 3742.
(88) Jansen, G.; Hess, B. A. *Phys. Rev. A* **1989**, *39*, 5016.
(89) Samzow, R.; Hess, B. A.; Jansen, G. *J. Chem. Phys.* **1992**, *96*, 1227.
(90) Wolf, A.; Reiher, M.; Hess, B. A. *J. Chem. Phys.* **2002**, *117*, 9215.
(91) Nakajima, T.; Hirao, K. *Chem. Rev.* **2011**, DOI: 10.1021/cr200040s.
(92) Nakajima, T.; Hirao, K. *Chem. Phys. Lett.* **1999**, *302*, 383.
(93) Visscher, L.; Visser, O.; Aerts, H.; Merenga, H.; Nieuwpoort, W. C. *Comput. Phys. Commun.* **1994**, *81*, 120.
(94) Saue, T.; Faegri, K.; Helgaker, T.; Gropen, O. *Mol. Phys.* **1997**, *91*, 937.
(95) Quiney, H. M.; Skaane, H.; Grant, I. P. *Adv. Quantum Chem.* **1999**, *32*, 1.
(96) Grant, I. P.; Quiney, H. M. *Int. J. Quantum Chem.* **2000**, *80*, 283.
(97) Mohanty, A.; Clementi, E. *Int. J. Quantum Chem.* **1991**, *39*, 487.
(98) Mohanty, A.; Clementi, E. *Int. J. Quantum Chem.* **1991**, *40*, 429.
(99) Pisani, L.; Clementi, E. *J. Comput. Chem.* **1994**, *15*, 466.
(100) Dyall, K. G.; Taylor, P. R.; Faegri, J. K.; Partridge, H. *J. Chem. Phys.* **1991**, *95*, 2583.
(101) Yanai, T.; Nakajima, T.; Ishikawa, Y.; Hirao, K. *J. Chem. Phys.* **2001**, *114*, 6526.
(102) Cao, X.; Dolg, M. *J. Phys. Chem. A* **2009**, *113*, 12573.
(103) Mosyagin, N. S.; Petrov, A. N.; Titov, A. V.; Tupitsyn, I. I. In *Recent Advances in the Theory of Chemical and Physical Systems*; Springer: Berlin, 2006; p 253.
(104) Andrae, D. *Phys. Rep.* **2000**, *336*, 413.
(105) Saue, T. Principles and applications of relativistic molecular calculations; PhD thesis, University of Oslo, Oslo, Norway, 1996.
(106) Visser, O.; Visscher, L.; Aerts, P. J. C.; Nieuwpoort, W. C. *Theor. Chim. Acta* **1992**, *81*, 405.
(107) Berestetski, V. B.; Lifshitz, E. M.; Pitaevskii, L. P. *Relativistic Quantum Theory*; Pergamon: Oxford, U.K., 1971.
(108) Thierfelder, C.; Schwerdtfeger, P. *Phys. Rev. A* **2010**, *82* No. 062503.
(109) Brown, G.; Ravenhall, D. G. *Proc. Roy. Soc. A* **1951**, *208*, 552.
(110) Sucher, J. *Phys. Rev. A* **1980**, *22*, 348.
(111) Schwarz, W. H. E.; Wechsel-Trakowski, E. *Chem. Phys. Lett.* **1982**, *85*, 94.
(112) Kutzelnigg, W. *Int. J. Quantum Chem.* **1984**, *25*, 107.
(113) Sucher, J. *Int. J. Quantum Chem.* **1984**, *25*, 3.
(114) Schwarz, W. H. E.; Wallmeier, H. *Mol. Phys.* **1982**, *46*, 1045.
(115) Sun, Q.; Liu, W.; Kutzelnigg, W. *Theor. Chem. Acc.* **2011**, *129*, 423.
(116) Nakashima, H.; Nakatsuji, H. *Theor. Chem. Acc.* **2011**, *129*, 567.
(117) Kutzelnigg, W. *Phys. Scr.* **1987**, *36*, 416.
(118) Chang, C.; Pélissier, M.; Durand, P. *Phys. Scr.* **1986**, *34*, 394.
(119) Heully, J.-L.; Lindgren, I.; Lindroth, E.; Lundqvist, S.; Mårtensson-Pendrill, A.-M. *J. Phys. B* **1986**, *19*, 2799.
(120) Katsuki, S.; Huzinaga, S. *Chem. Phys. Lett.* **1988**, *147*, 597.
(121) van Lenthe, E.; Baerends, E. J.; Snijders, J. G. *J. Chem. Phys.* **1993**, *99*, 4597.
(122) van Lenthe, E.; Baerends, E. J.; Snijders, J. G. *J. Chem. Phys.* **1994**, *101*, 9783.
(123) Faas, S.; Snijders, J. G.; van Lenthe, J. H.; van Lenthe, E.; Baerends, E. J. *Chem. Phys. Lett.* **1995**, *246*, 632.
(124) Barysz, M.; Sadlej, A. J.; Snijders, J. G. *Int. J. Quantum Chem.* **1997**, *65*, 225.
(125) Faas, S.; van Lenthe, J. H.; Hennum, A. C.; Snijders, J. G. *J. Chem. Phys.* **2000**, *113*, 4052.
(126) Barysz, M. *J. Chem. Phys.* **2001**, *114*, 9315.
(127) Barysz, M.; Sadlej, A. J. *J. Chem. Phys.* **2002**, *116*, 2695.
(128) Karwoski, J.; Kobus, J. *Int. J. Quantum Chem.* **1985**, 741.
(129) Barysz, M. In *Relativistic Methods for Chemists. Challenges and Advances in Computational Physics*; Springer: London, 2010; Vol. 10, p 165.
(130) Foldy, L. L.; Wouthuysen, S. A. *Phys. Rev.* **1950**, *78*, 29.
(131) Foldy, L. L.; Wouthuysen, S. A. *Phys. Rev.* **1950**, *78*, 345.
(132) Itoh, T. *Rev. Mod. Phys.* **1965**, *37*, 159.
(133) Douglas, M.; Kroll, N. M. *Ann. Phys.* **1974**, *82*, 89.
(134) Samzow, R.; Hess, B. A. *Chem. Phys. Lett.* **1991**, *184*, 491.
(135) Blume, M.; Watson, R. E. *Proc. Roy. Soc. A* **1962**, *270*, 127.
(136) Blume, M.; Watson, R. E. *Proc. Roy. Soc. A* **1963**, *271*, 565.
(137) Wadt, W. R. *Chem. Phys. Lett.* **1982**, *89*, 245.
(138) Koseki, S.; Gordon, M. S.; Schmidt, M. W.; Matsunga, N. *J. Phys. Chem.* **1995**, *99*, 12764.
(139) Koseki, S.; Schmidt, M. W.; Gordon, M. S. *J. Phys. Chem. A* **1998**, *102*, 10430.
(140) Koseki, S.; Fedorov, D. G.; Schmidt, M. W.; Gordon, M. S. *J. Phys. Chem. A* **2001**, *105*, 8262.
(141) Hess, B. A.; Marian, C. M.; Wahlgren, U.; Gropen, O. *Chem. Phys. Lett.* **1996**, *251*, 365.
(142) Marian, C. M.; Wahlgren, U. *Chem. Phys. Lett.* **1996**, *251*, 357.
(143) Schimmelpfennig, B.; Maron, L.; Wahlgren, U.; Teichteil, C.; Faegerli, H.; Gropen, O. *Chem. Phys. Lett.* **1998**, *286*, 267.
(144) Küchle, W.; Dolg, M.; Stoll, H.; Preuss, H. *Mol. Phys.* **1991**, *74*, 1245.
(145) Dolg, M.; Stoll, H.; Preuss, H. *J. Chem. Phys.* **1989**, *90*, 1730.
(146) Dolg, M.; Stoll, H.; Savin, A.; Preuss, H. *Theor. Chim. Acta* **1989**, *75*, 173.
(147) Andrae, D.; Häussermann, U.; Dolg, M.; Stoll, H.; Preuss, H. *Theor. Chim. Acta* **1990**, *77*, 123.
(148) Bergner, A.; Dolg, M.; Küchle, W.; Stoll, H.; Preuss, H. *Mol. Phys.* **1993**, *80*, 1431.
(149) Küchle, W.; Dolg, M.; Stoll, H.; Preuss, H. *J. Chem. Phys.* **1994**, *100*, 7535.
(150) Moritz, A.; Cao, X.; Dolg, M. *Theor. Chem. Acc.* **2007**, *117*, 473.
(151) Moritz, A.; Cao, X.; Dolg, M. *Theor. Chem. Acc.* **2007**, *118*, 845.
(152) Burkatzki, M.; Filippi, C.; Dolg, M. *J. Chem. Phys.* **2007**, *126*, No. 234105.
(153) Moritz, A.; Dolg, M. *Theor. Chem. Acc.* **2008**, *121*, 297.
(154) Burkatzki, M.; Filippi, C.; Dolg, M. *J. Chem. Phys.* **2008**, *129*, No. 164115.
(155) Hülsen, M.; Weigand, A.; Dolg, M. *Theor. Chem. Acc.* **2009**, *122*, 23.
(156) Seijo, L. *J. Chem. Phys.* **1995**, *102*, 8078.
(157) Casarrubios, M.; Seijo, L. *J. Mol. Struct.* **1998**, *426*, 59.
(158) Martin, R. L.; Hay, P. J. *J. Chem. Phys.* **1981**, *75*, 4539.
(159) Schwarz, W. H. E. *Fundamentals of Relativistic Effects in Chemistry*; Springer: Berlin, 1990; p 593.
(160) Schwerdtfeger, P.; Brown, J. R.; Laerdahl, J. K.; Stoll, H. *J. Chem. Phys.* **2000**, *113*, 7110.
(161) Schwarz, W. H. E. *Phys. Scr.* **1987**, *36*, 403.
(162) Schwarz, W. H. E.; van Wezenbeek, E. M.; Baerends, E. J.; Snijders, J. G. *J. Phys. B: At. Mol. Opt. Phys.* **1989**, *22*, 1515.
(163) Burke, V.; Grant, I. P. *Proc. Phys. Soc. London* **1967**, *90*, 297.
(164) Autschbach, J.; Siekierski, S.; Seth, M.; Schwerdtfeger, P.; Schwarz, W. H. E. *J. Comput. Chem.* **2002**, *23*, 804.
(165) Desclaux, J. P. *At. Data Nucl. Data Tables* **1973**, *12*, 311.
(166) Desclaux, J. P. *Comput. Phys. Commun.* **1977**, *13*, 71.
(167) Baerends, E. J.; Schwarz, W. H. E.; Schwerdtfeger, P.; Snijders, J. G. *J. Phys. B: At. Mol. Opt. Phys.* **1990**, *23*, 3225.
(168) Dolg, M. In *Encyclopedia of Computational Chemistry*; Wiley: Chichester, U.K., 1998; p 1478.

(169) Schwerdtfeger, P.; Dolg, M.; Schwarz, W. H. E.; Bowmaker, G. A.; Boyd, P. D.W. *J. Chem. Phys.* **1989**, *91*, 1762.
(170) Pitzer, K. S. *J. Chem. Phys.* **1975**, *63*, 1032.
(171) Pitzer, K. S. *J. Chem. Soc., Chem. Commun.* **1975**, 760.
(172) Dyall, K. G. *J. Chem. Phys.* **1992**, *96*, 1210.
(173) Metz, B.; Schweizer, M.; Stoll, H.; Dolg, M.; Liu, W. *Theor. Chem. Acc.* **2000**, *104*, 22.
(174) Metz, B.; Stoll, H.; Dolg, M. *J. Chem. Phys.* **2000**, *113*, 2563.
(175) Petrov, A. N.; Mosyagin, N. S.; Titov, A. V.; Tupitsyn, I. I. *J. Phys. B: At. Mol. Opt. Phys.* **2004**, *37*, 4621.
(176) Meyer, W.; Rosmus, P. *J. Chem. Phys.* **1975**, *63*, 2356.
(177) Rosmus, P.; Meyer, W. *J. Chem. Phys.* **1976**, *65*, 492.
(178) Müller, W.; Flesch, J.; Meyer, W. *J. Chem. Phys.* **1984**, *80*, 3297.
(179) Müller, W.; Meyer, W. *J. Chem. Phys.* **1984**, *80*, 3311.
(180) Fuentealba, P. *J. Phys. B: At. Mol. Phys.* **1982**, *15*, L555.
(181) Ishikawa, Y.; Malli, G. *J. Chem. Phys.* **1981**, *75*, 5423.
(182) Dolg, M. *Theor. Chim. Acta* **1996**, *93*, 141.
(183) Wittborn, C.; Wahlgren, U. *Chem. Phys.* **1995**, *201*, 357.
(184) Rakowitz, F.; Marian, C. M.; Seijo, L.; Wahlgren, U. *J. Chem. Phys.* **1999**, *110*, 3678.
(185) Rakowitz, F.; Marian, C. M.; Seijo, L. *J. Chem. Phys.* **1999**, *111*, 10436.
(186) Tsuchiya, T.; Nakajima, T.; Hirao, K.; Seijo, L. *Chem. Phys. Lett.* **2002**, *361*, 334.
(187) Paulovič, J.; Nakajima, T.; Hirao, K.; Seijo, L. *J. Chem. Phys.* **2002**, *117*, 3597.
(188) Schwarz, W. H. E. *Theor. Chim Acta* **1968**, *11*, 307.
(189) Schwarz, W. H. E. *Theor. Chim Acta* **1968**, *11*, 377.
(190) Schwarz, W. H. E. *Acta Phys. Hung.* **1969**, *27*, 391.
(191) Chang, T. C.; Habitz, P.; Pittel, B.; Schwarz, W. H. E. *Theor. Chim. Acta* **1974**, *34*, 263.
(192) Chang, T. C.; Habitz, P.; Schwarz, W. H. E. *Theor. Chim. Acta* **1977**, *44*, 61.
(193) Fock, V.; Vesselov, M.; Petrashen, M. *Zh. Eksp. Teor. Fiz.* **1940**, *10*, 723.
(194) Kahn, L. R.; Baybutt, P.; Truhlar, D. G. *J. Chem. Phys.* **1976**, *65*, 3826.
(195) Fuentealba, P.; Preuss, H.; Stoll, H.; v. Szentpály, L. *Chem. Phys. Lett.* **1982**, *89*, 418.
(196) Christiansen, P. A. *Chem. Phys. Lett.* **1986**, *127*, 50.
(197) Foucrault, M.; Millie, P.; Daudey, J. P. *J. Chem. Phys.* **1992**, *96*, 1257.
(198) Cao, X.; Dolg, M. In *WIREs Computational Molecular Science*; Wiley: Chichester, U.K., 2011; Vol. 1, p 200.
(199) Huzinaga, S.; Cantu, A. A. *J. Chem. Phys.* **1971**, *55*, 5543.
(200) Phillips, J. C.; Kleinman, L. *Phys. Rev.* **1959**, *116*, 287.
(201) Barandiarán, Z.; Seijo, L. *J. Chem. Phys.* **1988**, *89*, 5739.
(202) Wang, Y.; Flad, H.-J.; Dolg, M. *Phys. Rev. B* **2000**, *61*, 2362.
(203) Dolg, M.; Flad, H.-J. *J. Chem. Phys.* **1996**, *100*, 6147.
(204) Peterson, K. A.; Puzzarini, C. *Theor. Chem. Acc.* **2005**, *114*, 283.
(205) Pahl, E.; Figgen, D.; Thierfelder, C.; Peterson, K. A.; Calvo, F.; Schwerdtfeger, P. *J. Chem. Phys.* **2010**, *132*, No. 114301.
(206) Flad, H.-J.; Dolg, M. *J. Chem. Phys.* **1996**, *100*, 6152.
(207) Trail, J. R.; Needs, R. J. *J. Chem. Phys.* **2005**, *122*, No. 174109.
(208) Barandiarán, Z.; Seijo, L. *Can. J. Chem.* **1992**, *70*, 409.
(209) Llusar, R.; Casarrubios, M.; Barandiarán, Z.; Seijo, L. *J. Chem. Phys.* **1996**, *105*, 5321.
(210) Sakai, Y.; Miyoshi, E.; Klobukowski, M.; Huzinaga, S. *J. Chem. Phys.* **1997**, *106*, 8084.
(211) Doll, K.; Dolg, M.; Fulde, P.; Stoll, H. *Phys. Rev. B* **1997**, *55*, 10282.
(212) Weeks, J. D.; Rice, S. A. *J. Chem. Phys.* **1968**, *49*, 2741.
(213) Cohen, M. H.; Heine, V. *Phys. Rev.* **1961**, *122*, 1821.
(214) Goddard, W. A. *Phys. Rev.* **1967**, *157*, 73.
(215) Goddard, W. A. *Phys. Rev.* **1967**, *157*, 81.
(216) Kahn, L. R.; Goddard, W. A. *J. Chem. Phys.* **1972**, *56*, 2685.
(217) Melius, C. F.; Goddard, W. A. *Phys. Rev. A* **1974**, *10*, 1528.
(218) Melius, C. F.; Olafson, B. D.; Goddard, W. A. *Chem. Phys. Lett.* **1974**, *28*, 457.
(219) Topiol, S.; Moskowitz, J. W.; Melius, C. F. *J. Chem. Phys.* **1978**, *68*, 2364.
(220) Durand, P.; Barthelat, J.-C. *Chem. Phys. Lett.* **1974**, *27*, 191.
(221) Durand, P.; Barthelat, J.-C. *Theor. Chim. Acta* **1975**, *38*, 283.
(222) Barthelat, J.-C.; Durand, P. *Gaz. Chim. Ital.* **1978**, *108*, 225.
(223) Smallwood, C. J.; Larsen, R. E.; Glover, W. J.; Schwartz, B. J. *J. Chem. Phys.* **2006**, *125*, No. 074102.
(224) Smallwood, C. J.; Meija, C. N.; Glover, W. J.; Larsen, R. E.; Schwartz, B. J. *J. Chem. Phys.* **2006**, *125*, No. 074103.
(225) Heitler, W.; London, F. *Z. Phys.* **1927**, *44*, 455.
(226) Schwerdtfeger, P.; Stoll, H.; Preuss, H. *J. Phys. B: At. Mol. Opt. Phys.* **1982**, *15*, 1061.
(227) Schwerdtfeger, P.; Stoll, H.; Preuss, H. *J. Phys. B: At. Mol. Opt. Phys.* **1982**, *15*, 3111.
(228) http://www.nist.gov/pml/data/asd.cfm (accessed Aug 26, 2011).
(229) Heine, V.; Abarenkov, I. V. *Philos. Mag.* **1964**, *9*, 451.
(230) Abarenkov, I. V.; Heine, V. *Philos. Mag.* **1965**, *12*, 529.
(231) Kahn, L. R.; Goddard, W. A. *Chem. Phys. Lett.* **1968**, *2*, 667.
(232) Kahn, L. R.; Hay, P. J.; Truhlar, D. G. *J. Chem. Phys.* **1978**, *68*, 2386.
(233) Animalu, A. O. E. *Phil. Mag.* **1966**, *12*, 53.
(234) Hafner, P.; Schwarz, W. H. E. *J.Phys. B: At. Mol. Phys.* **1978**, *11*, 217.
(235) Lee, Y. S.; Ermler, W. C.; Pitzer, K. S. *J. Chem. Phys.* **1977**, *67*, 5861.
(236) Ermler, W. C.; Lee, Y. S.; Christiansen, P. A.; Pitzer, K. S. *Chem. Phys. Lett.* **1981**, *81*, 70.
(237) Pitzer, R. M.; Winter, N. W. *J. Phys. Chem.* **1988**, *92*, 3061.
(238) Cohen, J. S.; Wadt, W. R.; Hay, P. J. *J. Chem. Phys.* **1979**, *71*, 2955.
(239) Heinemann, C.; Koch, W.; Schwarz, H. *Chem. Phys. Lett.* **1995**, *245*, 509.
(240) Barthelat, J.-C.; Durand, P.; Serafini, A. *Mol. Phys.* **1977**, *33*, 159.
(241) Kolar, M. *Comput. Phys. Commun.* **1981**, *23*, 275.
(242) McMurchie, L. E.; Davidson, E. R. *J. Comput. Phys.* **1981**, *44*, 289.
(243) Bonifacic, V.; Huzinaga, S. *J. Chem. Phys.* **1974**, *60*, 2779.
(244) Sakai, Y.; Huzinaga, S. *J. Chem. Phys.* **1982**, *76*, 2537.
(245) Sakai, Y.; Huzinaga, S. *J. Chem. Phys.* **1982**, *76*, 2552.
(246) Huzinaga, S.; McWilliams, D.; Cantu, A. A. *Adv. Quantum Chem.* **1973**, *7*, 187.
(247) Höjer, G.; Chung, J. *Int. J. Quantum Chem.* **1978**, *14*, 623.
(248) Born, M.; Heisenberg, W. *Z. Phys.* **1924**, *23*, 388.
(249) Bardsley, J. N. *Chem. Phys. Lett.* **1970**, *7*, 517.
(250) Bottcher, C.; Dalgarno, A. *Proc. Roy. Soc. London Ser. A* **1974**, *340*, 187.
(251) Jeung, G. H.; Malrieu, J. P.; Daudey, J. P. *J. Chem. Phys.* **1982**, *77*, 3571.
(252) Jeung, G. H.; Daudey, J. P.; Malrieu, J. P. *J. Phys. B: At. Mol. Opt. Phys.* **1983**, *16*, 699.
(253) Gill, P. M. W.; Crittenden, D. L.; O'Neill, D. P.; Besley, N. A. *Phys. Chem. Chem. Phys.* **2006**, *8*, 15.
(254) Igel-Mann, G.; Stoll, H.; Preuss, H. *Mol. Phys.* **1988**, *65*, 1321.
(255) Igel-Mann, G.; Stoll, H.; Preuss, H. *Mol. Phys.* **1988**, *65*, 1329.
(256) Stoll, H.; Fuentealba, P.; Dolg, M.; Flad, J.; v. Szentpály, L.; Preuss, H. *J. Chem. Phys.* **1983**, *79*, 5532.
(257) Igel, G.; Dolg, M.; Fuentealba, P.; Preuss, H.; Stoll, H.; Frey, R. *J. Chem. Phys.* **1984**, *81*, 2737.
(258) Stoll, H.; Fuentealba, P.; Schwerdtfeger, P.; Flad, J.; v. Szentpály, L.; Preuss, H. *J. Chem. Phys.* **1984**, *81*, 2732.
(259) http://www.cfour.de (accessed Aug 26, 2011).
(260) http://www.univie.ac.at/columbus (accessed Aug 26, 2011).
(261) http://www.gaussian.com (accessed Aug 26, 2011).
(262) http://www.msg.chem.iastate.edu/gamess (accessed Aug 26, 2011).
(263) Willetts, A.; Gagliardi, L.; Ioannu, A. G.; Simper, A. M.; Skylaris, C. K.; Handy, N. C. *Int. Rev. Phys. Chem.* **2000**, *19*, 327.

(264) http://www.molcas.org (accessed Aug 26, 2011).
(265) http://www.molpro.net (accessed Aug 26, 2011).
(266) http://www.nwchem-sw.org/ (accessed Aug 26, 2011).
(267) http://www.turbomole.com (accessed Aug 26, 2011).
(268) http://www.q-chem.com (accessed Aug 26, 2011).
(269) http://www.tcm.phy.cam.ac.uk/~mdt26/casino2_introduction. html (accessed Aug 26, 2011).
(270) http://pages.physics.cornell.edu/~cyrus/champ.html (accessed Aug 26, 2011).
(271) http://www.cchem.berkeley.edu/walgrp/ (accessed Aug 26, 2011).
(272) http://www.crystal.unito.it (accessed Aug 26, 2011).
(273) Topp, W. C.; Hopfield, J. J. *Phys. Rev. B* **1973**, *7*, 1295.
(274) Preuss, H. *Z. Naturf. A* **1955**, *10*, 365.
(275) Flad, J.; Stoll, H.; Preuss, H. *J. Chem. Phys.* **1979**, *71*, 3042.
(276) Preuss, H.; Stoll, H.; Wedig, U.; Krüger, T. *Int. J. Quantum Chem.* **1981**, *19*, 113.
(277) Schwerdtfeger, P.; v. Szentpály, L.; Vogel, K.; Silberbach, H.; Stoll, H.; Preuss, H. *J. Chem. Phys.* **1986**, *84*, 1606.
(278) Schwerdtfeger, P.; v. Szentpály, L.; Stoll, H.; Preuss, H. *J. Chem. Phys.* **1987**, *87*, 510.
(279) Schwerdtfeger, P. *Phys. Scr.* **1987**, *36*, 453.
(280) Schwerdtfeger, P.; Fischer, T.; Dolg, M.; Igel-Mann, G.; Nicklass, A.; Stoll, H.; Haaland, A. *J. Chem. Phys.* **1995**, *102*, 2050.
(281) Leininger, T.; Nicklass, A.; Küchle, W.; Stoll, H.; Dolg, M.; Bergner, A. *Chem. Phys. Lett.* **1996**, *255*, 274.
(282) Leininger, T.; Nicklass, A.; Stoll, H.; Dolg, M.; Schwerdtfeger, P. *J. Chem. Phys.* **1996**, *105*, 1052.
(283) Dolg, M.; Wedig, U.; Stoll, H.; Preuss, H. *J. Chem. Phys.* **1987**, *86*, 866.
(284) Dolg, M.; Stoll, H.; Preuss, H.; Pitzer, R. M. *J. Phys. Chem. A* **1993**, *97*, 5852.
(285) Dolg, M. *Theor. Chem. Acc.* **2005**, *114*, 297.
(286) Stevens, W. J.; Krauss, M.; Basch, H.; Jasien, P. J. *Can. J. Chem.* **1992**, *70*, 612.
(287) Hurley, M. M.; Pacios, L. F.; Christiansen, P. A.; Ross, R. B.; Ermler, W. C. *J. Chem. Phys.* **1986**, *84*, 6840.
(288) Dolg, M.; Stoll, H.; Preuss, H. *Theor. Chim. Acta* **1993**, *85*, 441.
(289) Häussermann, U.; Dolg, M.; Stoll, H.; Preuss, H.; Schwerdtfeger, P.; Pitzer, R. M. *Mol. Phys.* **1993**, *78*, 1211.
(290) Seth, M.; Schwerdtfeger, P.; Dolg, M. *J. Chem. Phys.* **1997**, *106*, 3623.
(291) Figgen, D.; Rauhut, G.; Dolg, M.; Stoll, H. *J. Chem. Phys.* **2005**, *311*, 227.
(292) Lim, I. S.; Schwerdtfeger, P.; Metz, B.; Stoll, H. *J. Chem. Phys.* **2005**, *122*, No. 104103.
(293) Lim, I. S.; Stoll, H.; Schwerdtfeger, P. *J. Chem. Phys.* **2006**, *124*, No. 034107.
(294) Peterson, K. A.; Figgen, D.; Dolg, M.; Stoll, H. *J. Chem. Phys.* **2007**, *126*, No. 124101.
(295) Figgen, D.; Peterson, K. A.; Dolg, M.; Stoll, H. *J. Chem. Phys.* **2009**, *130*, No. 164108.
(296) http://bse.pnl.gov/bse/portal.
(297) http://www.tc.uni-koeln.de/PP/index.en.html.
(298) Nicklass, A.; Dolg, M.; Stoll, H.; Preuss, H. *J. Chem. Phys.* **1995**, *102*, 8942.
(299) Kaupp, M.; Schleyer, P. V.; Stoll, H.; Preuss, H. *J. Chem. Phys.* **1991**, *94*, 1360.
(300) Martin, J. M.; Sundermann, A. *J. Chem. Phys.* **2001**, *114*, 3408.
(301) Eichkorn, K.; Weigend, F.; Treutler, O.; Ahlrichs, R. *Theor. Chem. Acc.* **1997**, *97*, 119.
(302) Cao, X.; Dolg, M. *J. Chem. Phys.* **2001**, *115*, 7348.
(303) Cao, X.; Dolg, M. *J. Molec. Struct. (THEOCHEM)* **2002**, *581*, 139.
(304) Cao, X.; Dolg, M.; Stoll, H. *J. Chem. Phys.* **2003**, *118*, 487.
(305) Cao, X.; Dolg, M. *J. Molec. Struct. (THEOCHEM)* **2004**, *673*, 203.
(306) Peterson, K. A. *J. Chem. Phys.* **2003**, *119*, No. 11099.
(307) Peterson, K. A.; Figgen, D.; Goll, E.; Stoll, H.; Dolg, M. *J. Chem. Phys.* **2003**, *119*, No. 11113.
(308) Weigend, F.; Ahlrichs, R. *Phys. Chem. Chem. Phys.* **2005**, *7*, 3297.
(309) Armbruster, M. K.; Klopper, W.; Weigend, F. *Phys. Chem. Chem. Phys.* **2006**, *8*, 4862.
(310) Weigend, F.; Baldes, A. *Phys. Chem. Chem. Phys.* **2010**, *133*, No. 174102.
(311) Dolg, M.; Stoll, H.; Seth, M.; Schwerdtfeger, P. *Chem. Phys. Lett.* **2001**, *345*, 490.
(312) http://bases.turbo-forum.com/TBL/tbl.html (accessed Aug 26, 2011).
(313) Peterson, K. A.; Yousaf, K. E. *J. Chem. Phys.* **2010**, *133* No. 174116.
(314) http://tyr0.chem.wsu.edu/~kipeters/basis.html (accessed Aug 26, 2011).
(315) Werner, H.-J.; Knizia, G.; Manby, F. R. *Mol. Phys.* **2011**, *109*, 407.
(316) Armbruster, M. K.; Schimmelpfennig, B.; Plaschke, M.; Rothe, J.; Denecke, M. A.; Klenze, R. *J. Electron Spectrosc. Relat. Phenom.* **2009**, *169*, 51.
(317) Dolg, M.; Cao, X. In *Computational Inorganic and Bioinorganic Chemistry*; Wiley: Chichester, U.K., 2009; p 503.
(318) Field, R. W. *Ber. Bunsenges. Phys. Chem.* **1982**, *86*, 771.
(319) Dolg, M.; Stoll, H.; Preuss, H. *J. Mol. Struct. (THEOCHEM)* **1991**, *231*, 243.
(320) Dolg, M.; Stoll, H. *Theor. Chim. Acta* **1989**, *75*, 369.
(321) Dolg, M.; Stoll, H.; Preuss, H. *Chem. Phys.* **1990**, *148*, 219.
(322) Dolg, M.; Stoll, H.; Flad, H.-J.; Preuss, H. *J. Chem. Phys.* **1992**, *97*, 1162.
(323) Wang, Y.; Dolg, M. *Theor. Chem. Acc.* **1998**, *100*, 124.
(324) Yang, J.; Dolg, M. *Theor. Chem. Acc.* **2005**, *113*, 212.
(325) Christiansen, P. A.; Lee, Y. S.; Pitzer, K. S. *J. Chem. Phys.* **1979**, *71*, 4445.
(326) Hay, P. J.; Wadt, W. R. *J. Chem. Phys.* **1985**, *82*, 270.
(327) Hay, P. J.; Wadt, W. R.; Kahn, L. R. *J. Chem. Phys.* **1978**, *68*, 3059.
(328) Hamann, D. R.; Schlüter, M.; Chiang, C. *Phys. Rev. Lett.* **1979**, *43*, 1494.
(329) Kerker, G. P. *J. Phys. C* **1980**, *13*, L189.
(330) Troullier, N.; Martins, J. L. *Phys. Rev. B* **1991**, *43*, 1993.
(331) Titov, A. V.; Mosyagin, N. S. *Int. J. Quantum Chem.* **1999**, *71*, 359.
(332) Rappe, A. K.; Smedley, T. A.; Goddard, W. A. *J. Chem. Phys.* **1981**, *85*, 1662.
(333) Pacios, L. F.; Christiansen, P. A. *J. Chem. Phys.* **1985**, *82*, 2664.
(334) LaJohn, L. A.; Christiansen, P. A.; Ross, R. B.; Atashroo, T.; Ermler, W. C. *J. Chem. Phys.* **1987**, *87*, 2812.
(335) Ross, R. B.; Powers, J. M.; Atashroo, T.; Ermler, W. C.; LaJohn, L. A.; Christiansen, P. A. *J. Chem. Phys.* **1990**, *93*, 6654.
(336) Ross, R. B.; Powers, J. M.; Atashroo, T.; Ermler, W. C.; LaJohn, L. A.; Christiansen, P. A. *J. Chem. Phys.* **1994**, *101*, 10198.
(337) Ross, R. B.; Gayen, S.; Ermler, W. C. *J. Chem. Phys.* **1994**, *100*, 8145.
(338) Ermler, W. C.; Ross, R. B.; A.Christiansen, P. *Int. J. Quantum Chem.* **1991**, *40*, 829.
(339) Wildman, S. A.; DiLabio, G. A.; Christiansen, P. A. *J. Chem. Phys.* **1997**, *107*, 9975.
(340) Nash, C. S.; Bursten, B. E.; Ermler, W. C. *J. Chem. Phys.* **1997**, *106*, 5133.
(341) Nash, C. S.; Bursten, B. E.; Ermler, W. C. *J. Chem. Phys.* **1999**, *111*, 2347.
(342) http://www.clarkson.edu/~pac/reps.html (accessed Aug 26, 2011).
(343) Wallace, N. M.; Blaudeau, J.-P.; Pitzer, R. M. *Int. J. Quantum Chem.* **1991**, *40*, 789.
(344) Pacios, L. F.; Gomez, P. C. *Int. J. Quantum Chem.* **1994**, *49*, 817.
(345) Blaudeau, J.-P.; Curtiss, L. A. *Int. J. Quantum Chem.* **1997**, *61*, 943.

(346) Chang, A. H. H.; Pitzer, R. M. *J. Am. Chem. Soc.* **1989**, *111*, 2500.
(347) Pacios, L. F. *J. Chem. Phys.* **1990**, *169*, 281.
(348) Walker, E. C.; Christiansen, P. A.; Pacios, L. F. *Mol. Phys.* **1988**, *63*, 139.
(349) Pacios, L. F.; Olcina, V. B. *Int. J. Quantum Chem.* **1991**, *39*, 197.
(350) Zhang, Z.; Pitzer, R. M. *J. Phys. Chem. A* **1999**, *103*, 6880.
(351) Balasubramanian, K. *Chem. Rev.* **1989**, *89*, 1801.
(352) Balasubramanian, K. In *Handbook on the Physics and Chemistry of Rare Earths, Vol.* 18; Elsevier: Amsterdam, 1993; p 30.
(353) Balasubramanian, K. *J. Phys. Chem.* **1989**, *93*, 6585.
(354) Hay, P. J.; Wadt, W. R. *J. Chem. Phys.* **1985**, *82*, 299.
(355) Wadt, W. R.; Hay, P. J. *J. Chem. Phys.* **1985**, *82*, 284.
(356) Hay, P. J. *J. Chem. Phys.* **1983**, *79*, 5469.
(357) Hay, P. J.; Martin, R. L. *J. Chem. Phys.* **1998**, *109*, 3875.
(358) Ehlers, A. W.; Böhme, M.; Dapprich, S.; Gobbi, A.; Höllwarth, A.; Jonas, V.; Köhler, K. F.; Stegmann, R.; Veldkamp, A.; Frenking, G. *Chem. Phys. Lett.* **1993**, *208*, 111.
(359) Höllwarth, A.; Böhme, M.; Dapprich, S.; Ehlers, A. W.; Gobbi, A.; Jonas, V.; Köhler, K. F.; Stegmann, R.; Veldkamp, A.; Frenking, G. *Chem. Phys. Lett.* **1993**, *208*, 237.
(360) Check, C. E.; Faust, T. O.; Bailey, J. M.; Wright, B. J.; Gilbert, T. M.; Sunderlin, L. S. *J. Phys. Chem. A* **2001**, *105*, 8111.
(361) Hu, W.-P.; Huang, C.-H. *J. Am. Chem. Soc.* **1999**, *123*, 2340.
(362) Roy, L. E.; Hay, P. J.; Martin, R. L. *J. Chem. Theor. Comput.* **2008**, *4*, 1029.
(363) Teichteil, C.; Malrieu, J. P.; Barthelat, J.-C. *Mol. Phys.* **1977**, *33*, 181.
(364) Serafini, A.; Barthelat, J.-C.; Durand, P. *Mol. Phys.* **1978**, *36*, 1341.
(365) Jeung, G. H.; Barthelat, J.-C.; Pélissier, M. *Chem. Phys. Lett.* **1982**, *91*, 81.
(366) Bouteiller, Y.; Mijoule, C.; Nziam, M.; Barthelat, J.-C.; Daudey, J. P.; Pélissier, M.; Silvi, B. *Mol. Phys.* **1988**, *65*, 295.
(367) Hannachi, Y.; Barthelat, J.-C.; Jolly, L.-H.; Silvi, B.; Bouteiller, Y. *Int. J. Quantum Chem.* **1992**, *42*, 509.
(368) Pélissier, M.; Daudey, J. P.; Malrieu, J. P.; Jeung, G. H. In *Quantum Chemistry: The Challenge of Transition Metals and Coordination Chemistry*; Reidel: Dordrecht, the Netherlands, 1986; p 37.
(369) Cabrol, O.; Girard, B.; Spiegelmann, F.; Teichteil, C. *J. Chem. Phys.* **1996**, *105*, 6426.
(370) Tadjeddine, M.; Flament, J. P.; Teichteil, C. *Chem. Phys.* **1987**, *118*, 45.
(371) Teichteil, C.; Pélissier, M.; Spiegelmann, F. *Chem. Phys.* **1983**, *81*, 273.
(372) Teichteil, C.; Pélissier, M. *Chem. Phys.* **1994**, *180*, 1.
(373) Maron, L.; Teichteil, C. *Chem. Phys.* **1998**, *237*, 105.
(374) Stevens, W. J.; Basch, H.; Krauss, M. *J. Chem. Phys.* **1984**, *81*, 6026.
(375) Cundari, T. R.; Stevens, W. J. *J. Chem. Phys.* **1993**, *98*, 5555.
(376) Greeff, C. W.; W. A. Lester, J. *J. Chem. Phys.* **1998**, *109*, 1607.
(377) Ovcharenko, I.; Aspuru-Guzik, A.; W. A. Lester, J. *J. Chem. Phys.* **2001**, *114*, 7790.
(378) Zurita, S.; Rubio, J.; Illas, F.; Barthelat, J.-C. *J. Chem. Phys.* **1996**, *104*, 8500.
(379) Sellers, H.; Ove, R. *Chem. Phys. Lett.* **1990**, *170*, 523.
(380) Krauss, M.; Stevens, W. J. *J. Comput. Chem.* **1983**, *4*, 127.
(381) Krauss, M.; Stevens, W. J. *Mol. Phys.* **2003**, *101*, 125.
(382) Stevens, W. J.; Krauss, M. *Chem. Phys. Lett.* **1982**, *86*, 320.
(383) Mosyagin, N. S.; Titov, A. V.; Latajka, Z. *Int. J. Quantum Chem.* **1997**, *63*, 1107.
(384) Titov, A. V.; Mosyagin, N. S. *Russ. J. Phys. Chem.* **2000**, *74*, S376.
(385) Titov, A. V.; Mosyagin, N. S.; Isaev, T. A.; Petrov, A. N. *Phys. At. Nucl.* **2003**, *66*, 1152.
(386) Andzelm, J.; Radzio, E.; Barandiarán, Z.; Seijo, L. *J. Chem. Phys.* **1985**, *83*, 4565.
(387) http://www.tcm.phy.cam.ac.uk/~mdt26/casino2_pseudopotentials.html (accessed Aug 26, 2011).
(388) Titov, A. V.; Mosyagin, N. S.; Petrov, A. N.; Isaev, T. A. *Int. J. Quantum Chem.* **2005**, *104*, 223.
(389) Evarestov, R. A.; Losev, M. V.; Panin, A. I.; Mosyagin, N. S.; Petrov, A. N. *Phys. Stat. Sol. B* **2008**, *245*, 114.
(390) Petrov, A. N.; Mosyagin, N. S.; Titov, A. V.; Zaitsevskii, A. V.; Rykova, E. A. *Phys. At. Nucl.* **2009**, *72*, 396.
(391) Zaitsevskii, A. V.; Wüllen, C. V.; Titov, A. V. *Russ. Chem. Rev.* **2009**, *78*, 1173.
(392) Zaitsevskii, A.; Wüllen, C. V.; Rykova, E. A.; Titov, A. V. *Phys. Chem. Chem. Phys.* **2010**, *12*, 4152.
(393) Dolg, M.; Cao, X. *J. Phys. Chem. A* **2009**, *113*, 12573.
(394) Walch, S. P.; Goddard, W. A. *J. Am. Chem. Soc.* **1976**, *98*, 7908.
(395) Walch, S. P.; Goddard, W. A. *J. Am. Chem. Soc.* **1978**, *100*, 1338.
(396) Upton, T. H.; Goddard, W. A. *J. Am. Chem. Soc.* **1978**, *100*, 5659.
(397) Basch, H.; Osman, R. *Chem. Phys. Lett.* **1982**, *93*, 51.
(398) Mahé, L.; Barthelat, J.-C. *J. Mol. Struct. (THEOCHEM)* **1997**, *401*, 93.
(399) Mahé, L.; Boughdiri, S. F.; Barthelat, J.-C. *J. Phys. Chem. A* **1997**, *101*, 4224.
(400) Ceperley, D. M.; Alder, B. J. *Phys. Rev. Lett.* **1980**, *45*, 566.
(401) *Monte Carlo Methods in Ab Initio Quantum Chemistry*; Hammond, B. L., Lester, Jr.,W. A., Reynolds, P. J., Eds.; World Scientific: Singapore, 1994.
(402) Hammond, L.; Reynolds, P. J.; W. A. Lester, J. *J. Chem. Phys.* **1987**, *87*, 1130.
(403) Hurley, M. M.; Christiansen, P. A. *J. Chem. Phys.* **1987**, *86*, 1069.
(404) Christiansen, P. A. *J. Chem. Phys.* **1991**, *95*, 361.
(405) Lao, M. Z.; Christiansen, P. A. *J. Chem. Phys.* **1992**, *96*, 2161.
(406) Mitas, L. *Phys. Rev. A* **1994**, *49*, 4411.
(407) Flad, H.-J.; Dolg, M. *J. Chem. Phys.* **1997**, *107*, 7951.
(408) Fahy, S.; Wang, X. W.; Louie, S. G. *Phys. Rev. Lett.* **1988**, *61*, 1631.
(409) Fahy, S.; Wang, X. W.; Louie, S. G. *Phys. Rev. B* **1990**, *42*, 3503.
(410) Fahy, S.; Wang, X. W.; Louie, S. G. *Phys. Rev. B* **1991**, *43*, 9299.
(411) Trail, J. R.; Needs, R. J. *J. Chem. Phys.* **2005**, *122*, No. 014112.
(412) http://www.tcm.phy.cam.ac.uk/~mdt26/pseudo_lib/v/pseudo.html.
(413) http://www.tc.uni-koeln.de/data/psdb/intro.html (accessed Aug 26, 2011).
(414) Russo, T. V.; Martin, R. L.; Hay, P. J. *J. Phys. Chem.* **1995**, *99*, 17085.
(415) Jong, W. A. D.; Harrison, R. J.; Nichols, J. A.; Dixon, D. A. *Theor. Chem. Acc.* **2001**, *107*, 22.
(416) van Wüllen, C. *Int. J. Quantum Chem.* **1996**, *58*, 147.
(417) Mitin, A. V.; van Wüllen, C. *J. Chem. Phys.* **2006**, *124*, No. 064305.
(418) Schreckenbach, G.; Hay, P. J.; Martin, R. L. *J. Comput. Chem.* **1999**, *20*, 70.
(419) Batista, E. R.; Martin, R. L.; Hay, P. J.; Peralta, J. E.; Scuseria, G. E. *J. Chem. Phys.* **2004**, *121*, 2144.
(420) Louie, S. G.; Froyen, S.; Cohen, M. L. *Phys. Rev. B* **1982**, *26*, 1738.
(421) Delley, B. *Phys. Rev. B* **2002**, *66*, No. 155125.
(422) Teter, M. *Phys. Rev. B* **1993**, *48*, 5031.
(423) Bachelet, G.; Schlüter, M. *Phys. Rev. B* **1982**, *25*, 2103.
(424) Bachelet, G.; Hamann, D. R.; Schlüter, M. *Phys. Rev. B* **1982**, *26*, 4199.
(425) Kleinman, L. *Phys. Rev.* **1980**, *21*, 2630.
(426) Vanderbilt, D. *Phys. Rev. B* **1990**, *41*, 7892.
(427) Kleinman, L.; Bylander, D. M. *Phys. Rev. Lett.* **1982**, *48*, 1425.
(428) Blöchl, P. E. *Phys. Rev. B* **1990**, *41*, 5414.
(429) Pélissier, M.; Komiha, N.; Daudey, J. P. *J. Comput. Chem.* **1988**, *9*, 298.
(430) Fuchs, M.; Scheffler, M. *Comput. Phys. Commun.* **1999**, *119*, 67.
(431) Hartwigsen, C.; Goedecker, S.; Hutter, J. *Phys. Rev. B* **1998**, *58*, 3641.

(432) Goedecker, S.; Teter, M.; Hutter, J. *Phys. Rev. B* **1996**, *54*, 1703.
(433) Krack, M. *Theor. Chem. Acc.* **2005**, *144*, 145.
(434) http://www.physics.rutgers.edu/~dhv/uspp/ (accessed Aug 26, 2011).
(435) Datta, S. N.; Ewig, C. S.; van Wazer, J. R. *Chem. Phys. Lett.* **1978**, *57*, 83.
(436) Pyper, N. C. *Mol. Phys.* **1980**, *39*, 1327.
(437) Pyper, N. C. *Mol. Phys.* **1980**, *41*, 949.
(438) Pyper, N. C.; Marketos, P. *Mol. Phys.* **1981**, *42*, 1073.
(439) Klobukowski, M.; Huzinaga, S.; Sakai, Y. *Computional Chemistry: Reviews of Current Trends*, Vol. 3; World Scientific: Singapore, 1999; p 49.
(440) Huzinaga, S.; Seijo, L.; Barandiarán, Z.; Klobukowski, M. *J. Chem. Phys.* **1987**, *86*, 2132.
(441) http://www.uam.es/departamentos/ciencias/quimica/aimp/Data/AIMPLibs.html. (accessed Aug 26, 2011).
(442) Katsuki, S.; Huzinaga, S. *Chem. Phys. Lett.* **1988**, *152*, 203.
(443) Katsuki, S. *Chem. Phys. Lett.* **1990**, *165*, 535.
(444) Barandiarán, Z.; Seijo, L.; Huzinaga, S. *J. Chem. Phys.* **1990**, *93*, 5843.
(445) Pitzer, R. M.; Winter, N. W. *Int. J. Quan. Chem.* **1991**, *40*, 773.
(446) Barandiarán, Z.; Seijo, L. *J. Chem. Phys.* **1994**, *101*, 4049.
(447) Casarrubios, M.; Seijo, L. *J. Chem. Phys.* **1999**, *110*, 784.
(448) Seijo, L.; Barandiarán, Z.; Harguindey, E. *J. Chem. Phys.* **2001**, *114*, 118.
(449) Casarrubios, M.; Seijo, L. *Chem. Phys. Lett.* **1995**, *236*, 510.
(450) Seijo, L.; Barandiarán, Z.; Huzinaga, S. *J. Chem. Phys.* **1989**, *91*, 7011.
(451) Klobukowski, M. *J. Comput. Chem.* **1983**, *4*, 350.
(452) Sakai, Y.; Miyoshi, E.; Klobukowski, M.; Huzinaga, S. *J. Comput. Chem.* **1987**, *8*, 226.
(453) Sakai, Y.; Miyoshi, E.; Klobukowski, M.; Huzinaga, S. *J. Comput. Chem.* **1987**, *8*, 256.
(454) Osanai, Y.; Mon, M. S.; Noro, T.; Mori, H.; Nakashima, H.; Klobukowski, M.; Miyoshi, E. *Chem. Phys. Lett.* **2008**, *452*, 210.
(455) Osanai, Y.; Soejima, E.; Noro, T.; Mori, H.; Mon, M. S.; Klobukowski, M.; Miyoshi, E. *Chem. Phys. Lett.* **2008**, *463*, 230.
(456) Mori, H.; Ueno-Noto, K.; Osanai, Y.; Noro, T.; Fujiwara, T.; Klobukowski, M.; Miyoshi, E. *Chem. Phys. Lett.* **2009**, *476*, 317.
(457) Mane, J. Y.; Klobukowski, M. *Theor. Chem. Acc.* **2004**, *112*, 33.
(458) Miyoshi, E.; Sakai, Y.; Tanaka, K.; Masamura, M. *J. Mol. Struct. (THEOCHEM)* **1998**, *451*, 73.
(459) Miyoshi, E.; Mori, H.; Hirayama, R.; Osanai, Y.; Noro, T.; Honda, H. *J. Chem. Phys.* **2005**, *122*, No. 074104.
(460) Sakai, Y.; Miyoshi, E.; Tatewaki, H. *J. Mol. Struct. (THEOCHEM)* **1998**, *451*, 143.
(461) Zeng, T.; Fedorov, D. G.; Klobukowski, M. *J. Chem. Phys.* **2010**, *133*, No. 114107.
(462) Zeng, T.; Klobukowski, M. *J. Chem. Phys.* **2009**, *130*, No. 204107.
(463) Zeng, T.; Fedorov, D. G.; Klobukowski, M. *J. Chem. Phys.* **2010**, *132*, No. 074102.
(464) Fedorov, D. G.; Klobukowski, M. *Chem. Phys. Lett.* **2002**, *360*, 223.
(465) Song, C.; Gao, T.; Han, H.; Wan, M.; Yu, Y. *J. Mol. Struct. (THEOCHEM)* **2008**, *870*, 65.
(466) Zeng, T.; Fedorov, D. G.; Klobukowski, M. *J. Chem. Phys.* **2009**, *131*, No. 124109.
(467) Katsuki, S.; Taketa, H. *Int. J. Quantum Chem.* **1980**, *18*, 25.
(468) Katsuki, S.; Inokuchi, M. *J. Phys. Soc. Jpn.* **1982**, *51*, 3652.
(469) Andzelm, J.; Radzio, E.; Salahub, D. R. *J. Chem. Phys.* **1985**, *83*, 4573.
(470) Paulovič, J.; Nakajima, T.; Hirao, K.; Lindh, R.; Malmqvist, P. A. *J. Chem. Phys.* **2003**, *119*, 798.
(471) Motegi, K.; Nakajima, T.; Hirao, K.; Seijo, L. *J. Chem. Phys.* **2001**, *114*, 6000.
(472) Davidson, E.; Feller, D. *Chem. Rev.* **1986**, *86*, 681.
(473) Dunning, T. H.; Peterson, K. A.;Woon, D. E. In *Encyclopedia of Computational Chemistry*; Wiley: Chichester, U.K., 1998; p 88.
(474) Peterson, K. In *Computational Inorganic and Bioinorganic Chemistry*; Wiley: Chichester, U.K., 2009; p 187.
(475) Christiansen, P. A. *J. Chem. Phys.* **2000**, *112*, 10070.
(476) Blaudeau, J.-P.; Brozell, S. R.; Matsika, S.; Zhang, Z.; Pitzer, R. M. *Int. J. Quantum Chem.* **2000**, *77*, 516.
(477) McMurchie, L. E.; Davidson, E. R. *J. Comput. Phys.* **1978**, *26*, 218.
(478) Skylaris, C.-K.; Gagliardi, L.; Handy, N. C.; Ioannou, A. G.; Spencer, S.; Willetts, A.; Simper, A. M. *Chem. Phys. Lett.* **1998**, *296*, 445.
(479) van Wüllen, C. *J. Comput. Chem.* **2006**, *27*, 135.
(480) Kitaura, K.; Obara, S.; Morokuma, K. *Chem. Phys. Lett.* **1981**, *77*, 452.
(481) Cui, Q.; Musaev, D. G.; Svensson, M.; Morokuma, K. *J. Phys. Chem.* **1996**, *100*, 10936.
(482) van Wüllen, C.; Langermann, N. *J. Chem. Phys.* **2007**, *126*, No. 114106.
(483) Schwerdtfeger, P.; Silberbach, H. *Phys. Rev. A* **1988**, *37*, 2834.
(484) Schwerdtfeger, P.; Silberbach, H. *Phys. Rev. A* **1990**, *42*, 665.
(485) Smit, M. J. *Int. J. Quan. Chem.* **1999**, *73*, 403.
(486) Car, R.; Parrinello, M. *Phys. Rev. Lett.* **1985**, *55*, 2471.
(487) Jensen, J. O.; Carrirei, A. H.; Vlahacos, C. P.; Zeroka, D.; Hameka, H. F.; Merrow, C. N. *J. Comput. Chem.* **1993**, *14*, 986.
(488) Esser, M.; Butscher, W.; Schwarz, W. H. E. *Chem. Phys. Lett.* **1981**, *77*, 359.
(489) Esser, M. *Int. J. Quantum Chem.* **1984**, *26*, 313.
(490) Esser, M. *Chem. Phys. Lett.* **1984**, *111*, 58.
(491) Lee, S. Y.; Lee, Y. S. *J. Comput. Chem.* **1992**, *13*, 595.
(492) Kim, Y. S.; Lee, S. Y.; Oh, W. S.; Park, B. H.; Han, Y. K.; Park, S. J.; Lee, Y. S. *Int. J. Quantum Chem.* **1998**, *66*, 91.
(493) Lee, S. Y.; Lee, Y. S. *Chem. Phys. Lett.* **1991**, *187*, 302.
(494) Kim, M. C.; Lee, S. Y.; Lee, Y. S. *Chem. Phys. Lett.* **1996**, *253*, 216.
(495) Lee, H. S.; Han, Y. K.; Kim, M. C.; Bae, C.; Lee, Y. S. *Chem. Phys. Lett.* **1998**, *293*, 97.
(496) Kim, Y. S.; Lee, Y. S. *J. Chem. Phys.* **2003**, *119*, 12169.
(497) Kim, Y. S.; Lee, Y. S. *J. Chem. Phys.* **2004**, *120*, 5797.
(498) van Wüllen, C. *Z. Phys. Chem.* **2010**, *224*, 413.
(499) Armbruster, M. K.; Weigend, F.; van Wüllen, C.; Klopper, W. *Phys. Chem. Chem. Phys.* **2008**, *10*, 1748.
(500) Bischoff, F. A.; Klopper, W. *J. Chem. Phys.* **2010**, *132* No. 094108.
(501) Christiansen, P. A.; Balasubramanian, K.; Pitzer, K. S. *J. Chem. Phys.* **1982**, *76*, 5087.
(502) Teichteil, C.; Spiegelmann, F. *Chem. Phys.* **1983**, *81*, 283.
(503) Vallet, V.; Maron, L.; Teichteil, C.; Flament, J.-P. *J. Chem. Phys.* **2000**, *113*, 1391.
(504) Tilson, J. L.; Ermler, W. C.; Pitzer, R. M. *Comput. Phys. Commun.* **2000**, *128*, 128.
(505) Yabushita, S.; Zhang, Z.; Pitzer, R. M. *J. Phys. Chem. A* **1999**, *103*, 5791.
(506) Sjøvoll, M.; Gropen, O.; Olsen, J. *Theor. Chem. Acc.* **1997**, *97*, 301.
(507) Weigand, A.; Cao, X.; Vallet, V.; Flament, J.-P.; Dolg, M. *J. Phys. Chem. A* **2009**, *113*, 11509.
(508) Bader, R. F.W. *Atoms in Molecules—A Quantum Theory*; Oxford University Press: Oxford, U.K., 1990.
(509) Sierraalta, A.; Ruette, F. *J. Comput. Chem.* **1994**, *15*, 313.
(510) Vyboishchikov, S. F.; Sierraalta, A.; Frenking, G. *J. Comput. Chem.* **1996**, *18*, 416.
(511) Schwerdtfeger, P.; Assadollahzadeh, B.; Rohrmann, U.; Schäfer, R.; Cheeseman, J. R. *J. Chem. Phys.* **2011**, *134*, No. 204102.
(512) Buckingham, A. D.; Diesch, R. L.; Dunmur, D. A. *J. Am. Chem. Soc.* **1968**, *90*, 3104.
(513) Norman, P.; Schimmelpfennig, B.; Ruud, K.; Jensen, H. J. A.; Ågren, H. *J. Chem. Phys.* **2002**, *116*, 6914.
(514) Krause, D.; Klobukowski, M. *Can. J. Chem.* **1996**, *74*, 1248.

(515) Daasch, W. R.; McMurchie, L. E.; Davidson, E. R. *Chem. Phys. Lett.* **1981**, *84*, 9.
(516) Hetenyi, B.; Angelis, F. D.; Giannozzi, P.; Car, R. *J. Chem. Phys.* **2001**, *115*, 5791.
(517) Tupitsyn, I. I.; Sharapov, A. B.; Kuznetsov, V. G. *Opt. Spect.* **2008**, *105*, 52.
(518) Kaupp, M.; Malkin, V. G.; Malkina, O. L.; Salahub, D. R. *Chem. Phys. Lett.* **1995**, *235*, 382.
(519) Kaupp, M.; Malkin, V. G.; Malkina, O. L.; Salahub, D. R. *J. Am. Chem. Soc.* **1995**, *117*, 1851.
(520) Kaupp, M.; Malkin, V. G.; Malkina, O. L.; Salahub, D. R. *J. Am. Chem. Soc.* **1995**, *117*, 8492.
(521) Kaupp, M. *J. Chem. Soc., Chem. Commun.* **1996**, *117*, 1141.
(522) Kaupp, M. *Chem. Ber.* **1996**, *129*, 535.
(523) Straka, M.; Kaupp, M. *Chem. Phys.* **2005**, *311*, 45.
(524) Vaara, J.; Malkina, O. L.; Stoll, H.; Malkin, V. G.; Kaupp, M. *J. Chem. Phys.* **2001**, *114*, 61.
(525) Schreckenbach, G. *Int. J. Quantum Chem.* **2005**, *101*, 372.
(526) Schreckenbach, G.; Ziegler, T. *Theor. Chem. Acc.* **1998**, *99*, 71.
(527) Malkina, O. L.; Vaara, J.; Schimmelpfennig, B.; Munzarová, M.; Malkin, V. G.; Kaupp, M. *J. Am. Chem. Soc.* **2000**, *122*, 9206.
(528) Arbuznikov, A. V.; Vaara, J.; Kaupp, M. *J. Chem. Phys.* **2004**, *120*, 2127.
(529) Remenyi, C.; Reviakine, R.; Arbuznikov, A. V.; Vaara, J.; Kaupp, M. *J. Phys. Chem. A* **2004**, *108*, 5026.
(530) Pittel, B.; Schwarz, W. H. E. *Chem. Phys. Lett.* **1977**, *46*, 121.
(531) Dolg, M. *J. Chem. Phys.* **1996**, *104*, 4061.
(532) Dolg, M. *Chem. Phys. Lett.* **1996**, *250*, 75.
(533) Klobukowski, M. *Chem. Phys. Lett.* **1990**, *172*, 361.
(534) Seijo, L.; Barandiarán, Z. *Chem. Phys. Lett.* **1992**, *192*, 217.
(535) Rohlfing, C. M.; Hay, P. J.; Martin, R. L. *J. Chem. Phys.* **1986**, *85*, 1447.
(536) Frenking, G.; Fröhlich, N. *Chem. Rev.* **2000**, *100*, 717.
(537) Dolg, M. *Mol. Phys.* **1996**, *88*, 1645.
(538) Visscher, L.; Styszýnski, J.; Nieuwpoort, W. C. *J. Chem. Phys.* **1996**, *105*, 1987.
(539) Almlöf, J.; Taylor, P. *J. Chem. Phys.* **1987**, *86*, 4070.
(540) Dunning, T. H. *J. Chem. Phys.* **1989**, *90*, 1007.
(541) Visscher, L.; Dyall, K. G. *J. Chem. Phys.* **1996**, *104*, 9040.
(542) Pyykkö, P. *Inorg. Chim. Acta* **1987**, *139*, 243.
(543) Pepper, M.; Bursten, B. *Chem. Rev.* **1991**, *91*, 719.
(544) Kaltsoyannis, N. *Chem. Soc. Rev.* **2003**, *32*, 9.
(545) Schreckenbach, G.; Shamov, G. A. *Acc. Chem. Res.* **2010**, *43*, 19.
(546) Roos, B. O.; Lindh, R.; Malmqvist, P.-A.; Veryazov, V.; Widmark, P.-O- *Chem. Phys. Lett.* **2005**, *409*, 295.
(547) Roos, B. O.; Lindh, R.; Malmqvist, P.-Å.; Veryazov, V.; Widmark, P.-O.; Borin, A. C. *J. Phys. Chem. A* **2008**, *112*, 11431.
(548) Styszýnski, J. In *Relativistic Methods for Chemists. Challenges and Advances in Computational Physics*; Springer: London, 2010; Vol. 10, p 99.
(549) Cao, X.; Dolg, M. *Mol. Phys.* **2003**, *101*, 961.
(550) Cao, X.; Dolg, M. *Chem. Phys. Lett.* **2001**, *349*, 489.
(551) Thiel, C. W.; Sun, Y.; Cone, R. L. *J. Modern Optics* **2002**, *49*, 2399.
(552) Cao, X. *J. Chin. Chem. Soc.* **2003**, *50*, 665.
(553) Infante, I.; Eliav, E.; Kaldor, U.; Visscher, L. *J. Chem. Phys.* **2007**, *127*, No. 124308.
(554) Weigand, A.; Cao, X.; Vallet, V.; Flament, J.-P.; Dolg, M. *J. Phys. Chem.* **2010**, *113*, 11509.
(555) Barandiarán, Z.; Seijo, L. *J. Chem. Phys.* **2003**, *118*, 7439.
(556) Eliav, E.; Kaldor, U. *Phys. Rev. A* **1995**, *51*, 225.
(557) Gong, Y.; Zhou, M.; Andrews, L. *Chem. Rev.* **2009**, *109*, 6765.
(558) McDonald, S. A.; Rice, R. F.; Field, R. W.; Linton, C. *J. Chem. Phys.* **1990**, *93*, 7676.
(559) Dolg, M.; Stoll, H.; Preuss, H. *Chem. Phys.* **1992**, *165*, 21.
(560) Dias-Megias, S.; Seijo, L. *Chem. Phys. Lett.* **1999**, *299*, 613.
(561) Marian, C. M.; Wahlgren, U.; Gropen, O.; Pyykkö, P. *J. Mol. Struct. (THEOCHEM)* **1988**, *169*, 339.
(562) Averkiev, B. B.; Mantina, M.; Valero, R.; Infante, I.; Kovacs, A.; Truhlar, D. G.; Gagliardi, L. *Theor. Chem. Acc.* **2011**, *129*, 657.
(563) Heiberg, H.; Gropen, O.; Laerdahl, J.; Swang, O.; Wahlgren, U. *Theor. Chem. Acc.* **2003**, *110*, 118.
(564) Mosyagin, N. S.; Kozlov, M. G.; Titov, A. V. *J. Phys. B: At. Mol. Opt. Phys.* **1998**, *31*, L763.
(565) Cao, X.; Liu, W.; Dolg, M. *Sci. China, Ser. B: Chem.* **2002**, *45*, 91.
(566) Cao, X.; Moritz, A.; Dolg, M. *Chem. Phys.* **2008**, *343*, 250.
(567) Cao, X.; Dolg, M. *Mol. Phys.* **2003**, *101*, 1967.
(568) Dolg, M.; Stoll, H.; Preuss, H. *J. Mol. Struct. (THEOCHEM)* **1992**, *96*, 239.
(569) Zee, R. J. V.; Li, S.; Weltner, W. *J. Chem. Phys.* **1993**, *100*, 4010.
(570) Dolg, M.; Liu, W.; Kalvoda, S. *Int. J. Quantum Chem.* **2000**, *76*, 359.
(571) Buchachenko, A. A.; Chałasínski, G.; Szcęśniak, M. M. *Eur. Phys. J. D* **2007**, *45*, 147.
(572) Dolg, M.; Stoll, H.; Preuss, H. *J. Molec. Struct. (THEOCHEM)* **1991**, *251*, 327.
(573) Vallet, V.; Macak, P.; Wahlgren, U.; Grenthe, I. *Theor. Chem. Acc.* **2006**, *115*, 145.
(574) Odoh, S. O.; Schreckenbach, G. *J. Phys. Chem. A* **2010**, *114*, 1957.
(575) Iché-Tarrat, N.; Marsden, C. J. *J. Phys. Chem.* **2008**, *112*, 7632.
(576) Wiebke, J.; Moritz, A.; Cao, X.; Dolg, M. *Phys. Chem. Chem. Phys.* **2007**, *9*, 459.
(577) Ciupka, J.; Cao, X.; Wiebke, J.; Dolg, M. *Phys. Chem. Chem. Phys.* **2010**, *12*, 13215.
(578) David, F. H.; Fourest, B. *New J. Chem.* **1997**, *21*, 167.
(579) David, F.; Vokhmin, V.; Ionova, G. *J. Mol. Liq.* **2001**, *90*, 45.
(580) Marcus, Y. *J. Chem. Soc., Faraday Trans.* **1991**, *87*, 2995.
(581) Cao, X.; Heidelberg, D.; Ciupka, J.; Dolg, M. *Inorg. Chem.* **2010**, *49*, 10307.
(582) Clark, A. *J. Chem. Theory Comput.* **2008**, *4*, 708.
(583) Terrier, C.; Vitorge, P.; Gaigeot, M. P.; Spezia, R.; Vuilleumier, R. *J. Chem. Phys.* **2010**, *133*, No. 044509.
(584) Dinescu, A.; Clark, A. *J. Phys. Chem.* **2008**, *112*, 11198.
(585) Xiao, W.; Xia, Q.; Zhang, Y.; Ning, L.; Cui, Z. *Chin. J. Chem. Phys.* **2009**, *22*, 395.
(586) Buzko, V.; Sukhno, I.; Buzko, M. *J. Mol. Struct. (THEOCHEM)* **2009**, *894*, 75.
(587) Zhu, Y.; Chen, J.; Jiao, R. *Solvent Extr. Ion. Exch.* **1996**, *14*, 61.
(588) Cao, X.; Dolg, M. *Mol. Phys.* **2003**, *101*, 2427.
(589) Cao, X.; Li, Q.; Moritz, A.; Xie, Z.; Dolg, M.; Chen, X.; Fang, W. *Inorg. Chem.* **2006**, *45*, 3444.
(590) Lanza, G.; Varga, Z.; Kolonits, M.; Hargittai, M. *J. Chem. Phys.* **2008**, *128*, No. 074301.
(591) Groen, C. P.; Varga, Z.; Kolonits, M.; Peterson, K. A.; Hargittai, M. *Inorg. Chem.* **2009**, *48*, 4143.
(592) Pantazis, D.; Neese, F. *J. Chem. Theory Comput.* **2009**, *5*, 2229.
(593) Weigand, A.; Cao, X.; Yang, J.; Dolg, M. *Theor. Chem. Acc.* **2010**, *126*, 117.
(594) Varga, Z.; Groen, C. P.; Kolonits, M.; Hargittai, M. *Dalton Trans.* **2010**, *39*, 6221.
(595) Dolg, M. *AIP Conf. Proc.* **2011**preprint.
(596) Cundari, T. R.; Sommerer, S. O.; Strohecker, L. A.; Tippett, L. *J. Chem. Phys.* **1995**, *103*, 7058.
(597) Tsukamoto, S.; Mori, H.; Tatewaki, H. *Chem. Phys. Lett.* **2009**, *474*, 28.
(598) Lanza, G. *Int. J. Quantum Chem.* **2009**, *110*, 376.
(599) Straka, M.; Hrobarik, P.; Kaupp, M. *J. Am. Chem. Soc.* **2005**, *127*, 2591.
(600) Buzko, V. Y.; Kushkhov, K. B.; Buzko, M. B. *Rus. J. Inorg. Chem.* **2010**, *55*, 410.
(601) Kovács, A.; Konings, R. J. M.; Nemcsok, D. S. *J. Alloys Compd.* **2003**, *353*, 128.
(602) Batista, E. R.; Martin, R. L.; Hay, P. J. *J. Chem. Phys.* **2004**, *121*, 11104.

(603) Shamov, G. A.; Schreckenbach, G.; Vo, T. N. *Chem.—Eur. J.* **2007**, *13*, 4932.
(604) Kovács, A.; Konings, R. *J. Mol. Struct.* **2004**, *684*, 35.
(605) Schimmelpfennig, B.; Privalov, T.; Wahlgren, U.; Grenthe, I. *J. Phys. Chem. A* **2003**, *107*, 9705.
(606) Straka, M.; Patzschke, M.; Pyykkö, P. *Theor. Chem. Acc.* **2003**, *109*, 332.
(607) Moritz, A.; Dolg, M. *Chem. Phys.* **2007**, *327*, 48.
(608) *The Chemistry of the Actinide and Transactinide Elements*; Morss, L. R.; Edelstein, N. M.; Fuger, J.; Katz, J. J., Eds.; Springer: Dordrecht, The Netherlands, 2006.
(609) Denning, R. G. *J. Phys. Chem. A* **2007**, *111*, 4125.
(610) Vlaisavljevich, B.; Gagliardi, L.; Burns, P. C. *J. Am. Chem. Soc.* **2010**, *132*, 14503.
(611) Ricks, A. M.; Gagliardi, L.; Duncan, M. A. *J. Am. Chem. Soc.* **2010**, *132*, 15905.
(612) Wiebke, J.; Moritz, A.; Glorius, M.; Moll, H.; Bernhard, G.; Dolg, M. *Inorg. Chem.* **2008**, *47*, 3150.
(613) Shamov, G. A.; Schreckenbach, G.; Martin, R. L.; Hay, P. J. *Inorg. Chem.* **2008**, *47*, 1465.
(614) Puntus, L. N.; Lyssenko, K. A.; Pekareva, I. S.; Bünzli, J.-C. G. *J. Phys. Chem. B* **2009**, *113*, 9265.
(615) Pohl, R. H.; Wiebke, J.; Klein, A.; Dolg, M.; Maggiarosa, N. *Eur. J. Inorg. Chem.* **2009**, *17*, 2472.
(616) Maron, L.; Eisenstein, O.; Andersen, R. *Organometallics* **2009**, *28*, 3629.
(617) Maron, L.; Bourissou, D. *Organometallics* **2009**, *28*, 3686.
(618) Banik, N. L.; Schimmelpfennig, B.; Marquardt, C. M.; Brendebach, B.; Geist, A.; Denecke, M. *Dalton Trans.* **2010**, *39*, 5117.
(619) Castro, L.; Yahia, A.; Maron, L. *C. R. Chim.* **2010**, *13*, 870.
(620) Castro, L.; Yahia, A.; Maron, L. *Dalton Trans.* **2010**, *39*, 6682.
(621) Krogh-Jespersen, K.; Romanelli, M. D.; Melman, J. H.; Emge, T. J.; Brennan, J. G. *Inorg. Chem.* **2010**, *49*, 552.
(622) Vallet, V.; Fischer, A.; Szabo, Z.; Grenthe, I. *Dalton Trans.* **2010**, *39*, 7666.
(623) Todorova, T. K.; Gagliardi, L.; Walensky, J. R.; Miller, K. A.; Evans, W. J. *J. Am. Chem. Soc.* **2010**, *132*, 12397.
(624) Wiebke, J.; Weigand, A.; Weissmann, D.; Glorius, M.; Moll, H.; Bernhard, G.; Dolg, M. *Inorg. Chem.* **2010**, *49*, 6428.
(625) Apostolidis, C.; Schimmelpfennig, B.; Magnani, N; Lindqvist-Reis, P.; Walter, O.; Sykora, R.; Morgenstern, A.; Colineau, E.; Caciuffo, R.; Klenze, R.; Haire, R. G.; Rebizant, J.; Bruchertseifer, F.; Fanghaenel, T. *Angew. Chem., Int. Ed.* **2010**, *49*, 6229.
(626) Tassel, M. J.; Kaltsoyannis, N. *Dalton, Trans.* **2010**, *39*, 6719.
(627) Puntus, L. N.; Lyssenko, K. A.; Pekareva, I. S.; Antipin, M. Y. *Mol. Phys.* **2010**, *108*, 557.
(628) Guillaumont, D. *J. Phys. Chem. A* **2004**, *108*, 6893.
(629) Pascual, J. L.; Schamps, J.; Barandiarán, Z.; Seijo, L. *Phys. Rev. B* **2006**, *74*, No. 104105.
(630) Prodan, I. D.; Scuseria, G. E.; Martin, R. L. *Phys. Rev. B.* **2006**, *73*, No. 045104.
(631) Ordejon, B.; Vallet, V.; Flament, J. P.; Seijo, L.; Barandiarán, Z. *J. Lumin.* **2007**, *126*, 779.
(632) Gracia, L.; Seijo, L.; Barandiarán, Z.; Curulla, D.; Niemansverdriet, H.; van Gennip, W. *J. Lumin.* **2008**, *128*, 1248.
(633) Pascual, J. L.; Barros, N.; Barandiarán, Z.; Seijo, L. *J. Phys. Chem. A* **2009**, *113*, 12454.
(634) Sánchez-Sanz, G.; Seijo, L.; Barandiarán, Z. *J. Phys. Chem. A* **2009**, *113*, 12591.
(635) Sánchez-Sanz, G.; Seijo, L.; Barandiarán, Z. *J. Chem. Phys.* **2009**, *131*, No. 024505.
(636) Muñoz-García, A. B.; Seijo, L. *Phys. Rev. B* **2010**, *82*, No. 184118.
(637) Muñoz-García, A. B.; Pascual, J. L.; Barandiarán, Z.; Seijo, L. *Phys. Rev. B* **2010**, *82*, No. 064114.
(638) Sánchez-Sanz, G.; Seijo, L.; Barandiarán, Z. *J. Chem. Phys.* **2010**, *133*, No. 114506.
(639) Sánchez-Sanz, G.; Seijo, L.; Barandiarán, Z. *J. Chem. Phys.* **2010**, *133*, No. 114509.
(640) Sánchez-Sanz, G.; Seijo, L.; Barandiarán, Z. *Spectrosc. Lett.* **2010**, *43*, 393.
(641) Yang, J.; Dolg, M. *J. Solid State Chem.* **2007**, *180*, 2763.
(642) Balducci, G.; Brutti, S.; Ciccioli, A.; Gigli, G.; Palenzona, A.; Pani, M. *J. Phys.Chem. B* **2007**, *111*, 5132.
(643) Masys, S.; Mickevicius, S.; Grebinskij, S.; Jonauskas, V. *Phys. Rev. B* **2010**, *82*, No. 165120.
(644) Schwerdtfeger, P.; Seth, M. In *Encyclopedia of Computational Chemistry*; Wiley: Chichester, U.K., 1998; p 2480.
(645) Seth, M.; Cooke, F.; Schwerdtfeger, P.; Heully, J. L.; Pélissier, M. *J. Chem. Phys.* **1998**, *109*, 3935.
(646) Seth, M.; Faegri, K.; Schwerdtfeger, P. *Angew. Chem., Int. Ed.* **1998**, *37*, 2493.
(647) Han, Y. K.; Bae, C.; Lee, Y. S. *J. Chem. Phys.* **1999**, *110*, 8969.
(648) Seth, M.; Schwerdtfeger, P.; Faegri, K. *J. Chem. Phys.* **1999**, *111*, 6422.
(649) Seth, M.; Dolg, M.; Fulde, P.; Schwerdtfeger, P. *J. Am. Chem. Soc.* **1995**, *117*, 6597.
(650) Nash, C. S. *J. Phys. Chem. A* **2005**, *109*, 3493.
(651) Pershina, V. *Russ. Chem. Rev.* **2009**, *78*, 1153.
(652) Hermann, A.; Furthmueller, J.; Gaeggeler, H. W.; Schwerdtfeger, P. *Phys. Rev. B* **2010**, *82*, No. 155116.
(653) Pyykkö, P.; Atsumi, A. *Chem.—Eur. J.* **2009**, *15*, 186.
(654) Pershina, V. In *Relativistic Methods for Chemists. Challenges and Advances in Computational Physics*; Springer: London, 2010; Vol. 10, p 451.